Composite beams with openings in metal-ribbed decking slabs.

Baharom, Shahrizan

College of Engineering

Swansea University

Prifysgol Abertawe
Swansea University

Composite Beams with Openings in Metal-Ribbed Decking Slabs

SHAHRIZAN BAHAROM

Thesis submitted to the Swansea University
In candidature for the degree of Doctor of Philosophy

August 2010

Specimen Layout for Declaration/Statements page to be included in Higher Degree Thesis

DECLARATION

This work has not previously been accepted in substance for any degree and is not being concurrently submitted in candidature for any degree

Signed .... (candidate)

Date .....4/3/2011.....

STATEMENT 1

This thesis is the result of my own investigations, except where otherwise stated. Other sources are acknowledged by footnotes giving explicit references. A bibliography is appended.

Signed ..... (candidate)

Date .....4/3/2011.....

STATEMENT 2

I hereby give consent for my thesis, if accepted, to be available for photocopying and for inter-library loan, and for the title and summary to be made available to outside organizations.

Signed ..... (candidate)

Date .....4/3/2011.....

NB: *Candidates on whose behalf a bar on access has been approved by the University, should use the following version of Statement 2*:

I hereby give consent for my thesis, if accepted, to be available for photocopying and for inter-library loans, **after expiry of a bar on access approved by Swansea University on the special recommendation of the Constituent Institution / University concerned.**

Signed ..... (candidate)

Date .....4/3/2011.....

Acknowledgement

I would like to thank Prof. R.Y Xiao for providing supervision, encouragement and help during the course of the research. I am also thankful to all my friends who helped me in so many ways and made my stay at Swansea University so pleasant and unforgettable.

I would like to express my sincere thanks and appreciation to Prof. N E Shanmugam for his valuable suggestions and advice in preparing my thesis. My sincere thanks are extended to Prof. R Taha and Prof. W Hamidon, University Kebangsaan Malaysia for their consistent encouragements to continue my PhD degree.

I would like to express my gratitude to National University of Malaysia (UKM) and Malaysia Government, who have provided the necessary fund for the project.

I would like to acknowledge my wife Norhafezah Kasmuri and my son, Amir Hakim who have accompanied me in Wales. I express my sincere indebtedness for their sacrifices, patience and understanding which have been inevitable to make this work possible. I also acknowledge my sincere gratitude to all my families, especially to my mother, Rapiah Ahmad and my late father, Baharom Md. Amin, for their love throughout my live. Finally, all praise goes to almighty Allah for being kind to me.

Abstract

This thesis deals with the finite element simulation of composite beam with openings in metal-ribbed decking slab. A three-dimensional (3D) finite element model is proposed using general purpose finite elemnt sotware, ANSYS, to carry out non-linear analyses to investigate the effect of openings in metal-ribbed decking slabs on strength and deformation. Firstly, the finite element (FE) model had been developed to predict the behaviour of composite beams without openings in metal-ribbed decking slab as a reference before the influence of the openings in metal-ribbed decking slab was investigated. The FE model developed has been validated with the experimental test carried out by other researchers. It is proposed to implement 3D shear stud modelling in composite beam to simulate the real deformation of shear studs in composite beam with metal-ribbed decking slab. Close agreements for ultimate load and load-deflection curve plot have been recorded between the finite element model and experimental results. Having obtained the capability to predict the ultimate moment capacity of composite beam, a parametric study of the effect of openings in composite beam flange on the moment capacity of composite beam was carried out to study the influence of different parameters. The parameters such as openings size in tranverse and longitudinal direction, openings location and load location were considered. It is observed from investigation that the opening size in tranverse direction and load location produced significant effect in moment capacity due to openings. The investigation to study suitable method to increase moment capacity of composite beam with openings also has been carried out. It is observed from investigation that, concrete strength, thickness of slab and diameter of reinforcement bar can be used to increase the ultimate moment capacity of compsoite beam with opening up to the moment capacity of composite beam without openings. A design method is suggested to predict the ultimate moment of composite beam with openings. Comparisons between results of the proposed design method and corresponding FE analysis have shown that the derived formulae are able to predicts the moment capacity and stiffness of composite beams due to openings in the flange.

Content List

Chapter 4 Numerical Simulation and Validation

Chapter 6 Analytical Method

Chapter 7 Conclusions and Recommendations

Appendix

List of Figures

Chapter 4 Numerical Simulation and Validation

List of Tables

Notations

A	Cross-sectional area
A_0	$(A_s A_c)/(nA_s + A_c)$
A'	$A_0/(I_0+A_0 d_c^2)$
A_c	area of concrete cross-section
A_s	area of steel cross-section
A_{sc}	area of shear connector cross-section
B_e	effective breadth of concrete slab
D	beam depth
d	diameter; depth; distance
D_p	profiled depth
D_s	overall slab thickness
E_c	elastic modulus of concrete
E_s	elastic modulus of steel
E_{sh}	elastic modulus of steel at strain hardening
EI	rigidity of section
f	strength of material
f_{cu}	compressive strength of cubic concrete block.
f_t^u	the ultimate tensile strength of concrete
f_{sy}	yield strength of steel
f_{su}	ultimate strength of steel
f_u	yield strength of shear stud connector
f'_c	cylinder compressive strength of concrete
f_{cu}	compressive strength of concrete cube
h	height; thickness
I	Second moment inertia
I_0	$I_c/n + I_s$
I_c	moment inertia of concrete
I_s	moment inertia of steel
K	shear stiffness of shear stud

k_s	degree of shear interaction
L	beam span
M	bending moment
M_c	moment capacity
M_u	ultimate bending moment
M_{BS5950}	ultimate moment of beam calculated according to BS5950
M_{EC4}	ultimate moment of beam calculated according to EC4
M_{FE}	ultimate moment of beam from finite element analysis
M_{uo}	ultimate moment of beam with openings
M_{no}	ultimate moment of composite beams without openings
n	modular ratio; number of shear stud
P_u	ultimate load
P_o	ultimate load of composite beam with openings
P_{no}	ultimate load of composite beams without openings
p	longitudinal spacing of shear stud
p_f	longitudinal spacing of shear stud for full composite action
R_c	compressive resistance of concrete
R_q	longitudinal shear resistance of shear connector
R_r	tensile/compression force of reinforcement bar
R_s	resistance of steel section
R_{st}	tensile resistance of steel section
R_{sc}	compression resistance of steel section
R_w	tensile resistance of web
T	thickness of steel flange
t	thickness of steel web
σ	the stress
σ_y	the yield stress
σ_s	the stress of steel
σ_{yr}	yield stress of reinforcement bar
δ	deflection of beam
δ_a	deflection for steel beam acting alone

δ_c	deflection for composite beam with full shear connection
δ_{EC4}	deflection obtained from method proposed by EC4
δ_{FE}	deflection obtained from finite element analysis
δ_{Nie}	deflection obtained from method proposed by Nie. J
ε	the strain
ε_t^u	strain at ultimate tensile strength of concrete.
ε_u	ultimate concrete strain in compression (= 0.0035).
ε_s	strain of steel
ε_{sh}	strain at the beginning of steel hardening
ε_{su}	ultimate strain of steel
ε'_c	concrete strain at maximum yield stress
ξ	parameter of slip effect
v	poisson's ratio

Chapter 1

INTRODUCTION

1.1 Overview

The idea of combining two or more different materials together to increase their structural performance has been around for more than hundred years and has continued up to the present time. Instead, ancient people, Eastern and Western, built houses with the combination of mud and chopped straw, which may also be considered as composite structures. Composite structures offer many advantages over simple structures. One of the most advantageous features of composite construction is its flexibility in design, offering the designers virtually infinite possibility to "tailor" both the geometric shape and material to optimise the structural performance. As a result, for a similar shape and size, a composite structural member can have greater stiffness, higher load carrying capacity and resistance against material damage and higher collapse capacity. Consequently, composite members can provide better economy of material and construction.

Traditionally, in structural engineering applications, composite construction refers to casting of concrete slab on steel section, using the whole assembly as a single structural unit. This system is termed as steel-concrete composite system. Reinforced concrete is inexpensive, massive and stiff while steel members are strong, lightweight and easy to assemble. With the advance of new technologies and materials, composite structures now, may include all types of construction that are formed by arranging two or more structural materials. Among these is the introduction and widespread use of composite-steel decks that serve initially as work platforms and concrete formwork and as slab reinforcement in resisting loads after the concrete has hardened. A typical modern composite-floor system is shown in Figure 1.1. The composite floor system consists of four principal components, which are steel beam section, steel deck, headed shear stud and concrete slab. In composite frame system, the beam supports the floor slab and at each intersection between beams and columns, the columns are usually continuous and the beams are attached to their external faces by connections. These are usually assumed in design to act as pin joints, but they may be semi-rigid or rigid. Composite slabs and semi-rigid connections constitute a new type of semi-rigid connection.

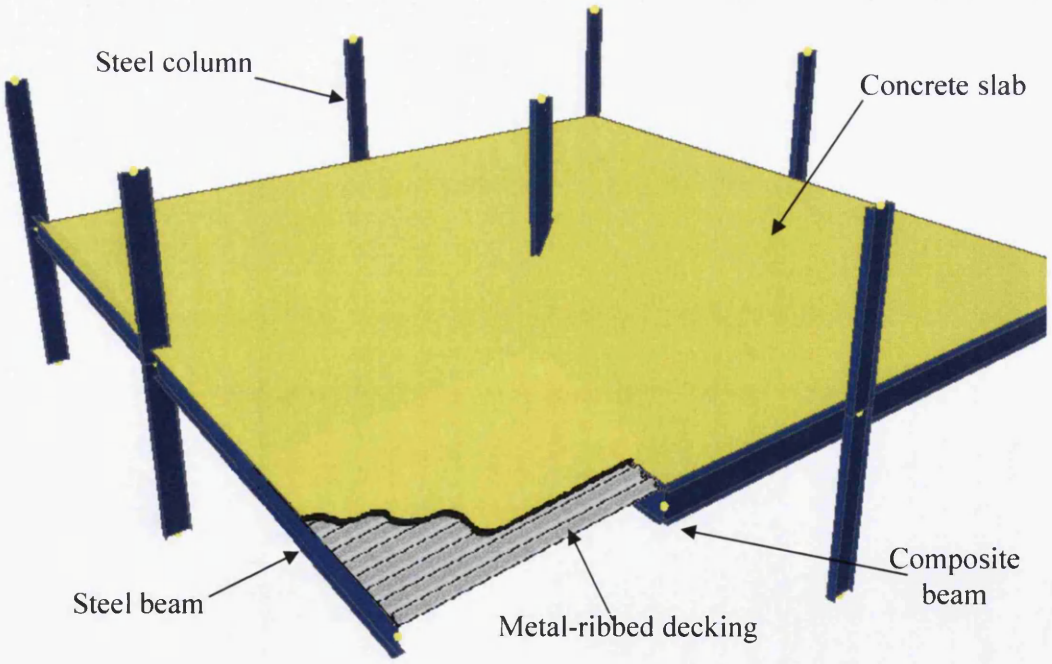

Figure 1.1: Typical composite floor system

1.2 Statement of problem

Composite floor system has a widespread use in construction because of the benefits of efficiently combining the two construction materials, steel and concrete. It is economic in terms of labour saving on site, construction timing and shallower structural size. A composite slab is normally designed as a deformed deck-slab by using shear connectors to transfer interface shear to act as the base for the concrete floors as shown in Figure 1.2.

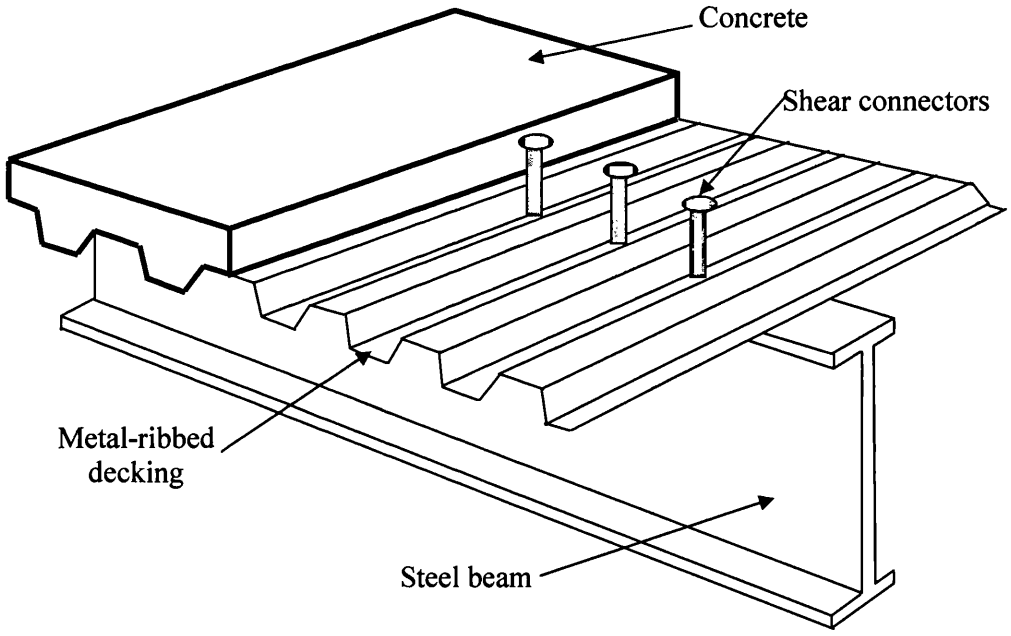

Figure 1.2: Composite beam components in composite floor system

However, openings frequently occur in commercial or hospital buildings which may contain pipelines, risers, placing heating, ducts and ventilation. These may require a large opening in the composite slab (as shown in Figure 1.3) which has the potential to reduce composite beam capacities and to have influence on moment resistance of the whole composite system. In composite beam and slab design, designers are often faced with this problem (Xiao 1998).

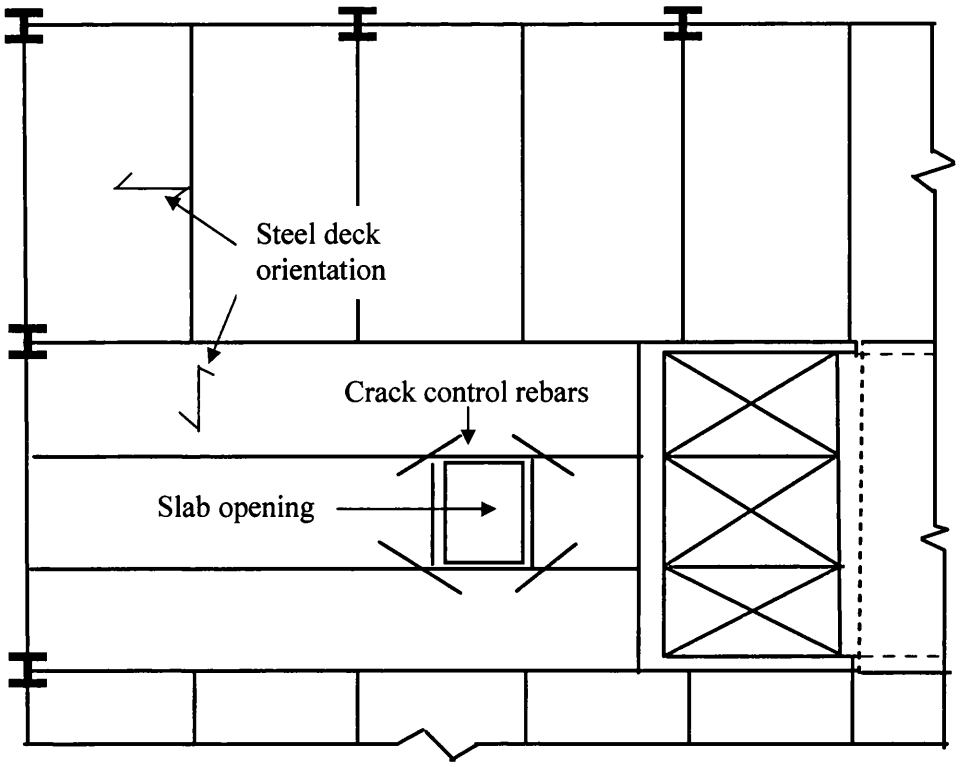

Figure 1.3: Opening in composite floor system

Openings are varied in terms of size and position. Openings can be located anywhere in the composite beam flange, symmetrically and asymmetrically. BS5950 Part 4 (BSI 1994) gives little guidance on the design for openings, referring instead to BS8110 (BSI 1997) for the slab design itself. No details are given and the metal decking suppliers themselves give only minimal recommendation covering extra reinforcement or trimming steel to satisfy local slab checks as shown in Figure 1.4. The composite floor system relies for its strength on steel beam acting compositely with a concrete slab via metal ribbed decking and shear connector. Hence, it is clear, when a composite beam is weakened by opening, this potentially affects the moment resistance of the whole composite system.

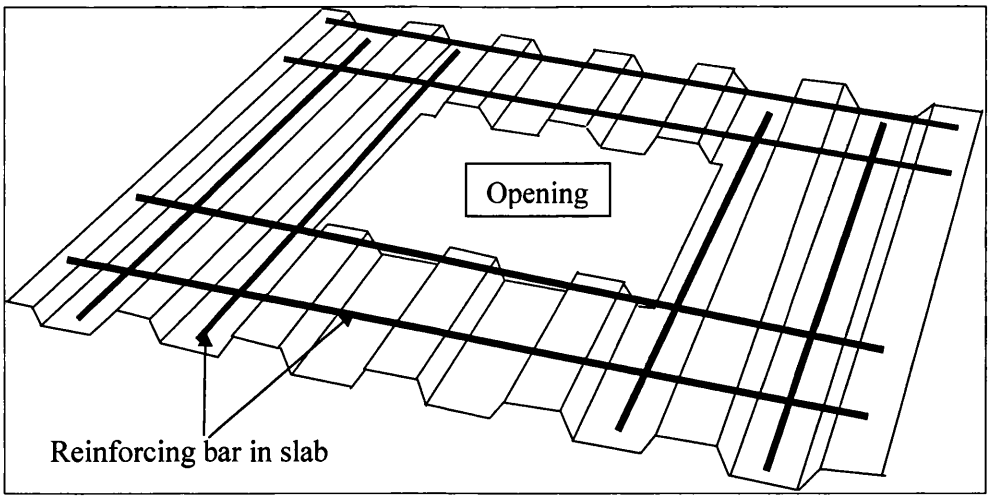

Figure 1.4: Cut-out and reinforcing bar in the metal-ribbed decking

1.3 Previous work

Xiao et. al. (1998) have proposed a design method for calculating the moment resistance of composite slab with openings in the sagging moment region. The ultimate strength of the composite section can be determined from its plastic capacity. A design formula for composite beam with openings was derived by inclusion of the opening effect into plastic analysis. Openings were assumed within the effective breadth of the composite beam. Only the net effective width of the composite beams flange was considered in plastic analysis. This method is termed as the effective width method. The modified section then was used in the calculation of the composite section with compliance to BS 5950 (BSI 1990) composite beam design. Xiao et al. (1998) have also proposed the continuity design approach to counter the influence of openings.

The design formula was programmed in design software and a parametric study carried out. The parameters considered were steel strength, beam section size, beam span, metal decking slab or solid slab, concrete strength and slab depth. The conclusions from the research were as follows:-

- Moment resistance of the composite beam was significantly affected by the presence of openings in the composite slab.
- A small steel section is more sensitive to the opening effect in the slab.
- Continuity in the support regions could counter the influence of openings on the moment resistance of the structure.

1.4 Objectives of research

The structural response of a composite beam with metal ribbed decking is predominantly nonlinear. By locating openings in the composite beam flange, it is expected that the positive moment capacity of a simply supported composite beam will decrease. However, due to a lack of knowledge of their performance, design of composite beam with openings in the metal ribbed decking composite slab can be either too conservative or inadequate. To predict accurately the structural response to loading in order to design safely such structures, a realistic analysis should be carried out to consider all nonlinearities in metal ribbed decking composite beam with and without opening.

With this consideration, this research has been conducted as an extension to the previous research work by Xiao et. al. (Xiao 1998) to achieve the following goals:-

- To develop a nonlinear finite element model of metal ribbed decking composite beam on a single span, incorporating the nonlinear aspects of behaviour.
- To develop a nonlinear finite element model of metal ribbed decking composite beam with openings in the composite beam flange on a single span to investigate the behaviour of structure with associated parameters.
- Development of a theoretical prediction method based on finite element simulation results.
- To give guidelines to designers and contractors to take into consideration the influence of openings.
- Methods to improve strength of composite beams with openings.

1.5 Research programme

To achieve the objectives set in this thesis, finite element software package *ANSYS* (ANSYS Release 10) has been used to carried out the research. ANSYS is selected as a tool due to its capability in nonlinear analysis. The research was carried out in the following order:-

- Development and verification of the finite element (FE) model of composite beam without openings in metal ribbed decking slab.
- Investigation of the effects of openings in the composite beam by using the aforementioned FE model.
- Investigation on suitable method to increase the capacity of composite beam with openings in metal-ribbed decking slab
- Development of a design equation for composite beam with opening in the metal-ribbed decking slab.

1.6 Scope of the thesis

This thesis presents the details of the research work on modelling the behaviour of composite beam with and without openings in metal ribbed decking composite slabs. The thesis is divided into seven chapters.

Chapter 1 describes the composite system, statement of problem, previous work, objectives of the research work, research programmes and scope of thesis.

Chapter 2 introduces the reader to the literature review, which assesses the research conducted in the fields relevant to this project: Composite beam with metal ribbed decking slabs, including both experimental and numerical modelling conducted by other researchers. The materials used to construct composite beam with metal ribbed decking and composite connections also are discussed.

In Chapter 3, an introduction of analytical methods especially the finite element (FE) software (ANSYS) is highlighted. Material modelling and the type of element used in FE modelling also are described in detail.

In Chapter 4, the development of a nonlinear three-dimensional FE model of composite beam with metal ribbed decking is described in detail. The modelling technique especially the implementation of FE modelling of headed shear stud into the composite beams modelling, is the focus in this chapter. The modelling of composite beams with metal ribbed decking slab is verified by experimental tests which have been conducted by other researchers. A parametric study has been conducted by using the new modelling technique of composite beam with metal ribbed decking slabs.

Chapter 5 is devoted to the FE modelling of composite beam with openings in the metal-ribbed decking slab. Intensive FE analyses have been carried out to gain an understanding of structural behaviour and their moment capacity reduction when openings are located in the composite beam flange. The final part of this chapter is a parametric study of the suitable method to increase the ultimate moment of composite beam with openings.

Chapter 6 presents an analytical method for calculating moment capacity of composite beam with opening in metal-ribbed decking slab. Also results are compared with corresponding finite element results obtained using model proposed in Chapter 4.

Finally, Chapter 7 summarises the major findings of the research and recommendations for further study.

1.7 References

ANSYS (Release 10). ANSYS Documentations, Manual Set and Theory Reference Manual, ANSYS Inc.

BSI (1990). BS 5950 Structural use of steel work in building, Part 3, section 3.1: Code of practice for design of composite beams. London, BSI.

BSI (1994). BS5950 Structural use of steelwork in building, Part 4: Code of practice for design of composite slab with profiled sheeting, BSI.

BSI (1997). BS8110 Structural use of concrete, Part 1: Code of practice for design and construction, London, BSI.

Xiao, R. Y., Dibb-Fuller, D., and, Wood, G.A., (1998). "Opening in composite slabs - design implication." Journal of Constructional Steel Research 46(1-3): Paper no. 354.

Chapter 2

LITERATURE REVIEW

2.1 Introduction

Most of the composite floor systems built today are of steel-concrete composite. It is a fact, however, that engineers are increasingly designing composite and mixed building systems of structural steel and reinforced concrete to produce more efficient structures than the ones designed using only one of those materials. Continuous development has been carried out to optimise the structural form, which has led to designs that are lighter, more efficient and economic. In fact, the drive for designing lighter and more economical structures has always been a major motivation in building construction. In order to achieve improved economy, an efficient and speedy construction technique is essential. Steel is considered to be the most suitable material for quick and efficient construction, as the steel member can be fabricated in factory to the correct dimensions, minimising tolerances and wastage. The high ratio of strength to weight of steel also makes the material easy to transport and handle in the workshop. Steel is

preferred as it is lighter, has lower energy consumption in production, experiences less damage during handling and has an excellent recycling value.

This chapter summarises and reviews important findings from a number of researchers, who have examined composite beam with metal-ribbed decking. Special attention is given to the composite beam with openings in metal-ribbed decking slab. To study composite beams with metal-ribbed decking, it is also useful to know about its basic design which is discussed in depth in this chapter.

2.2 Composite beam with a metal-ribbed decking slab

2.2.1 Introduction

One of the components in a composite frame system is composite beam. A composite beam is designed using a combination of concrete slab, shear studs, steel section and profiled steel sheeting. Structurally, a composite beam behaves like a series of parallel T beams with thin, wide flanges. An effective breadth of slab is identified, which acts in conjunction with the steel beam. The steel shape is used primarily to resist tension and shear, while the concrete slab acts as a compression-resisting element, when the structure is subjected to sagging (positive) moment. Thus, the composite beam is usually designed as a simply supported construction. The slab also restraints the upper flange of the steel section against local and lateral buckling. This type of beam normally can be designed to achieved a span of 1 – 40 m (Hayward 2002).

A conventional composite T-beam is a combination of solid slab with steel beam I-section. However, with the introduction of metal decking, the change from solid slab to decking slab is developing rapidly. Metal decking was first used as a non-composite material, where it was used as roofing and working platforms on which to cast concrete slabs. Nowadays composite-steel deck floor system is used in almost all multistory, steel-framed buildings for economical reasons (Chien 1993).

One of the factors that has made the composite beam popular is the development of welded headed studs. Headed shear studs provide a mechanical shear connection between the top flange of the steel beam, the concrete and the steel deck. A push-off

test is used to determine the shear capacity of the connector in a composite beam instead of the full-scale composite-beam test. Since the shear capacity is one of the most important parameters in the determination of composite-beam strength, the push-off test is considered to be a very important test. In addition, it is not as costly as the full-scale beam test. Due to the popularity of composite steel-deck construction, much research on composite beams with metal-ribbed decking has been carried out, using full-scale composite beams, push-off tests or computer modelling.

2.2.2 Experimental study

Robinson (1967) carried out an experimental programme to investigate the influence of rib geometry on the general performance of beams. Fifteen simple-span beams and thirty-nine push-off specimens were tested. From the results, he concluded that the stiffness and load-carrying capacity of composite beams could be increased by the improvement of the composite action between the decking, the concrete slab and the steel beam. If the correct interaction is achieved, the mode of cracking is influenced by the geometry of the ribs. He also found that the geometry of the metal decking played an important role in rib cracking, where the concrete cracking of the rib occurred in an elastic range for the height– width ratio greater than 1; while for the height– width ratio less than 1, it occurred close to the time when local yielding of the beam was initiated. All the beams that were tested, failed, due to inadequate shear connection; great deformation and concrete crushing and cracking was only a secondary effect, which was mostly initiated around the point-load region.

Fisher (1970) proposed a formula for the reduction in shear capacity of the shear connector of a composite beam with metal-ribbed decking. The formula was developed after he found that composite beams could be modelled with a haunch slab, which was equal in thickness to the solid slab and part of the rib above. The formula is given in Equation (2-1)

$$Q_{rib} = A\left(\frac{w}{h}\right)Q_{sol} \leq Q_{sol} \qquad (2\text{-}1)$$

Where,

Q_{rib} = Shear strength of connection in a rib

A = numerical coefficient (0.5 for beams)

w = average rib width

h = height of rib

Q_{sol} =shear strength of connector in solid slab

Robinson et al. (1973) presented results from two series of tests on a composite beam with metal-ribbed decking slab. The experimental programme consisted of tests on twelve push-out test and nine simple span composite beams. Single studs and double studs were used in the push-off and composite tests. The objective of the investigation was to verify the use of ultimate strength computation, based on partial connection and to study various connectors spaced up to 914.4 mm apart. It was found that the strength of a connection with two studs is approximately 50% greater than one with a single stud. The factors affecting the strength of connection in a metal-decking slab include width of the slab, embedment length of the stud in a solid slab, width of ribs, and stud diameter. He also found that a partial connection ratio of 0.5 enabled a beam to attain 82% of the full ultimate flexural capacity. However, for the 0.27 ratio, connections had failed slightly above working-load level.

Grant et al. (1977) reported the evaluation of the work done in Lehigh University in 1971, which involved seventeen full-scale tests on composite beams with metal decking and an additional fifty-eight tests conducted by other researchers. They proposed a formula for calculating the capacity of shear studs in the ribs of composite beams with metal-ribbed decking, by incorporating the parameters of the average rib width–height ratio, height of the rib, embedment of the connector and number of connectors. He modeled the reduction in shear capacity by formula shown in Equation (2-2).

$$Q_{rib} = \frac{0.85}{\sqrt{N}}\left(\frac{H-h}{h}\right)\left(\frac{w}{h}\right)Q_{sol} \le Q_{sol} \qquad (2\text{-}2)$$

Where,

N = number of studs in a rib

H = height of shear connector

Q_{sol} = strength of the stud shear connector in a solid slab

Robinson (1988) reported on the studies of the behaviour of multiple stud shear connections in deep-ribbed metal decking. Seventeen different types of push-off specimens were tested, using a variety of ribbed, metal profiles, a number of different connectors and locations of headed stud, and two full-scale beams. Each push-out test specimen consisted of either a single or a pair of headed shear studs. The purpose of the push-off test was to determine the ultimate strength of the shear specimens to be used in the design of a composite beam. The theoretical result of the pairs–single stud ratio was derived from Equation (2-2), which was introduced by Grant (1977); this was compared with the experimental result of the pair–single stud ratio. From the theoretical and experimental results, there were no cases of the double studs having two times the interfacial strength of the single studs. The ratio of the ultimate flexural moment of a composite beam, between the theory and the test, was nearly 1.0, which shows very good agreement. He concluded that having one lateral row of single or pairs of headed shear studs in the push-off test gave reliable shear strength results, which were comparable to the shear connection in composite beams.

Jayas et al. (1988; 1989) carried out an experiment on the behaviour of headed studs using a push-out test and a full-size composite beam with metal-ribbed decking. The first phase of the research was reported in year 1998 and consisted of eighteen full-size, push-out tests. The second phase of the research, in year 1989, consisted of four full-size composite beams and two full-size push-off tests. From the research, Jayas et al. (1989) proposed empirical equation for specimens with depth of decks of 38mm and 76mm. The equations are given as below:

$$V_c = 0.35\lambda\sqrt{f'_c}A_c \le Q_u \qquad \text{For metal decks with 76 mm depth} \qquad (2\text{-}3)$$

$$V_c = 0.61\lambda\sqrt{f'_c}A_c \le Q_u \qquad \text{For metal decks with 38 mm depth} \qquad (2\text{-}4)$$

Where,

V_c = shear capacity due to concrete pull-out failure (N)

f'_c = concrete compressive strength (MPa)

A_c = area of concrete pull-out failure surface (mm^2)

λ = 1.0 for normal density concrete, 0.85 for semi-low density concrete, 0.75 for density concrete.

He found that the predicted values of flexural capacity, which were calculated using plastic analysis by incorporating Equations (2-3) and (2-4), were in good agreement with those observed in the full-size beam specimens tested.

Harding (1990) reported his experimental research on metal-ribbed decking composite beams with partial shear connection. The interaction was between 26% and 77%. The parameters considered were overall span, different types of British metal decking profiled with parallel or transverse decking orientation, degree of shear connection, type of concrete and effective slab width. He found that the mode of failure of the composite beams with partial stud shear connection was interfacial shear due to the critical loss of shear connection between the steel deck slab and steel beam. However, for the composite beam with full shear connection, the beam failed in flexural mode. It was found that the influence of shear lag can be ignored for a maximum slab-span–width ratio of 3. He also found that the end-slip was at about 1.5–2.0mm for the beam failed in the interfacial mode and about 0.5 mm for flexural mode of failure. Interfacial slip was shown to significantly reduce both stiffness and strength of a composite beam.

Nie et al. (2007) reported on an experimental study of the performance of a metal-ribbed-decking composite beam with partial shear connection. In the test, degree of shear connection was varied between 0.25 and 1.85. The degree of shear connection 1.85 is a theoretical value which means the number of shear studs provided is 85% more than number of shear stud required for full interaction. The experiment consisted of three series, including: a simply-supported beam subjected to positive-bending and negative-bending, and continuous beams with two or three spans. The ultimate moment from the test was compared with EC4 and AISC equivalent methods, which showed that the method overestimated the bending strength by about 2.7% to 9.7%, respectively and closely predicted the negative-bending strength. For a continuous beam with partial interaction, it was found that both positive and negative bending could be predicted by using the EC4 method. He also found that the deflection of a continuous beam at 50% of the ultimate load was increased by about 45% to 98%, compared to the beam with full shear connection.

2.2.3 Computer modelling

Full-size composite beam test and full-size push-out test require facilities that are costly to implement. Nowadays, computer modelling is considered a very important tool to predict the behaviour of such structures. Computer modelling of metal-decking composite beams and push-out tests could reduce the use of full-size tests and enable a number of repetitive analyses to be carried out so that a comprehensive parametric analysis could be conducted. Computer modelling, carried out by many researchers, is described in this literature review.

Wright (1990) introduced the folded-plate method in composite-beam modelling, which used an exact elastic solution. The composite beam is idealised as components plates, considering the slab as concrete plates and the steel beam as individual steel plate as shown in Figure 2.1. A 'dummy element' that connected a steel beam to a slab was developed, which was considered to be a more flexible approach. The method had been used previously in the modelling of a metal decking composite beam (Wright 1990). Discrete, non-linear connections can be taken into account by disconnecting the 'dummy' element from the beam, thus creating a free-slip surface. The forces introduced give rise to a differential slip and, with some iteration, it is possible to match the load and slip to the relationship obtained from the push-off test. As each stud load and resulting slip is applied individually to the analysis, non-linear effects are automatically included. As each stud load and resulting slip is applied individually to the analysis, non-linear effects are automatically included.

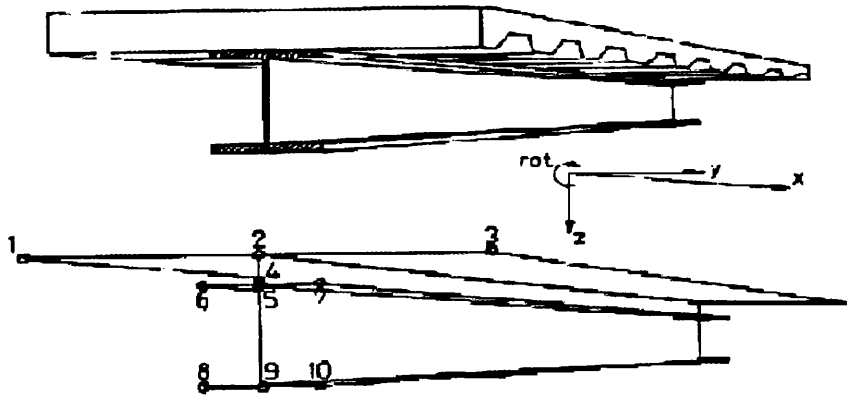

Figure 2.1: Folded plate approach of composite beam proposed by Wright (1990).

Computer modelling was proposed by Wang et al.(2008) and Fahmy et al. (2008) recently. Both of them used ABAQUS in the finite element modelling. Wang et al. used 2-D models by employing a plane stress element in order to examine the structural behaviour of perforated steel beam web of composite beams with metal-ribbed decking. He used horizontal and vertical spring elements for shear and axial deformation, as shown in Figure 2.2. Equation (2-5), was used as constitutive load-slip curve. On the other hand, Fahmy et al. (2008) proposed that 3-D, non-linear modelling to investigate longitudinal cracking of concrete slabs in a metal-ribbed-decking composite beam. He also used the spot-weld option, which is available in ABAQUS, to model the shear stud. The model is shown in Figure 2.3. The hyperbolic curve, as in Equation (2-6), was used to idealise the actual load-slip curve. Generally, both of the models can effectively predict the behaviour of composite beams, when the comparison of the load-deflection curves from FE model is compared with the experimental curve.

$$F_s = P_s(1-e^{-\beta s})^{\alpha} \tag{2-5}$$

Where,

P_s = shear resistance of headed shear stud

F_s = longitudinal shear force developed in the headed

s = slippage (mm)

α = non-dimensional parameter with the value between 0.5 and 1.5

β = parameter with unit of mm^{-1}, typical values between 0.5 and 2.0

$$Q = \frac{C}{\gamma - A} + B \tag{2-6}$$

Where,

Q = shear force in connector

γ = slip

A,B,C = constant

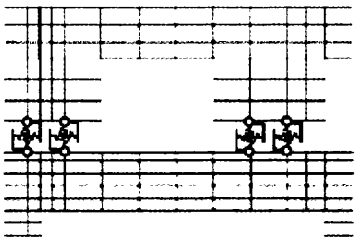

Figure 2.2: Spring Element in composite beam proposed by Wang et.al (2008)

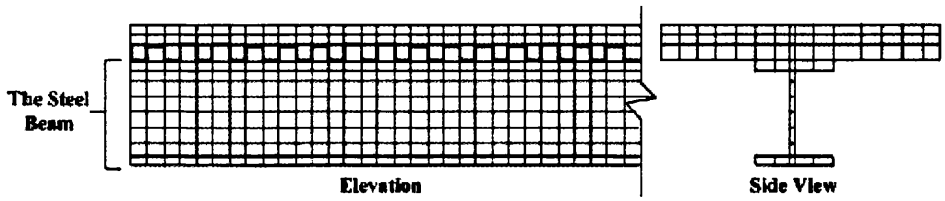

Figure 2.3: Composite beam model proposed by Fahmy et. al (2008)

From the literature mentioned above, it is found that modelling of shear connection of a metal-ribbed-decking composite slab is very important issue. Kim et al. (2001) used FE modelling to model a push-off test for the shear connection between steel beams and a metal-ribbed-decking composite slab, which used through-deck, welded shear connectors. He modelled the push-off test using a 2D (linear and non-linear) and 3D (linear-only) model. The stud was assumed to be a rectangular element. He used double nodes between concrete and stud to simulate the separation. The same nodes for the concrete and the metal decking were also used in the model. It was found using linear 3D FE model, load-slip curve comparison between experimental and finite element analysis was close in elastic range and deviate away in the inelastic range.

For the non-linear 2D, the load-slip curve obtained from the FE model seemed to deviate away from experimental curve. The FE model is shown in Figure (2.4).

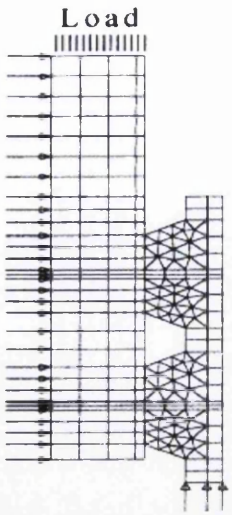

Figure 2.4: FE model of push-off proposed by Kim et. al.(2001)

Ellobody et al. (2006) proposed a different approach in FE modelling of the push-off test, to investigate the behaviour of the headed shear connection in a composite beam with a metal-ribbed-decking slab. He modelled using a 3D non-linear analysis. It was found, load-slip curve predicted by the non-linear 3D FE was close agreement with experimental load-slip curve. The FE model is shown in Figure (2.5).

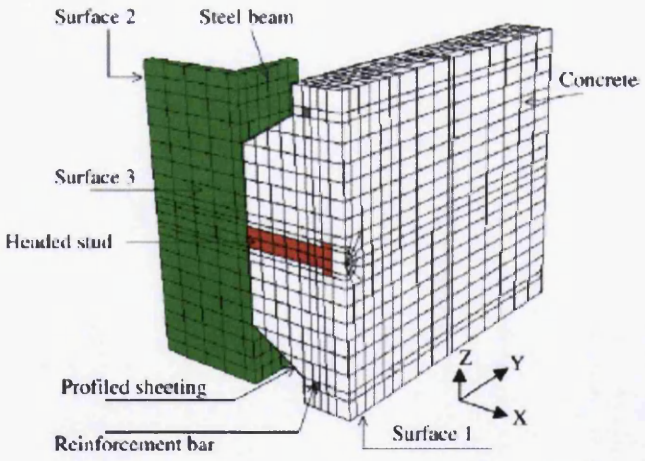

Figure 2.5: Finite element model of push-off proposed by Ellobody et. al. (2006)

Most researchers used spring element to simulate shear stud interaction in composite beam modelling. However, to use spring element, actual load-slip relation needs to be

obtained from the push-off test before the analysis. Furthermore, shear stud in composite beam may behave differently, depending on their position. In the other hand, the capacity of the shear connection, the load-slip behaviour of headed studs connection and failure modes were accurately predicted by 3D finite element model (Ellobody et al. (2006)). Due to this reason, in this thesis, used of 3D shear stud modelling technique by was proposed using the FEM for composite beams with metal-ribbed decking.

2.4 Composite beam with openings in metal-ribbed decking slab

The steel–concrete composite constructions of floor systems have been widely accepted and used in industrial and residential buildings, because of their numerous advantages. However, designers frequently find it necessary to introduce openings in commercial or residential buildings to facilitate access for services and inspection. In composite beams, openings are placed in the steel web, in the composite beam flange, or in both. The holes for, amongst other things, piping, electrical wiring and plumbing, have to be provided in a composite beam. Such openings have the potential to significantly affect the moment resistance of the whole composite system. Loss of strength due to openings can easily exceed 25% of the total moment resistance (Xiao 1998). It is possible to position additional reinforcement around the opening to ensure that the strength lost by the cut-out is recovered; however, introducing additional reinforcement is an expensive operation on account of the welding and handling costs involved. The need for reinforcement must, therefore, be established by a fairly precise assessment of the effects of the openings (Shanmugam 1997). For openings in a composite slab, no details are given and the metal decking suppliers themselves give only minimal recommendations, covering extra reinforcement or trimming steel, to satisfy a local slab check (Xiao 1998). BS 5950: Part 3 (1990) gives little guidance on the design for openings referring instead to BS 8110 (1997) for the design of the slab itself. To the writer's knowledge, only two reports on composite beams with openings in flange available.

Investigation into the effects of openings in the web has been carried out by many researchers (Fahmy 1996; Veríssimo 1998; Chung 2001; Park 2003; Lawson 2006;

Wang. 2008). However, only a few of them were concerned with the performance of composite beams containing openings in composite beam flange. To the writer's knowledge, the first study on composite beams with openings in the slab was carried out by Xiao et al. (1998) who modified the composite beam design equation (BS 5950) to be implemented in design software. The ultimate bending resistance is calculated by subtracting the width of the openings from the effective width of the flange, which is termed, the net effective width method. The details of their work are described in Chapter 1.

Nie et al. (2006) reported experimental and theoretical study on composite beams with openings in the solid slab. Based on the test results and analyses, they proposed design equation on the moment reduction of a composite beam with the opening in a solid slab. Unlike Xiao et al. (Xiao 1998), they used regression analysis to find the reduction coefficient. The value calculated by using this method improved the accuracy of the net effective width method and the result agreed well with the test results. Nie et al. also reported the fact that, when the opening ratio 20%–50%, the composite beams exhibited a typical flexural failure mode, namely, the crushing of the concrete slab in compression, or the yielding of the steel beam in tension.

2.5 Composite beam with 'full interaction' and 'partial interaction'

Composite beams with full interaction can exhibit full composite action and it is assumed that the slip between beam and slab is zero. Composite beams with partial shear interaction lack in strength to provide full composite action and are likely to fail at shear connection. Nowadays, partial shear connection is very common in composite beam design. This is because the full interaction is not always necessary when the strength of the composite section is greater than the required strength to satisfy applied service load. The composite beam interaction can be determined using plastic design. In plastic design, the shear connection is designed to resist the longitudinal shear force, transferred between concrete and steel. If each connector has the same resistance to shear and the number in each shear span is N, the degree of shear connection is defined as in Equation (2-7) (Chien 1984; Lawson 1990; Johnson 1994).

$$k_s = \frac{N}{N_f} \tag{2.7}$$

Where,

k_s = degree of shear connection

N_f = Number of connectors required for full shear connection

N = Number of connectors provided

The definition of degree of shear connection described above will be used through out this thesis.

2.6 Effective width of composite beam flange

A composite beam is composed of a series of T-beams that are interconnected so that the beam responds to different loads as a single unit. An effective flange width of a composite beam is the width of a slab deemed to be effective when calculating the composite sectional properties for strength and stiffness. A common approach in plastic design is to consider the effective width as a proportion of the beam span. EC4 and BS 5950: Part 3 defines the effective width as span/8 on each side but not exceeding the actual slab width considered to act with each beam. Connection deformability in composite beams plays an important role in evaluating an effective width for stress analysis of steel-concrete composite beams (Amadio 2002). Effective widths specified by EC4 (span/4) will be used in this thesis for all models.

2.7 European Code EC4 (1994) and British Standard BS5950 (1990)

Code provisions in BS5950 and EC4 are based on limit state design with loading factors and material safety factors. The ultimate moment is calculated from plastic stress distribution over the cross-section. Both design code considered the influence of deck shape on shear connection. The strength reduction factor relative to solid slab for decking placed transversely to beam adopted formula introduced by Grant et al.

(1977). However in EC4, the coefficient 0.85 is reduced to 0.70 based on results from more recent test on European profiles.

EC4 and BS5950 used similar equation to calculate deflection of simple composite beam at working load, where partial shear connection is used, as given below;

$$\frac{\delta}{\delta_c} = 1 + \varphi\left[1 - \frac{N}{N_f}\right]\left[\frac{\delta_a}{\delta_c} - 1\right] \tag{2.8}$$

Where factor φ is taken as 0.5 for propped beams and 0.3 for unpropped beam, δ_c and δ_a are deflections of composite beam and steel beam respectively.

2.8 Alternative method to calculate deflection

Nie. J. et. al (2003) proposed an alternative method to calculate deflection of composite beam. They have derived formula to account for slip effects and shows significantly improved the accuracy of deflection when compared with available test result. The effective stiffness parameter of cross-section of composite beam including slip is given as below;

$$EI_{eff} = \frac{EI}{1+\xi} \tag{2.9}$$

The function of rigidity reduction factor as follows,

$$\xi = \eta\left(\frac{1}{2} - \frac{1}{\alpha L}\right) \tag{2.10}$$

In equation (2.10), α and η are two functions of cross-section of the member and stiffness of its shear connection. These are defined by following equation,

$$\frac{1}{A_o} = \frac{n}{A_c} + \frac{1}{A_s} \tag{2.11}$$

$$\frac{1}{A'} = d_c^2 + \frac{I_o}{A_o} \tag{2.12}$$

$$I_o = \frac{I_c}{n} + I_s \tag{2.13}$$

$$\alpha^2 = \frac{K}{pE_s I_o A'} \tag{2.14}$$

$$\beta = \frac{A' pd_c}{K} \tag{2.15}$$

$$\eta = \frac{24EI\beta}{L^2 h} \tag{2.16}$$

In equation 2.14 and 2.15, shear connector stiffness not normally given in design codes. The stiffness of studs varies along the beam in terms of loading cases and boundary condition. Wang (1998) and Nie et. al (2003) has proposed the estimation value for shear connector stiffness as

$$K = 0.66 N_s P_{\max} \tag{2.17}$$

Where

N_s = number of shear studs per row

P_{max} = design shear resistance of stud

2.9 Conclusions

First part of this chapter has presented a description of composite beams with a metal-ribbed decking. The development in the field of composite-beam construction is reviewed with special focus on the composite beam with metal-ribbed decking. A few of the experimental studies regarding push-off test and full-scale beam test have been reviewed. Even though some of the studies are rather old, the findings from those study are important and still be referred by many researchers and also has been adopted in current design codes. Most of the researches which involved laboratory testing were carried out between 1950's and 1980's. Since laboratory testing is very costly, starting in early 90's, research has moved to the use of computer modelling to study the behaviour of composite beams. The technique used in computer modelling has been reviewed in this chapter. A special consideration is given to the modelling of connection between slab and beam.

The objective of author research is to study the effect of openings in metal-ribbed decking slab to composite beam. There are not many researches in this field. The papers involved design concept and also only a few experiments on composite beam with solid slab. Further research is, therefore, needed to investigate the effect of openings in metal-ribbed decking of composite beam. The present study deal with finite element investigation with the main objective is to examine the effect of opening's parameters on ultimate moment of composite beam.

2.9 References

Amadio, C., and, Fragiacomo, M., (2002). "Effective width evaluation for steel-concrete composite beams." Journal of Constructional Steel Research 58: 373-388.

BSI (1990). BS 5950 Structural use of steel work in building, Part 3, section 3.1: Code of practice for design of simple and continuous composite beams. London: British Standard Institute.

BSI (1997). BS8110 Structural use of concrete, Part 1: Code of practice for design and construction, London, BSI.

BSI (1994). Eurocode 4, Design of composite steel and concrete structures, Part 1.1: General rules and rules for buildings. London.

Chien, E. Y. L., and Ritchie, J.K., (1984). "Design and Construction of Composite Floor System", Canadian Institute of Steel Construction.

Chien, E. Y. L. and. Ritchie, J.K., (1993). "Composite floor system- a mature design option." Journal of Constructional Steel Research 25: 107-139.

Chung, K. F., and, Lawson, R.M, (2001). "Simplified design of composite beams with large web openings to Eurocode 4." Journal of Constructional Steel Research 57(2): 135-164.

Ellobody, E., Young, B., (2006). "Performance of shear connection in composite beams with profiled steel sheeting." Journal of Constructional Steel Research 62: 682-694.

Fahmy, E. H. (1996). "Analysis of composite beams with rectangular web openings." Journal of Constructional Steel Research 37(1): 47-62.

Fahmy, E. H., and Abu-Amra, T.H., (2008). "Longitudinal cracking of concrete slabs in composite beams with ribbed metal deck." Journal of Constructional Steel Research 64(6): 670-679.

Fisher, J., W., (1970). "Design of composite beams with formed metal deck." Engineering Journal of the American Institution of Steel Construction 7(3).

Grant, J., A., Fisher, J., W., and Slutter, R.,G., (1977). "Composite beams with formed steel decking." Engineering Journal of the American Institution of Steel Construction 14(First Quater).

Harding, P. W. (1990). Composite floors with Profiled Steel Sheeting. Civil and Structural Engineering. Cardiff, University of Wales, College of Cardiff. Ph.D.

Hayward, A., Weare., F. (2002). Steel Designers' Manual, Blackwell publishing.

Jayas., B. S., and, Hosain, M. U., (1988). "Behaviour of headed studs in composite beams: push-out tests." Can. J. Civ. Eng. 15: 240-253.

Jayas., B. S., and, Hosain., M., U., (1989). "Behaviour of headed studs in composite beams: full-size tests." Can. J. Civ. Eng. 16: 712-724.

Johnson, R. P. (1994). "Composite Structures of Steel and Concrete-Beams,Slabs,Columns, and Frames For Building". Oxford, Blackwell Scientific Publications.

Kim, B., Wright, H. D., Cairns. R. (2001). "The behaviour of through-deck welded shear connectors: an experimental and numerical study." Journal of Constructional Steel Research 57: 1359-1380.

Lawson, R. M. (1990). Commentary on BS 5950: Part 3: Section 3.1 "Composite Beams", The Steel Construction Institute.

Lawson, R. M., Lim, J., Hicks, S.J., and, Simms, W.I, (2006). "Design of composite asymmetric cellular beams and beams with large web openings." Journal of Constructional Steel Research 62(6): 614-629.

Nie, J. G., Cai, (2003). "Steel-concrete composite beams considering shear slip effects" Journal of Structural Engineering, ASCE 129(4): 495-506.

Nie, J. G., Cai, C.S., Wu., H., and Fan, J.S., (2006). "Experimental and theoretical study of steel-concrete composite beams with opening in concrete flange." Engineering Structures 28: 992-1000.

Nie, J. G., Fan, J., and,Cai, C.S. (2007). "Experimental study of partially shear-connected composite beams with profiled sheeting." Engineering Structures 30(1): 1-12.

Park, J. W., Kim, C.H., and, Yang, S.C., (2003). "Ultimate Strength of ribbed slab composite beams with web openings." Journal of Structural Engineering, ASCE 129(6): 810-817.

Robinson, H. (1967). "Composite beams incorporating cellular steel decking." Journal of the Structural Division, ASCE 93(ST4).

Robinson, H. (1988). "Multiple stud shear connection in deep ribbed metal deck." Can. J. Civ. Eng. 15: 553-569.

Robinson, H., and, Wallace, I.,W., (1973). "Composite beams with 1-1/2 inch metal deck and partial and full shear connection." The Engineering Journal 16(A-8).

Shanmugam, N. E. (1997). "Openings in thin-walled steel structures." Thin-walled Structures 28: 355-372.

Veríssimo, G. S., and Fakury, R.H, (1998). "Design of steel and composite beams with web openings." Journal of Constructional Steel Research 46(1-3): 207.

Wang., A. J., and, Chung, K.C, (2008). "Advance finite element modelling of perforated composite beams with flexible shear connector." Engineering Structures: 1-15.

Wang, Y. C. (1998). "Deflection of steel-concrete composite beams with partial shear interaction." Journal of Structural Engineering, ASCE 124(10): 1148-1158.

Wright, H. D. (1990). "The deformation of composite beams with discrete flexible connection." Journal of Constructional Steel Research 15: 49-64.

Wright, H. D. (1990). "A plate model for composite slab analysis." Thin-walled Structures 10: 299-328.

Xiao, R. Y., Dibb-Fuller, D., and, wood, G.A., (1998). "Opening in composite slabs - design implication." Journal of Constructional Steel Research 46(1-3): Paper no. 354.

Chapter 3

MATERIAL MODELLING AND FINITE ELEMENT INPUT PARAMETER

3.1 Introduction

In finite element analysis, it is important to understand the constitutive relationships for material properties and failure modes of the model. In this study, the material properties for universal beam, shear stud, metal-ribbed decking, steel reinforcement, and concrete elements have been considered. General purpose finite element software, namely, ANSYS Ver.10, has been employed to carry out the analyses.

The first part of this chapter will review the analytical methods available and, the selection of the finite element method as an analytical tool will be discussed.

The second part of this chapter will describe the constitutive model for non-linear analyses, which is adopted throughout this thesis and is either standard or has been used by the others. This section will explain in detail, the plasticity theory, used in

ANSYS. This will be followed by an examination of the constitutive model that was used for each material throughout this thesis. Finally, an explanation regarding the input data and ANSYS modelling will be provided.

The finite element analysis package, ANSYS (ANSYS Release 10) has several types of elements, suitable for numerical analysis. Amongst others, these elements are: two-dimensional elements (2-D), three-dimensional elements (3-D), 2-D and 3-D spar elements, beam elements, shell elements, and contact elements. The last section of this chapter will describe how different types of elements were selected.

3.2 Review of analytical methods

3.2.1 Classical partial interaction approach

Analysis of the influence of slip in composite beams (Newmark 1951; Johson 1975; Johson 1981; Yam 1981; Johnson 1991) has, in general, been based on an approach attributed to Newmark (1951). A second order differential equation, governing the behaviour of two elastic beam elements connected longitudinally by a linearly elastic connection, was derived and solved, in terms of either the resultant axial force or interface slip, and was substituted back into the basic equilibrium and compatibility equation. This equation was solved to give displacement and strains throughout the beam. These solutions were particularly relevant to traditional, concrete, steel composite construction.

This type of solution is suitable for simply-supported, single-span beams, subjected to loading. However, for composite beams with complicated boundary conditions, like in the case of the composite beam with openings (due to its discontinuities) proposed in this thesis, the use of this approach is not applicable.

3.2.2 Classical folded plate approach

This approach is suitable for structures that can be idealised as a system of simply-supported, single-span plate elements. Various shapes of plates and degrees of curvature can be incorporated into the method. The approach was first developed by Goldberg and Leve (1957), which employed the classical two-way elasticity theory for determination of membrane stresses and the two-way slab theory, for determination of bending and twisting of the slabs from prismatic isotropic folded-plate structures. Wright (1988) programmed Johnson's resulting equation for computer solutions and applied it to analyse single-span composite beams with metal-ribbed decking.

However, many practical structures lie outside the range of application of the elasticity method of folded-plate analysis. The presence of openings and complicated boundary conditions commonly found in practical situations cannot be analysed accurately by the elasticity method.

3.2.3 Numerical finite element method

In recent years, the finite element method has become widely accepted by the engineering profession as an extremely valuable method of analysis. Its application has enabled satisfactory solutions to many problems.

The finite element method represents the extension of matrix methods originally proposed for skeletal structures to the analysis of continuum. This method, the continuum is divided into a number of plate elements, interconnected at their corners only. This subdivision means that continuity requirements between adjacent elements are relaxed, except at their nodal points. However, the individual elements are constrained and deformed in specific patterns, due to the choice of a suitable function to represent the displacement of each element so that although continuity is only specified at the nodal points, the deflection of the edge of the elements is also controlled. Once the initial subdivision of the continuum has been carried out and the stiffness matrices of the individual elements have been established, the steps in the finite element method are identical to the conventional matrix method.

A considerable amount of research into the use of the finite element method has been conducted by researchers such as Zienkiewicz (1965), Cheung (1964) and Argyris (1965) – in the United Kingdom, and by Clough (1960, 1965), Melosh (1961) and many others in America. These studies have shown that accurate solutions for plane stress and plate bending problems can be obtained by this method. Furthermore, by combining the plane stress and plate flexure analyses, solutions for continuously-curved shell structures have also been established. Several researchers (Rockey 1967; Wegmuller and Amer H.N. 1975; Hamada 1977; Rockey 1983; Razaqpur 1989; Tan 1989; Jiang 1997) have exploited finite element analysis in order to analyse composite construction, sandwich panels, folded-plate structures, stiffened plates or clad structures.

In this research, the non-linear, finite element method has been used for modelling the composite beam with metal-ribbed decking. Commercial, general-purpose, finite element software, namely, ANSYS Ver.10, has been used for all analyses in this thesis. The ANSYS pre-processing option supports on-screen modelling and offers excellent options, which model typical sections of the structures. Its post-processing option includes colour plots of stress and strain contours and the deformed shape of the model defined by three-dimensional displacement vectors.

3.3 Constitutive models

3.3.1 Introduction

Constitutive model adopted throughout the thesis are either standard or that used by the others. The following section gives details of about theory of plasticity and the theory of constitutive model. This section also gives the details for each of the material models used in the finite element model.

3.3.2 Steel beam and column

The von Mises yield criterion with multilinear isotropic hardening (MISO) is used to represent steel behaviour. The stress-strain relation used by Gattesco (Gattesco 1999) has been adopted for all models through out this thesis. Nonlinear equation in strain hardening branch up to ultimate stress is given in this model. The use of nonlinear curve will increase the degree of accuracy compared with linear curve.

The relation is linearly elastic up to yielding as shown in Equation (3-33)

$$\sigma_s = E_s \varepsilon_s \tag{3-33}$$

and perfectly plactic between the elastic limit and beginning of strain hardening as shown in Equation (3-34)

$$\sigma_s = f_{sy} \tag{3-34}$$

After the perfectly plastic part, the curve will start to behave as strain hardening and follows the Equation (3-35)

$$\sigma_y = f_{sy} + \left(f_{su} - f_{sy}\right)\left(1 - e^{\left(\frac{(\varepsilon_{sh} - \varepsilon_s)}{k}\right)}\right) \tag{3.35}$$

where f_{sy} and f_{su} are the yielding and ultimate tensile stress of steel component respectively ; E_{sh} and ε_{sh} are the strain hardening modulus and strain hardening of the steel component, respectively. Strain at ultimate strength (ε_{su}) is depending on steel ductility. Lower steel strength will give higher steel ductility. Total strain at fracture and the ratio of ultimate strength to yield strength should be at least 18 per cent and 1.2, respectively (Hayward A. 2005). Factor k is defined as in Equation (3-36).

$$k = k_x \frac{(\varepsilon_{sh} - \varepsilon_{su})}{(\varepsilon_{sh} - 0.16)} \tag{3-36}$$

Value of k_x is taken as 0.028 (Gattesco 1999). The complete stress strain curve is shown as in Figure 3.1.

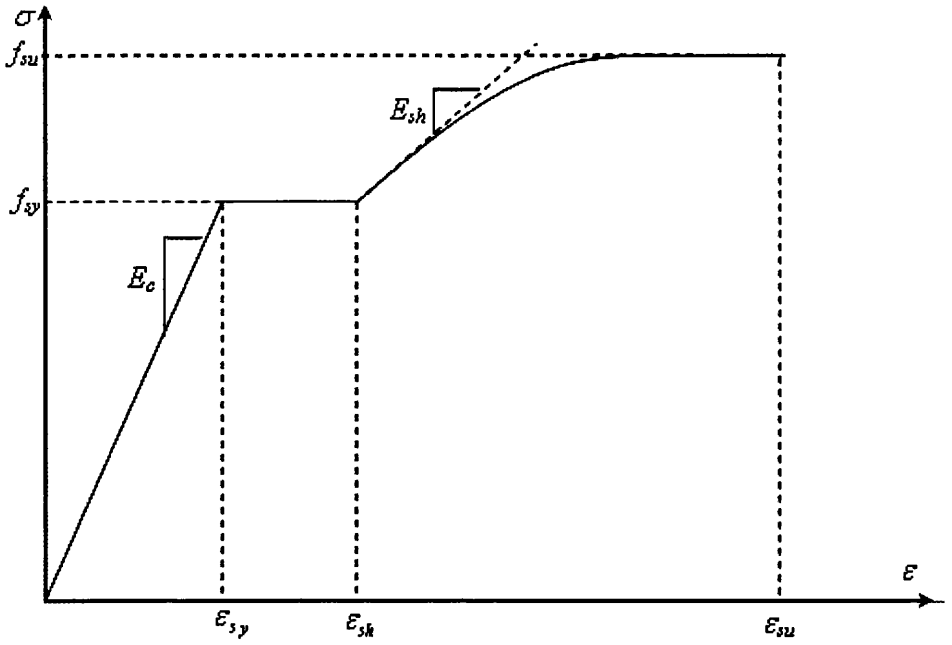

Figure 3.1: Stress-strain curve for steel beam

3.3.3 Concrete

The concrete slab behaviour is modelled by multilinear isotropic hardening relationship (MISO), using von Mises yield criterion coupled with an isotropic work hardening assumption; similar assumption has been made by Queiroz et.al (2006). To model the nonlinear behaviour of concrete slab, the equivalent uniaxial presentation for stress-strain curve of concrete is show in Figure. 3.2.

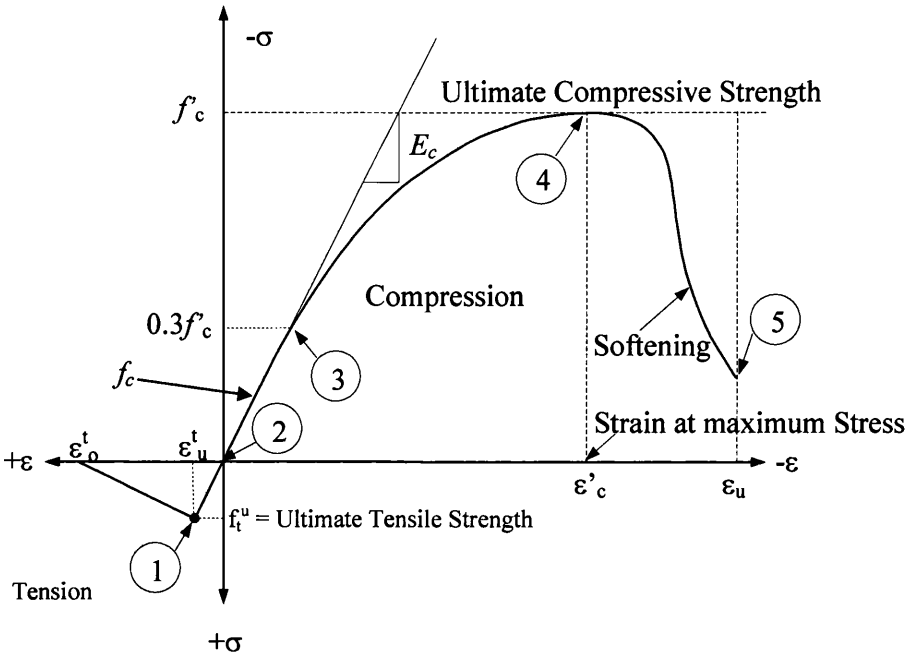

Figure 3.2: Concrete stress-strain curve for concrete

The first part of stress-strain curve is assumed elastic. The value of the proportional limit stress is taken as $0.3(f'_c)$, the same value taken by Queiroz et. al.(2006) and Shanmugam et.al (2002). The compressive stress, f'_c, is equal to 0.78 (f_{cu}), where f_{cu} is the compressive cube strength of concrete. The stress-strain curve is assumed parabolic from Point 3 to f'_c, *at* Point 4. This part of curve can be determined from Equations (3-37) and Equation (3-38) (Carreira 1985):

$$f_c = \frac{f'_c \zeta \left[\frac{\varepsilon}{\varepsilon'_c}\right]}{\zeta - 1 + \left[\frac{\varepsilon}{\varepsilon'_c}\right]^{\zeta}} \tag{3-37}$$

$$\zeta = \left[\frac{f'_c}{32.4}\right]^3 + 1.55 \tag{3-38}$$

$$\varepsilon'_c = 2.4 \times 10^{-4} \sqrt{\frac{f_{cu}}{\gamma_m}} \tag{3-39}$$

Where f'_c is the cylinder strength of concrete in MPa and ε is the strain in concrete. The strain (ε'_c) at which the maximum compressive stress occurs, is taken as in Equation (3-39) (BSI 1997). Starting from the maximum stress at Point 4, the curve starts descending, which is the softening branch up to the ultimate strain of concrete at failure, ε_{cu}, at Point 5, taken as 0.0035 (BSI 1997). Equation (3-37) is able to simulate the ascending and descending branch of the stress-strain curve of concrete.

The poisson's ratio of concrete is taken as 0.2 (Ellobody, 2006). The young's modulus is reasonably calculated by the empirical Equation (3-40) (ACI, 2000).

$$E_c = 4730\sqrt{f'_c} \tag{3-40}$$

In tension, the stress-strain curve for concrete is assumed linearly elastic up to ultimate tensile strength, at Point 1, as shown in Equation (3-41). Concrete cracks beyond this point and the strength decrease to zero (ANSYS Release 10) where,

$$f_t^u = 0.55\sqrt{f_c'} \quad \text{(MPa)} \tag{3-41}$$

$$\varepsilon'_u = \frac{f_t^u}{E_C} \tag{3-42}$$

$$\varepsilon_o^t = 6\varepsilon_u^t \tag{3-43}$$

The material model in ANSYS could predict failure of brittle materials. In ANSYS, the 'TB, CONCR' accesses this material model is available with the reinforced concrete element SOLID65. For failure surface criteria, two constants: ultimate tensile strength (f_t^u) and ultimate compressive strength (f'_c), need to be input under the 'TB, CONCR' command. The other three constants, ambient hydrostatic stress state (σ^a_h), ultimate compressive strength for a state of biaxial compression superimposed on hydrostatic stress state (f_1) and ultimate compressive strength for a state of uniaxial compression superimposed on hydrostatic stress state (f_2), default to William et al. (1975).

One more constant to be input under the 'TB, CONCR' command is the concrete element shear-transfer coefficient (β_t). This is required to represents a shear strength reduction factor for subsequent loads that induce sliding (shear) across the crack face. The values range from 0 to 1, where 0 represents a smooth crack, meaning a complete loss of shear transfer, and 1 represents a rough crack meaning no loss of shear transfer. The amount of shear transfer across a crack can be varied between full-shear transfer and no-shear transfer at a crack section (Shah 1995).The concrete element shear-transfer coefficients assumed in this thesis are 0.2 for open crack and 0.3 for closed crack.

The last constant is the stiffness multiplier for the cracked condition. This constant is used as the stress relaxation coefficient, the device that helps accelerate convergence when cracking is imminent. The default value of 0.6 was used in this analysis.

3.3.4 Steel decking, shear stud and steel reinforcement

The shear stud, metal-ribbed decking and steel reinforcement were simulated using a bi-linear stress strain curve with the BISO option in ANSYS. Bilinear stress-strain curve is capable of representing elastic-perfectly plastic material behaviour, with equal yield stresses, f_{sy}, in tension and compression as well as with the hardening option (Figure 3.3). The materials behave as linear elastic material, and becomes fully plastic or with strain hardening beyond this stage.

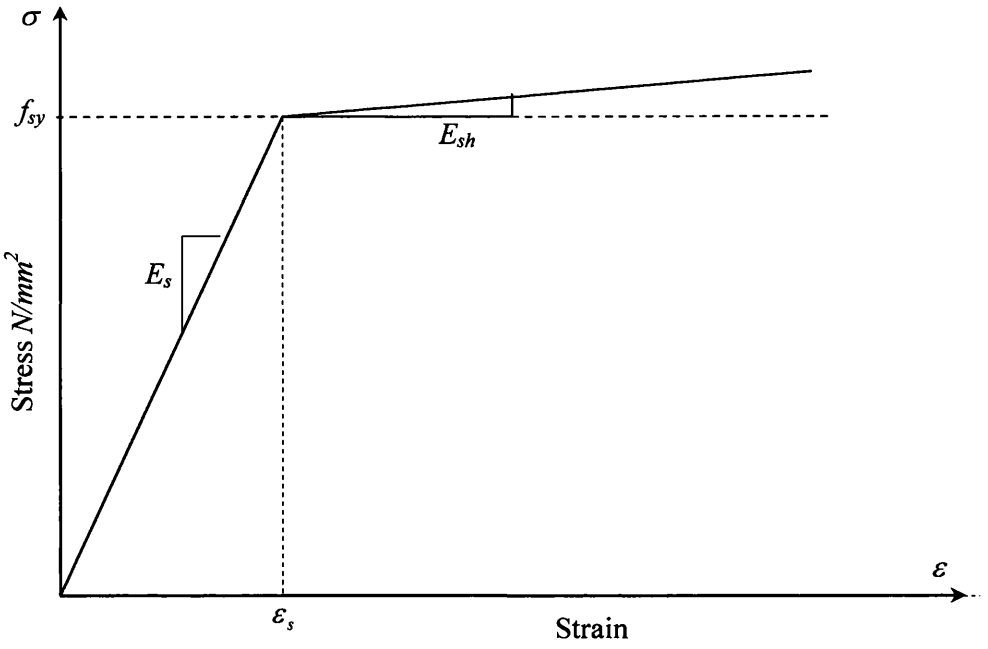

Figure 3.3: Stress-strain curve for steel decking, shear stud and reinforcing bar

3.3.5 Convergence criteria

Like any other type of non-linear analysis the ANSYS programme performs a series of linear approximations with corrections. A convergence failure can indicate a physical instability in the structure or it can merely be the result of some numerical problem in the finite element model. Convergence criteria indicate to what extent an equilibrium state has been achieved. The programme will continue to do equilibrium iterations until the convergence criteria (CNVTOL) are satisfied. Several choices of convergence for successive iterations are offered in the ANSYS programme. The convergence of a solution can be controlled by tolerances based on forces, moments, displacements, or rotations, or on any combinations of these items. By default, the programme will check for force (and, when rotational degrees of freedom are active, moment) convergence by comparing the square root sum of the squares (SRSS) of the force imbalances against the product of SRSS of applied forces (or, for applied displacements, of the Newton-Raphson restoring forces) with tolerance. The value of tolerance used is between 0.005 and 0.001. Tighter convergence criteria will improve

the accuracy of the results, but at the cost of more iteration and this is done by changing the tolerance value.

The force-based convergence serves as an absolute measurement of convergence, while displacement-based convergence provides only a relative measurement of apparent convergence. Additionally, for the modelling of a system including concrete elements, after crushing occurs at an integration point, the strain of concrete at that point increases intensely. This may invalidate displacement–based convergence checking. So, force convergence should always be employed and used as convergence checking. Consequently, the force-based convergence checking is adopted as the convergence criteria. The values of the criteria were determined for each particular model.

The ANSYS programme provides three different vector norms to use for convergence checking:

- The *infinite norm* repeats the single-DOF check at each DOF in the model.
- The *L1 norm* compares the convergence criterion against the sum of the absolute values of force (and moment) imbalance for all DOFs.
- The *L2 norm* performs the convergence check using the square root sum of the squares of the force (and moment) imbalances for all DOFs. (Additional L1 or L2 checking can be performed for a displacement convergence check.)

In all analysis in this thesis, L2-Norm of the force is considered. ANSYS also offer a few types of equation solvers which will help to overcome the convergence problem. However sparse direct solver has been used since it can minimize the memory used in solution process and capable to overcome convergence problem for the modeling used in this thesis.

3.4 Element-type selection

3.4.1 Steel decking and steel beam.

Shell 143 has been chosen to model steel decking and steel beams. This type of element is well suited to model non-linear, flat or warped, thin-to-moderately-thick shell structures. The element is defined by four nodes. However triangular-shaped element also can be formed by defining the same nodes number, for example nodes K and L as shown in Figure 3.4. The geometry of the element is shown in Figure 3.4. The element has six degrees of freedom at each node: translation in x, y, and z directions; and rotations about the nodal x, y, and z axes. The deformation shapes are linear in both in-plane directions. For the out-of-plane, it uses a mixed interpolation of tensorial components.The element has plasticity, creep, stress stiffening, large deflection, and small strain capabilities. The flanges and web of beams and decking were modelled with this type of element.

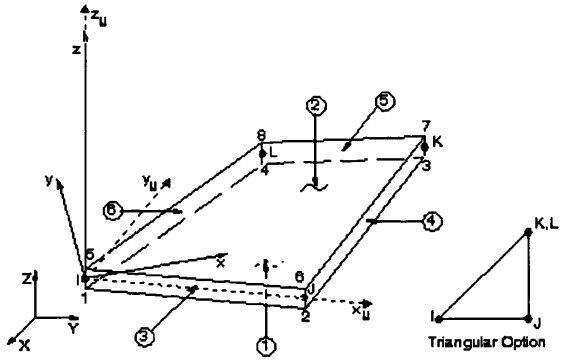

Figure 3.4: Shell 143 elements geometry; Alphabets I-L and the circled integers represent the nodes and element surfaces respectively (ANSYS Release 10)

3.4.2 Shear stud

SOLID45 was used for the 3D modelling of shear stud. The element is defined by eight nodes having three degrees of freedom at each node: translations in the nodal x, y, and z directions. The element is capable of orthotropic material properties by defining different properties in x-, y- and z-axis direction. The element has plasticity, creep, swelling, stress stiffening, large deflection, and large strain capabilities. The geometry of the element is shown in Figure 3.5.

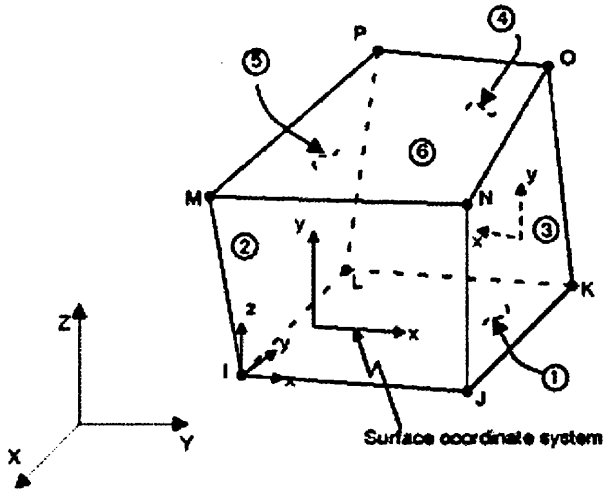

Figure 3.5: Solid 45 element geometry; Alphabets I-P and the circled integers represent the nodes and element surfaces respectively (ANSYS Release 10)

3.4.3 Concrete slab

Concrete is assumed to be isotropic material prior to cracking and is difficult to simulate (Kachlakev 2001). 3D solid element, namely SOLID65 was chosen to simulate the concrete slab since only this element was available in ANSYS to support the concrete model. The element has eight nodes with three degrees of freedom (translations) at each node. The element is capable of cracking, crushing, plastic deformation and creep. The geometry of the element is shown in Figure 3.6.

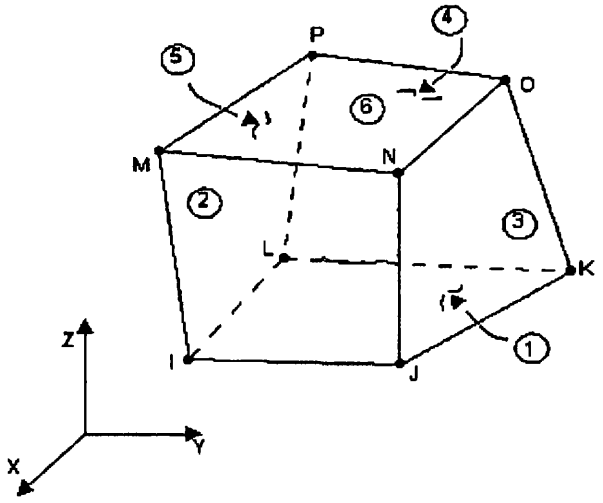

Figure 3.6: Solid65 element geometry; Alphabets I-P and the circled integers represent the nodes and element surfaces respectively (ANSYS Release 10)

3.4.4 Interaction element

- TARGE170

The contact and target surfaces constitute a 'Contact Pair'. TARGE170 is used to represent various 3D target surfaces for the associated contact elements (CONTA173). The contact elements themselves overlay the solid elements describing the boundary of a deformable body that is potentially in contact with the rigid target surface, defined by TARGE170. Hence, a 'target' is simply a geometric entity in space that senses and responds when one or more contact elements move into a target segment element. Each target segment is a single element with a specific shape or segment type. The reaction forces on the entire rigid target surface are obtained by summing all the nodal forces of the associated contact elements.

- CONTA173

CONTA173 is defined as a 3D 4-node surface-to-surface contact element that is used to represent contact and sliding between 3D 'target' surfaces (TARGE170) and a deformable surface. This element is located on the surfaces of 3D solid or shell elements without mid-side nodes. It has the same geometric characteristics as the solid or shell element face. Contact occurs when the element surface penetrates one of the target segment elements (TARGE170) on a specified target surface. Coulomb and shear stress friction is allowed. The element is defined by four nodes (the underlying solid or shell element has no mid-side nodes).

3.4.5 Reinforcement bar

LINK8 is 3D bar element and is an uniaxial tension-compression element with three degrees of freedom at each node: translations in the nodal x, y, and z directions. The element is defined by two nodes, cross-sectional area, initial strain, and material properties. The initial strain in the element is given by Δ/L, where Δ is the difference between the element length, L, (as defined by I and J node locations) and zero strain length. The geometry of the elements is shown in Figure 3.7.

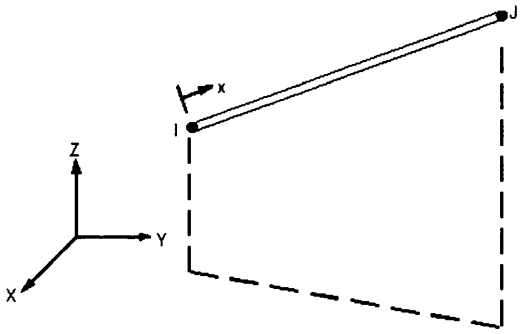

Figure 3.7: LINK8 spar element geometry (ANSYS Release 10)

3.5 Summary

This chapter presented the concept of selected numerical analysis, finite element and material constitutive model used in the analysis. General-purpose finite element software ANSYS version 10, was selected for the modelling and the analysis. Details of selected element types used in the modelling were also explained.

3.6 References

ACI Committee. (2000). Cement and Concrete Terminology (ACI 116R-00), Farmington Hills, American Concrete Institute.

ANSYS (Release 10). ANSYS Documentations, Manual Set and Theory Reference Manual, ANSYS Inc.

Argyris, J. H. (1965). Continua and Discontinua, Matrix methods in Structural Mecahnics, Ohio.

BSI (1997). BS8110 Structural use of concrete, Part 1: Code of practice for design and construction, London, BSI.

Carreira, D. J., and Chu, K.H (1985). "Stress-Strain relationship for plain concrete in compression." ACI Journal Proceeding 82(11): 797-804.

Cheung, Y. K. (1964). Finite Element Methods, University of Wales, Swansea. Ph.D.

Clough, R. W. (1960). The Finite Element Method in Plane Stress Analysis. Conference of Electronic Computation, Pittsburgh, A.S.C.E.

Clough, R. W. (1965). The Finite Element in Structural Mechanics in "Stress Analysis", John Willy and Co.

Ellobody, E., Young, B., (2006). "Performance of shear connection in composite beams with profiled steel sheeting." Journal of Constructional Steel Research 62: 682-694.

Gattesco, N. (1999). "Analytical Modelling of Nonlinear Behaviour of Composite Beams with Deformable Connection." Journal of Constructional Steel Research 52: 195-218.

Goldberg, J. E. a. L., H.L (1957). "Theory of Prismatic Folded Plate Structures." Publ. Int. Assn. Bridge & Structural Engg 17: 59-86.

Hamada, S., and Arizumi, Y., (1977). "Finite Element Analysis of Continuous Composite Beams with Incomplete Interaction." Journal of Constructional Steel Research 9: 64-67.

Hayward, A. and Weare, F. (2002), Steel Detailers' Manual, 2 Ed, Blackwell Science, Oxford, U.K.

Jiang, W., Bao. G., Roberts, J.C., (1997). "Finite Element Modelling of Stiffened and Unstiffened Orthotropic Plates." Computers &Structures 63(1).

Johnson, R. P., Molestra, N. (1991). "Partial Shear Connection in Composite Beams for Buildings." Proc. Instn. of Civ. Engineer, London, England 2: 679-704.

Johson, R. P. (1975). Composite Structure of Steel and Concrete - Beams, Slabs, Column, Frames and Application in Buildings, Granada Publishing.

Johson, R. P. (1981). "Loss of Interaction in Short Span Composite Beams and Plates." Journal of Constructional Steel Research 1(2): 11-16.

Kachlakev, D. I., Miller, T., Yim, S., Chansawat, K., and Potisuk, T. (2001). Finite Element Modeling of Reinforced Concrete Structures Strengthened With FRP Laminates. Report for Oregon Department of Transportation, Research Group, 200 Hawthorne SE, Suite B-240 Salem, OR 97301-5192, And Federal Highway Administration, 400 Seventh Street SW, Washington, DC 20590, Civil, Construction and Environmental Engineering Department, Oregon State University.

Melosh, R. J. (1961). "A Stiffness Matrix for the Analysis of Thin Plates in Bending." Journal of the aero-Space Science 28(January): 34-42.

Newmark, N. M., Siess, C. P., Vest I. M. (1951). "Test and Analysis of composite Beams with Incomplete Interaction." Proc. Society for Experimental Stress Analysis. 9(1).

Queiroz, F. D., Vellasco, P.C.G.S., and Nethercot, D.A. (2006). "Finite Element Modelling of Composite Beams with Full and Partial Shear Connection." Journal of Constructional Steel Research.

Razaqpur, A. G., Nofal, M. (1989). "Finite Element for Modelling the Nonlinear Behaviour of Shear Connectors in Composite Structures." Computers &Structures 32(1): 169-174.

Rockey, K. C., and Evans, H.R. (1967). A Finite Element Solution for Folded Plate Structures. Conference of Space-Structures, Oxford, Blacwell.

Rockey, K. C., Evans, H.R.,Griffiths, D.W., and Nethercot, D.A., (1983). The Finite Element Method. A Basic Introduction for Engineers, Collins Professional and technical Books.

Shah, S. P., Swartz S. E., and Ouyang C (1995). Fracture Mechanics of Concrete. New York, Wiley & Sons, Inc.

Shanmugam, N. E., Kumar, G., Thevendran, V., (2002). "Finite Element Modelling of Double Skin Composite Slabs." Finite Elements in Analysis and Design 38: 579-599.

Tan, K. H., Montague,P. and Norris, C. (1989). "Steel Sandwich Panels: Finite Element, Closed Solution and Experimental Comparison on a 6m by 2.1m Panel." The Structural Engineers 67: 159-166.

Wegmuller and Amer H.N. (1975). "Nonlinear Response of Composite Steel-Concrete Bridge." Computers &Structures 7: 161-169.

Willam, K. J., and Warnke, E. D (1975). Constitutive Model for the Triaxial Behaviour of concrete. International Association for bridge and structure, Bergamo, Italy.

Wright, H. D. (1988). Design Floor Decks Utilising Profiled Steel Sheeting & Through Deck Welded Stud, University College Cardiff, University of Wales, U.K. Ph.D.

Yam, C. P. (1981). Design of Composite Steel Concrete Structures. London, Surrey University Press.

Zienkiewicz, O. C. (1965). Finite Element Procedure in the Solution of Plates & shell Problems in Stress Analysis, John Willey and Co.

Chapter 4

NUMERICAL SIMULATION AND VALIDATION

4.1 Introduction

The primary objective of this chapter is to develop non-linear finite element model of composite beam formed with metal-ribbed decking and through deck welded shear stud. General-purpose finite element software, namely, ANSYS Ver.10 was used to conduct the analyses. This chapter highlighted the numerical simulations of experiments conducted by other researchers and this will pave the way for the parametric simulations in this and next chapters. To serve as a guideline for the development of a finite element model (FEM), the first part of this chapter reviews the current research and knowledge-base for the FE modelling of composite beams.

This is followed by a verification study. The modelling of headed shear stud is important in simulating the shear interaction between steel beam and composite slab. The technique used in modelling the headed shear stud in composite beam will be introduced. Then the proposed model is analysed to compare the results with the corresponding test results.

Finally, in order to find out the factors that have the most influence on the behaviour of composite beams with metal-ribbed decking using a proposed technique. A parametric investigation took place, using the FEM to study the effects of concrete compressive strength, beam interaction, type of decking, steel decking thickness and steel decking yield stress on composite beams.

4.2 Review on finite element modelling of composite beams with partial interaction

The analysis of composite beam with partial shear interaction is very complex. Most of the relevant, advanced models of partial interaction analysis of composite slabs and beams, which account for geometric and numerical non-linearities, are based on non-linear, numerical methods of finite elements (Fabbrocino 1999; Gattesco 1999; Queiroz 2006; Fahmy 2008), finite difference (Roberts 1985) or finite strip (Plank 1974; Uy 1994) methods.

Most of the researchers who have investigated the behaviour of composite beams using three-dimensional FEMs (Sun 2005; Queiroz 2006; Fahmy 2008) use a non-linear spring element to simulate the shear stud and the interaction between the slab and steel beam. However, to use spring element, actual load-slip relation needs to be obtained from the push-off test before the analysis. Furthermore, shear stud in composite beam may behave differently, depending on their position. Due to this reasons, in this chapter, 3D FE modelling of headed shear stud is proposed to be implemented in composite beam modelling and will be explained in detail in the next section.

4.3 Verification Study of Composite beam

4.3.1 General

For a successful numerical model of composite beam, all different components associated with the composite beams must be properly presented. The components of

a composite beam with metal-ribbed decking are: composite slab with metal-ribbed decking, shear stud and steel beam.

In this section, the numerical model combining all composite beam components (metal-ribbed decking slab, steel beam and headed shear stud) will be established. Furthermore, the implementation of shear stud modelling in the composite beams will be presented with partial interaction accounted. This interaction can vary for parametric study purpose.

The FEM developed will be used to investigate the behaviour of composite beams with partial interaction. Ultimate moment and moment-deflection curve obtained from the analyses will be used to investigate the effects of openings in the flange of composite beams. The study will be presented in the next chapter.

4.3.2 Review on full-scale test of composite beams with metal-ribbed decking

Full-scale test on composite beams carried out by Nie et al. (2005) were selected to validate the FEM. These composite beams have been analysed by the proposed finite element. The composite beams had transverse orientation of deck ribs on them. All composite beams tested were of single span and simply-supported. The arrangement for the tests is shown in Appendix A.

Five, full-scale composite beams (SB1 to SB5) were tested by Nie et al. (2005), who used metal-ribbed decking of 1.0 mm thick. Two types of decking narrow-ribbed and wide-ribbed have been used. The arrangements for the tests are shown in Appendix E. Composite beams of 3.9 m span with 0.8 m wide and 105 mm deep slab, were used. Concrete in the composite slabs had different cube strengths. The steel beam was I-section (I20a) with: total depth = 200 mm, flange = 100 mm wide and 11.4 mm thick, and web = 177.2 deep mm and 7 mm thick. The shear studs were 19 mm in diameter and 90 mm in height, spaced at 390 mm, welded on the top flange of the steel beams through the profiled steel sheeting. The parameters of the specimens is summarised in Table 4.1.

Table 4.1: Details of composite beams parameter

Beam Model	Span (m)	Slab width (m)	Stud per rib	Metal decking classification	Degree of shear interaction k_s (%)
SB1	4.0	0.8	1	Wide-ribbed	47
SB2	4.0	0.8	2	Wide-ribbed	67
SB3	4.0	0.8	2	Wide-ribbed	67
SB4	4.0	0.8	1	Narrow-ribbed	32
SB5	4.0	0.8	2	Narrow-ribbed	44

4.3.3 Modelling of composite beams with partial interaction

The experimental study was undertaken by Nie et al. (2005) have been analysed by the proposed finite element method. In this part, solid element to model headed shear stud in composite beam was proposed. The solid element was used to connect the top flange of steel beam and meta-ribbed decking slab to represent the shear stud. The composite beam was modelled with a small gap between the top flange of steel beam and metal-ribbed decking in order to simulate contact area.

It was observed by Jayas et al. (1988), Johnson et al. (1981) and Kim et al. (2001) that separation of concrete behind the shear connector occurred even at low load levels. Based on this observation, in FE model, the nodes behind the shear stud from surrounding concrete (in the direction of the load) has been detached. The same approach was used by Ellobody et al. (2006), Lam et al. (2005), Kim et al. (2001) and Kalfas et al. (1997). Figure 4.1 shows the detached nodes in proposed FE model. The nodes are detached from the surrounding concrete nodes with the other nodes of shear stud and the location is shown in Figure 4.1 (marked with a red line). Same nodes for the top surface of shear stud and concrete were used since it is assumed that the headed shear stud has sufficient resistance to uplift. This is shown in Figure 4.1 (mark with green line). In simulation, direction of loading is similar to direction of concrete slip as show in Figure 4.1.

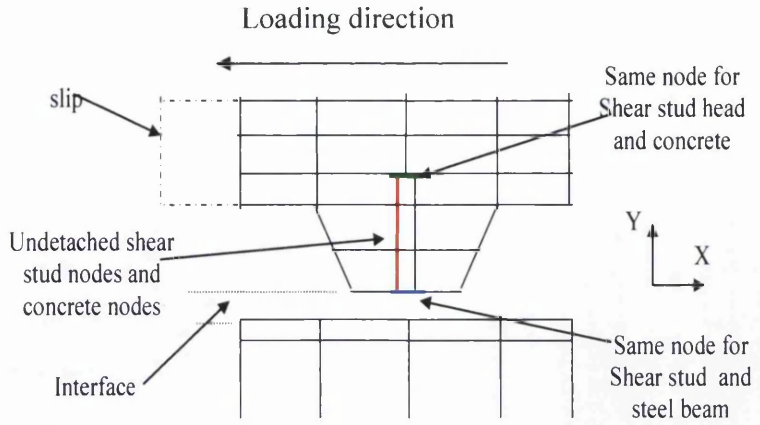

Figure 4.1: Shear stud modelling in composite beam

The combination of components in composite beam is shown in Figure 4.2. The first horizontal crack occurred in the concrete through, was located near the support of the composite beams, when the load reached 0.6 to 0.7 of ultimate load (Nie. J. 2008). Therefore, it is assumed that separation of profiled steel sheeting from the concrete slab at a certain load level has little effect on the concrete slab. A similar assumption was also made by other researchers (Kim 2001; Ellobody 2006; Queiroz 2006; Fahmy 2008). Hence, the same nodes were used for metal ribbed-decking and for the concrete. The same value of yield stress for steel beams, concrete and shear studs, which were defined in the experiment, was also used in the modelling of composite beams.

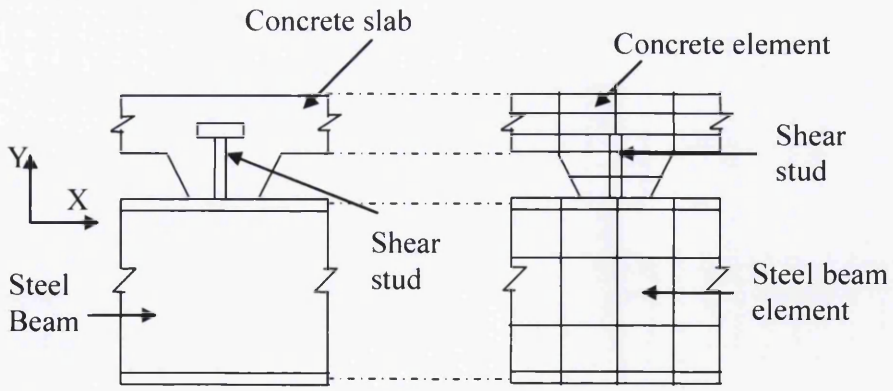

Figure 4.2: Finite element idealisation

Interaction between metal-ribbed decking and steel beams is not fully bonding. Due to this reason, surface to surface contact element was used as an interface element between the steel decking and the steel beam to prevent any penetration of steel decking with the steel beam. Modelling based on interaction between two materials has been used in conjunction with surface interaction technique available in ANSYS. Direct nodal connection between steel element and steel decking elements was avoided in this technique and, slip between the two surfaces with a predefined allowable tensile and frictional stresses was allowed. The location of the interface element is shown in Figure 4.1. A 3D contact pair element, namely CONTA173 and TARGE170 were used as a contact element. A brief description about the elements was outlined in the Chapter 3.

All contact problems require stiffness between the two contact surfaces. The amount of penetration between two surfaces can be controlled by this stiffness. There were twenty-six real constants available for the elements. However, only FKN (normal penalty stiffness factor), FTLON (penetration tolerance factor) and FKT (tangent penalty stiffness) needed to be defined, since the aim was to prevent penetration. The stiffness factor needed to be defined; had a range between 0.001 and 1.0. A smaller value provides for easier convergence but more penetration. The FKN and FTLON factors were adjusted to control the penetration. The pilot model was run to select the appropriate factor, which gave better results in preventing penetration. Factors of 1.0 for the FKN and 0.01 for FTLON were selected. For FKT, the factor of 0.1 was used as this model permitted sliding. The same factor values were used for all composite beam models.

4.3.4 Boundary conditions

Symmetry of the composite beams is taken into account by modelling only one half of the beam span. All nodes of the concrete, profiled steel sheeting and steel beam which lie on the surface of symmetry at the mid span position are restrained from moving in the x-axis direction. All nodes for the steel beam which lie along the line of the symmetry also are restrained from rotation (y and z axis) because of symmetry. A typical finite element model and the boundary conditions are shown in Figure 4.3.

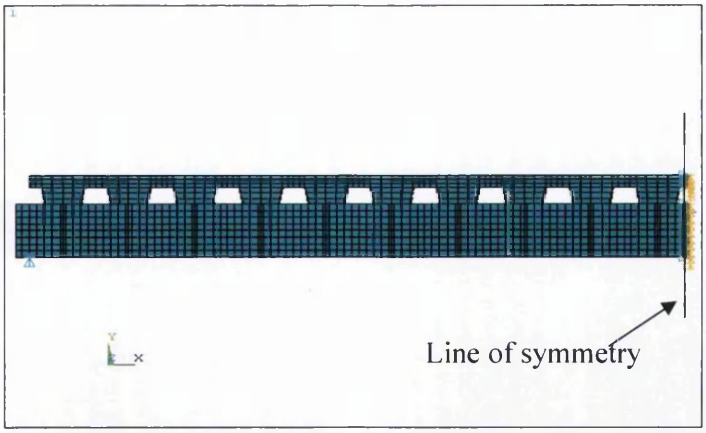

Elevation

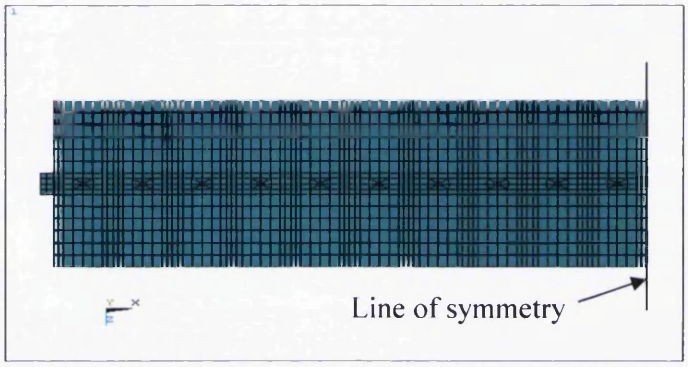

Plan

Figure 4.3: Composite beam with metal-ribbed decking FE model

4.3.5 Application of load

Concentrated loads are incrementally applied to the model by means of an equivalent displacement to overcome convergence problems and the similar technique has been used by Queiroz (2006). For load other than concentrated load, the associated error is controlled by comparison between applied forces and reaction forces.

4.3.6 Convergence study

Convergence studies were carried out. Three different types of mesh were used to asses the sensitivity of the results to mesh refinement for the composite beams model, as shown in Figure 4.4. The finer mesh, model S1, consisted of three layers of solid

elements for concrete above top of ribs of metal-ribbed decking, whilst for the concrete rib, four layers of solid elements were used. The medium mesh, model S2, consisted of three layers of solid elements for the concrete above top of ribs of metal-ribbed decking, whilst three layers of solid elements were used in the concrete rib. The final model (S3) considered as coarse mesh had two layers of solid elements for concrete above top of ribs of metal-ribbed decking and two layers of solid elements in the concrete rib. The three meshes are shown in Figure 4.4.

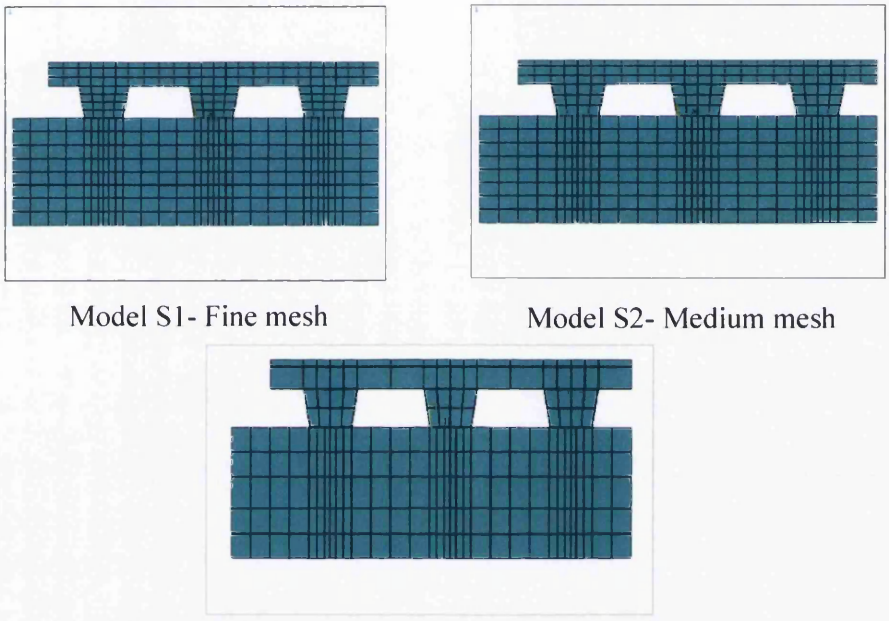

Model S1- Fine mesh

Model S2- Medium mesh

Model S3- Coarse mesh

Figure 4.4: The Finite element mesh for convergence study

The load-deflection curves corresponding to each of the meshes were plotted and compared as shown in Figure 4.5. Use of the coarse mesh (S3) predicted a higher load than the medium and fine mesh; the load limit for the medium and fine meshes was quite close. However, the fine mesh (S1) was more complex and involved longer time to converge compared to the medium mesh. Fine and medium mesh (S2) was used for the analysis depending on the geometry of the composite beams; however, the medium mesh was used in most cases.

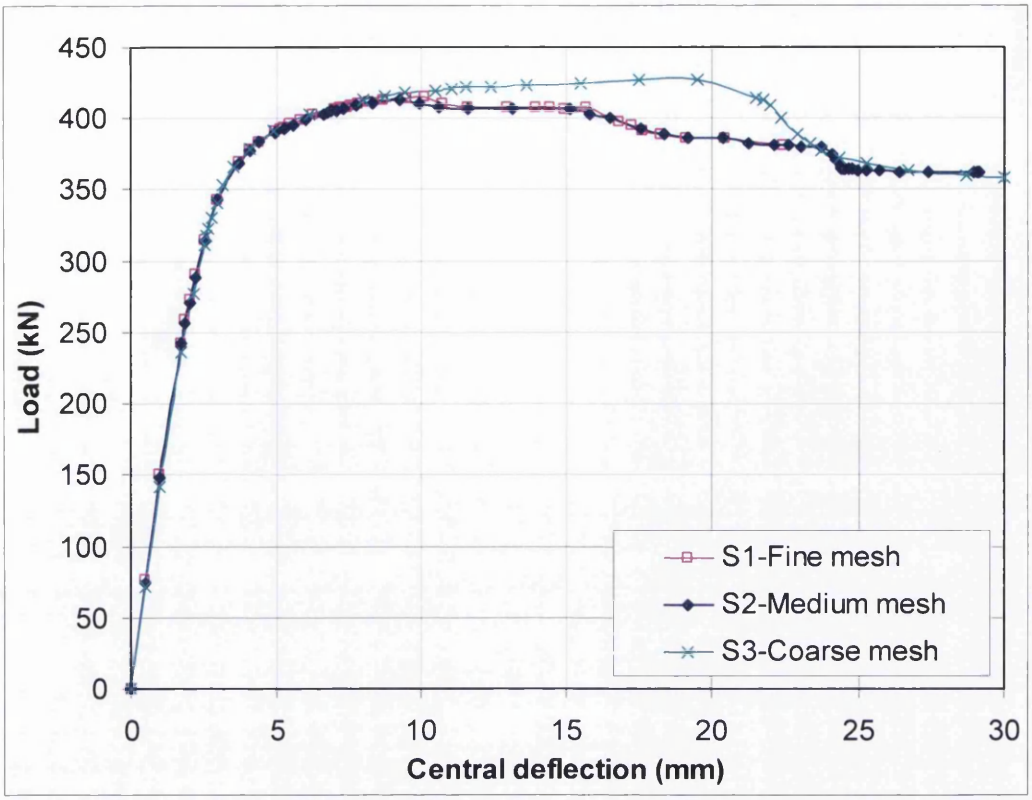

Figure 4.5: Load-deflection curve of composite beams models for convergence study

4.3.7 Verification of finite element models

To verify the accuracy of the proposed modelling approach, five of the full-scale experimental beams reported in the literature were analyzed and the analytical result compared with the experimental results for each case. The parameters used in the modelling are summarized in Table 4.2 to Table 4.4.

Specimens designated as SB1 to SB5 were reported by Nie. et. al (2005). The degree of shear connection k_s was varied from 0.315 to 0.666 as defined by EC4 (BSI 1990) specifications, with one or two studs being welded in each trough of the sheeting.

Table 4.2: Composite beams parameter

Beam Model	Span (m)	Slab width (m)	Stud per rib	Total studs	Degree of shear interaction, k_s *(EC4) (%)*	Steel beam serial size (Fig.4.7)	Type of decking (Fig. 4.6)
SB1	4.0	1.0	1	9	49	I20a	B
SB2	4.0	1.0	2	18	64	I20a	B
SB3	4.0	1.0	2	18	69	I20a	B
SB4	4.0	1.0	1	9	32	I20a	A
SB5	4.0	1.0	2	18	47	I20a	A

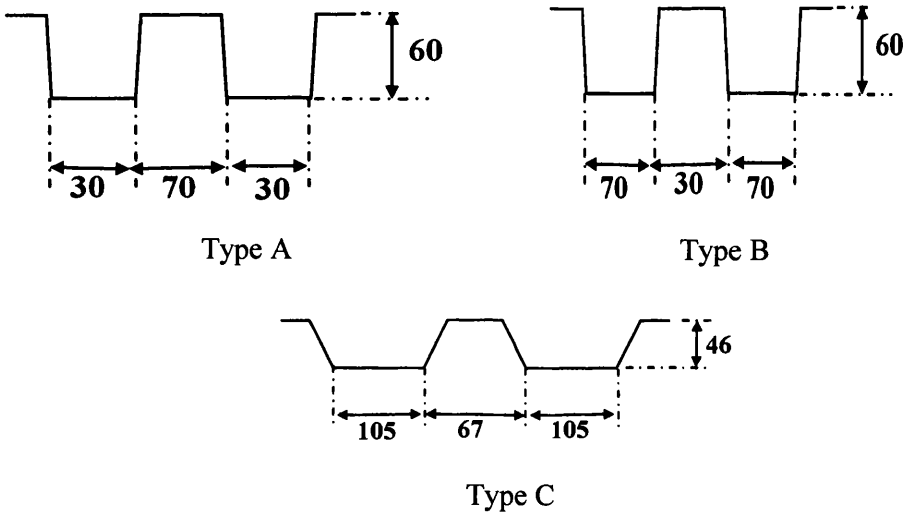

Figure 4.6: Metal-ribbed decking dimensions, unit in mm (not to scale)

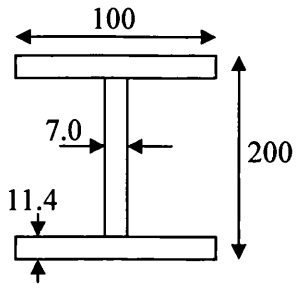

Figure 4.7: Steel beam (I20a) dimensions, unit in mm (not to scale)

Table 4.3: Material properties for concrete and steel beam used in finite element modeling

Model	Concrete				Steel Beam		
	f_{cu} (MPa)	f_c (MPa)	E_c (MPa)	v_c	f_{ys} (MPa)	f_{yu} (MPa)	v_s
SB1	43.6	31.68	2.97×10^4	0.2	291	371.2	0.3
SB2	47.3	34.36	2.77×10^4	0.2	291	371.2	0.3
SB3	43.5	31.60	2.66×10^4	0.2	291	371.2	0.3
SB4	43.4	31.53	2.66×10^4	0.2	291	371.2	0.3
SB5	42.9	31.17	2.64×10^4	0.2	291	371.2	0.3

Table 4.4: Material properties for steel decking and shear stud considered for finite element modeling

Model	Steel Decking			Shear Stud		
	f_{yp} (MPa)	v_p (MPa)	E_{yp} (MPa)	f_u (MPa)	v_u (MPa)	E_s (MPa)
SB1	280	0.3	2.1×10^5	480	0.3	2.0×10^5
SB2	280	0.3	2.1×10^5	480	0.3	2.0×10^5
SB3	280	0.3	2.1×10^5	480	0.3	2.0×10^5
SB4	280	0.3	2.1×10^5	480	0.3	2.0×10^5
SB5	280	0.3	2.1×10^5	480	0.3	2.0×10^5

4.3.8 Comparison of load-deflection curve

In order to study the suitability of the non-linear finite element model, key design parameters such as load-deflection response and ultimate load behaviour, predicted by the non-linear finite element model, were compared with the experimental data. Figures 4.8 to 4.12 show the load-deflection curves the experimental and the finite.

The load-deflection behaviour results obtained from the analyses are similar to the corresponding experimental curves in all cases. It was observed that all beams in the experimental tests showed softening behaviour in the load-deflection curve; the modelling technique could also simulate this behaviour. It was seen that there were some differences in the softening sections, where the analytical curve deviated away from the experimental result. This was due to the concrete material modelling used in the finite element analysis (FEA). Nevertheless the models were also able to simulate closely the transition between linear and non-linear behaviour of the composite beams.

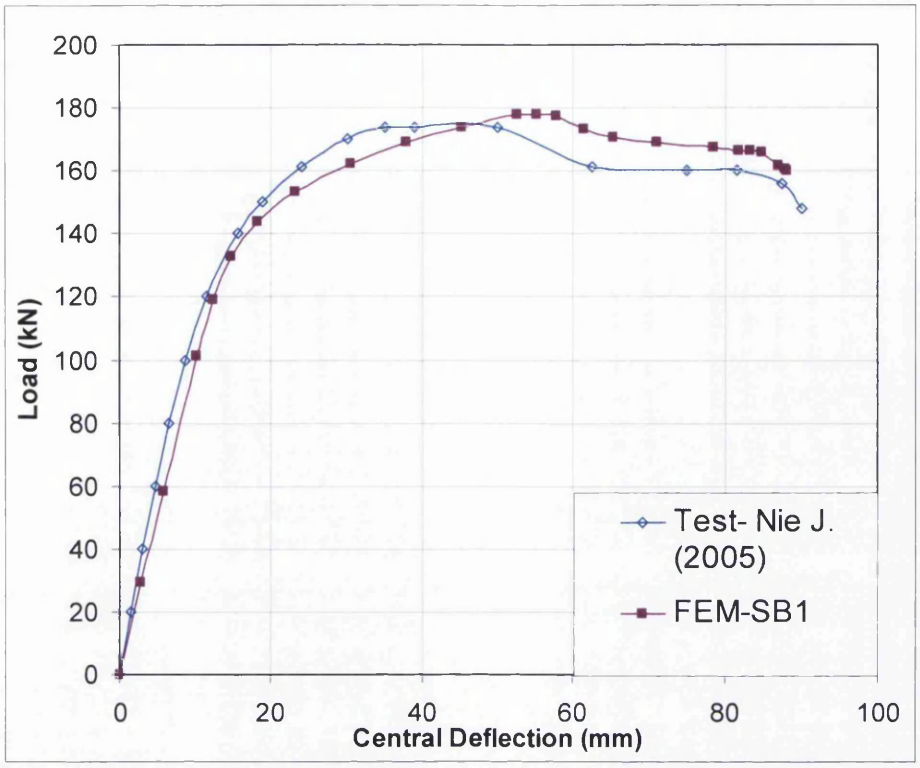

Figure 4.8: Comparison of moment-deflection curve of composite beam (SB1) between experimental test result and finite element prediction.

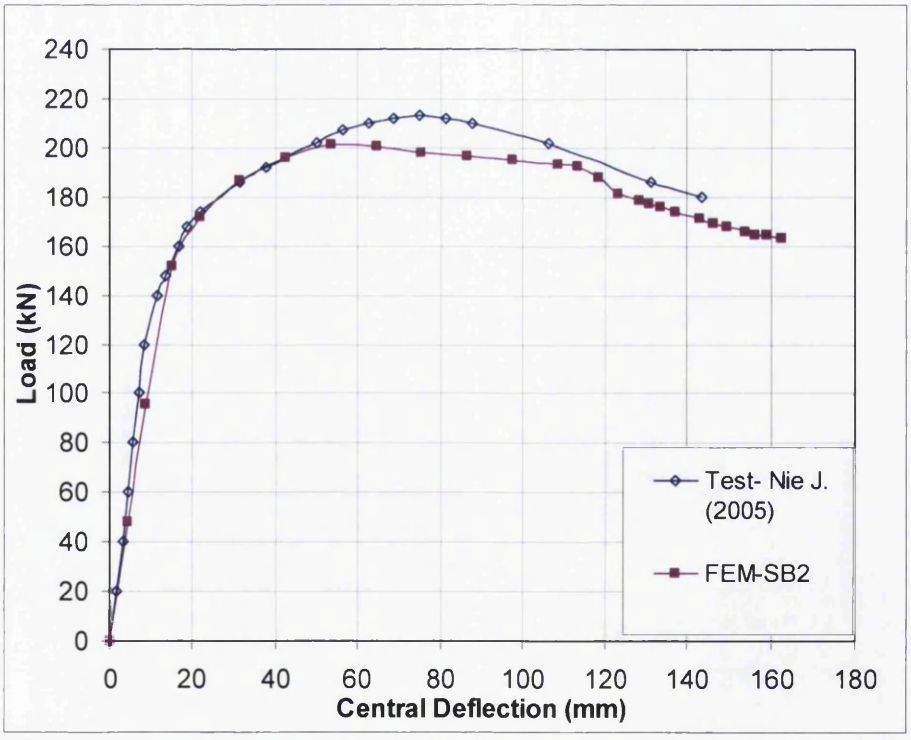

Figure 4.9: Comparison of moment-deflection curve of composite beam (SB2) between experimental test result and finite element prediction

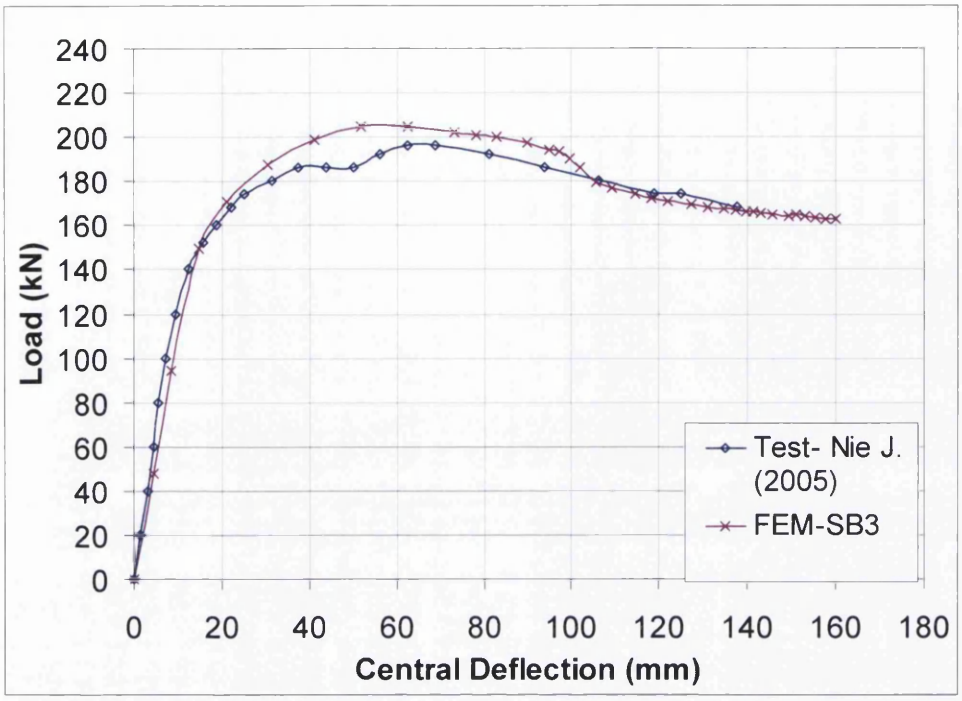

Figure 4.10: Comparison of moment-deflection curve of composite beam (SB3) between experimental test result and finite element prediction

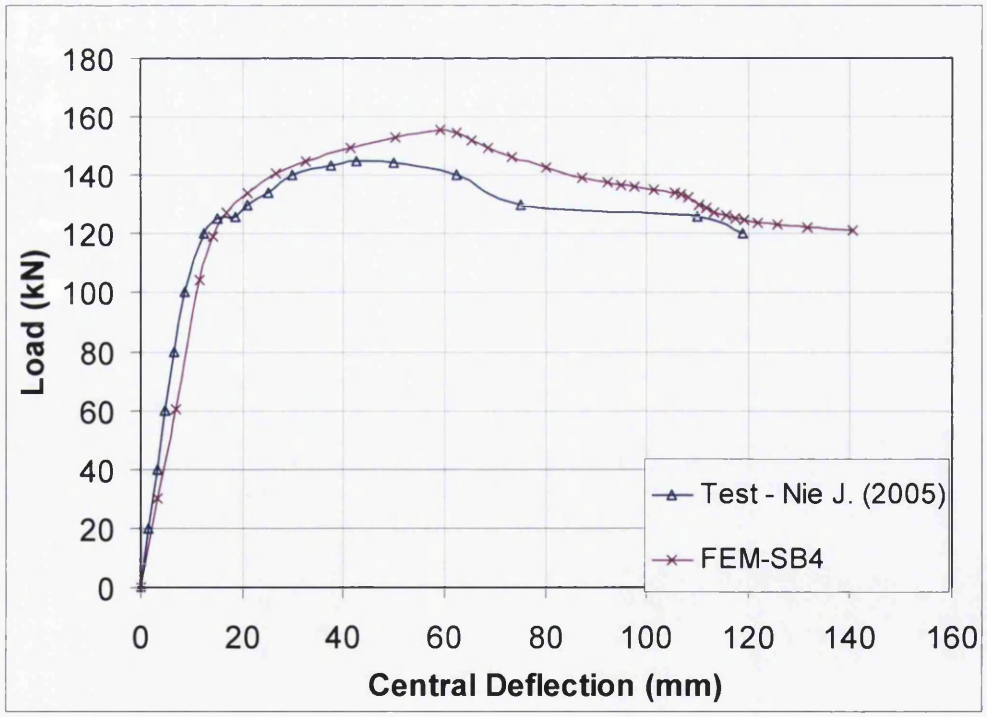

Figure 4.11: Comparison of moment-deflection curve of composite beam (SB4) between experimental test result and finite element prediction

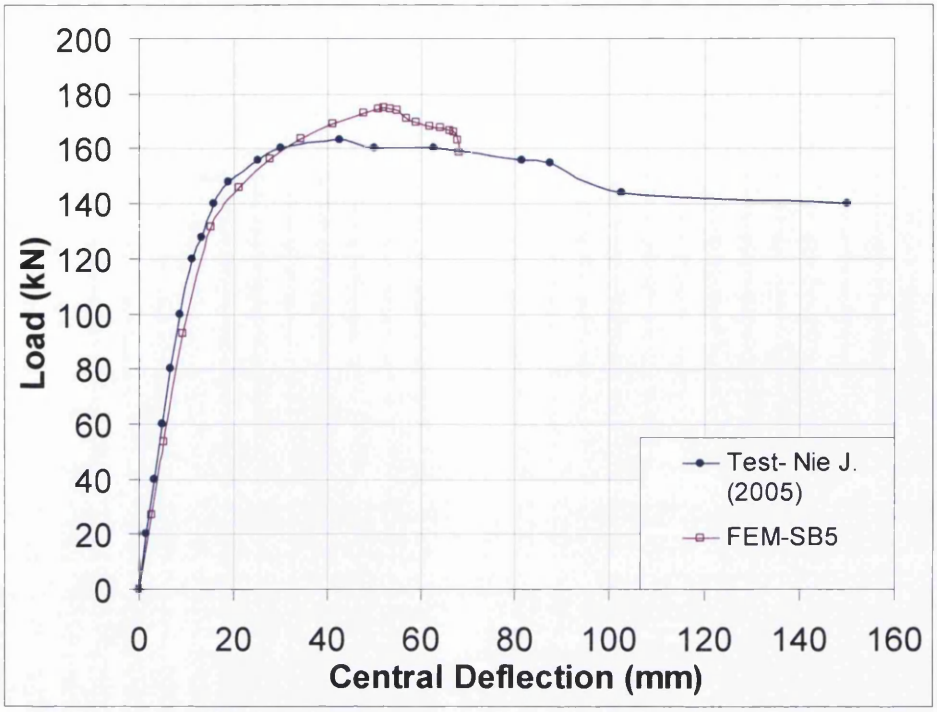

Figure 4.12: Comparison of load-deflection curve of composite beam (SB5) between experimental test result and finite element prediction

The non-linear finite element predictions for the ultimate load capacity seen to differ by -8% to 6% compared to the experimental results, as shown in Table 4.5. It can be observed that, in most cases, the finite element method overestimates the ultimate load compared to the experimental results except for model SB2. The differences are within allowable variation of 15%, (ASCE 1984; AISI 1996) in structural testing.

The ultimate moment of composite beams can be defined by calculating the load-deflection curve. The ultimate moment M_{FE} obtained from the FE analyses are compared with flexural strength M_{EC4} predicted by Eurocode 4 (2004) specifications for composite beam with a partial shear connection (Table 4.5). The plastic moments and design strength are calculated using the measured material properties shown in Table 4.2 to Table 4.4. The design strengths predicted by Eurocode 4 are conservative for most cases with 1% to 8% difference compared to FE method.

Therefore, the non-linear finite element modelling can be used in design without any loss of accuracy or of being too overestimate or conservative. Considering the extent

of the assumptions and simplification made in numerical modelling, the result is satisfactory and can be used in the design of composite beams.

Table 4.5: Comparison of ultimate moment between experimental, Finite Element and EC4

Specimen	M_u (Test) (kN.m)	M_{FE} (kN.m)	M_u / M_{FE}	M_{EC4} (equivalent method)	M_{EC4} / M_{FE}
SB1	143.5	146.89	0.98	140.07	0.95
SB2	175.6	169.95	1.06	156.41	0.94
SB3	160.9	169.01	0.95	155.64	0.92
SB4	119.5	128.07	0.93	125.93	0.98
SB5	132.5	144.14	0.92	137.68	0.96

4.3.9 Mode of failure for composite beams

The ultimate moment capacity of composite beams depends on the degree of shear connection, the compressive resistance of concrete slab and steel beam (where the neutral axis falls within steel section), and the tensile resistance of the steel beam section. Three flexural modes of failure exist (Chien 1984), shear connection failure, crushing of the concrete, and full yielding of the steel beam section. In FE analysis, the mode of failure can be defined by plotting the yielding sequence (stress versus central deflection) of composite beam components (concrete and shear stud). In this sequence, if the stud yielding point is located before the concrete crushing point, then the mode of failure of the composite beams is considered as stud failure. Conversely, if the stud yielding point is located after the concrete crushing point, the mode of failure is assumed to be concrete crushing. The FE contour stress also can be used to confirm the failure mode. In FE modelling, when crushing of concrete and shear studs occur, this will cause the steel beam sections to reach their ultimate stress and will cause a large deflection prior to failure. While, the failure modes from experimental observation are described in details by Nie et. al. (2005). A typical mode of failure from experimental and FE analysis was compared in Appendix A.

Figure 4.13 to figure 4.17 show the yielding sequence for the composite beams components, SB1 to SB5. The yielding sequence of composite beam components was

obtained by plotting the stress-deformation curve and observation from stress contours obtained from FE analysis as shown in Appendix B to Appendix F. The beams SB1, SB4 and SB5 failed due to shear stud since the yielding of shear studs occur before the concrete reached its compressive strength. This was also confirmed by the experimental observation where some shear studs were found broken (Nie et. al; 2005). Beams SB2 and SB3 failed due to concrete crushing, since the concrete crushing occurred before the shear stud yielding. This mode of failure also occurred in the experimental test where the concrete had crushed at the central of slab (Nie et. al; 2005). Concrete crushing failure occurred in the composite beam SB2 and SB3 because both beams had higher degree of interaction (more than 50%) compared to other beams (less than 50%). The calculations of shear stud interaction are based on EC4 (2004). At the final load, for all FE models, the steel section had reached the ultimate stress.

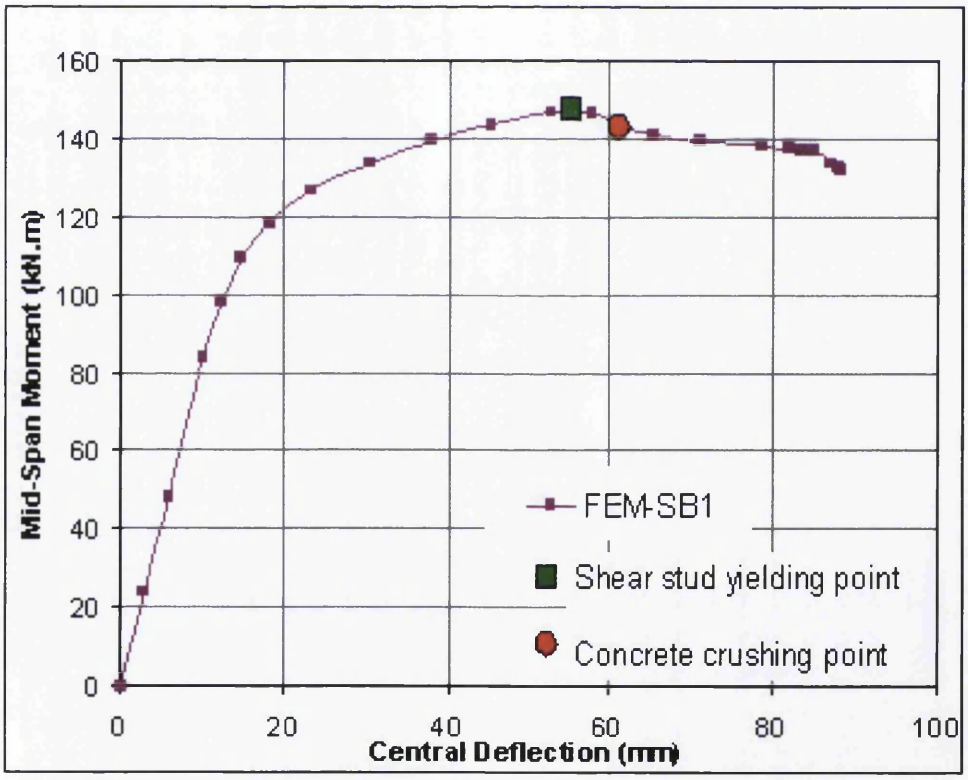

Figure 4.13: Sequence of failure point for composite beams (SB1)

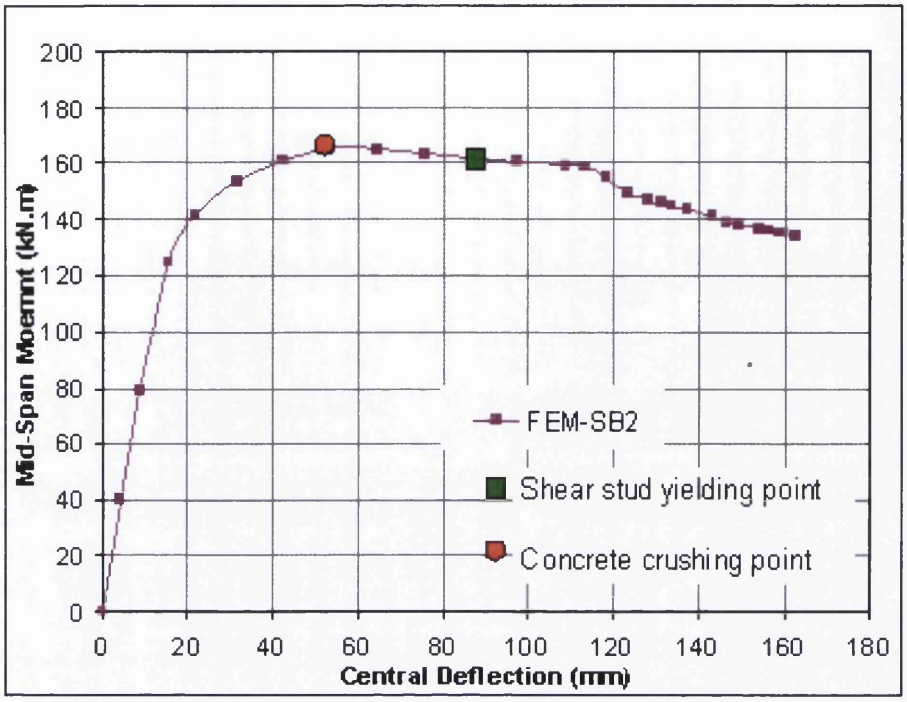

Figure 4.14: Sequence of failure point for composite beams (SB2)

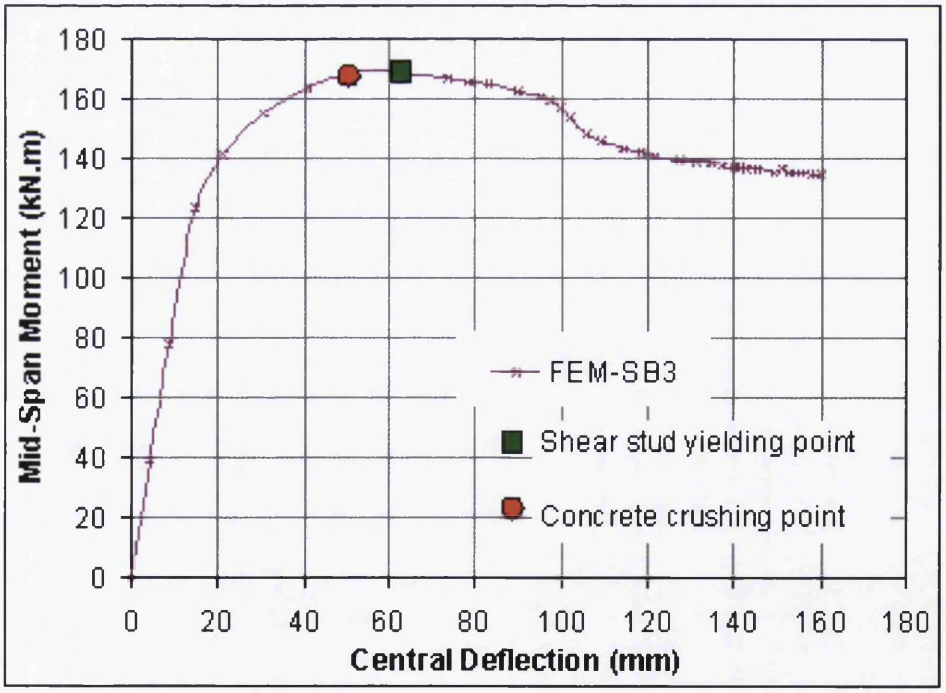

Figure 4.15: Sequence of failure point for composite beams (SB3)

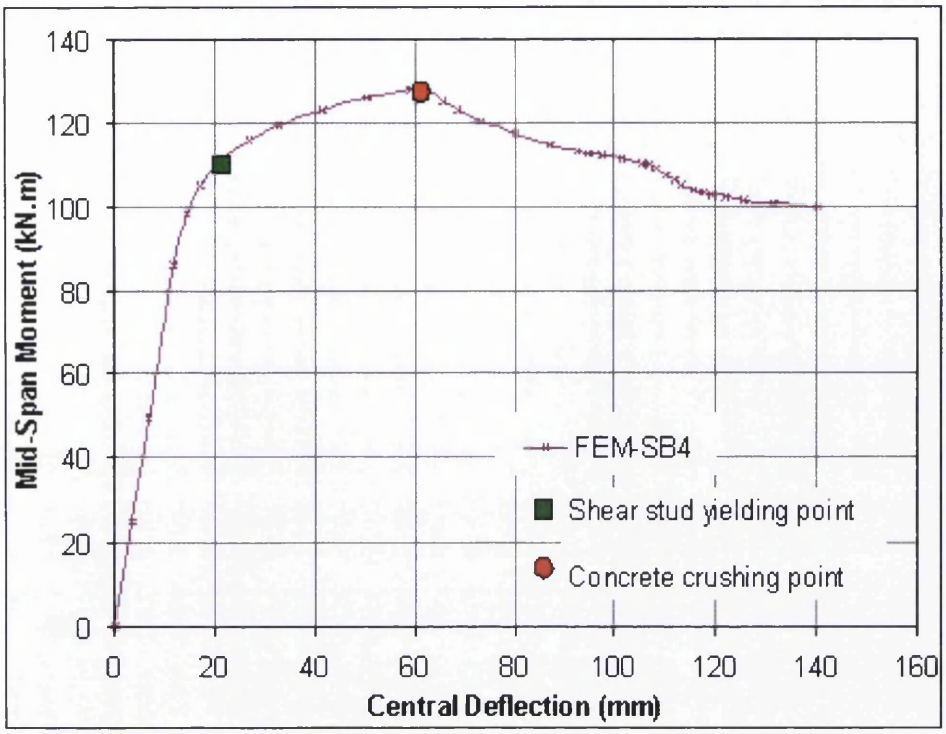

Figure 4.16: Sequence of failure point for composite beams (SB4)

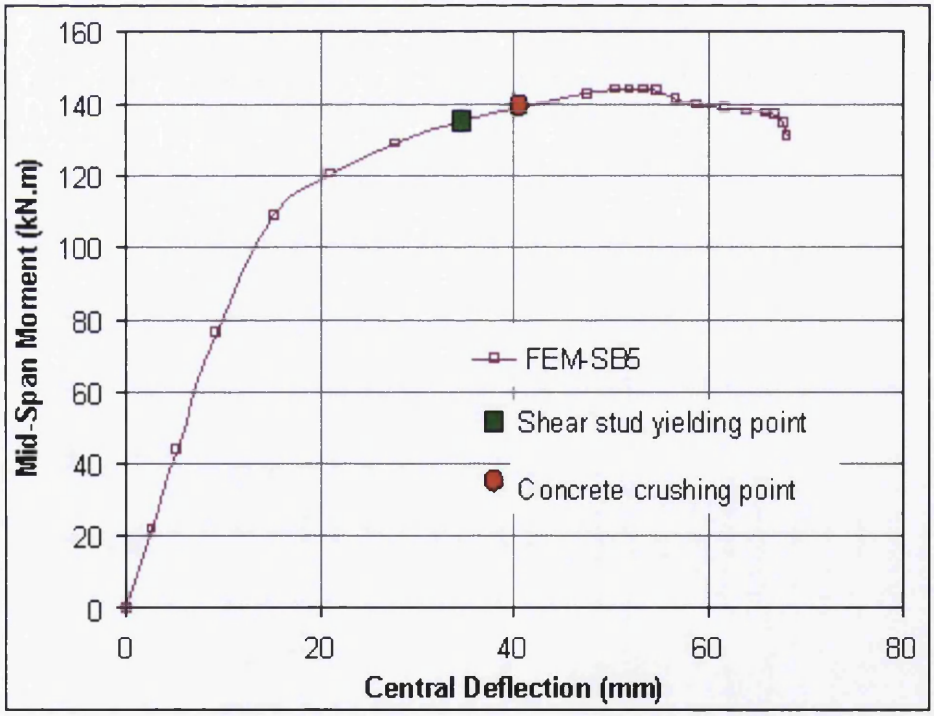

Figure 4.17: Sequence of failure point for composite beams (SB5)

4.4 Finite element model of metal-ribbed decking composite beams without openings

4.4.1 Introduction

This section is focused on the modelling of nines 3D FEMs of composite beam without openings which were used to compare with composite beam with openings in Chapter 5. The parametric studies also were carried out to study the major parameter affecting the load carrying capacity of composite beam. Nine simply-supported composite beams were analysed in three groups. The group were classified as A, B and C, based on their decking shape as shown in Figure 4.6. The groups were also classified by their concrete strength. Decking-shape B and C were classified as wide-rib, while decking-shape A was classified as narrow-rib. The classification was based on BS 5950 (Hayward; 2002). Parameters of the models used in the parametric study are shown in Table 4.6 to Table 4.8.

Table 4.6: Composite beams model parameter for model A1 to A3

Model	L (mm)	B (mm)	D_s (mm)	D_p (mm)	f_c (MPa)	k_s (%)	Decking Shape (Ref. Fig. 4.6)
A1	4000	1000	105	60	43.4	51	A
A2	4000	1000	105	60	26	68	A
A3	4000	1000	105	60	35	61	A

Table 4.7: Composite beams model parameter for model B1 to B3

Model	L (mm)	B (mm)	D_s (mm)	D_p (mm)	f_c (MPa)	k_s (%)	Decking Shape (Ref. Fig. 4.6)
B1	4000	1000	105	60	43.4	76	B
B2	4000	1000	105	60	26	100	B
B3	4000	1000	105	60	35	91	B

Table 4.8: Composite beams model parameter for model C1 to C3

Model	L (mm)	B (mm)	D_s (mm)	D_p (mm)	f_c (MPa)	k_s (%)	Decking Shape (Ref. Fig 4.6)
C1	4000	1000	105	46	43.4	54	C
C2	4000	1000	105	46	26	71	C
C3	4000	1000	105	46	35	63	C

For steel beam properties, elongation at ultimate load and the ratio of ultimate strength to yield strength is taken as 15% and 1.2, respectively. Material properties for steel beams, steel decking and shear studs are shown in Table 4.9 and were used in the FE analyses. All models consisted of shear stud with 19 mm in diameter and 95 mm in height. The steel beam section, with serial number 203x33xUB30, was used for all beams. Figure 4.18 shows the steel beam dimension. The thickness of the solid part of the concrete slab was kept constant at 105 mm, while the height of the ribs was varied depending on their decking shape. The other variables considered were concrete strength and degree of shear interaction.

Table 4.9: Material properties for steel beam, steel decking and shear stud considered for finite element modeling

Material	f_y	v_p (MPa)	E_s (MPa)
Steel beam	300	0.3	2.06×10^5
Steel decking	280	0.3	2.1×10^5
Shear stud	450	0.3	2.0×10^5

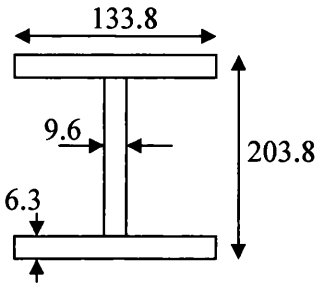

Figure 4.18: Steel beam (203x133xUB30) dimension, unit in mm (not to scale)

4.4.2 Result and Discussion

4.4.2.1 General

Figures 4.19 to 4.21 show the moment-deflection curves for classified model A, B and C, base on their decking shape.

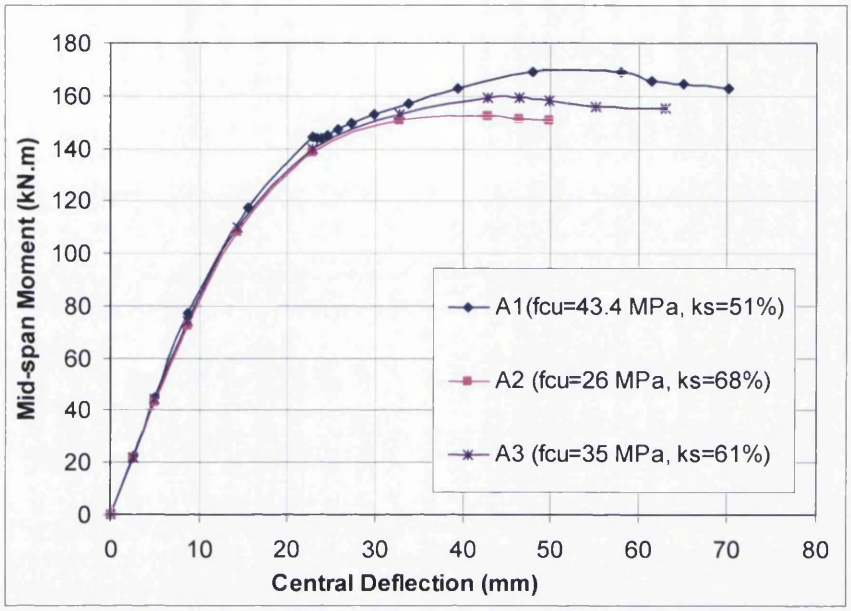

Figure 4.19: Moment-deflection curve of composite beams for model A1 to A3

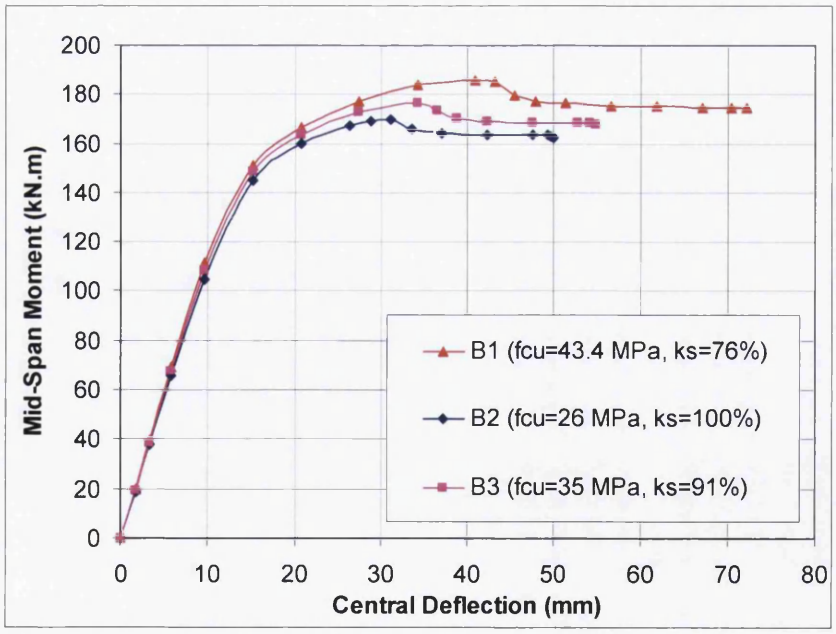

Figure 4.20: Moment-deflection curve of composite beams for model B1 to B3

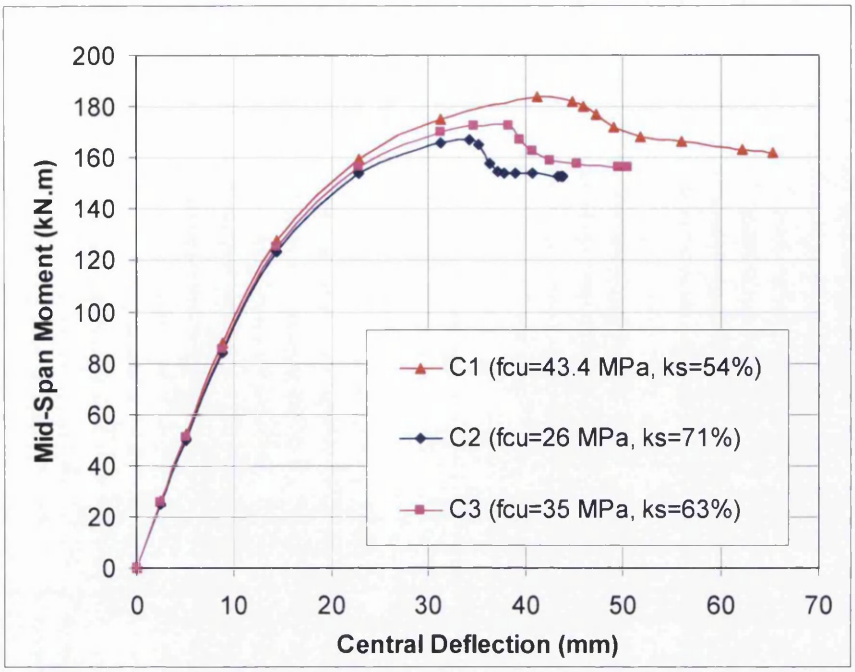

Figure 4.21: Moment-deflection curve of composite beams for model C1 to C3

Generally, numerical moment-deflection curves are linear up to the first yield load about 90 kN, 150 kN and 100 kN for decking type A, B and C, respectively and its becomes non-linear thereafter. For similar concrete cube strength, Decking type B and C has higher ultimate load compared to decking type C. Models A1 and C1 has lower degree of interaction, 51% and 54%, respectively. It can be observed from Figure 4.21 to figure 4.22, all models failed due to flexural mode of failure since concrete crushing point located before shear stud yielding point. Yielding sequence and stress contours of composite beam components for beam A1, B1 and C1 obtained from FE analyses are shown in Appendix G to Appendix I. It can be concluded that composite beam with more than 50% degree of shear interaction used in this study failed due to flexural mode of failure.

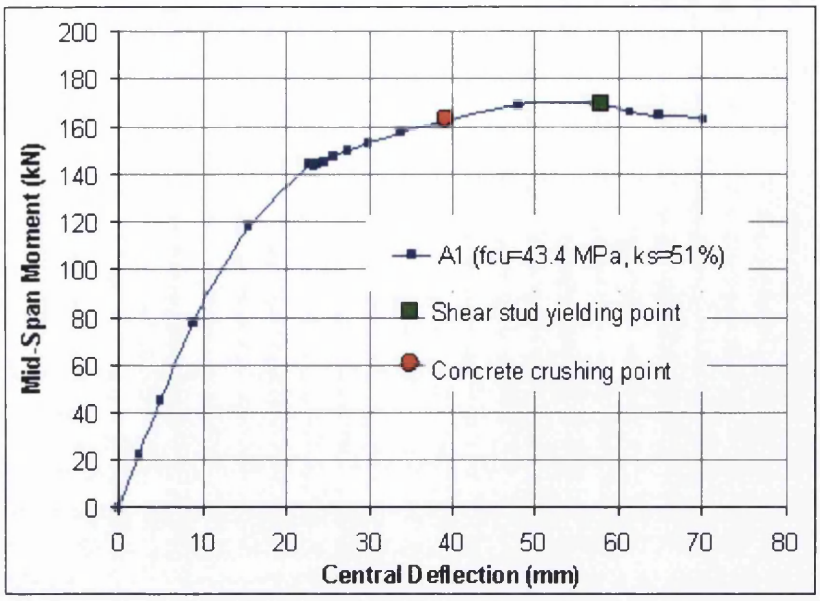

Figure 4.22: Sequence of failure point for composite beams (A1)

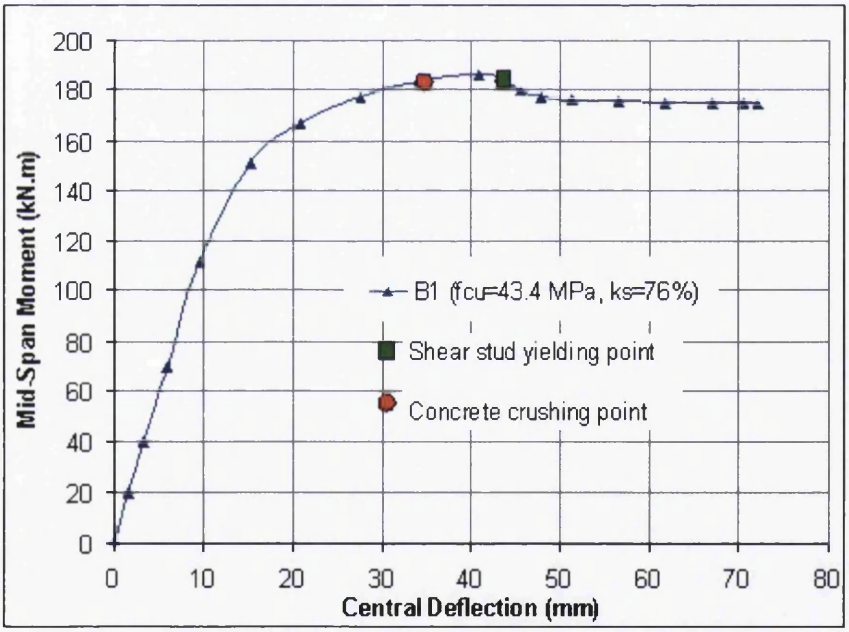

Figure 4.23: Sequence of failure point for composite beams (B1)

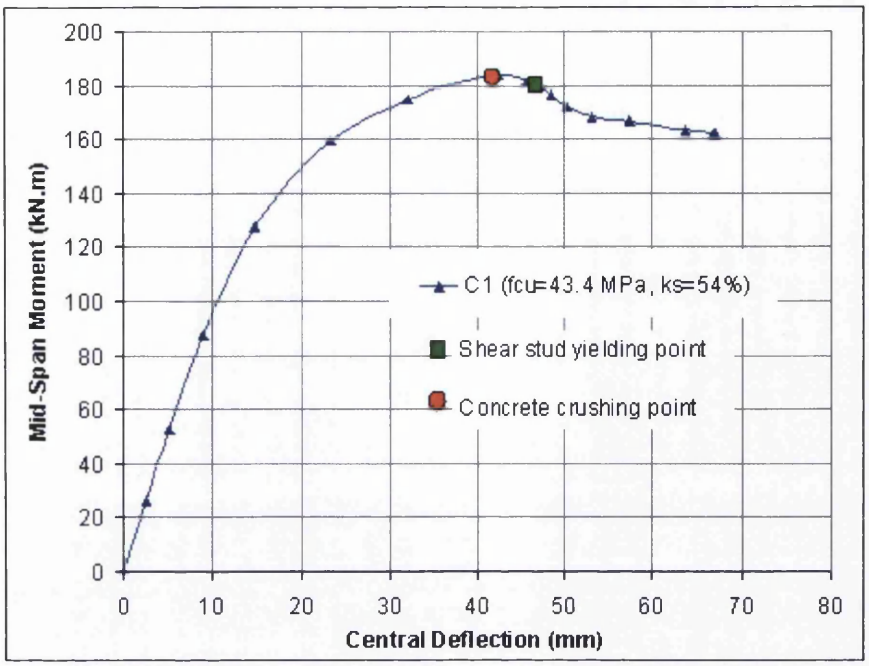

Figure 4.24: Sequence of failure point for composite beams (C1)

The ultimate moment of composite beam data obtained from FE analysis were compared with design method. The bending strength can be calculated by an equivalent method proposed by Eurocode 4 (2004) and BS5950 (1990). The comparisons of ultimate moment obtained from the FE analysis with flexural strength predicted by Eurocode 4 and BS5950 is shown in Table 4.10. In the table, M_{FE} is ultimate moment obtained from numerical analysis. While, M_{EC4} and M_{BS5950} are moment capacity calculated using plastic analysis as recommended by European Code and British Standard, respectively. From $\frac{M_{EC4}}{M_{FE}}$ ratio, it can be observed that the finite element results overestimate the moment capacity averagely 5%, when compared with Eurocode 4 prediction. However from $\frac{M_{BS5950}}{M_{FE}}$ ratio, the deviation of two values obtained from finite element and BS5950 prediction is between +1% to -3%. However the different is considered small. In view of the material and geometrical nonlinearity involved in FE modelling, the finite element modelling can be considered accurate for design purpose. Furthermore, the Eurocode 4 design may be conservative compared to BS 5950. Eurocode 4 have introduced reduction factor 0.70, in calculating a reduction factor for deck shape compared with 0.85 in BS 5950.

Table 4.10: Comparison of ultimate moment between finite element, EC4 and BS5950

Specimen	M_{FE} *(kN.m)*	M_{EC4} (equivalent method)	$\frac{M_{EC4}}{M_{FE}}$	M_{BS5950} *(kN.m)*	$\frac{M_{BS5950}}{M_{FE}}$
A1	169.55	152.87	0.90	164.05	0.97
A2	152.19	142.61	0.94	153.40	1.01
A3	159.12	150.38	0.95	160.22	1.01
B1	185.96	171.45	0.92	185.33	1.00
B2	169.74	156.06	0.92	168.11	0.99
B3	176.18	167.17	0.95	178.57	1.01
C1	183.89	166.61	0.91	180.02	0.98
C2	167.13	152.64	0.91	164.73	0.99
C3	172.28	162.87	0.95	169.87	0.99

4.4.2.2 Concrete compressive strength

The effect of changing the compressive strength of the concrete was investigated. Models numbered with 1 (A1, B1 and C1) had higher compressive strengths with 43.3 MPa compared to models with the numbers 2 (A2, B2 and C2) and 3 (A3, B3 and C3) with compressive strength 26 MPa and 35 MPa, respectively. A comparison of the moment-deflection curves is shown in Figures 4.19 to 4.21. The results show that, by increasing the concrete compressive strength from 26 MPa to 43.3 MPa, (a 40% increment) increased ultimate moment of composite beams with metal decking was approximately 9% to 11%. This also has been proved by design calculation of Eurocode 4, where the moment capacity was increased by 7% to 10%. The significant increment is due to plastic neutral axis lies within steel beam and this caused all of concrete section act as compressive forces. These will subsequently increase the moment capacity of composite beam by increasing the concrete compressive strength.

4.4.2.3 Beam interaction

In this parametric study the shear connection interaction is varied between 51% and 100%. Increasing beam interaction improved the stiffness and load carrying capacity of the composite beams with metal-ribbed decking. This was observed from the comparison of moment-deflection curve between models A1, A2 and A3, B1, B2 and B3, and C1, C2 and C3, as shown in Figures 4.19 to 4.21. The increment of moment capacity is because of the full strength of concrete can be achieved with the higher degree of shear connector.

4.4.2.4 Type of decking

Three types of decking were used for this study, which were A, B and C. The comparison of the moment-deflection curve for different shapes of decking is shown in Figure 4.25. For A and B type, the decking height was 60 mm; were only different is in their ribbed width. The used of wide-rib, B type (B1), compared to narrow-rib, A type (A1), increased the stiffness and ultimate moment of the composite beams. The decking, C type was 46 mm high and had a wide-rib classification. Although the beam A1 used higher metal-ribbed decking compared to beam C1, beam C1 was stiffer and had a larger ultimate moment capacity due to its wide-rib effect, see Figure 4.25. Shear resistance of shear connector in ribbed metal decking normally lower than in a solid slab. Shear resistance of shear connector in narrow-rib reduced more compared to wider-rib. This will subsequently reduced a percentage of shear connector interaction. Due to this reasons, A type decking has lower moment capacity compared to B type and C type. This is proved by a calculation of moment capacity using a design method as shown in Table 4.9. In the design method, Eurocode 4 and BS 5950, have specifies reduction factors due to this effect. These factors are based on formulae developed by Grant et. al (1997) as has been described in literature review.

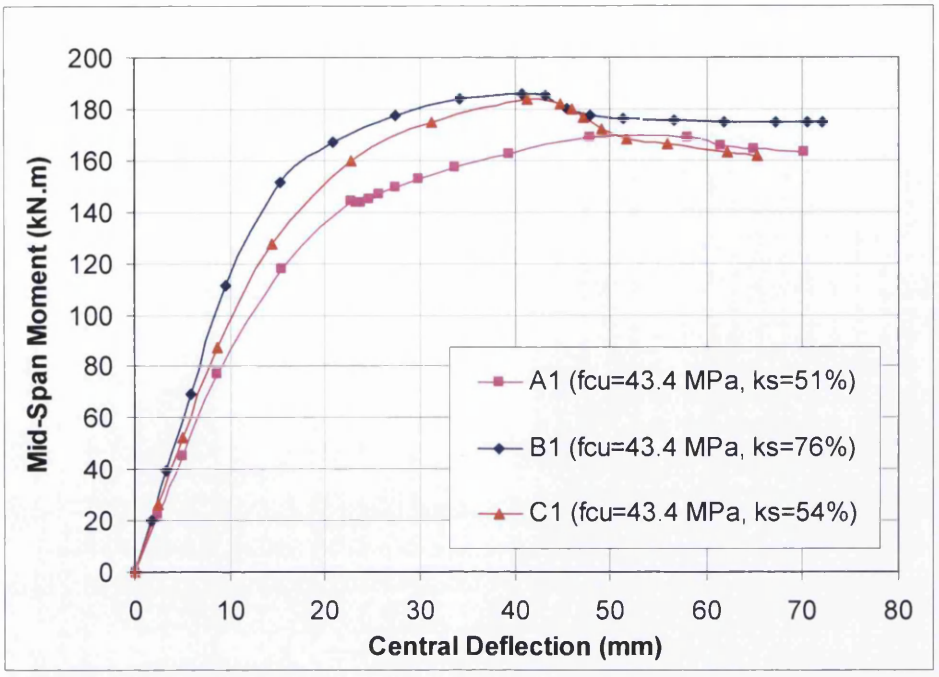

Figure 4.25: Moment-deflection curve comparison of composite beams for different type of decking.

4.4.2.5 Metal-ribbed decking thickness and yield stress

The effect of changing the thickness and yield strength of the metal-ribbed decking was investigated in relation to central load only. Beam A1 was used to study this effect. Comparison of the moment-deflection results is shown in Figure 4.26 and Figure 4.27. The results show that increased thickness and yield strength of ribbed decking will not improved the stiffness and capacity of the composite beams. Metal decking can be considered as orthotropic material due to its geometry. Since the investigation only focusing on the composite slab perpendicular to steel beam, the steel decking do not have tensile strength in the parallel direction to steel beam. Due to this reason, the steel decking thickness and yield strength do not have an effect to composite beam strength.

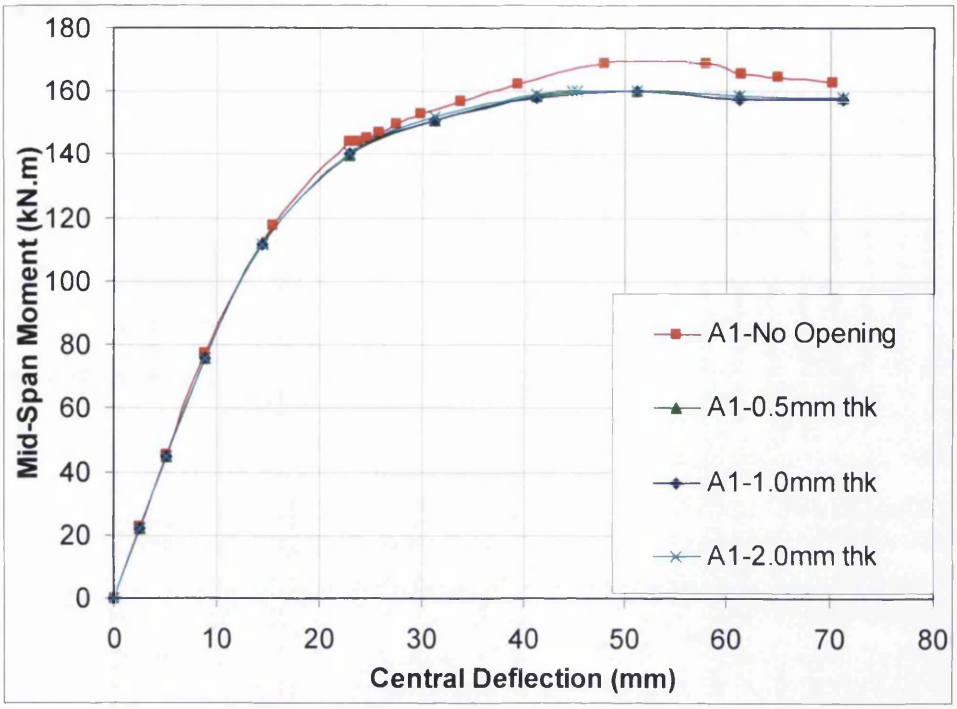

Figure 4.26: Moment-deflection curve comparison of composite beams for different decking thickness

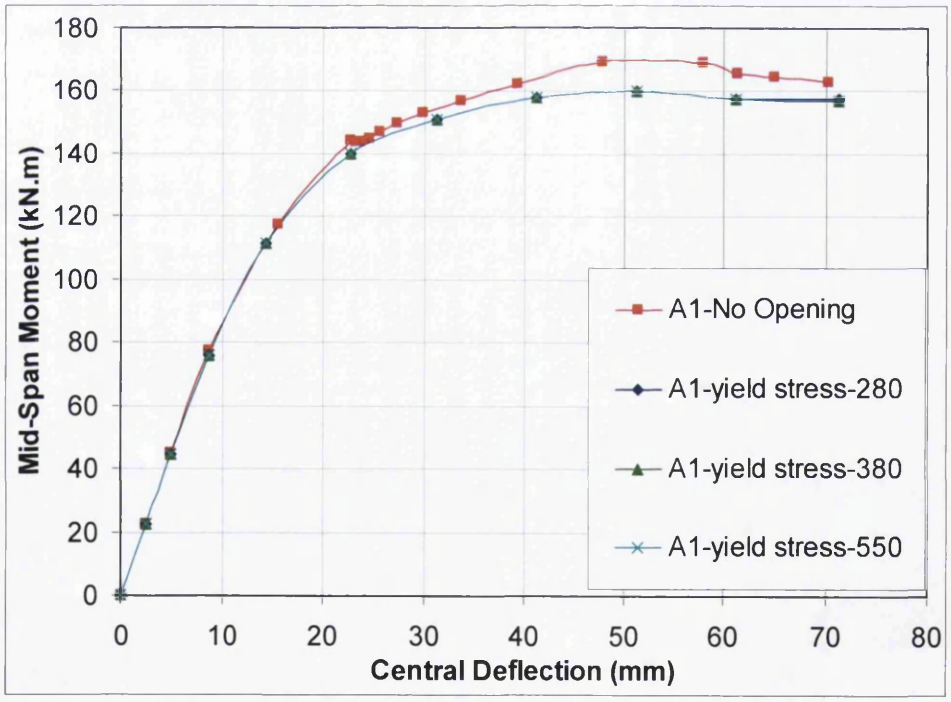

Figure 4.27: Moment-deflection curve comparison of composite beams for different yield stress of steel decking

4.4.2.6 Deflection of composite beam

Deflection of composite beam measured from FE analysis is compared with the value calculated according to Eurocode 4 (2004). Comparison of deflection value obtained from FE analysis and calculated value is shown in Table 4.11. The values obtained from finite element analysis δ_{FEM} for corresponding load are higher than the values of δ_{EC4} calculated by design method. This is because in linear range, finite element analysis ignores the stiffness of concrete behind the shear stud.

Table 4.11: Comparison of deflection

Specimen	Service Load (kN)	δ_{FEM} (mm)	δ_{EC4} (mm)	$\frac{\delta_{EC4}}{\delta_{FE}}$
A1	70	7.78	6.09	0.78
A2	60	6.80	4.95	0.73
A3	65	7.50	5.47	0.73
B1	95	8.00	7.01	0.88
B2	90	8.10	5.97	0.74
B3	95	8.30	6.73	0.81
C1	80	7.88	6.82	0.87
C2	70	7.10	5.67	0.80
C3	75	7.50	6.23	0.83

4.5 Conclusion

This chapter was divided into two sections. In the first sections, details of the FEM were presented. The three-dimensional FEM technique of composite beams with metal-ribbed decking was discussed. Most researchers used spring element to simulate shear stud interaction in composite beam modelling. Used of 3D shear stud modelling technique was proposed using the FEM for composite beams with metal-ribbed decking. Even though this technique has been used by some researchers to model push-off test, this chapter showed that the technique also can be implemented in composite beam. The FEM used the proposed technique and was verified using the

experiment's results, which are available in the literature. Validation of the proposed FEM was satisfactory. The FEM has, to a large extent, proved capable of predicting elastic and inelastic load-deflection curve for composite beams. The models are also capable of accurately predicting ultimate moment.

Nines FEMs were analysed and the results for ultimate moment and stiffness were verified using the design code, BS5950 and EC4. Good agreement between numerical and design codes results were achieved. Parametrical study also was carried out using finite element analysis. From the finite element analysis, it can be concluded that the major parameter affecting the load carrying capacity of composite beams with metal-ribbed decking are: concrete compressive strength, beam interaction and type of decking.

4.6 References

AISI, C. (1996). Commentary on the 1996 edition of the specification for the design of cold forned steel structural members. Washington, American Iron and Steel Institute.

ASCE (1984). Specification for the design and construction of composite slab. New York, ASCE.

BSI (1990). BS 5950, Part 3, section 3.1: Code of practice for design of simple and continuous composite beams. London: British Standard Institution.

BSI. DD ENV 1994-1-1 (1991). EC4: Design of composite steel and concrete structure-Part 1-1: General rules for buildings. London: British Standard Institution.

Chien, E. Y. L., and Ritchie, J.K., (1984). Design and Construction of Composite Floor System, Canadian Institute of Steel Construction.

Ellobody, E., Young, B., (2006). "Performance of shear connection in composite beams with profiled steel sheeting." Journal of Constructional Steel Research 62: 682-694.

Fabbrocino, G., Manfredi,G., Cosenza, E., (1999). "Non-linear analysis of composite beams under positive bending." Computers & Structures 70: 77-89.

Fahmy, E. H., and Abu-Amra, T.H., (2008). "Longitudinal cracking of concrete slabs in composite beams with ribbed metal deck." Journal of Constructional Steel Research 64(6): 670-679.

Fahmy, E. H., and Robinson, H., (1986). "Analysis and tests to determine the effective widths of composite beams in unbraced multi-story frames." Can. J. Civ. Eng. 13(1): 66-75.

Gattesco, N. (1999). "Analytical Modelling of Nonlinear Behaviour of Composite Beams with Deformable Connection." Journal of Constructional Steel Research 52: 195-218.

Grant, J., A., Fisher, J., W., and Slutter, R.,G., (1977). "Composite beams with formed steel decking." Engineering Journal of the American Institution of Steel Construction 14(First Quater).

Jayas B. S., Hosain, M. U. (1988). "Behaviour of headed studs in composite beams: push-out tests." Can. J. Civ. Eng. 15: 240-253.

Johson, R. P., Oehlers, D.J., (1981). Analysis and design for longitudinal shear in composite T-beams, Proceeding Instn. Civil Engineers Part 2.

Kalfas, C., and, Pavlidis, P., (1997). Load-slip curve of shear connector evaluated by FEM analysis. Composite Construction-Conventional and innovative, Innsbruck, Austria.

Kim, B., Wright, H. D., Cairns, R., (2001). "The behaviour of through-deck welded shear connectors: an experimental and numerical study." Journal of Constructional Steel Research 57: 1359-1380.

Lam, D., Ellobody, E., (2005). "Behaviour of headed stud shear connectors in composite beam." Journal of Structural engineering, ASCE 131(1): 96-107.

Nie, J. G., Cai, C.S., Wang, T., (2005). "Stiffness and capacity of steel-concrete composite beam with profiled sheeting." Engineering Structures 27: 1074-1085.

Nie, J. G., Fan, J., Cai, C.S., (2008). "Experimental study of partially shear-connected composites beams with profiled sheeting" Engineering Structures, 30:1-12.

Ollgaard, J. G. (1971). "Shear Strength of stud connectors in lightweight sand and normal weight concrete." Engineering Journal of the American Institution of Steel Construction 5.

Plank, R. J., and,Wittrick, W.H, (1974). "Buckling under combined loading of thin, flat-walled structures by complex finite strip method." Numerical Methods in Engineering 8(2): 323-339.

Queiroz, F. D., Vellasco, P.C.G.S., and Nethercot, D.A. (2006). "Finite Element Modelling of Composite Beams with Full and Partial Shear Connection." Journal of Constructional Steel Research. 63(4): 505-521

Roberts, T. M. (1985). "Finite difference analysis of composite beam with partial interaction." Computers & Structures 21(3): 469-473.

Sun, F. F. (2005). A beam element for steel-concrete composite beams with shear lag and area load. 4th Conference on Advance in Steel Structures, Shanghai, China.

Uy, B., and Bradford, M.A., (1994). "Inelastic local buckling of cold form thin steel plates in profiled composite beams." The Structural Engineers 72(16): 259-267.

Hayward, A. and Weare, F. (2002). Steel detailers' manual, 2 Ed Blackwell Science, Oxford, U.K.

Chapter 5

PARAMETRIC STUDIES ON COMPOSITE BEAM WITH OPENINGS IN THE METAL-RIBBED DECKING SLAB

5.1 Introduction

Composite floor systems are used widely in construction because of benefits of efficiently combining the two construction materials, steel and concrete. They are also economic in terms of labour on site, construction time and shallower structural member. A composite slab is normally designed as a deformed deck-slab by using shear connectors for interface shear transfer at the base of the concrete floor.

However, openings are frequently placed in floor slab of buildings that contain pipelines for heating, ducts and ventilation. These large openings in the composite slab tend to reduce the capacity of the composite beam. The moment resistance of the whole composite system is affected. Openings can be located anywhere in composite beam flanges, symmetrically or asymmetrically.

There has been a great deal of research was carried out on composite beam behaviour and strength. However, studies on the behaviour of composite beams with openings in slabs with steel decking have not been reported well, despite their importance.

The FEM was used in these studies as to provide a better understanding of the behaviour of composite beam with openings in the metal-ribbed decking composite slab. A three-dimensional finite element model was established with all the main structural parameters and associated material non-linearities included for steel beam, shear stud, concrete and steel decking. The computer code ANSYS is used in this studies.

The main characteristics of finite element analyses on composite beam with metal-ribbed decking were described in detail in Chapter 4. Due to good agreement between the experimental and numerical models, the validated numerical models have been used to carry out parametric studies in this chapter.

This chapter is divided into three parts. First part deals with investigation of the opening effect on the ultimate moment capacities of composite beams. Parameters considered include opening sizes in transverse and longitudinal axis, location of the openings and position of load.

Openings in metal-ribbed decking slab reduce the moment capacity of composite beam. Therefore, the second part is related to various slab thickness and reinforcement bars which increase the moment capacity of composite beam with openings.

For simplification in the FE models, openings were assumed to have symmetry on z-axis and x-axis. Therefore, half the beam was modelled giving due consideration for the boundary conditions of the models along the line of symmetry. For purpose of standardisation and easy reference, all the numerical models used a standard steel grade of f_y = 300 N/mm^2 and f_u = 415 N/mm^2. All numerical models were simply supported, loaded with single point load at the mid-span of the beam, except for model used for the study load location. A total of 180 finite elements models of 4.0 m span with 1 m slab wide were used for this study. In this research, the focus was on

symmetrical structure due to location of openings. As mentioned in the previous chapter, there are three type of decking, A, B and C used in this study.

5.2 Size of opening

5.2.1 Opening size in the transverse direction

Fifty four composite beam models were used to investigate the effect of this parameter on the ultimate moment capacity. Figure 5.1 shows the layout of opening size in transverse direction. In the layout, opening size in transverse direction is denoted as 'a'; 'f' refers to openings size in longitudinal direction, B_f the width of composite beam flange and 'L' length of composite beam. The opening size in transverse direction, **a,** was varied while, **f,** was kept constant.

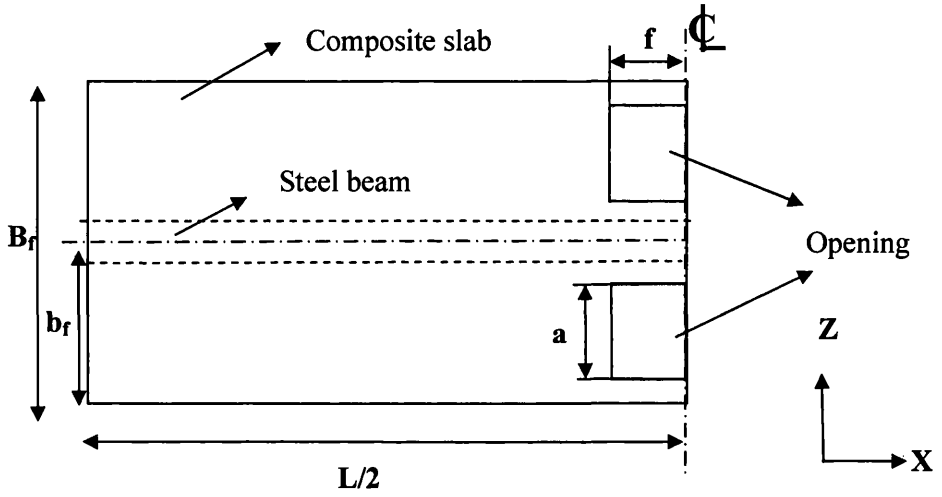

Figure 5.1: Layout of composite beam model with different openings size in transverse direction in metal-ribbed decking slab.

Numerical models for the studies on opening size in transverse direction were numbered from A1 to A18 for decking type A, B1 to B18 for decking type B and C1 to C18 for decking type C. Table 5.1 to Table 5.3 show the details of the parameters.

Table 5.1: Details of composite beams with different opening size in the transverse direction, type A

Beam Model	Degree of shear interaction, k_s	Concrete cube strength, f_{cu} *(MPa)*	Opening size	
			a (mm)	f (mm)
A1	0.51	43.3	50	100
A2	0.51	43.3	100	100
A3	0.51	43.3	140	100
A4	0.51	43.3	170	100
A5	0.51	43.3	200	100
A6	0.51	43.3	250	100
A7	0.68	26	50	100
A8	0.68	26	100	100
A9	0.68	26	140	100
A10	0.68	26	170	100
A11	0.68	26	200	100
A12	0.68	26	250	100
A13	0.61	35	50	100
A14	0.61	35	100	100
A15	0.61	35	140	100
A16	0.61	35	170	100
A17	0.61	35	200	100
A18	0.61	35	250	100

Table 5.2: Details of composite beams with different opening size in the transverse direction, type B

Beam Model	Degree of shear interaction, k_s	Concrete cube strength, f_{cu} *(MPa)*	Opening size	
			a (mm)	f (mm)
B1	0.76	43.3	50	100
B2	0.76	43.3	100	100
B3	0.76	43.3	140	100
B4	0.76	43.3	170	100
B5	0.76	43.3	200	100
B6	0.76	43.3	250	100
B7	1.00	26	50	100
B8	1.00	26	100	100
B9	1.00	26	140	100
B10	1.00	26	170	100
B11	1.00	26	200	100
B12	1.00	26	250	100
B13	0.91	35	50	100
B14	0.91	35	100	100
B15	0.91	35	140	100
B16	0.91	35	170	100
B17	0.91	35	200	100
B18	0.91	35	250	100

Table 5.3: Details of composite beams with different opening size in the transverse direction, type C

Beam Model	Degree of shear interaction, k_s	Concrete cube strength, f_{cu} *(MPa)*	Opening size	
			a (mm)	f (mm)
C1	0.54	43.3	50	100
C2	0.54	43.3	100	100
C3	0.54	43.3	140	100
C4	0.54	43.3	170	100
C5	0.54	43.3	200	100
C6	0.54	43.3	250	100
C7	0.71	26	50	100
C8	0.71	26	100	100
C9	0.71	26	140	100
C10	0.71	26	170	100
C11	0.71	26	200	100
C12	0.71	26	250	100
C13	0.63	35	50	100
C14	0.63	35	100	100
C15	0.63	35	140	100
C16	0.63	35	170	100
C17	0.63	35	200	100
C18	0.63	35	250	100

5.2.2 Openings size in the longitudinal direction

Layout of composite beam models used to investigate the effect of openings size in longitudinal direction (second parameter) is shown in Figure 5.2. The opening size in the transverse direction, **a,** was kept constant, while the opening size in the longitudinal direction, **f** varied.

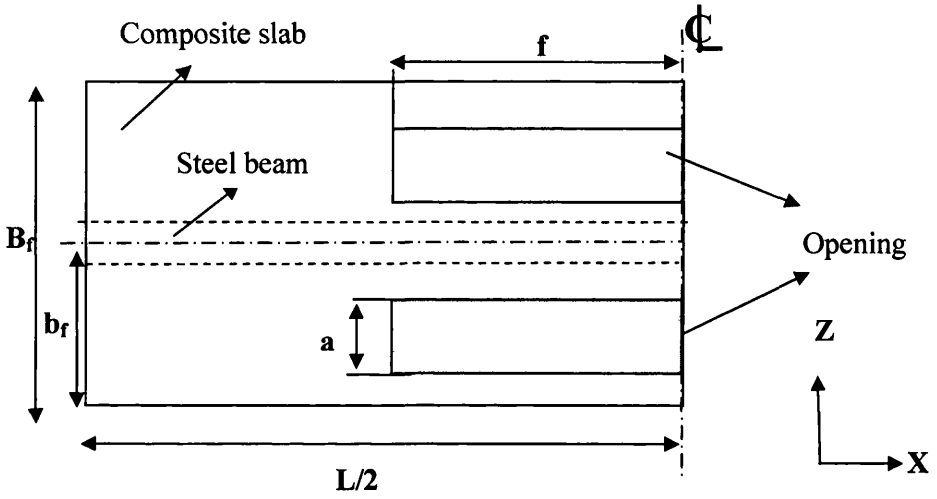

Figure 5.2: Layout of composite beam model with different openings size in longitudinal direction in metal-ribbed decking slab.

Nine models (A1-f1, A1-f2, A1-f3, B1-f1, B1-f2, B1-f3, C1-f1, C1-f2, C1-f3) were studied in the investigation. They are identified in terms of openings size in the longitudinal direction, **f**. Cube strength was selected as 43.1 MPa. Details of the openings for these models are shown in Table 5.4.

Table 5.4: Details of composite beams with different opening size in the longitudinal direction

Beam Model	Degree of shear interaction, k_s	Concrete cube strength, f_{cu} *(MPa)*	Opening size	
			a (mm)	f (mm)
A1-f1	0.51	43.3	250	200
A1-f2	0.51	43.3	250	400
A1-f3	0.51	43.3	250	900
B1-f1	0.76	43.3	250	100
B1-f2	0.76	43.3	250	400
B1-f3	0.76	43.3	250	900
C1-f1	0.54	43.3	250	100
C1-f2	0.54	43.3	250	400
C1-f3	0.54	43.3	250	900

5.3 Location of Openings

5.3.1 Openings location in longitudinal direction

Third parameter investigated was the effect of opening location. The distance of openings (d) is measured from the mid-span of the beam. In the FE analysis, the opening locations in the longitudinal direction were varied. Three different locations (d) examined in this study were 300mm, 500mm and 900mm. Eighteen models were used. Layout of composite beam model is shown in Figure 5.3. Table 5.5 summarises the parameters of the models used.

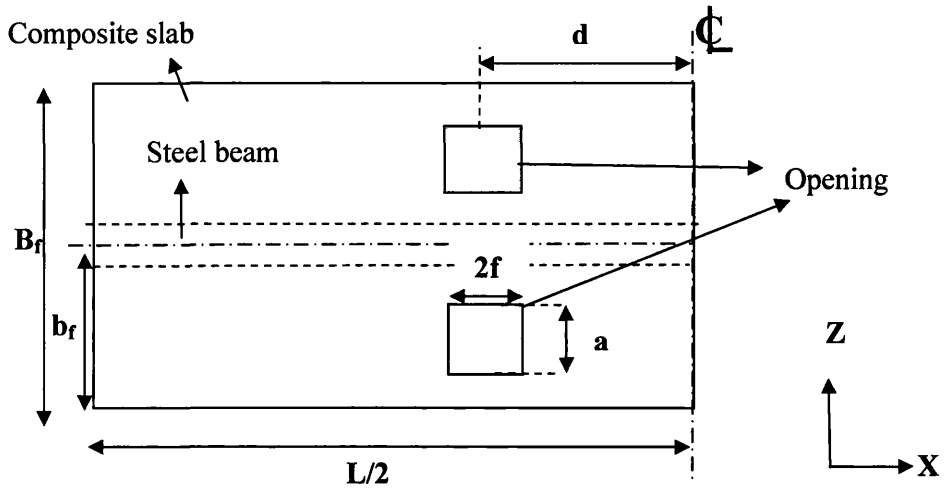

Figure 5.3: Layout of composite beam model with different openings locations

Table 5.5: Details of composite beams with different opening locations

Beam Model	Degree of shear interaction, k_s	Concrete cube strength, f_{cu} *(MPa)*	Opening parameter		
			a (mm)	f (mm)	d (mm)
A1-L1	0.51	43.3	170	100	400
A1-L2	0.51	43.3	170	100	800
B1-L1	0.76	43.3	170	100	400
B1-L2	0.76	43.3	170	100	800

5.3.2 Openings with different load location

Fourth parameter investigated was the load location on composite beams with openings. All models were simply supported, loaded by concentrated loads applied symmetrically about the mid-span of the beam with different spacing ($2l_d$). The distance of load (l_d) was defined from central of the beam. The composite beam model used for the investigation is shown in Figure 5.4. In the numerical analyses, the load locations along the span were varied for each of the opening positions kept the same. Two different opening locations **(d)** used in this study were 600mm and 1000mm from the mid-span of the beam. Load was located at three different locations namely, opening front section, opening central section and opening end section shown in the Figure 5.4. There different load locations (l_d) for each opening location (d) were investigated. For opening with d=600mm, distance of load (l_d) were 400mm (front section), 600mm (central section) and 800mm (end section). For opening with d=1000mm, distance of load (l_d) were 800mm (front section), 1000mm (central section) and 1200mm (end section). Table 5.6 summarises the parameters of the models used for this study.

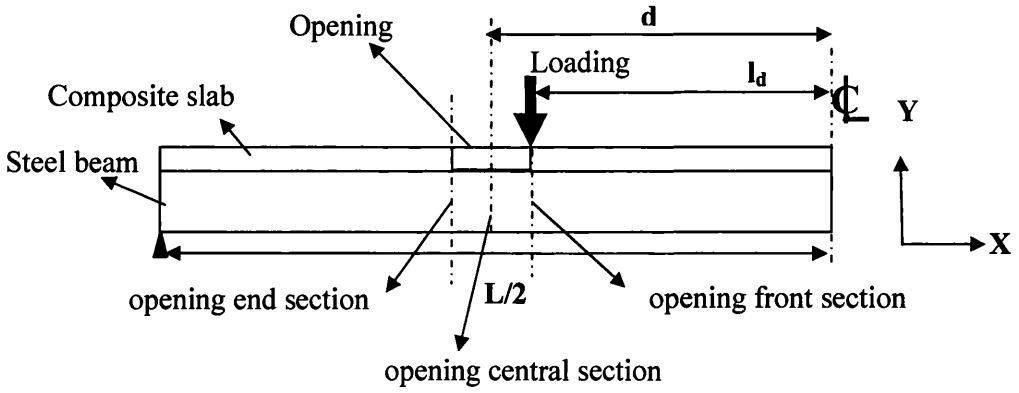

Figure 5.4: Layout of composite beam with openings with different load locations

Table 5.6: Details of the composite beams with openings and with different load locations

Beam Model	Degree of shear interaction, k_s	Concrete cube strength, f_{cu} (MPa)	Opening parameter			
			l_d (mm)	a (mm)	f (mm)	d (mm)
A1- Ld1	0.51	43.3	400	170	200	600
A1- Ld2	0.51	43.3	600	170	200	600
A1- Ld3	0.51	43.3	800	170	200	600
A1- Ld4	0.51	43.3	800	170	200	1000
A1- Ld5	0.51	43.3	1000	170	200	1000
A1- Ld6	0.51	43.3	1200	170	200	1000
B1- Ld1	0.51	43.3	400	170	200	600
B1- Ld2	0.76	43.3	600	170	200	600
B1- Ld3	0.76	43.3	800	170	200	600
B1- Ld4	0.76	43.3	800	170	200	1000
B1- Ld5	0.76	43.3	1000	170	200	1000
B1- Ld6	0.76	43.3	1200	170	200	1000

5.3.3 Two openings with different position

Another case was the positions of two openings in composite beam flange. If there are two openings, its can be located either in same flange side or different flange side as shown in Figure 5.5. In Figure 5.5, openings are numbered as 1 and 2. Reason for this study is to investigate the difference in moment capacity between two openings position (same flange side or different flange side). Table 5.7 summarise the parameters used for this study.

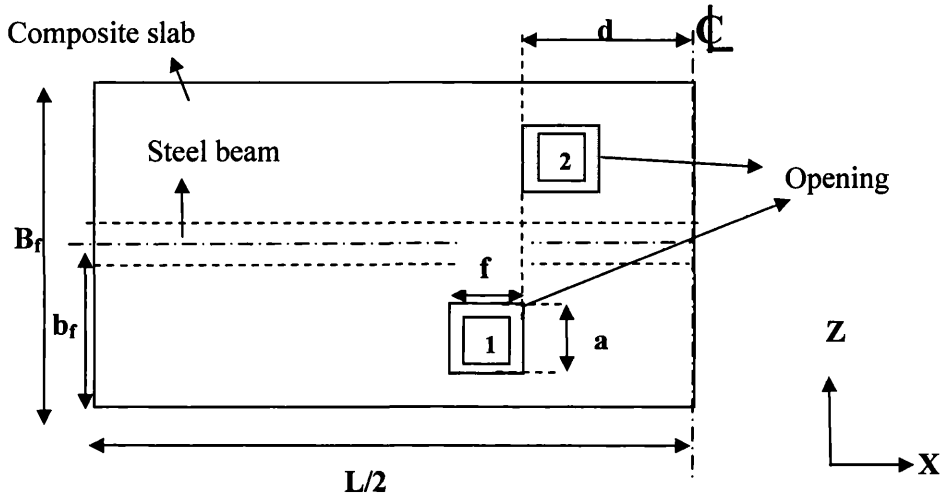

a) Openings located at different side of flange

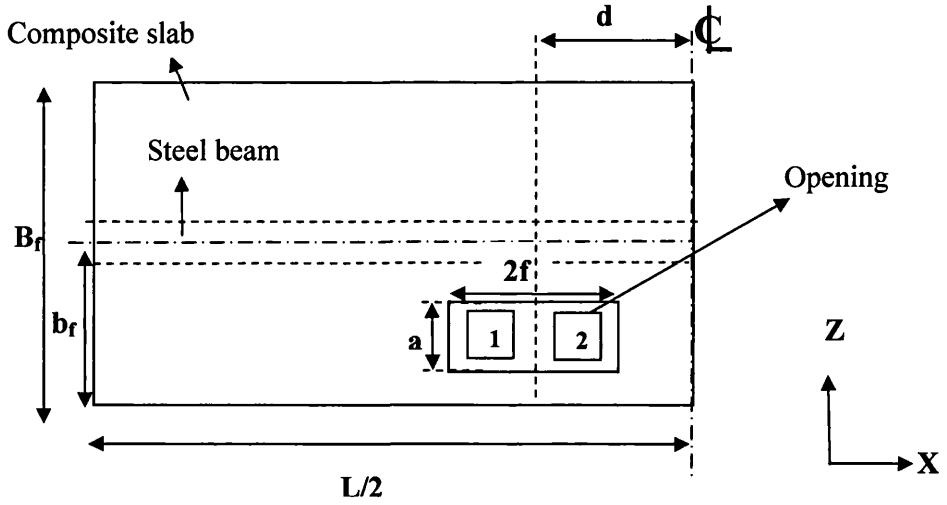

b) Openings located at same side of flange

Figure 5.5: Layout of composite beam with different opening position (same side of flange or similar side of flange)

Table 5.7: Details of the composite beams with two openings with different location (same side of flange or different side of flange)

Beam Model	Beam Span, L (mm)	Degree of shear interaction, k_s	Slab width, B_f, (mm)	Concrete cube strength, f_{cu} *(MPa)*	Opening parameter			
					Location of openings on flanges (one side or both side)	a (mm)	f (mm)	d (mm)
A1-P1	4.0	0.51	1000	43.3	one side	170	200	600
A1-P2	4.0	0.51	1000	43.3	both side	170	200	600
A1-P3	4.0	0.51	1000	43.3	one side	250	200	600
A1-P4	4.0	0.51	1000	43.3	both side	250	200	600
B1-P1	4.0	0.76	1000	43.3	one side	170	200	600
B1-P2	4.0	0.76	1000	43.3	both side	170	200	600
B1-P3	4.0	0.76	1000	43.3	one side	250	200	600
B1-P4	4.0	0.76	1000	43.3	both side	250	200	600

5.4 Parametric study on the method to increase the ultimate moment of composite beams with openings in metal-ribbed decking slab

5.4.1 General

Openings will reduce the moment capacity of the composite beams. Contractor's and engineer's often increase slab thickness, install steel reinforcement bar (rebar) or increase steel beam dimension to counter the openings effect in composite beam slab. Even though this technique will normally increase the capacity of composite beam without openings, the aim of this study is to investigate how the beam capacity is maintained in order to avoid too costly approach or leading to inadequate in beam design. Hence the parametric study was conducted to study the suitable methods to increase the moment capacity of the composite beams with openings in metal-ribbed decking. The parameters considered were the concrete strength, overall slab thickness and steel reinforcement bar (rebar). Fifty four FE model with three different

dimensions of metal-ribbed decking (type A, type B and type C as shown in Fig.4.6) and openings size, a, 140 mm were considered in this study.

5.4.2 Concrete strength

Results in Chapter 4, section 4.4.2.2 show that, by increasing the concrete compressive strength from 26 MPa to 43.3 MPa ultimate moment of composite beams with metal decking is increased approximately by 9% to 11%. However, these results refer to composite beams without openings. In order to study composite beam with opening in metal-ribbed decking slab analyses were carried out in which openings size was varied in transverse axis direction as shown in Table 5.1 to Table 5.3 with cube strength 43.3 MPa and 26 MPa.

5.4.3 Slab thickness

This section describes a comprehensive parametric study to investigate the difference in moment capacity of composite beam with openings with different overall slab thickness. Four different slab thicknesses were used, 110 mm, 115 mm, 120 mm and 125mm. One of the models in **section 5.2.1** (T1) has been used as a reference. This model had an overall slab thickness of 105 mm, opening size in transverse direction (a) and longitudinal direction (f), 140mm and 200mm, respectively. Parameters of all models are shown in Table 5.8 to Table 5.10.

Table 5.8: Details of the composite beams with openings and with different overall slab thickness, A Type

Beam Model	Degree of shear interaction, k_s (%)	Concrete cube strength, f_{cu} *(MPa)*	Slab thickness (mm)	Opening size	
				a (mm)	f (mm)
A-T1	51	43.3	105	140	200
A-T2	46	43.3	110	140	200
A-T3	41	43.3	115	140	200
A-T4	40	43.3	120	140	200
A-T5	40	43.3	125	140	200
A-T6	68	26	105	140	200
A-T7	61	26	110	140	200
A-T8	56	26	115	140	200
A-T9	51	26	120	140	200
A-T10	47	26	125	140	200
A-T11	61	35	105	140	200
A-T12	55	35	110	140	200
A-T13	50	35	115	140	200
A-T14	45	35	120	140	200
A-T15	42	35	125	140	200

Table 5.9: Details of the composite beams with openings and with different overall slab thickness, B Type

Beam Model	Degree of shear interaction, k_s (%)	Concrete cube strength, f_{cu} *(MPa)*	Slab thickness (mm)	Opening size	
				a (mm)	f (mm)
B-T1	123	43.3	105	140	200
B-T2	111	43.3	110	140	200
B-T3	101	43.3	115	140	200
B-T4	92	43.3	120	140	200
B-T5	85	43.3	125	140	200
B-T6	179	26	105	140	200
B-T7	161	26	110	140	200
B-T8	146	26	115	140	200
B-T9	134	26	120	140	200
B-T10	124	26	125	140	200
B-T11	146	35	105	140	200
B-T12	131	35	110	140	200
B-T13	119	35	115	140	200
B-T14	109	35	120	140	200
B-T15	101	35	125	140	200

Table 5.10: Details of the composite beams with openings and with different overall slab thickness, C Type

Beam Model	Degree of shear interaction, k_s (%)	Concrete cube strength, f_{cu} *(MPa)*	Slab thickness (mm)	Opening size	
				a (mm)	f (mm)
C-T1	85	43.3	105	140	200
C-T2	78	43.3	110	140	200
C-T3	72	43.3	115	140	200
C-T4	67	43.3	120	140	200
C-T5	63	43.3	125	140	200
C-T6	124	26	105	140	200
C-T7	113	26	110	140	200
C-T8	105	26	115	140	200
C-T9	98	26	120	140	200
C-T10	91	26	125	140	200
C-T11	92	35	105	140	200
C-T12	84	35	110	140	200
C-T13	78	35	115	140	200
C-T14	72	35	120	140	200
C-T15	68	35	125	140	200

5.4.4 Area of reinforcement bar (rebar)

In this section, the effect of variation in steel reinforcement area will be assessed. The results obtained were used to propose suitable design method to design composite beam with openings reinforced with reinforcing bar which described in details in Chapter 6. The rebars were placed on the longitudinal axis, at the top of shear studs, as shown in Figure 5.6. Rebars were placed within the effective width of composite beam. Six different cross section area of rebar were used in this study, which were: 56.56 mm^2 (2xR6), 226.22 mm^2 (2xR12), 402.18 mm^2 (2xR16), 113.11 mm^2 (4xR6), 452.45 mm^2 (4xR12), and 804.35 mm^2 (4xR16). For the two rebars case, bars were

located at outermost side of flange next to opening. Four rebars, bars were located at outermost side and innermost side of flange next to opening.

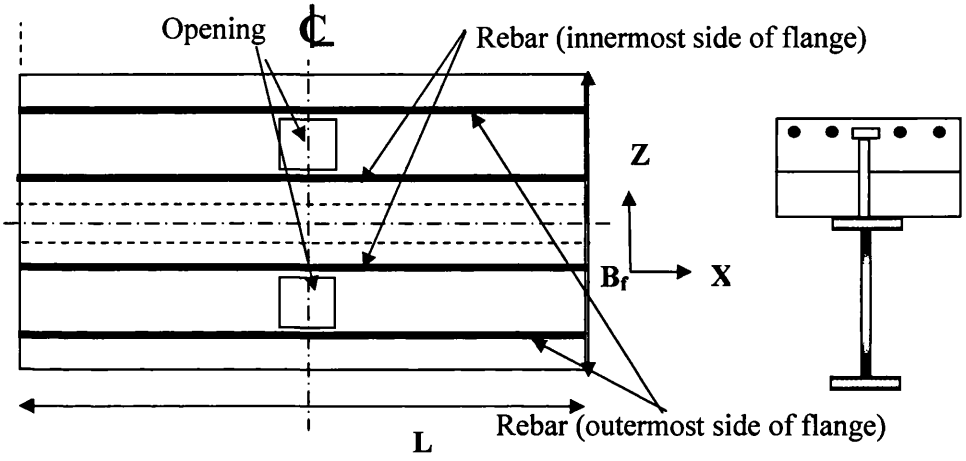

Figure 5.6: Layout of rebar next to the openings.

Rebar was idealised in the FE model by using the LINK8 element and was assumed to have full bonding with the concrete. To provide a perfect bond, the link element for steel reinforcing was connected between the nodes of each adjacent concrete solid element, so the two materials shared the same nodes. Figure 5.7 illustrates the element connectivity. Tables 5.11 to 5.13 summarise the parameters used in this study.

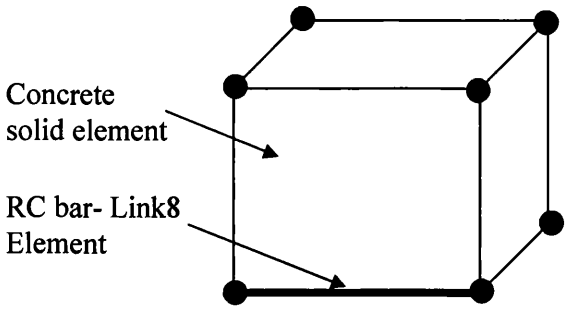

Figure 5.7: Element connectivity between concrete-solid element and rebar-link element.

Table 5.11: Details of the composite beams with openings and with different rebar area, A Type

Beam Model	Concrete cube strength, f_{cu} *(MPa)*	Rebar area (mm^2)	Opening size	
			a (mm)	f (mm)
A-R1	43.3	(2R6) 56.56	140	200
A-R2	43.3	(2R12) 226.22	140	200
A-R3	43.3	(2R16) 402.18	140	200
A-R4	43.3	(4R6) 113.11	140	200
A-R5	43.3	(4R12) 452.45	140	200
A-R6	26	(4R16) 804.35	140	200
A-R7	26	(2R6) 56.56	140	200
A-R8	26	(2R12) 226.22	140	200
A-R9	26	(2R16) 402.18	140	200
A-R10	26	(4R6) 113.11	140	200
A-R11	26	(4R12) 452.45	140	200
A-R12	26	(4R16) 804.35	140	200
A-R13	35	(2R6) 56.56	140	200
A-R14	35	(2R12) 226.22	140	200
A-R15	35	(2R16) 402.18	140	200
A-R16	35	(4R6) 113.11	140	200
A-R17	35	(4R12) 452.45	140	200
A-R18	35	(4R16) 804.35	140	200

Table 5.12: Details of the composite beams with openings and with different rebar area, B Type

Beam Model	Concrete cube strength, f_{cu} *(MPa)*	Rebar area (mm^2)	Opening size	
			a (mm)	f (mm)
B-R1	43.3	(2R6) 56.56	140	200
B-R2	43.3	(2R12) 226.22	140	200
B-R3	43.3	(2R16) 402.18	140	200
B-R4	43.3	(4R6) 113.11	140	200
B-R5	43.3	(4R12) 452.45	140	200
B-R6	26	(4R16) 804.35	140	200
B-R7	26	(2R6) 56.56	140	200
B-R8	26	(2R12) 226.22	140	200
B-R9	26	(2R16) 402.18	140	200
B-R10	26	(4R6) 113.11	140	200
B-R11	26	(4R12) 452.45	140	200
B-R12	26	(4R16) 804.35	140	200
B-R13	35	(2R6) 56.56	140	200
B-R14	35	(2R12) 226.22	140	200
B-R15	35	(2R16) 402.18	140	200
B-R16	35	(4R6) 113.11	140	200
B-R17	35	(4R12) 452.45	140	200
B-R18	35	(4R16) 804.35	140	200

Table 5.13: Details of the composite beams with openings and with different rebar area, C Type

Beam Model	Concrete cube strength, f_{cu} *(MPa)*	Rebar area (mm^2)	Opening size	
			a (mm)	f (mm)
C-R1	43.3	(2R6) 56.56	140	200
C-R2	43.3	(2R12) 226.22	140	200
C-R3	43.3	(2R16) 402.18	140	200
C-R4	43.3	(4R6) 113.11	140	200
C-R5	43.3	(4R12) 452.45	140	200
C-R6	26	(4R16) 804.35	140	200
C-R7	26	(2R6) 56.56	140	200
C-R8	26	(2R12) 226.22	140	200
C-R9	26	(2R16) 402.18	140	200
C-R10	26	(4R6) 113.11	140	200
C-R11	26	(4R12) 452.45	140	200
C-R12	26	(4R16) 804.35	140	200
C-R13	35	(2R6) 56.56	140	200
C-R14	35	(2R12) 226.22	140	200
C-R15	35	(2R16) 402.18	140	200
C-R16	35	(4R6) 113.11	140	200
C-R17	35	(4R12) 452.45	140	200
C-R18	35	(4R16) 804.35	140	200

5.5 Result and Discussion

5.5.1 Openings size in transverse direction

For type A decking (narrow-ribbed), all the curves are linear up to the first yield load and become non-linear thereafter. Most of the models sustain the linear stage approximately up to 80 kN. It can be seen from Figures 5.8 to 5.10 that the ultimate loads decrease with the increase of openings size in transverse direction, '**a**', (Refer to Fig.5.1). As in the case of model A12 which has lowest ultimate load for the A group (narrow-ribbed), the load-deflection behaviour is linear up to the first yield load equal to 77.02 kN and it becomes nonlinear thereafter. It is observed for model A1, A7 and A13 with opening ratio of 10% in transverse direction the ultimate load value were 165.62 kN, 151.15 kN and 156.56 kN, respectively, corresponding to a deflection of 52.81 mm, 41.87 mm and 41.87 mm, respectively. The corresponding ultimate load value is 153.88 kN, 143.49 kN and 147.35 kN with the opening size increased to 50%.

It can be seen from Table 5.14, the $\frac{P_o}{P_u}$ ratio shows that ultimate loads were reduced with the increase of opening ratio. In the table, P_o is ultimate load for composite beams with opening while P_u is ultimate load for composite beam without openings. The lowest value of $\frac{P_o}{P_u}$ ratio means higher reduction in ultimate load capacity. The results show that by increasing the openings size in transverse direction will decrease the ultimate load of composite beam. The results show that the ultimate load decrease by 2%, 1% and 2% when the opening size is increased by 10% in the direction of transverse axis for model A1, A7 and A8, respectively. The corresponding drop in ultimate load is 9%, 6% and 10% when the opening size increased to 50%. The results obtained are shown in Tables 5.14.

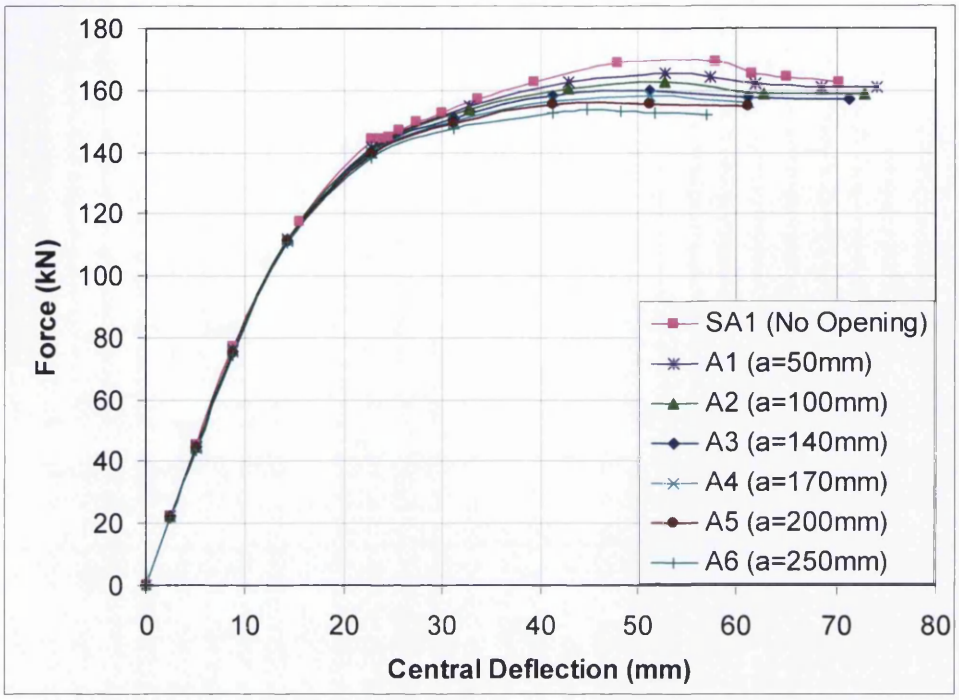

Figure 5.8: Load-deflection curves for composite beams with different openings size in transverse direction, (f_{cu}= 43.3 MPa)

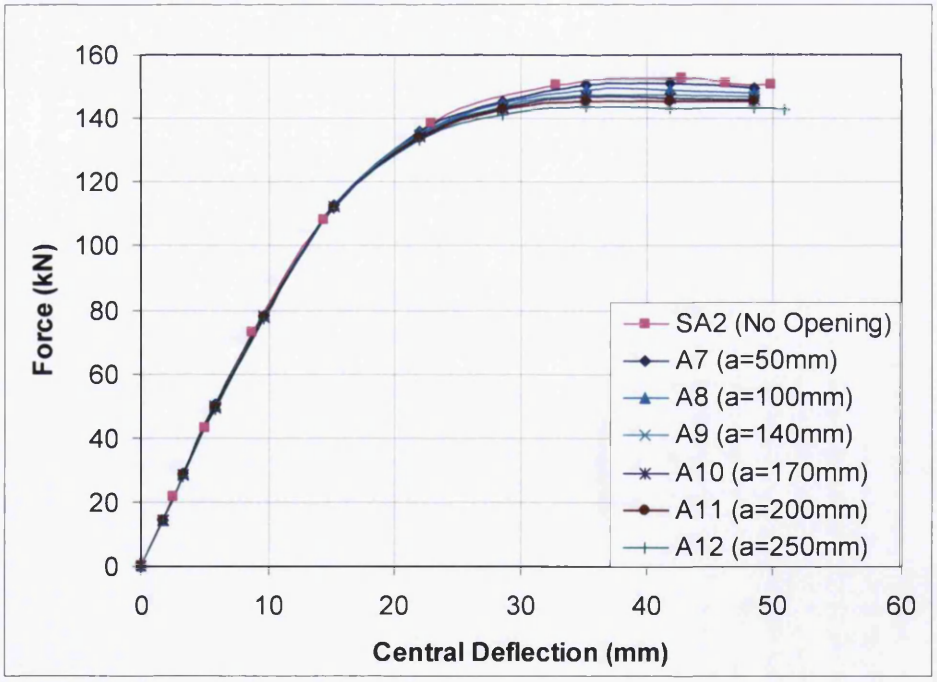

Figure 5.9: Load-deflection curves for composite beams with different openings size in transverse direction, (f_{cu}= 26 MPa)

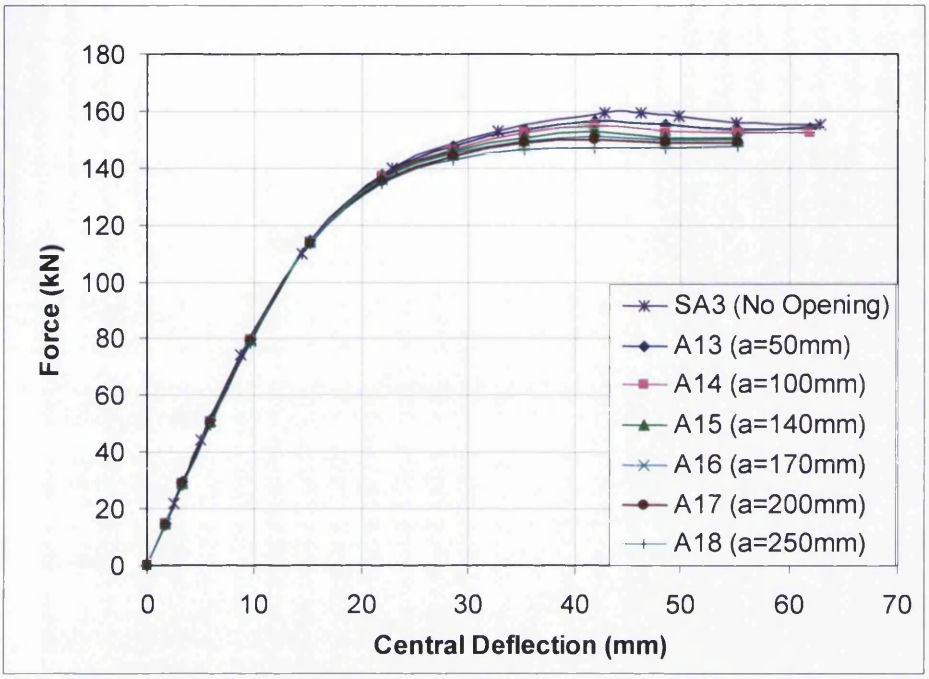

Figure 5.10: Load-deflection curves for composite beams with different openings size in transverse direction, (f_{cu} =35 MPa)

Table 5.14: Results for composite beam with different openings size in transverse direction, A type

Beam Model	Concrete cube strength, f_{cu} *(MPa)*	Opening parameter		Opening Ratio %	Ultimate Load (kN)	P_o/P_u
		a (mm)	f (mm)			
SA1	43.3	0	0	0	169.04	1.00
A1	43.3	50	100	10	165.62	0.98
A2	43.3	100	100	20	162.54	0.96
A3	43.3	140	100	28	160.06	0.95
A4	43.3	170	100	34	158.05	0.93
A5	43.3	200	100	40	155.68	0.92
A6	43.3	250	100	50	153.88	0.91
SA2	26	0	0	0	159.34	1.00
A7	26	50	100	10	156.56	0.98
A8	26	100	100	20	154.71	0.97
A9	26	140	100	28	152.80	0.96
A10	26	170	100	34	151.30	0.95
A11	26	200	100	40	149.69	0.94
A12	26	250	100	50	147.35	0.90
SA3	35	0	0	0	152.58	1.00
A13	35	50	100	10	151.15	0.99
A14	35	100	100	20	148.9	0.98
A15	35	140	100	28	147.66	0.97
A16	35	170	100	34	146.65	0.96
A17	35	200	100	40	145.56	0.95
A18	35	250	100	50	143.49	0.94

Load-deflection curves behaviour for B type model (wide-ribbed) are shown in Figure 5.11 to 5.13. Linear behaviour is observed at early stage of loading, after reaching the ultimate load, vertical deflection increased rapidly with the load. The load-deflection behaviour for this group is linear up to the first yield load averagely equal to 105 kN

and it becomes non-linear thereafter. It is observed that B1, B7 and B13 with opening ratio of 10%, ultimate load value is 181.54 kN, 165.48 kN and 171.63 kN, respectively. However for 50% opening ratio, the ultimate load were 165.53 kN, 144.61 kN and 154.53 kN, for B6, B12 and B18, respectively. As in the case of model B12, it has lowest ultimate load value which is 144.61 kN. The model has 26 MPa cube strength and 50% of opening ratio. The load-deflection plot of this model is almost linear up to 65% of the ultimate load and the beam show larger deflection with smaller increase in load above this point.

The results show that the ultimate load drops by 2%, 3% and 3%, when the opening size is increased by 10% in the direction of transverse direction for model B1, B7 and B8, respectively. The corresponding drop in ultimate load is 11%, 15% and 12% in ultimate load when the opening size increased to 50%. The results obtained for B type model is shown in Tables 5.15.

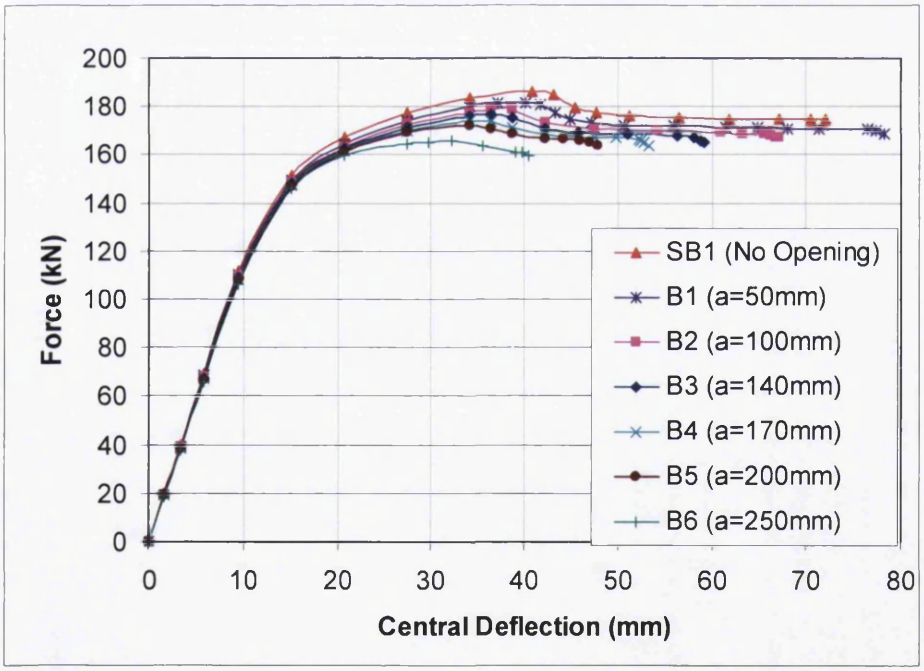

Figure 5.11: Load-deflection curves for composite beams with different openings size in transverse direction, (f_{cu}= 43.3 MPa)

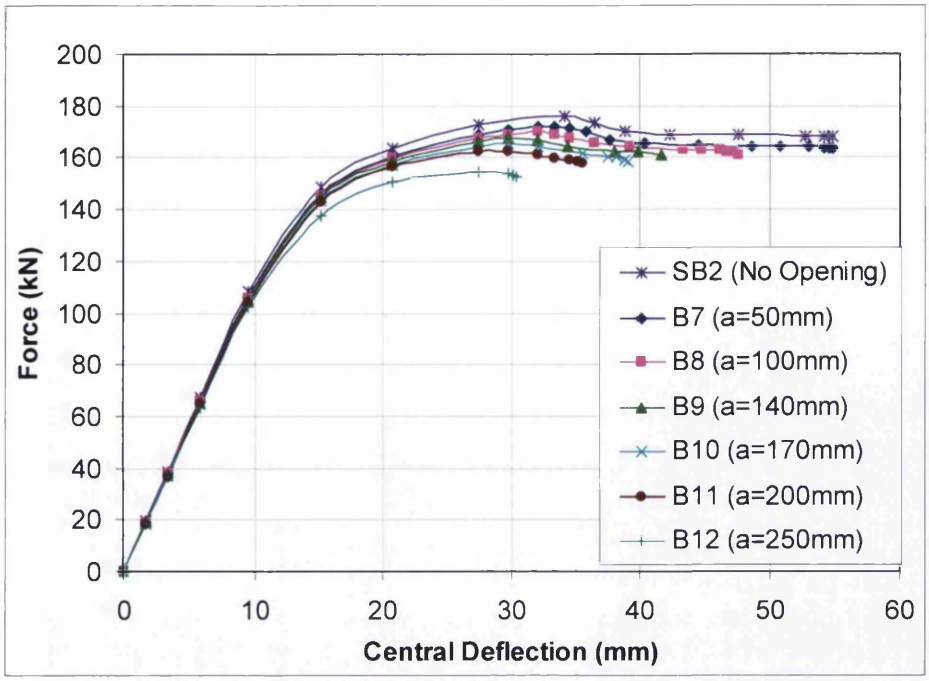

Figure 5.12: Load-deflection curves for composite beams with different openings size in transverse direction, (f_{cu}= 26 MPa)

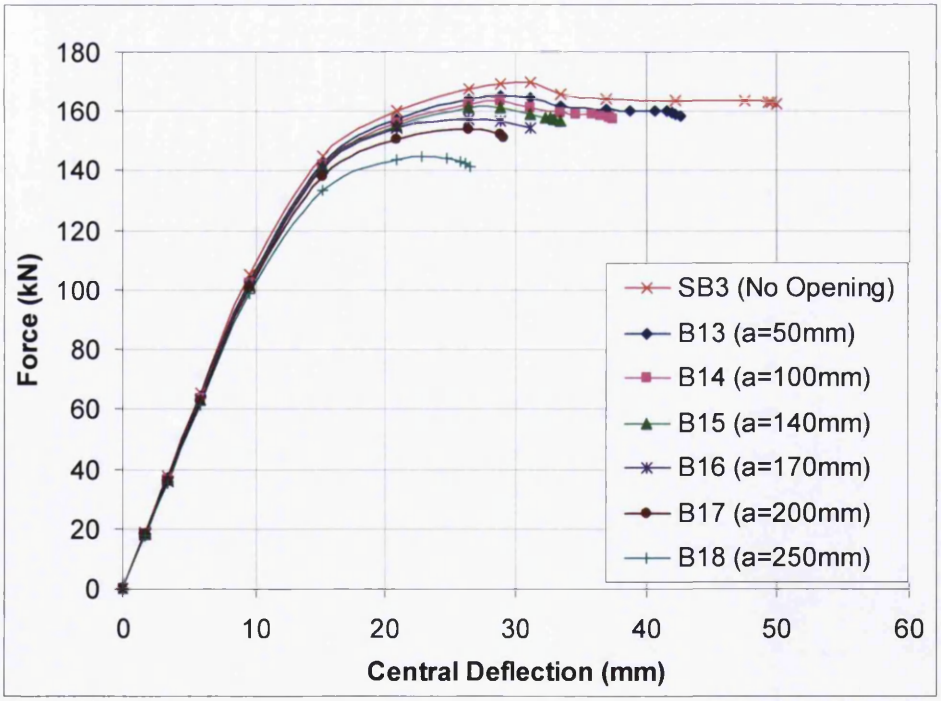

Figure 5.13: Load-deflection curves for composite beams with different openings size in transverse direction, (f_{cu}= 35 MPa)

Table 5.15: Results for composite beam with different openings size in transverse direction, B type

Beam Model	Concrete cube strength, f_{cu} *(MPa)*	Opening parameter		Opening Ratio %	Ultimate Load (kN)	P_o/P_u
		a (mm)	f (mm)			
SB1	43.3	0	0	0	185.96	1.00
B1	43.3	50	100	10	181.54	0.98
B2	43.3	100	100	20	178.55	0.96
B3	43.3	140	100	28	176.42	0.95
B4	43.3	170	100	34	173.97	0.94
B5	43.3	200	100	40	172.15	0.93
B6	43.3	250	100	50	165.53	0.89
SB2	26	0	0	0	169.74	1.00
B7	26	50	100	10	165.48	0.97
B8	26	100	100	20	163.50	0.96
B9	26	140	100	28	161.07	0.95
B10	26	170	100	34	157.43	0.93
B11	26	200	100	40	153.68	0.91
B12	26	250	100	50	144.61	0.85
SB3	35	0	0	0	176.18	1.00
B13	35	50	100	10	171.63	0.97
B14	35	100	100	20	169.78	0.96
B15	35	140	100	28	167.46	0.95
B16	35	170	100	34	165.24	0.94
B17	35	200	100	40	162.49	0.92
B18	35	250	100	50	154.53	0.88

Load-deflection plots for C groups are presented in Figures 5.14 to 5.16. The metal decking used in this group is classified as wide-ribbed similar classification to B groups but different in decking dimension. Similar pattern of load-deflection curve was observed when compared with A and C group. Load-deflection behaviour of this group is almost linear up to 80 to 85 kN and the showed a large deflection with increasing load thereafter. The stiffness of composite section contributed up to 55% of ultimate load. It is observed that for beam with 10% opening ratio, the ultimate load is 177.17 kN, 161.30 kN and 167.80 kN, for C1, C7 and C13, respectively. It is observed that model having higher opening ratio which is 50%, the ultimate load value is 161.30 kN, 144.18 kN and 152.57 kN, for C6, C12 and C18, respectively.

The results show that the ultimate load drops by 4%, 3% and 3%, when the opening size is increased by 10% in the direction of transverse direction for model C1, C7 and C8, respectively. The corresponding drop in ultimate load is 12%, 14% and 11% in ultimate load when the opening size increased to 50%.The results obtained are shown in Tables 5.16.

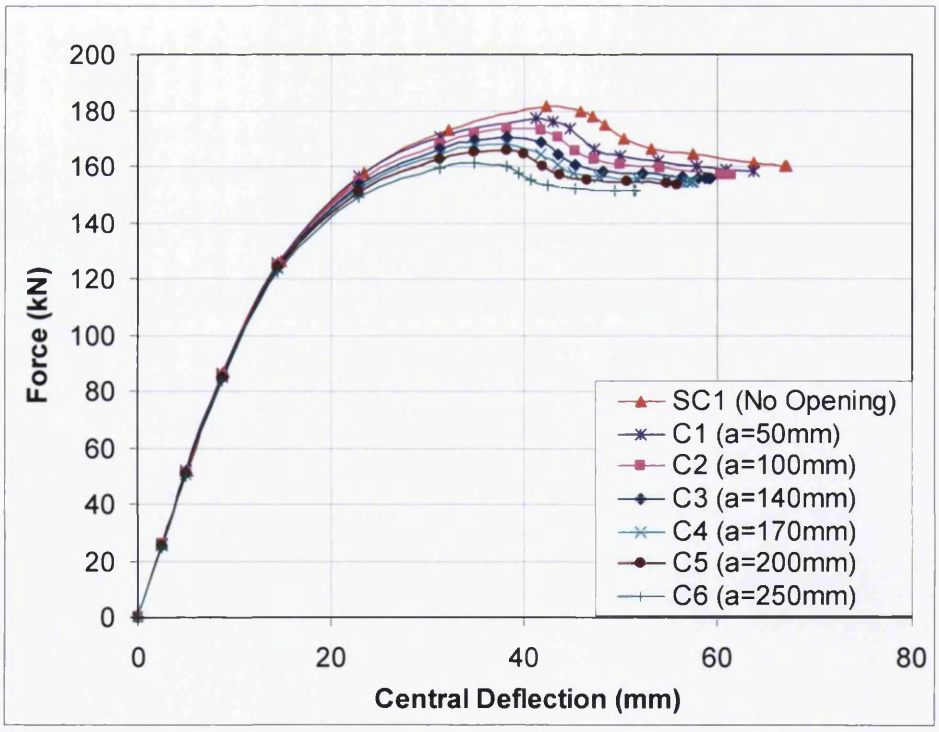

Figure 5.14: Load-deflection curves for composite beams with different openings size in transverse direction, (f_{cu}= 43.3 MPa)

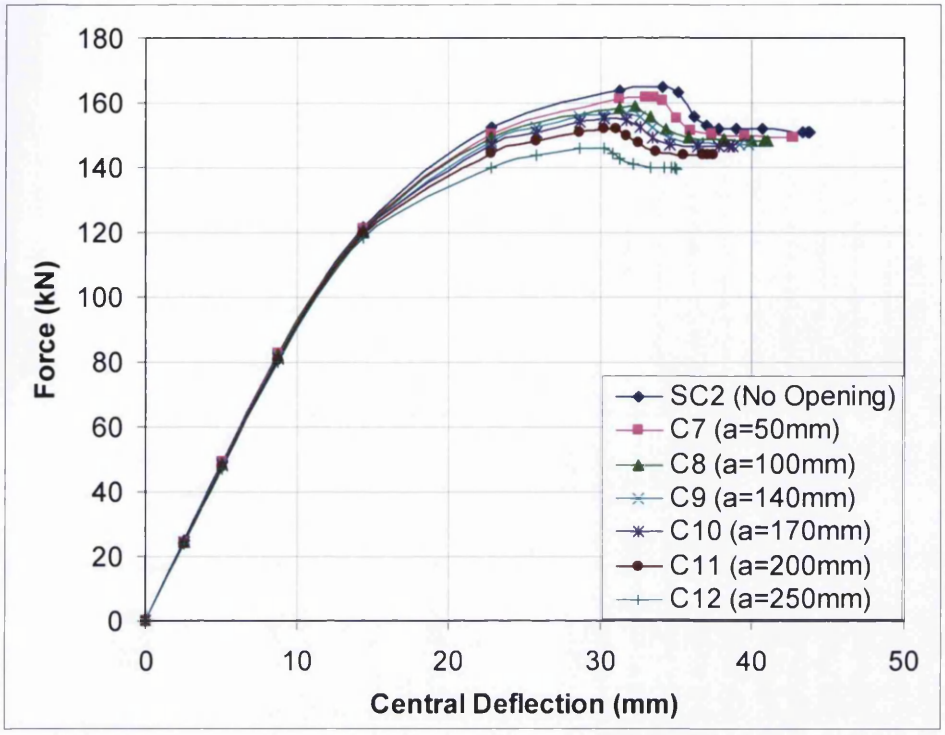

Figure 5.15: Load-deflection curves for composite beams with different openings size in transverse direction, (f_{cu}= 26 MPa)

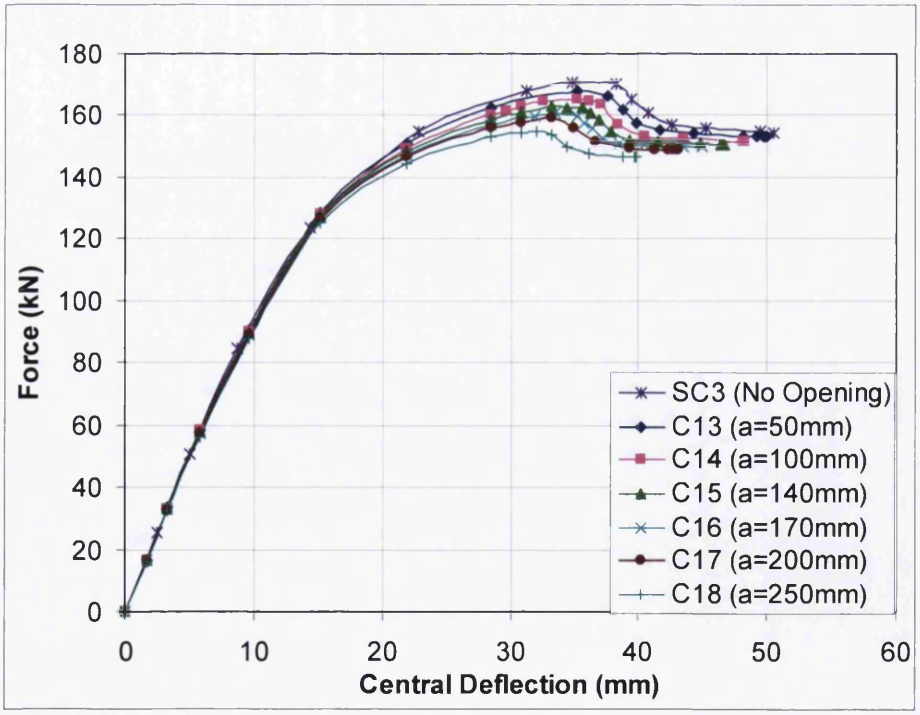

Figure 5.16: Load-deflection curves for composite beams with different openings size in transverse direction, (f_{cu}= 35 MPa)

Table 5.16: Results for composite beams with different openings size in transverse direction, C type

Beam Model	Concrete cube strength, f_{cu} *(MPa)*	Opening parameter		Opening Ratio %	Ultimate Load (kN)	P_o/P_u
		a (mm)	f (mm)			
SC1	43.3	0	0	0	183.89	1.00
C1	43.3	50	100	10	177.17	0.96
C2	43.3	100	100	20	173.59	0.94
C3	43.3	140	100	28	170.60	0.93
C4	43.3	170	100	34	168.15	0.91
C5	43.3	200	100	40	165.47	0.90
C6	43.3	250	100	50	161.30	0.88
SC2	26	0	0	0	167.13	1.00
C7	26	50	100	10	161.63	0.97
C8	26	100	100	20	158.82	0.95
C9	26	140	100	28	155.91	0.93
C10	26	170	100	34	154.79	0.93
C11	26	200	100	40	149.93	0.90
C12	26	250	100	50	144.18	0.86
SC3	35	0	0	0	172.28	1.00
C13	35	50	100	10	167.80	0.97
C14	35	100	100	20	164.75	0.96
C15	35	140	100	28	162.68	0.94
C16	35	170	100	34	160.74	0.93
C17	35	200	100	40	158.94	0.92
C18	35	250	100	50	152.57	0.89

As explained in the parametric study in section 4.6.2, composite slab serves as compressive component. The capacity of composite beam depends on its compressive strength. Openings reduce the flange width at cross section corresponding to the opening position, which consequently reduce the effective width of the flange, as shown in Figure 5.17. Beyond the ultimate load, the composite slab loses its load

carrying capacity due to concrete crushing, and the models eventually failed when a plastic hinge formed in the steel beam. All models failed in bending.

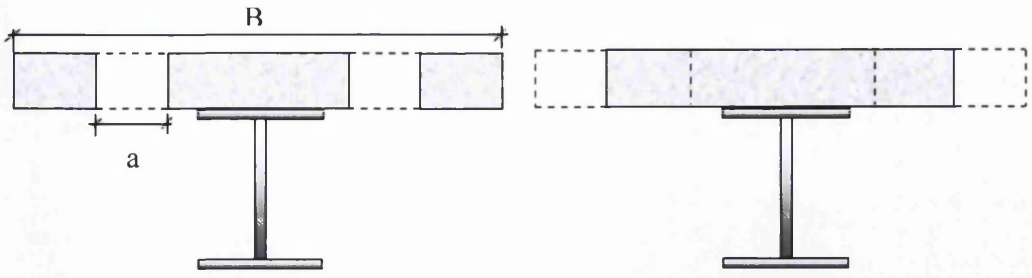

(a) Flange with opening (b) Net effective width

Figure 5.17: Typical section of the composite beams with openings

A typical stress contour of composite beams obtained from finite element analysis is shown in Fig. 5.18. The figure shows the formation of yield stress at mid-span of the beam. The development of plastic hinge is shown by yield stress formed in the steel beam. The high level of yielding in the steel beam can be clearly seen in the diagram. High stress in steel beam starts just after the development of high compressive stress in concrete slab and extends to other region of steel beam with the increase of load.

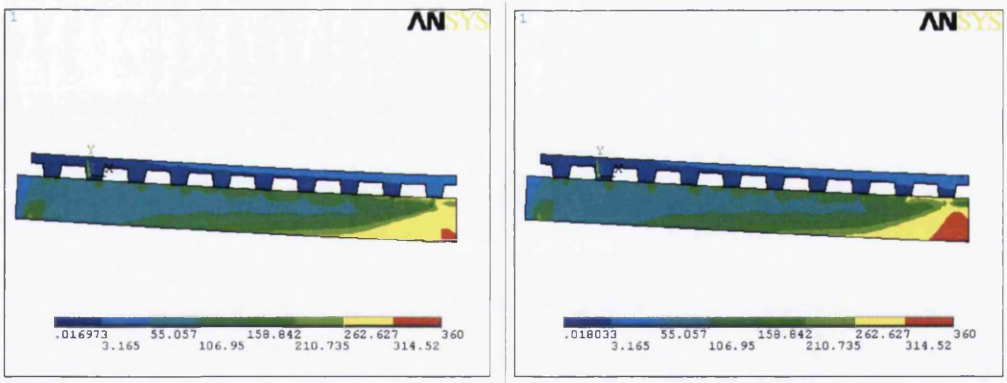

a) At first yield b) At final load

Figure 5.18: Development of yield stress in the steel beam, unit in MPa

The initiation and development of stress in ribbed decking slab is shown in Fig 5.19 and 5.20 for model A2 and A6, respectively. Generally, with the increase in load, development of high compressive stress is initiated at beam centre and outermost side of opening and then high compressive stress extends to the whole side of opening. For higher openings ratio, as in the case of model A6, development of high compressive

stress is initiated at lower applied load compared to model A1 which has lower opening ratio.

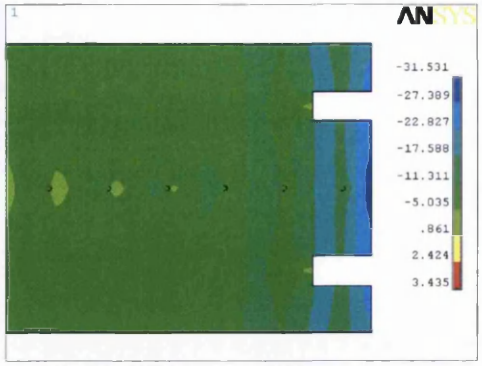

a) Load 140.76 kN

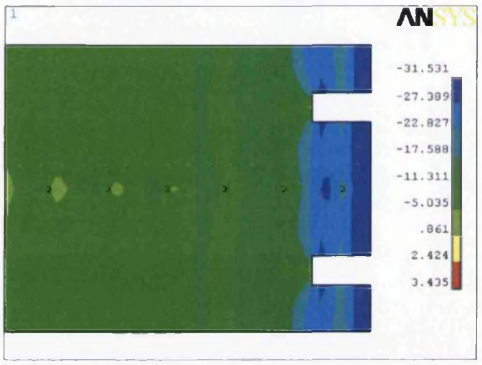

b) Load 153.49 kN

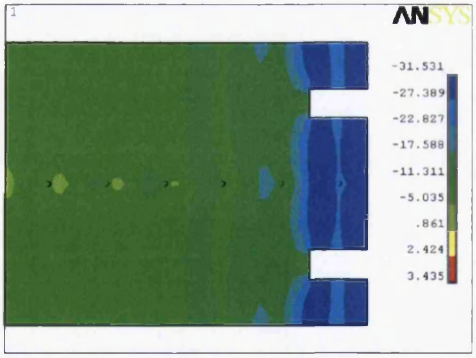

c) Load 160.32 kN

Figure 5.19: Developemnt of stress in slab for model A2, unit in MPa

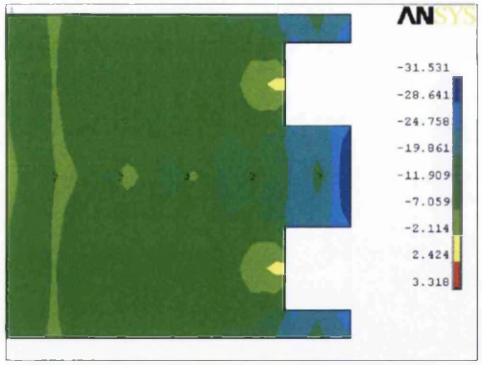

a) Load 138.14 kN

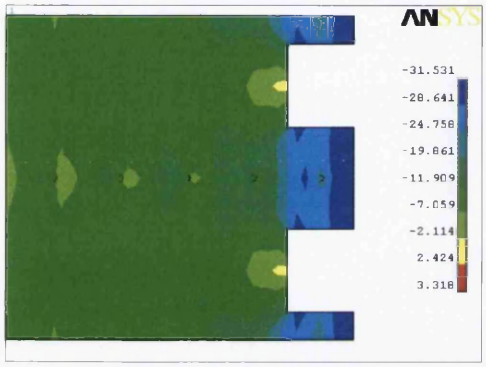

b) Load 147.70 kN

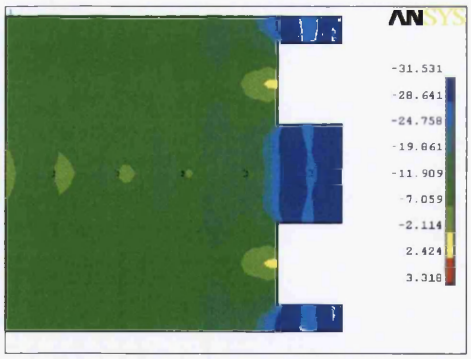

c) Load 152.76 kN

Figure 5.20: Development of stress in slab for model A6, unit in MPa

5.5.2 Opening size in the longitudinal direction

Figures 5.21 to 5.23 show the comparison of load-deflection curves for models with opening size in the direction of longitudinal axis. It can be seen from the figures that increase the openings size in longitudinal axis direction does not affect the ultimate load. This behaviour is contrary to the results for the models with opening size in transverse axis direction. Negligible effect on ultimate load is due to the fact that the width of composite beam flange is not reduced.

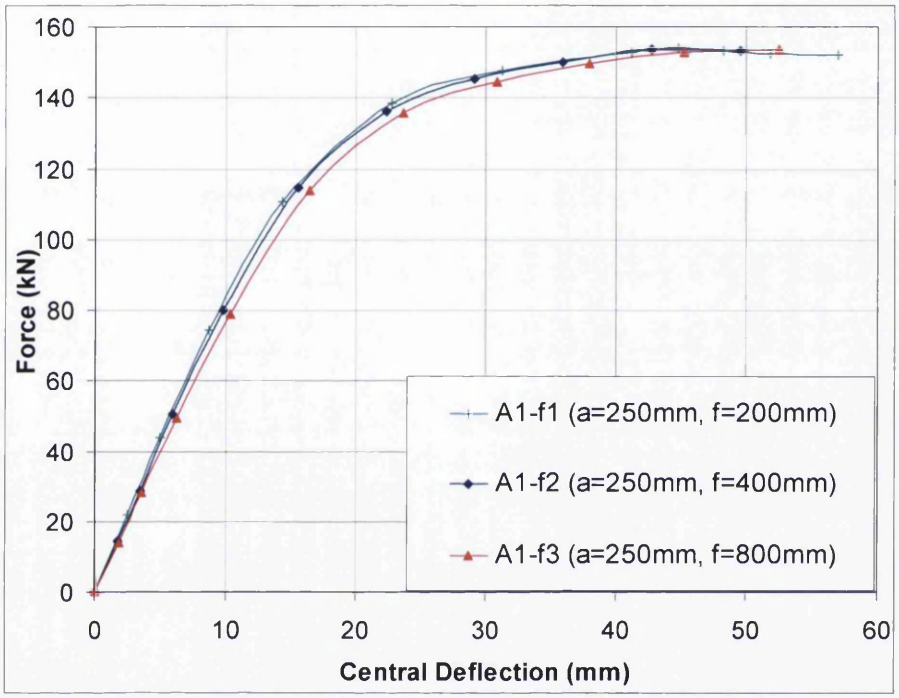

Figure 5.21: Load-deflection curves for different opening size in longitudinal axis, A type

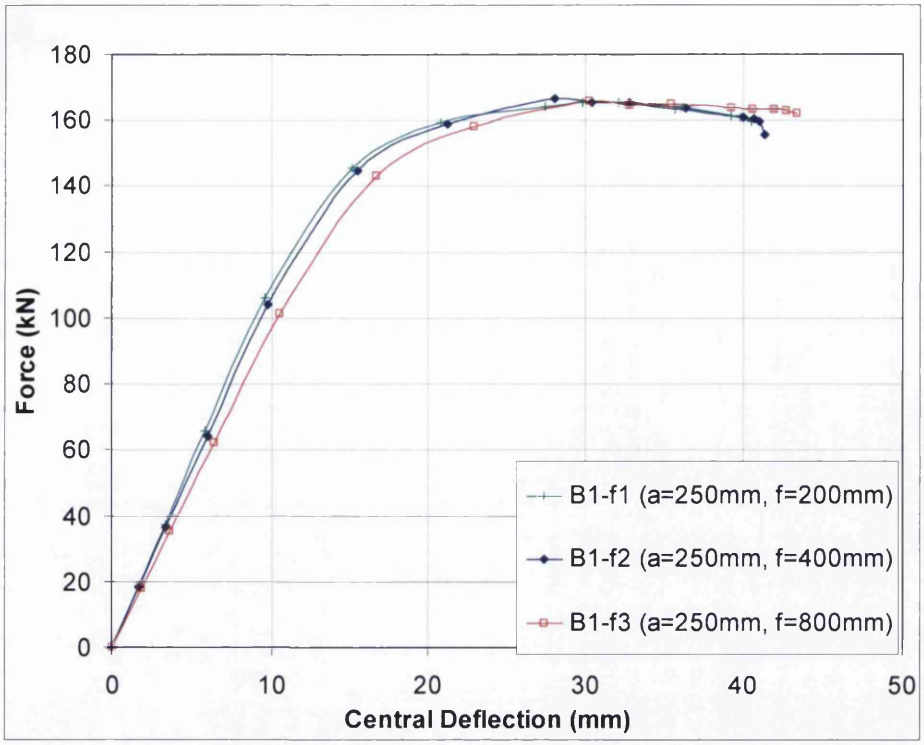

Figure 5.22: Load-deflection curves for different opening size in longitudinal axis, B type

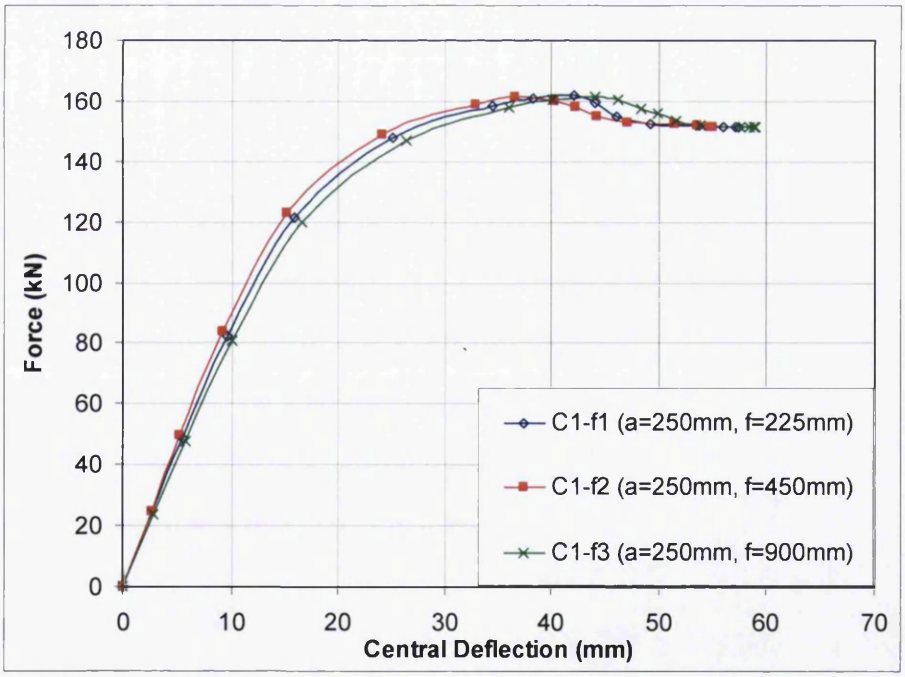

Figure 5.23: Load-deflection curves for different opening size in longitudinal axis, C type

Reduction in stiffness of the beams is, however, observed in the linear range with increase in the size of openings **(f)** as shown in Figures 5.24 to Figure 5.26. Reduction is attributed due to change of geometry of composite beams in the longitudinal axis. Reduction in stiffness can be associated with opening ratio. Opening ratio is defined by opening size in longitudinal direction divided by beam length.

Table 5.17 summarises the results from the parametric study. In the table, δ is deflection of composite beam with opening and δ_{no} is deflection for composite beam without opening. The table 5.17 show that $\frac{\delta}{\delta_{no}}$ ratio is increase with the increase of opening ratio (%). With opening ratio of 10%, the reduction of stiffness is approximately 4% compared with composite beam without opening. For opening ratio 40%, the reduction of stiffness is as high as 22%, as in the case of model B1-f3. From the numerical results, it can be concluded that the effect is significant when opening ratio is more than 20%.

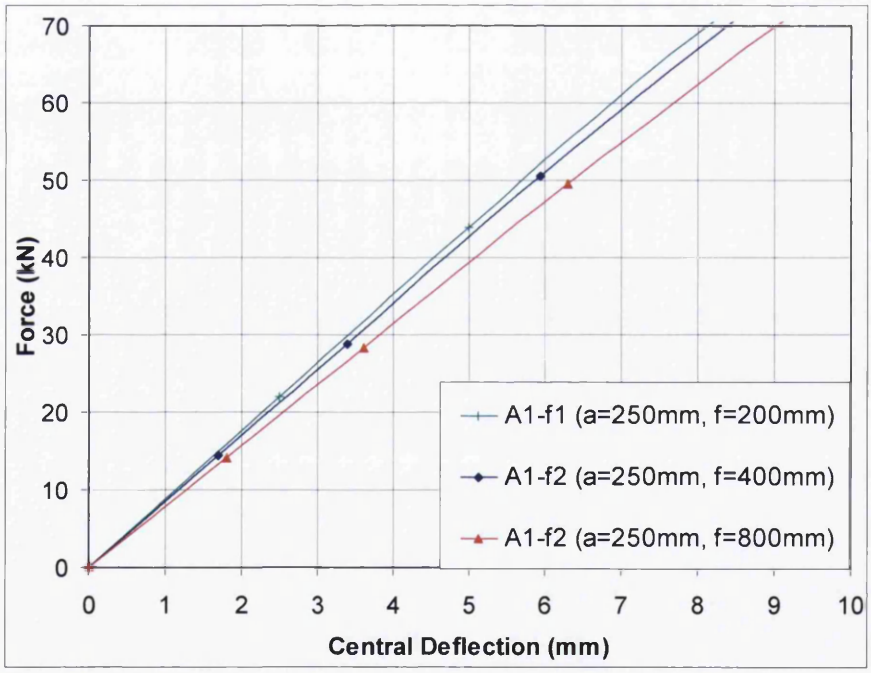

Figure 5.24: Load-deflection curves for different opening size in longitudinal axis, A type

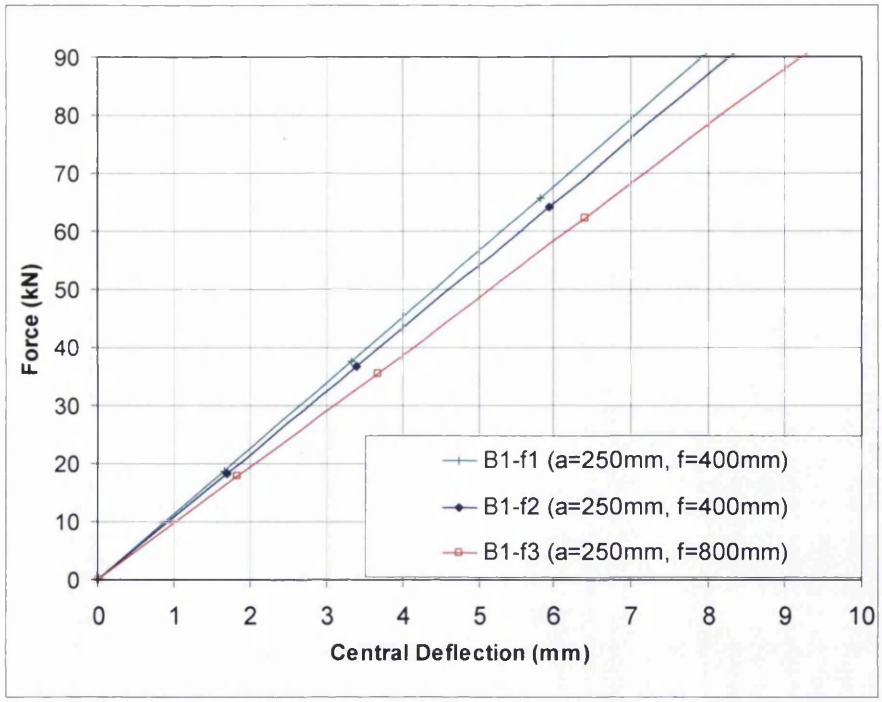

Figure 5.25: Load-deflection curves for different opening size in longitudinal axis, B type

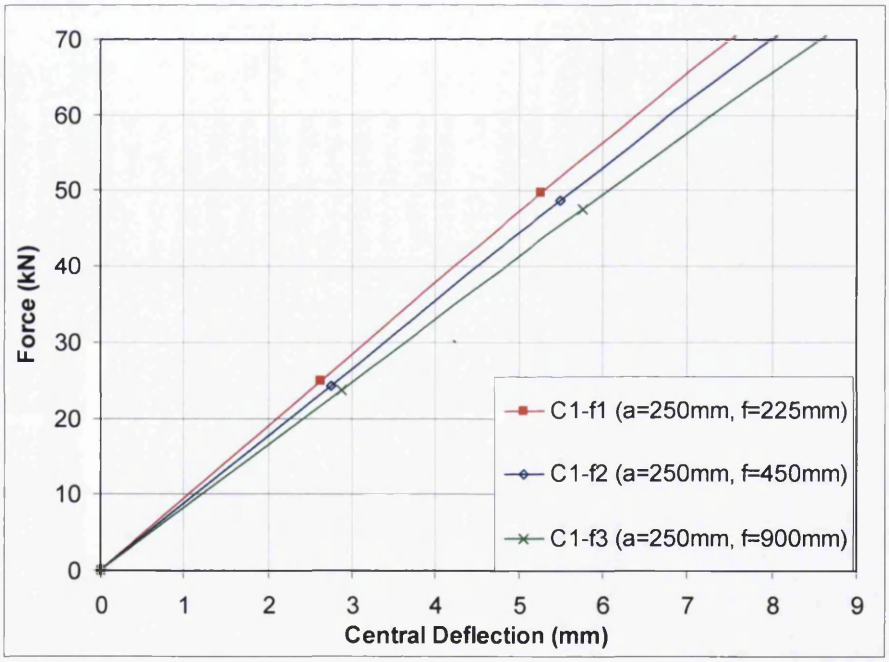

Figure 5.26: Load-deflection curves for different opening size in longitudinal axis, C type

Table 5.17: Results for opening size in the direction of longitudinal axis

Beam Model	Opening parameter		Opening Ratio (%)	Load at Deflection (kN)	δ (mm)	$\frac{\delta}{\delta_{no}}$
	a (mm)	f (mm)				
A1-f1	250	200	10	70	8.1	1.04
A1-f2	250	400	20	70	8.4	1.08
A1-f3	250	900	40	70	9.0	1.16
B1-f1	250	100	10	90	7.8	1.03
B1-f2	250	400	20	90	8.3	1.09
B1-f3	250	900	40	90	9.3	1.22
C1-f1	250	100	10	70	7.5	1.04
C1-f2	250	400	20	70	7.9	1.10
C1-f3	250	900	50	70	8.5	1.18

5.5.3 Location of Openings

5.5.3.1 Opening location in longitudinal direction

Figures 5.27 and 5.28 show the effect of opening location on load-deflection curves. Two different locations d=400mm and d=800mm were considered in the study. It can be seen that the beam stiffness and ultimate load are least affected when the openings are placed away from the mid-span.

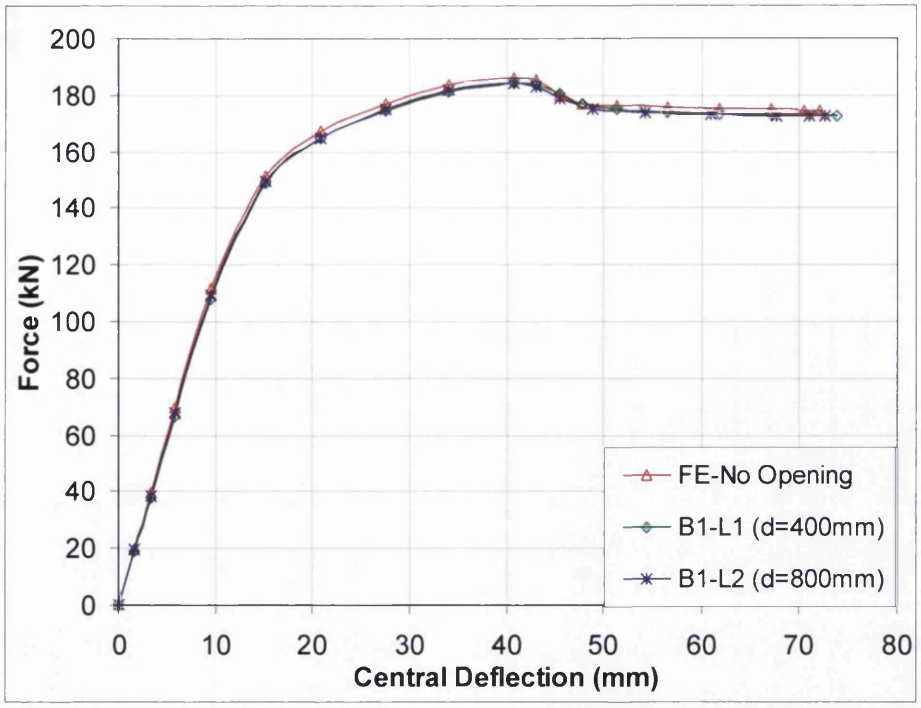

Figure 5.27: Load-deflection curves for different opening size in longitudinal axis.

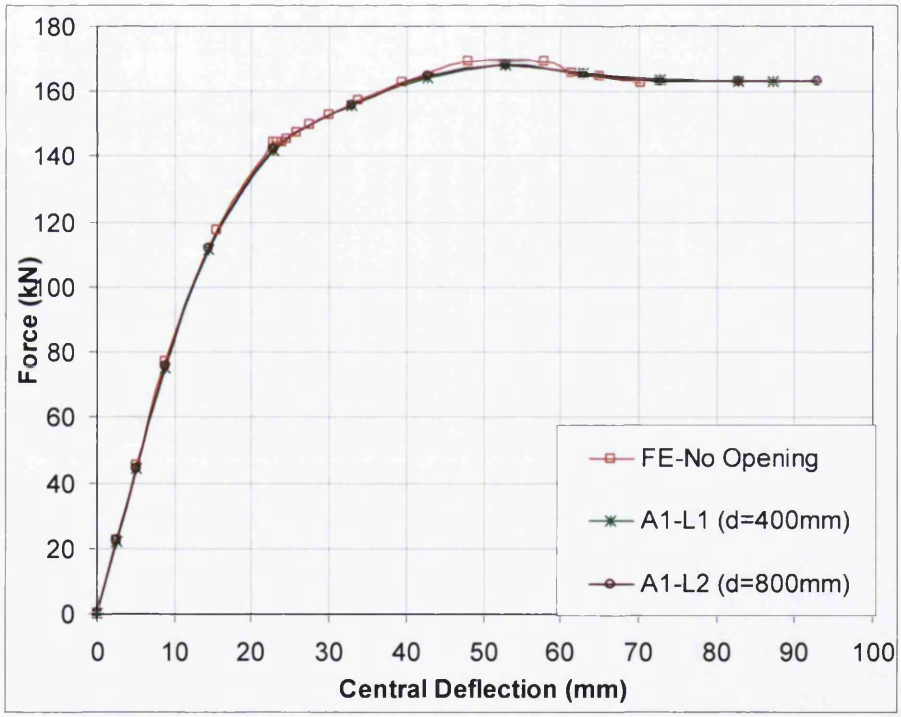

Figure 5.28: Load-deflection curves for different opening size in longitudinal axis.

Typical stress contour for this study obtained from finite element analysis is shown in Fig. 5.29. From the figure it can bee seen that for the beam subjected to central

loading, the high compressive stress in slab at beam centre does not affected by openings placed away from mid-span. Due to this reason, openings away from mid-span do not affect the load carrying capacity of composite beam.

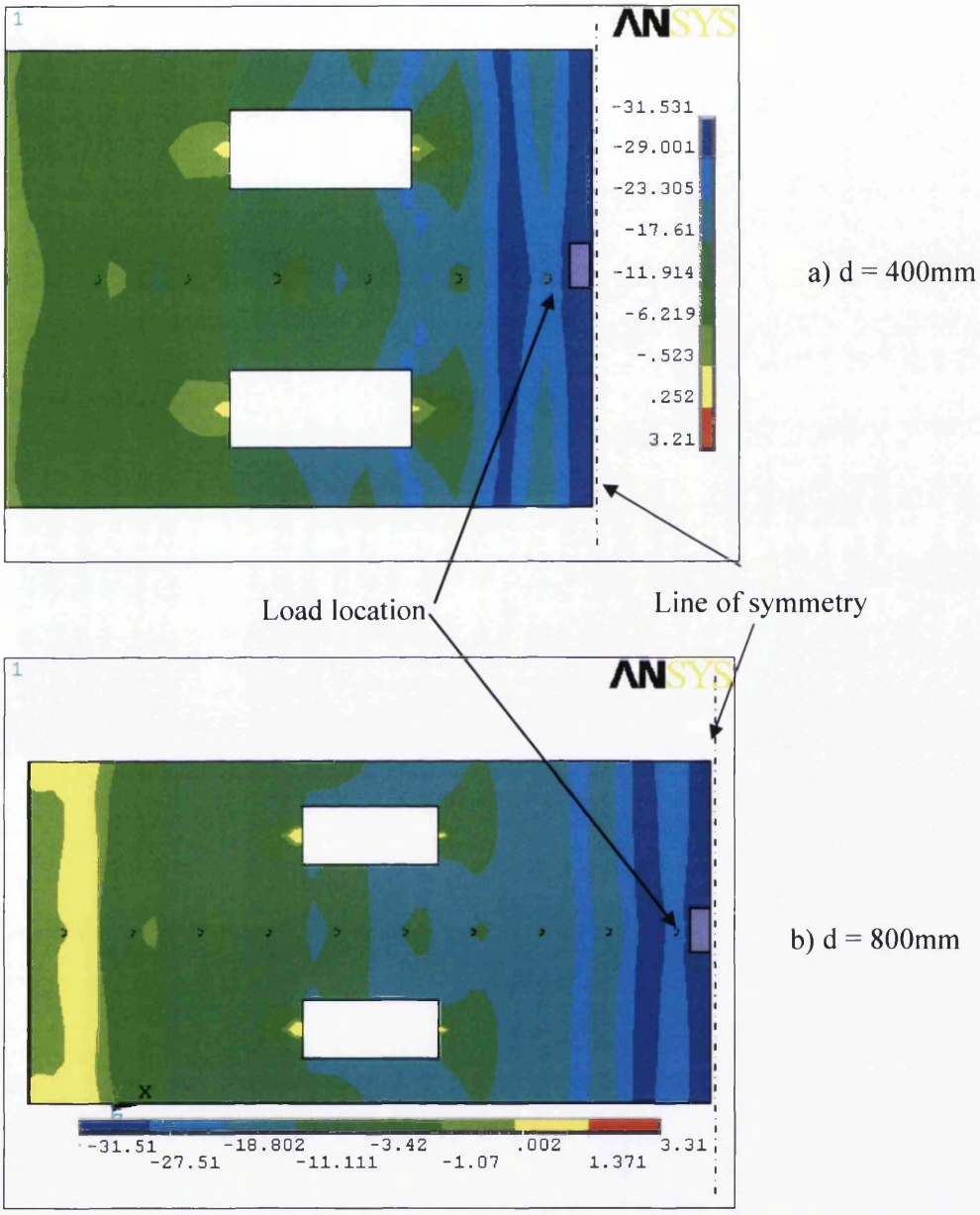

Figure 5.29: Stress contour in composite slab for different opening location (B1 Model), unit in MPa

5.5.3.2 Location of load

Figure 5.30 to 5.41 show the moment-deflection curves which illustrate the effect of load location on composite beams with openings. Results are compared with those corresponding to the without openings subjected to similar loading. In order to compare the results for different load locations, applied force were converted to applied moment.

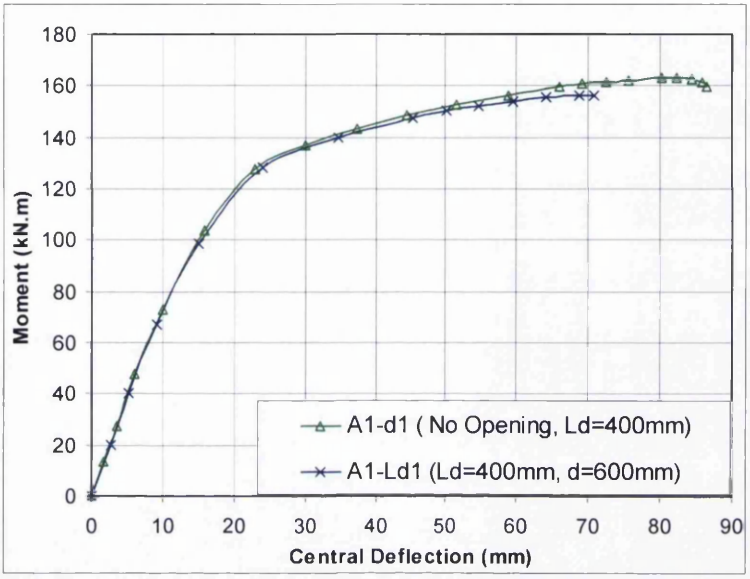

Figure 5.30: Moment-deflection curves for A type model with load applied at 400mm and opening located at 600mm from mid-span of the beam

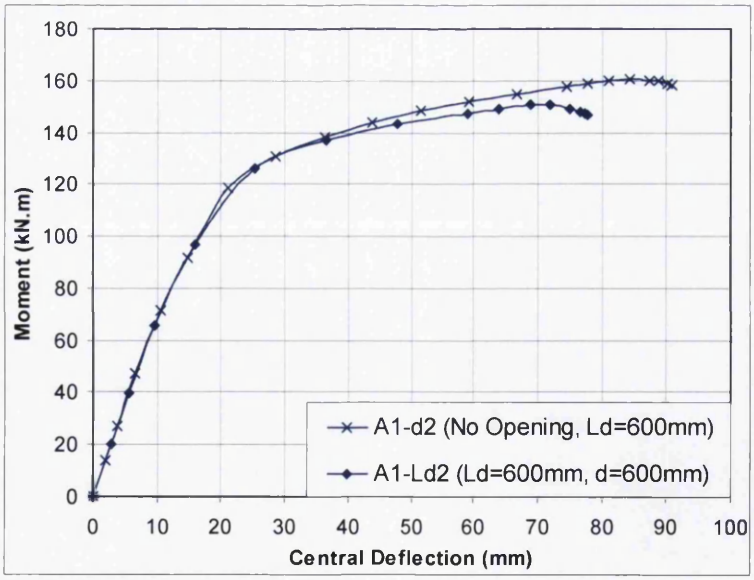

Figure 5.31: Moment-deflection curves for A type model with load applied at 600mm and opening located at 600mm from mid-span of the beam

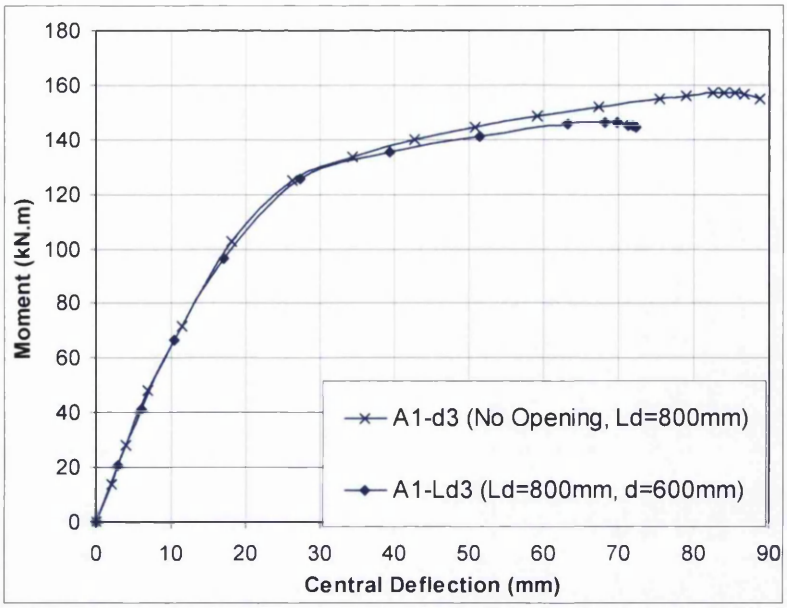

Figure 5.32: Moment-deflection curves for A type model with load applied at 800mm and opening located at 600mm from mid-span of the beam

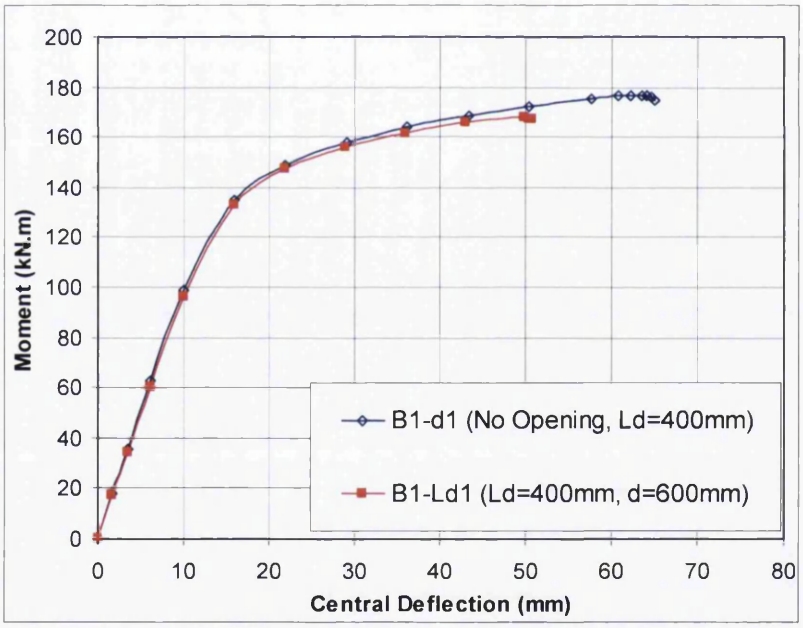

Figure 5.33: Moment-deflection curves comparison for B type model with load applied at 400mm and opening located at 600mm from mid-span of the beam

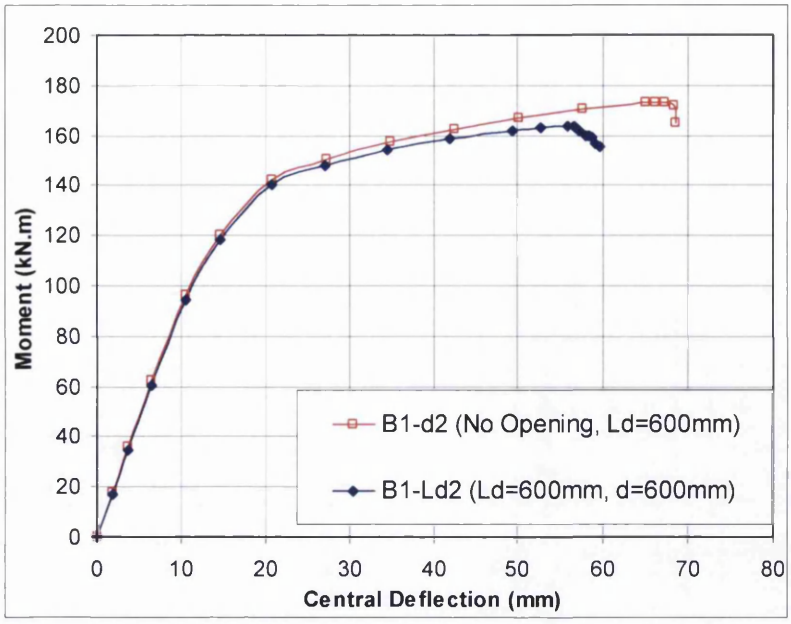

Figure 5.34: Moment-deflection curves for B type model with load applied at 600mm and opening located at 600mm from mid-span of the beam

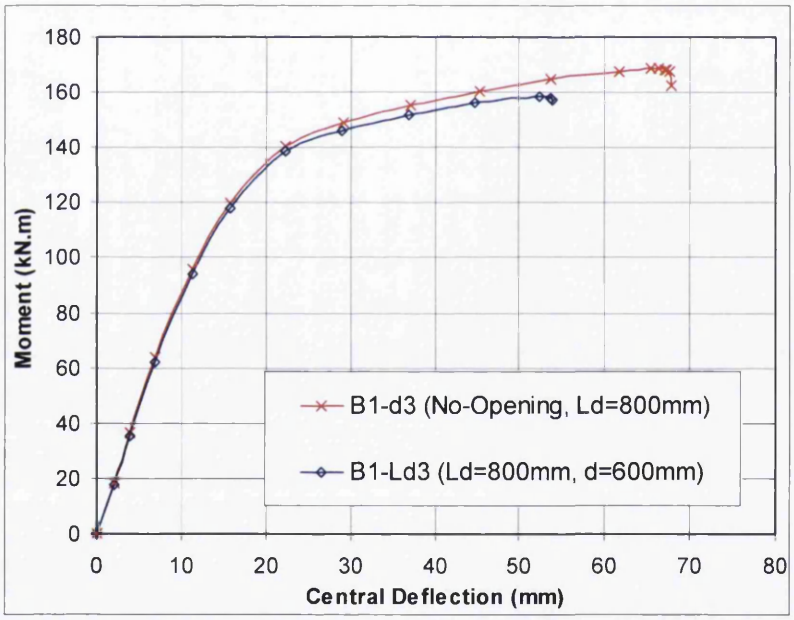

Figure 5.35: Moment-deflection curves for B type model with load applied at 800mm and opening located at 600mm from mid-span of the beam.

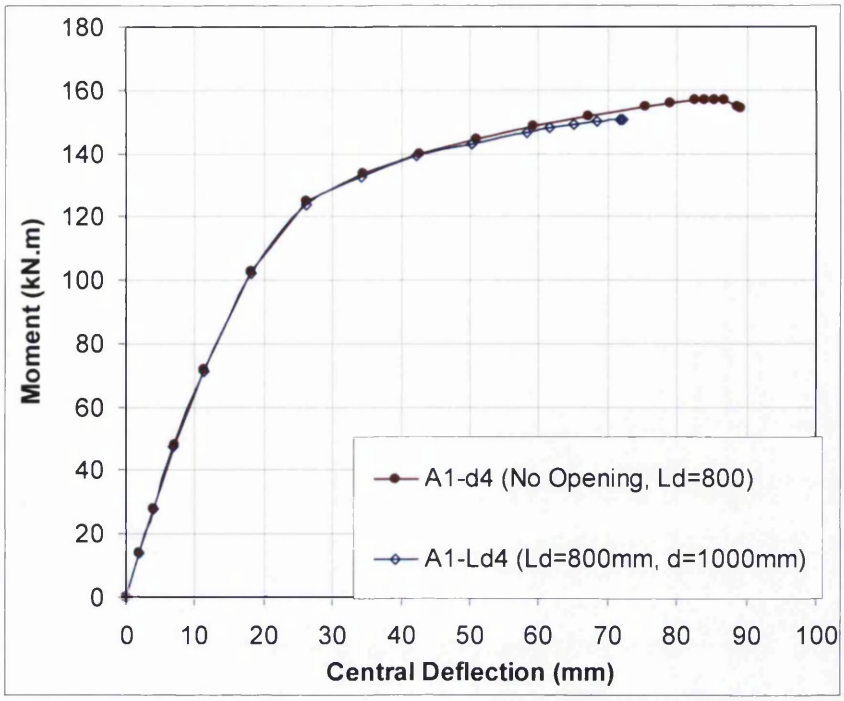

Figure 5.36: Moment-deflection curves for A type model with load applied at 800mm and opening located at 1000mm from mid-span of the beam

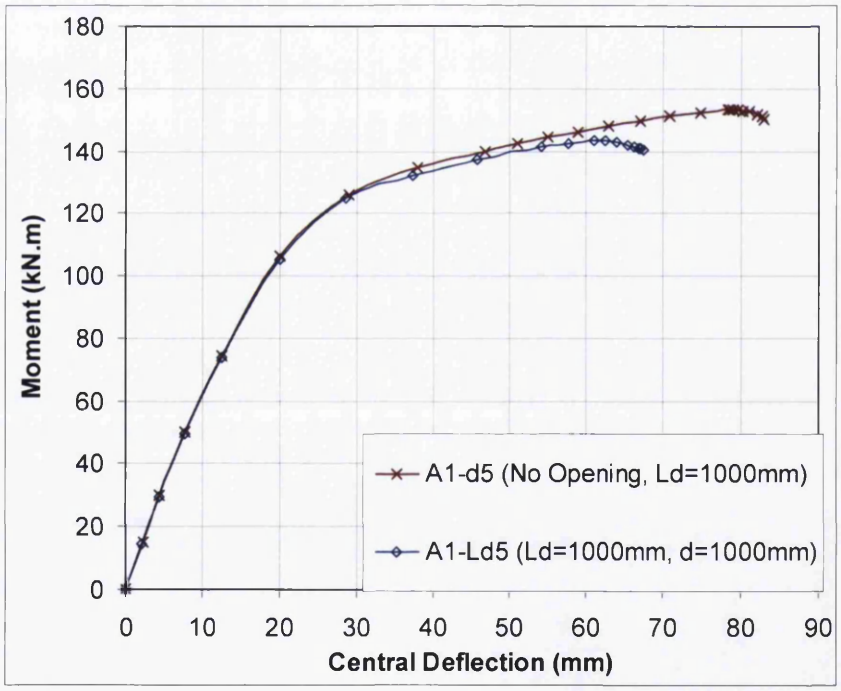

Figure 5.37: Moment-deflection curves for A type model with load applied at 1000mm and opening located at 1000mm from mid-span of the beam

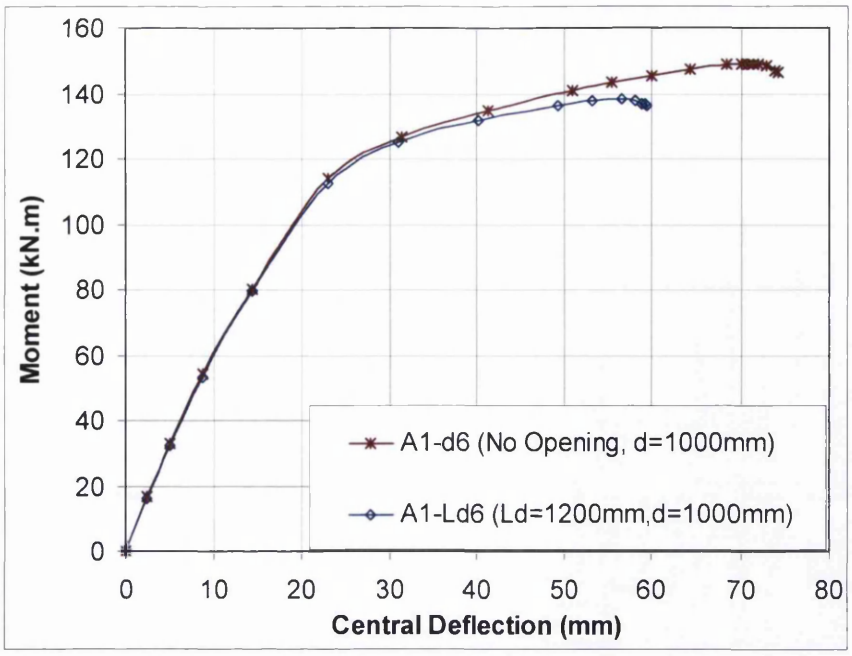

Figure 5.38: Moment-deflection curves for A type model with load applied at 1200mm and opening located at 1000mm from mid-span of the beam

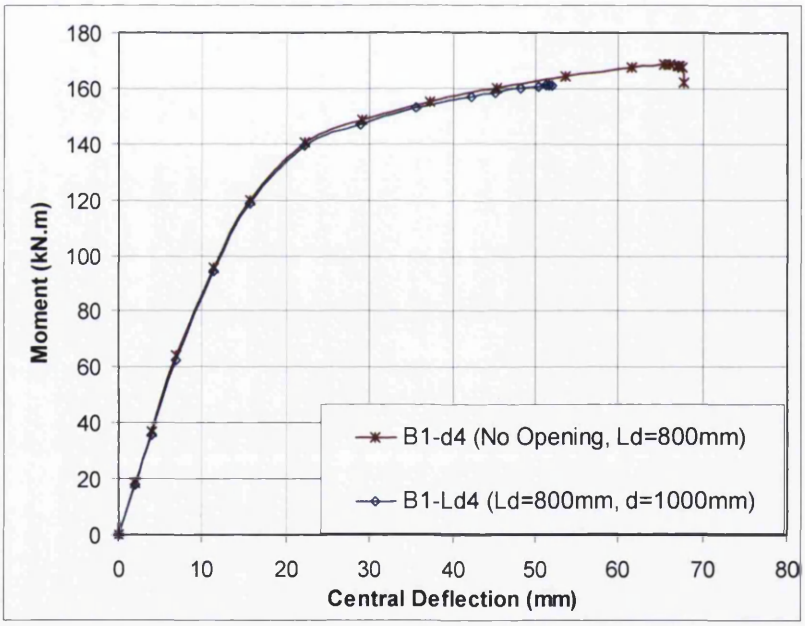

Figure 5.39: Moment-deflection curves for B type model with load applied at 800mm and opening located at 1000mm from mid-span of the beam

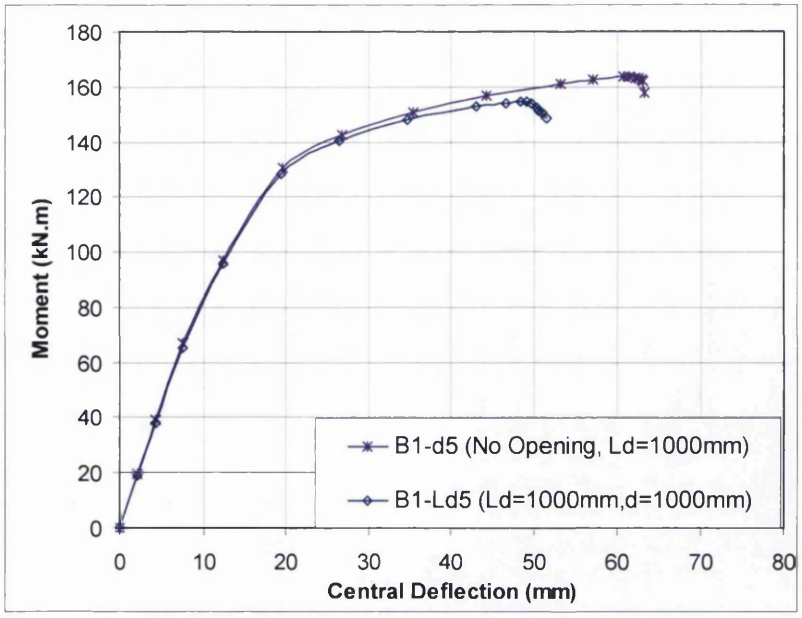

Figure 5.40: Moment-deflection curves for B type model with load applied at 1000mm and opening located at 1000mm from mid-span of the beam

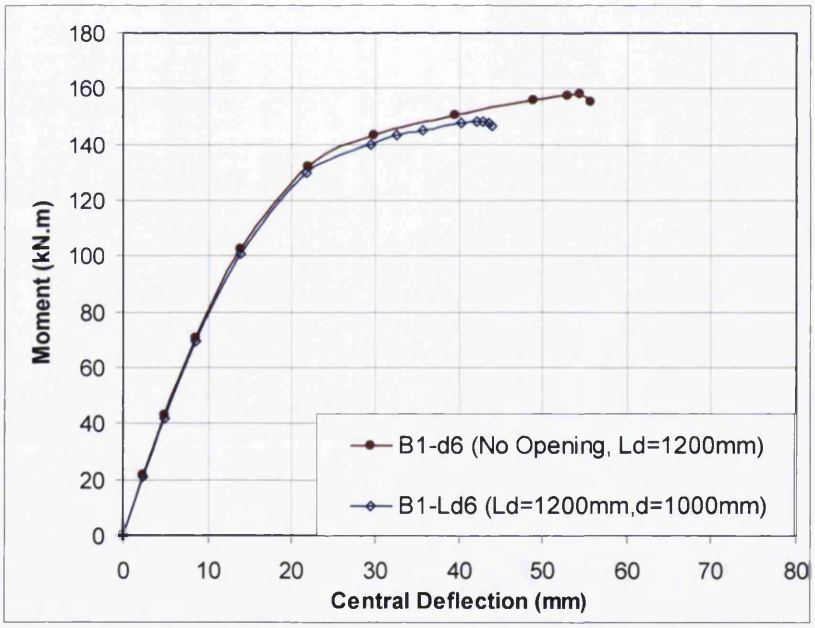

Figure 5.41: Moment-deflection curves for B type model with load applied at 1200mm and opening located at 1000mm from mid-span of the beam

Moment-deflection curves show that there is reduction on moment capacity of composite beam even when opening is not located at mid-span. The reduction of

moment capacity is found to be influenced by applied load location. As mention in section 5.4, load is applied at different locations which are before opening (front section), opening centre (central section) and after opening (end section).

Summary of results from the parametric study is given in Table 5.18. In the table, M_{uo} is the ultimate moment of composite beam with opening and M_{no} is the ultimate moment of beam without openings. Moment is reduced up to 4%, 6% and 7% for load applied at the front section, central section and end section of openings, respectively. It was observed that the moment reduction is more when load is located at opening end section compared to front section. It was also observed that the opening influences more if it is applied within the region of maximum bending moment. For central loading, the maximum bending moment is at the central of the beam while for two point load cases, the maximum bending moment is in between the two loads as shown in Figure.5.42.

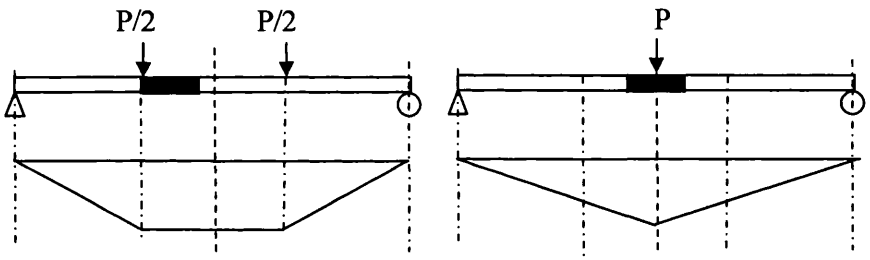

a) Two point load b) Single point load

Figure 5.42: Opening within maximum bending moment region

It is observed that when openings were located outside maximum bending moment region the ultimate moment are least effected as shown in previous section, 5.8.3. Due to this reason, ultimate moment is reduced more for the model Ld3 compared to the model Ld1. In model Ld3, load was applied at opening end section compared to model Ld1 where the load was applied at the openings front section as shown in Figure 5.43.

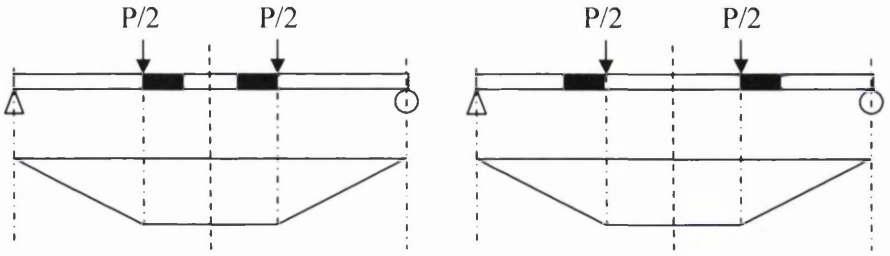

a) Openings within maximum bending moment region.

b) Openings outside maximum bending moment region.

Figure 5.43: Opening within and outside maximum bending moment region

Figures 5.44 to 5.46 present typical stress contours in composite beam with opening with different load locations. It is interesting to note that for openings located outside maximum bending moment region (load applied at front section), high compressive stress in slab is formed at mid-span (Figs 5.44). For load applied at the opening centre (Figs 5.45) and opening end section (Figs 5.46), high compressive stress in slab is distributed at opening area, along innermost and outermost side of beam flange. The location of high compressive stress is changing from mid-span to opening area due to reduction of slab section.

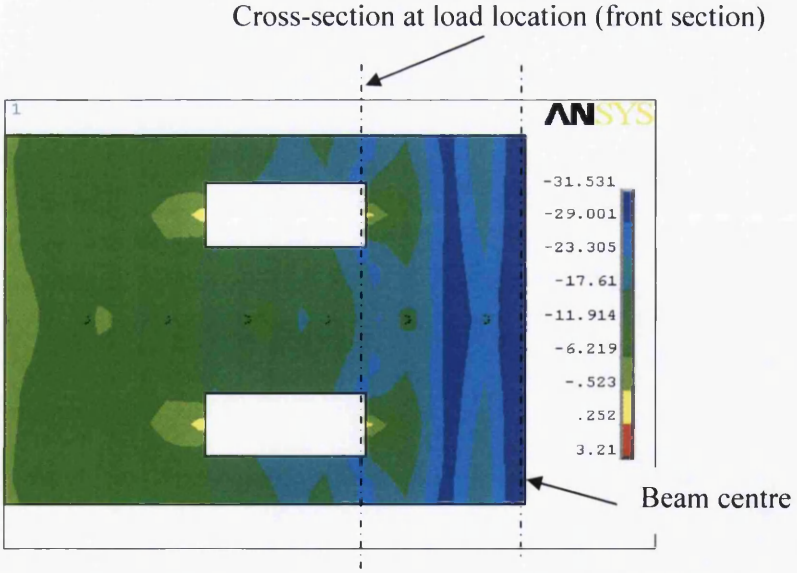

Figure 5.44: Stress contour in composite slab for B1 Model- Load at opening front section, unit in MPa

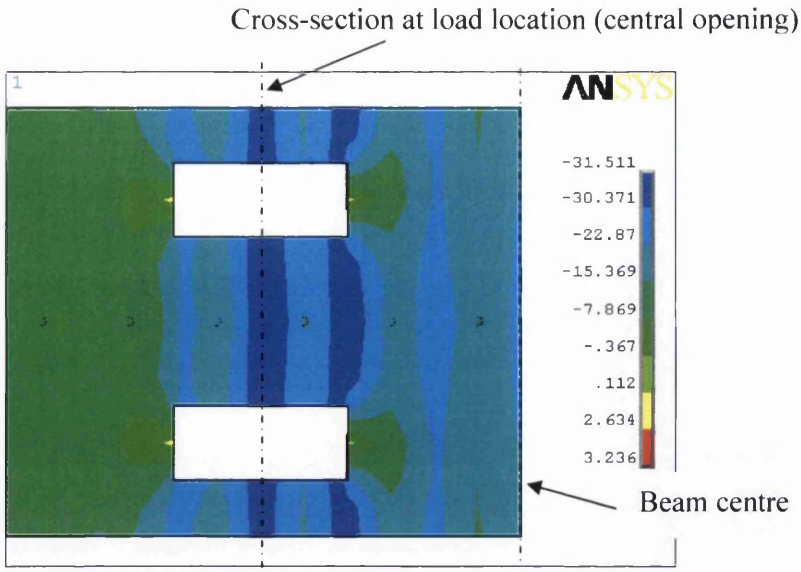

Figure 5.45: Stress contour in composite slab for B1 Model- Load at central opening, unit in MPa

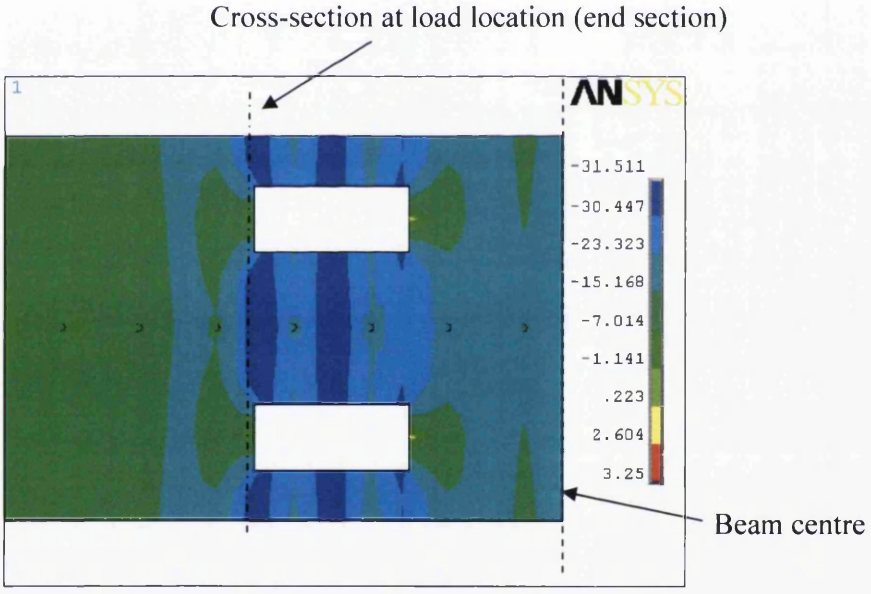

Figure 5.46: Stress contour in composite slab for B1 Model- Load at opening end section, unit in MPa

Table 5.18: Result for composite beams with opening and with different load locations

Beam Model	Opening parameter		M_{uo} or M_{no} (kN.m)	$\frac{M_u}{M_{no}}$
	L_d (mm)	d (mm)		
A1-d1	400	0	163.24	
A1- Ld1	400	600	156.31	0.96
A1-d2	600	0	160.47	
A1- Ld2	600	600	150.71	0.94
A1-d3	800	0	157.02	
A1- Ld3	800	600	146.43	0.93
A1-d4	800	0	157.00	
A1- Ld4	800	1000	150.57	0.96
A1-d5	1000	0	153.08	
A1- Ld5	1000	1000	143.37	0.94
A1-d6	1200	0	149.08	
A1- Ld6	1200	1000	138.34	0.93
B1-d1	400	0	174.98	
B1- Ld1	400	600	167.56	0.96
B1-d2	600	0	172.86	
B1- Ld2	600	600	163.43	0.95
B1-d3	800	0	168.65	
B1- Ld3	800	600	158.32	0.94
B1-d4	800	0	168.65	
B1- Ld4	800	1000	161.08	0.96
B1-d5	1000	0	163.75	
B1- Ld5	1000	1000	153.91	0.94
B1-d6	1200	0	157.73	
B1- Ld6	1200	1000	146.32	0.93

5.5.3.3 Two opening with different position

Figures 5.47 and 5.48 show load-deflection plots for beams with different opening position. It can be seen from the load-deflection curve, that a reduction of ultimate load for two openings located at both side of beam flange is more than that of openings located at one side of beam flange.

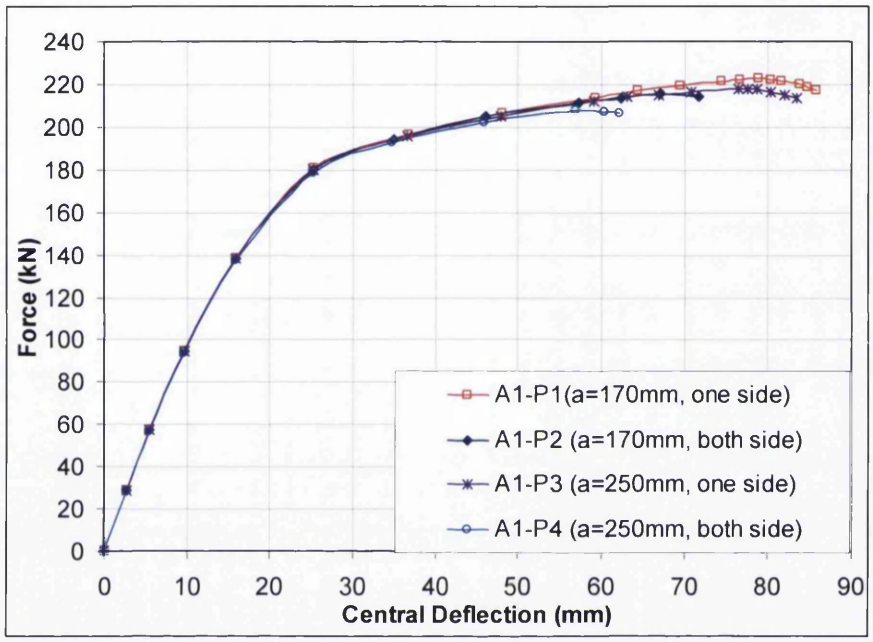

Figure 5.47: Load-deflection curves for composite beam with two openings at different positions, A type

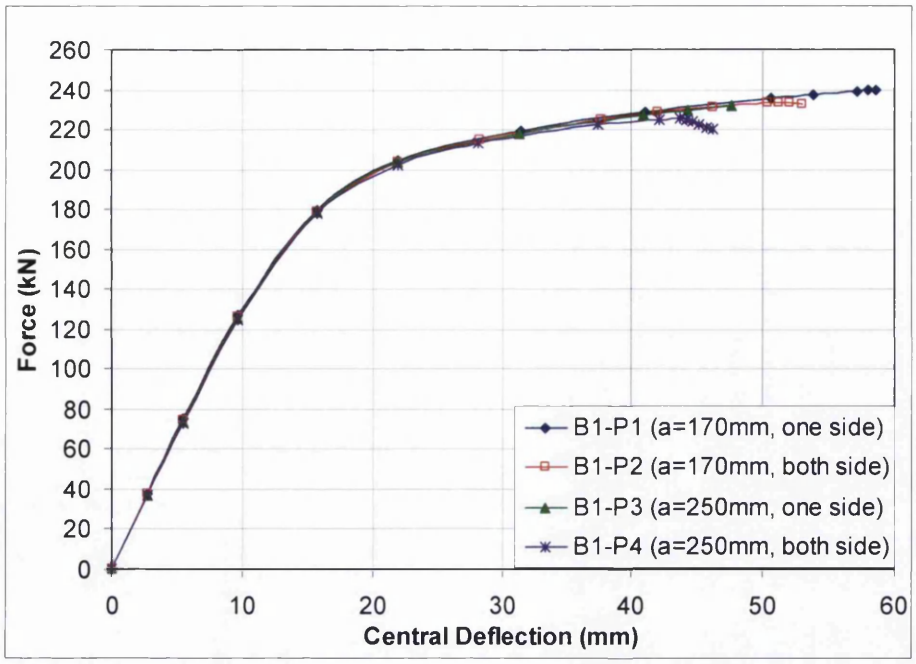

Figure 5.48: Load-deflection curves for composite beam with two openings at different positions, B type

Table 5.19 shows the summary of results obtained in this study. In the table M_{u1} refer to ultimate moment for composite beam with openings located at one side of flange whereas M_{u2} the ultimate moment for the beam with opening located at both side of flange. The table shows that the difference in ultimate moment between these opening positions is between 3% and 5%. This study involves the openings located at 600 mm and 1000mm from beam centre. It should be mention, the analyses were carried out using model with openings located away from mid-span. The ultimate moment could be reduced more if openings are located at mid-span of the beam.

Figure 5.49 shows the comparison of stress contour for different opening positions, located at one side or both side of flange. It can be observed, when opening is positioned at both sides of beam flange, high compressive stress developed at corner side of opening. Between these two openings, high compressive stress developed from one opening corner to another opening corner. It shows that the stress distribution is influenced by these two openings. Calculation of effective width should include these two openings even though both opening is located at different cross section. For opening located at one side of flange, high compressive stress is distributed at load location area.

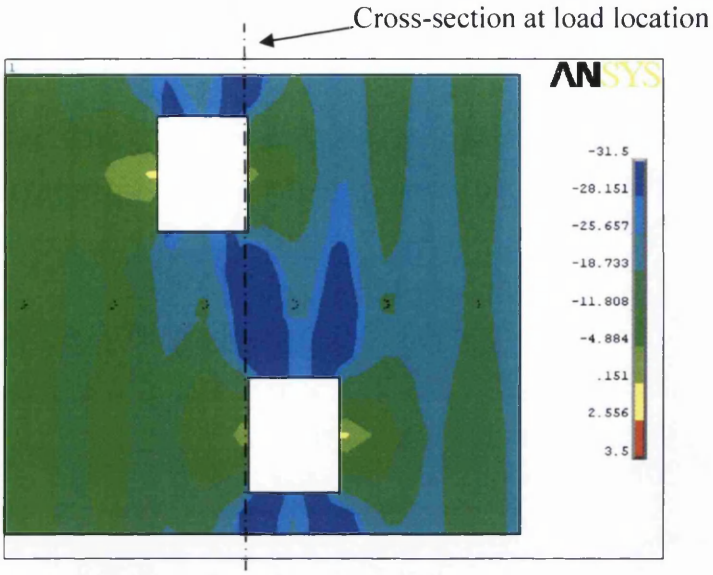

a) Two openings at different side of flange

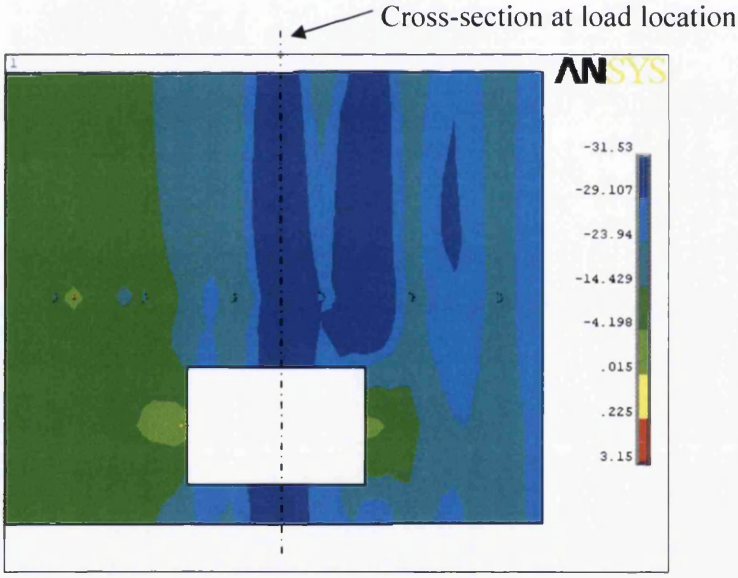

b) Two openings at similar side of flange

Figure 5.49: Stress contour in composite slab for different opening location (A1 Model), unit in MPa

Table 5.19: Results for composite beams with two openings at different positions

Beam Model	Opening parameter				M_{u1} or M_{u2} (kN.m)	$\frac{M_{u1}}{M_{u2}}$
	Location of two openings on flanges (one side or both side)	a (mm)	f (mm)	d (mm)		
A1-P1	one side	170	200	600	222.49	
A1-P2	both side	170	200	600	214.79	0.97
A1-P3	one side	250	200	600	217.55	
A1-P4	both side	250	200	600	207.04	0.95
B1-P1	one side	170	200	600	239.28	
B1-P2	both side	170	200	600	231.52	0.97
B1-P3	one side	250	200	600	233.61	
B1-P4	both side	250	200	600	225.14	0.96

5.8.4 Effect of change in concrete strength

The primary aim of this study is to investigate the effect of ultimate load of composite beam with openings in metal-ribbed decking slab by increasing the concrete strength. Comparison of results obtained from the analyses of opening size in transverse axis direction with cube strength of 26 MPa and 43.3 MPa are listed in Table 5.20. In the table, $P_{fcu-43.3}$ and P_{fcu-26} is ultimate load for composite beam with openings with cube strength of 43.3 MPa and 26 MPa, respectively. P_{no} is ultimate load for composite beam without opening corresponding to similar cube strength.

It can be seen from the table that the ultimate load is increased by about 10% when the cube strength of composite beam with opening is increased from 26 MPa to 43.3 MPa. It is observed, the beam ultimate load are affected more for lower opening ratio with the increase in concrete cube strength. As in the case of models A1, B1 and C1 which has 10% opening ratio, ultimate load is increased about 7% over the composite beam without openings when the cube strength is increased from 26 MPa to 43.3 MPa. As in the case of model A6, B6 and C6 which has higher opening ratio (50%), the ultimate load is increased about 1% over the composite beam without opening when the cube strength is increased from 26 MPa to 43.3 MPa. The fact is this increase is due to higher compressive force for higher concrete strength.

It can be concluded that the ultimate load increment by increasing cube strength is influence by openings ratio. By increasing the concrete cube strength, for higher openings ratio, the increase in ultimate load is lower compare to smaller openings ratio.

Table 5.20: Results for composite beams containing openings with different cube strength

Beam Model	f_{cu} (MPa)	P_u (kN)	$\frac{P_u}{P_o}$	Beam Model	f_{cu} (MPa)	Opening Ratio %	P_u (kN)	$\frac{P_u}{P_o}$	$\frac{P_{fcu-43.3}}{P_{fcu-26}}$	$\frac{P_{fcu-43.3}}{P_{no}}$
A1	43.3	151.15	0.99	A7	26	10	165.62	0.98	1.10	1.09
A2	43.3	148.90	0.98	A8	26	20	162.54	0.96	1.09	1.07
A3	43.3	147.66	0.97	A9	26	28	160.06	0.95	1.08	1.05
A4	43.3	146.65	0.96	A10	26	34	158.05	0.93	1.08	1.04
A5	43.3	145.56	0.95	A11	26	40	155.68	0.92	1.07	1.02
A6	43.3	143.49	0.94	A12	26	50	153.88	0.91	1.07	1.01
B1	43.3	181.54	0.98	B7	26	10	165.48	0.97	1.10	1.07
B2	43.3	178.55	0.96	B8	26	20	163.50	0.96	1.09	1.05
B3	43.3	176.42	0.95	B9	26	28	161.07	0.95	1.10	1.04
B4	43.3	173.97	0.94	B10	26	34	157.43	0.93	1.11	1.02
B5	43.3	172.15	0.93	B11	26	40	153.68	0.91	1.12	1.01
B6	43.3	165.53	0.89	B12	26	50	144.61	0.85	1.14	0.98
C1	43.3	177.17	0.96	C7	26	10	161.63	0.97	1.10	1.07
C2	43.3	173.59	0.94	C8	26	20	158.82	0.95	1.09	1.05
C3	43.3	170.60	0.93	C9	26	28	155.91	0.93	1.09	1.03
C4	43.3	168.15	0.91	C10	26	34	154.79	0.93	1.09	1.02
C5	43.3	165.47	0.90	C11	26	40	149.93	0.90	1.10	1.00
C6	43.3	161.30	0.88	C12	26	50	144.18	0.86	1.12	0.98

5.5.5 Effect of change in concrete slab thickness

This section describes comprehensive parametric studies of the ultimate load of composite beam containing openings in flange with different overall slab thicknesses. Four different slab thicknesses 10 mm, 115 mm, 120 mm and 125mm were used. The models, which have been analysed in the previous section (5.8.1), had an overall slab thickness of 105 mm are used as reference to examine the beams with different slab thicknesses. Figures 5.50 and 5.58 show the load-deflection curve for the changes in overall slab thickness.

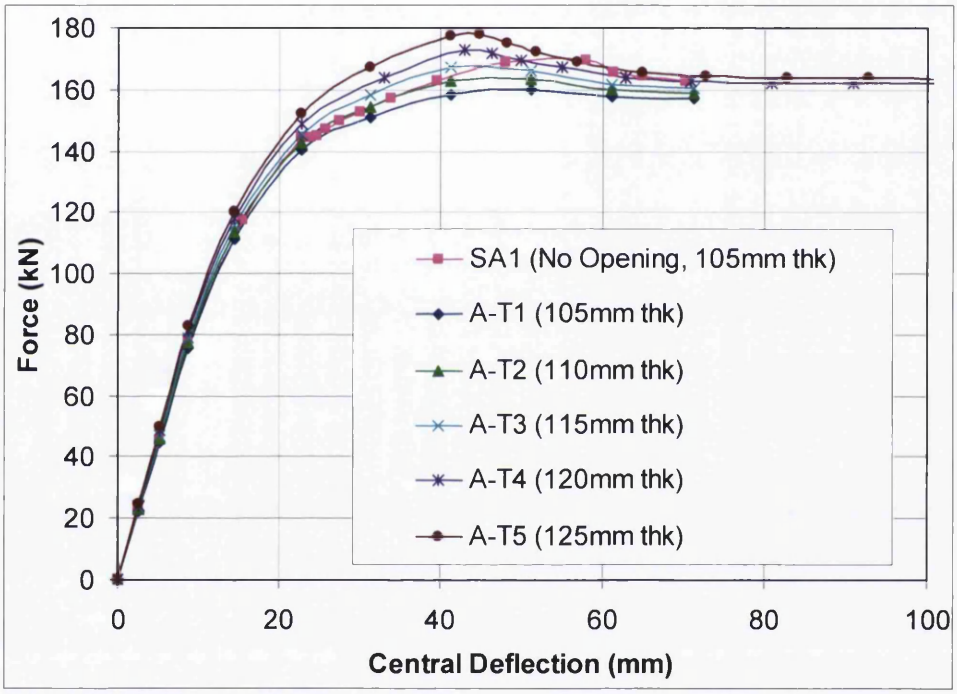

Figure 5.50: Effect of slab thickness on ultimate load of composite beam with openings, type A with concrete strength, 43.3 N/mm^2

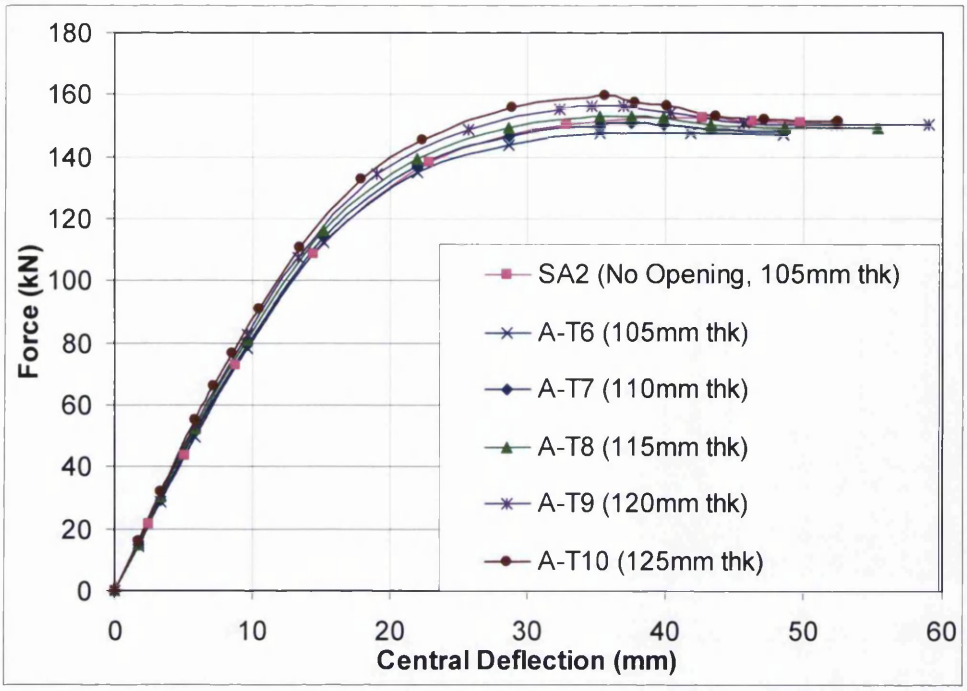

Figure 5.51: Effect of slab thickness on ultimate load of composite beam with openings, type A with concrete strength, 26 N/mm^2

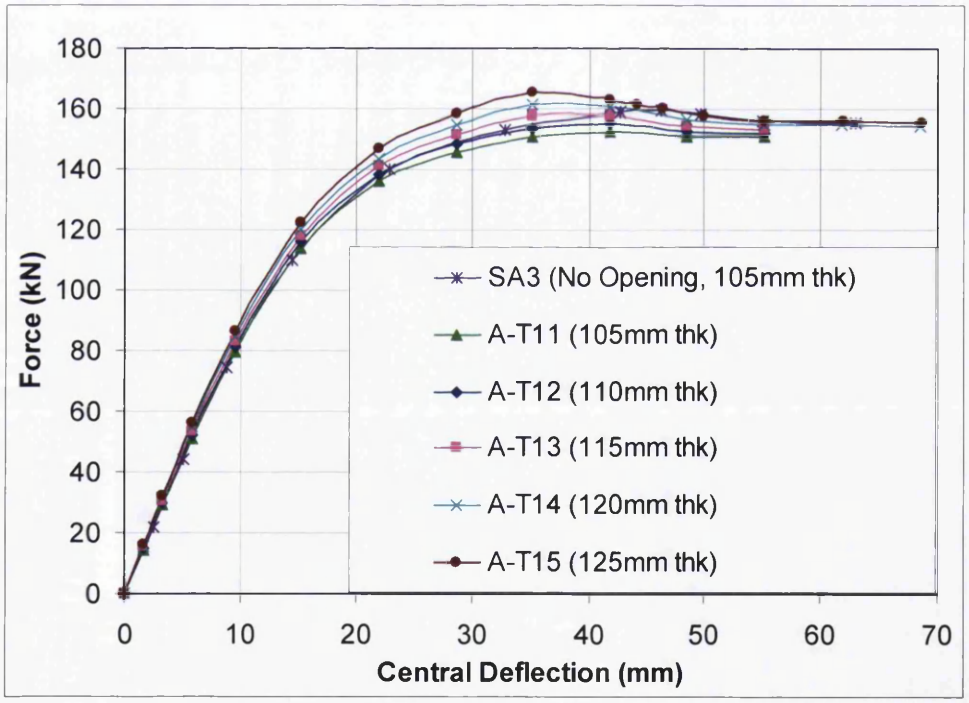

Figure 5.52: Effect of slab thickness on ultimate load of composite beam with openings, type A with concrete strength, 35 N/mm^2

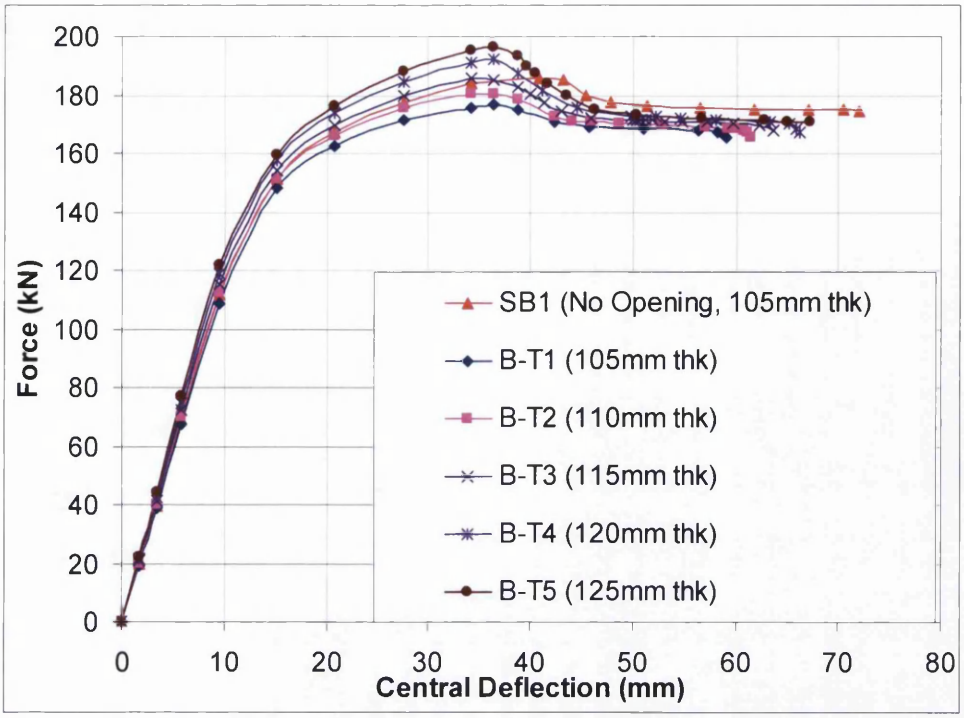

Figure 5.53: Effect of slab thickness on ultimate load of composite beam with openings, type B with concrete strength, 43.3 N/mm^2

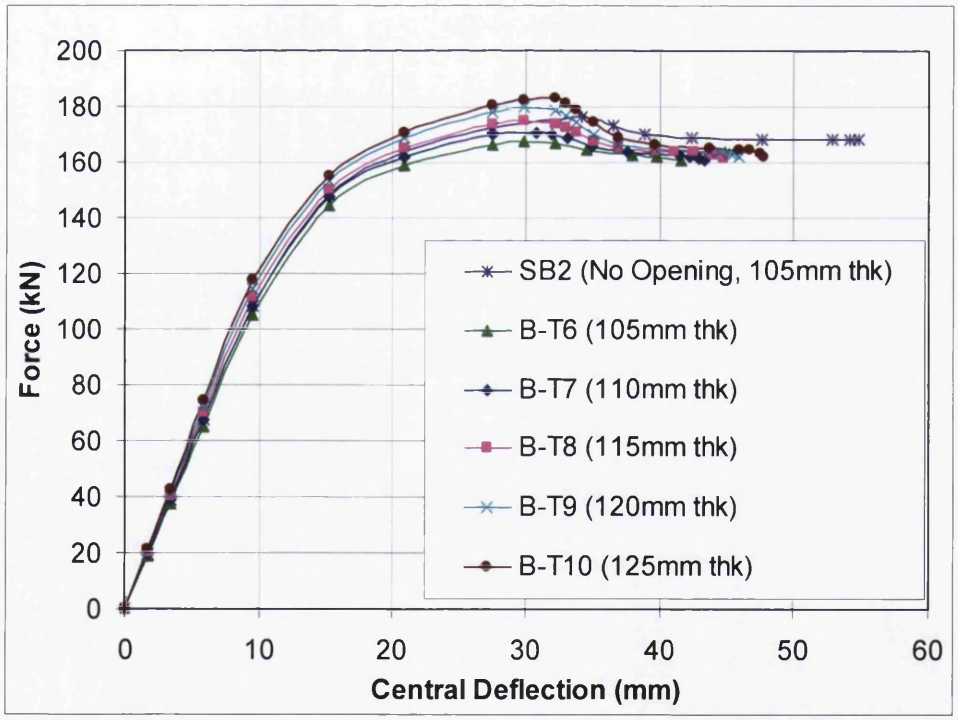

Figure 5.54: Effect of slab thickness on ultimate load of composite beam with openings, type B with concrete strength, 26 N/mm^2

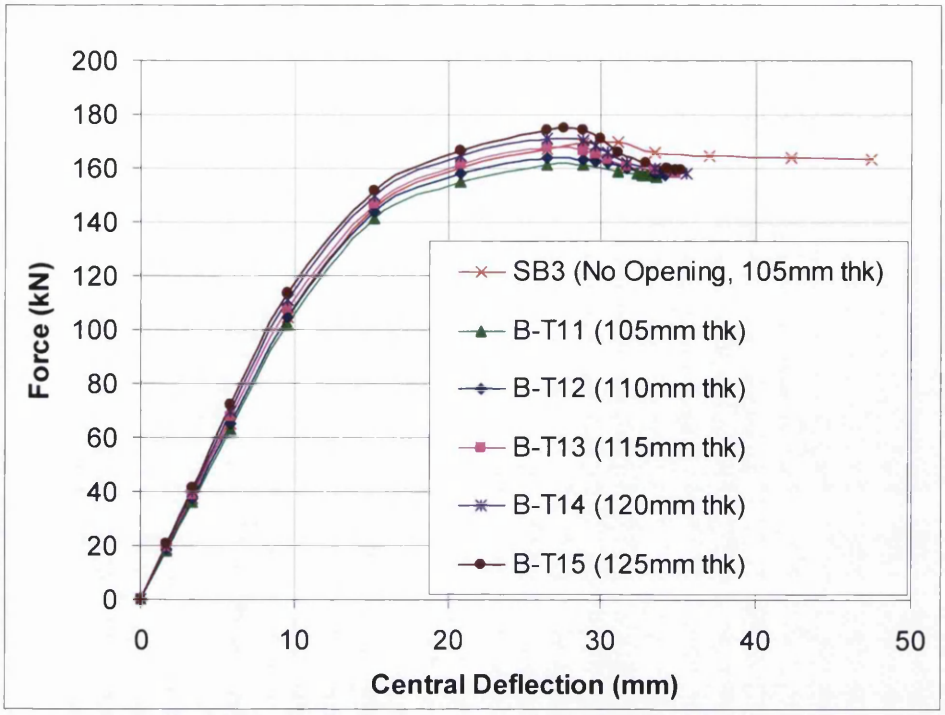

Figure 5.55: Effect of slab thickness on ultimate load of composite beam with openings, type B with concrete strength, 35 N/mm^2

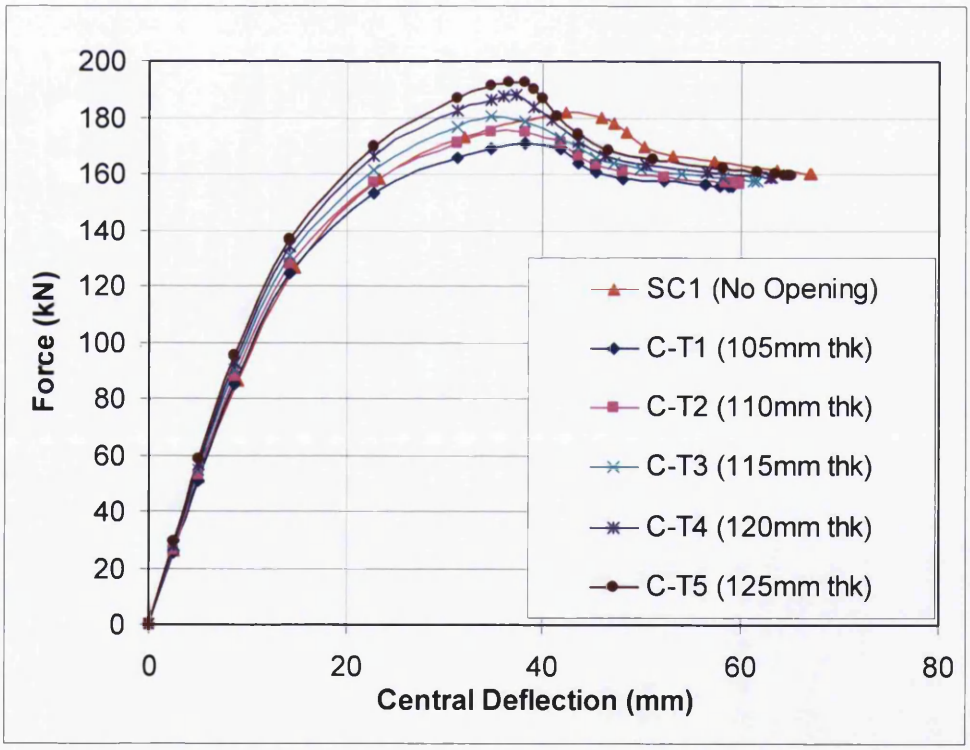

Figure 5.56: Effect of slab thickness on ultimate load of composite beam with openings, type C with concrete strength, 43.3 N/mm^2

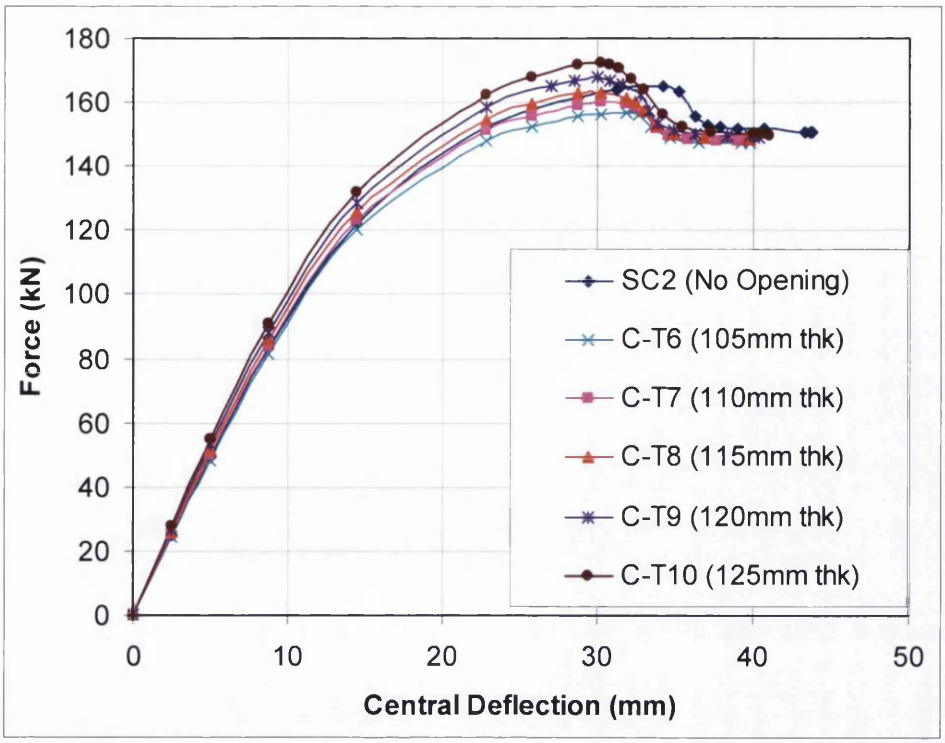

Figure 5.57: Effect of slab thickness on ultimate load of composite beam with openings, type B with concrete strength, 26 N/mm^2

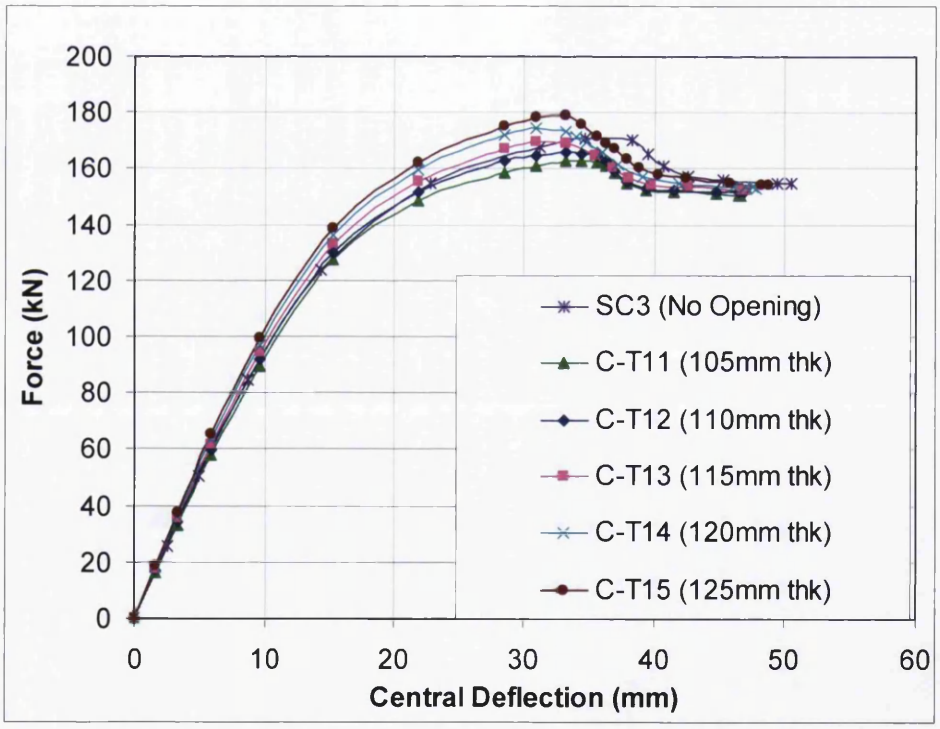

Figure 5.58: Effect of slab thickness on ultimate load of composite beam with openings, type C with concrete strength, 35 N/mm^2

By analysing the load-deflection curves (Figures 5.50 to 5.58), it is observed that an increase in the overall slab thickness resulted an increase in the ultimate load of the composite beam. Complete results from the study are shown in Table 5.21 to 5.23. In the tables P_u is ultimate load for composite beam with openings, P_o for reference model and P_{no} for composite beam without openings. While $\frac{t}{t_{ref}}$ is ratio of slab increment over the reference model.

From $\frac{P_u}{P_o}$ ratio it can be observed that on average, the increment of 5% of overall slab thickness will increase the ultimate load of composite beams by about 1% to 3%. The maximum of $\frac{P_u}{P_o}$ ratio is 1.13 which is for model C-T5. This shows that by increasing the overall slab thickness by about 20% compared to reference model slab thickness the ultimate load is increased as high as 13%.

It is interesting to note that, the ultimate load is increased to the situation of a composite beam without openings when the slab thickness is increased up to 10% for the reference model. This result shows that approximately only 10% slab thickness increment needed from reference models as a composite beam with openings is required to recover the lost of composite beam strength caused by openings in slab.

In all cases, it is observed that the ultimate load is increased more than a complete composite beam without openings when the slab thickness is increased more than 10% for the reference model. As in the case of model B-T5, the ultimate load is increased by 7% over the composite beam without openings when the slab thickness is increased by 19% for the thickness of reference model. These results show that the composite beam with openings will be over design when the slab thickness is increased more than 10% for the thickness of reference model. Location of plastic neutral axis (PNA) is a possible reason for its increment. The increment in slab thickness moves plastic neutral axis (PNA) upwards and hence increase the lever arm between compression force and tension force. This results in increment in moment capacity of composite beam.

Table 5.21: Results for composite beams with openings with different slab thickness, type A

Beam model	Slab thickness (mm)	$\frac{t}{t_{ref}} x100$ (%)	P_u	$\frac{P_u}{P_o}$	$\frac{P_u}{P_{no}}$
A-T1	105	0	160.06	1.00	0.94
A-T2	110	5	162.67	1.02	0.96
A-T3	115	10	167.07	1.04	0.99
A-T4	120	14	172.72	1.08	1.02
A-T5	125	15	177.78	1.11	1.05
A-T6	105	0	147.66	1.00	0.97
A-T7	110	5	150.57	1.02	0.99
A-T8	115	10	153.27	1.04	1.01
A-T9	120	14	156.56	1.06	1.03
A-T10	125	15	159.61	1.08	1.05
A-T11	105	0	152.80	1.00	0.96
A-T12	110	5	155.27	1.02	0.98
A-T13	115	10	157.52	1.03	0.99
A-T14	120	14	161.38	1.06	1.01
A-T15	125	15	165.37	1.08	1.04

Table 5.22: Results for composite beams with openings and with different slab thickness, type B

Beam model	Slab thickness (mm)	$\frac{t}{t_{ref}} x100$ (%)	P_u	$\frac{P_u}{P_o}$	$\frac{P_u}{P_{no}}$
B-T1	105	0	176.42	1.00	0.96
B-T2	110	5	180.31	1.02	0.98
B-T3	115	10	185.61	1.05	1.01
B-T4	120	14	192.20	1.09	1.04
B-T5	125	15	196.19	1.11	1.07
B-T6	105	0	161.07	1.00	0.96
B-T7	110	5	164.09	1.02	0.98
B-T8	115	10	167.50	1.04	1.00
B-T9	120	14	171.03	1.06	1.02
B-T10	125	15	174.11	1.08	1.04
B-T11	105	0	167.46	1.00	0.96
B-T12	110	5	170.74	1.02	0.98
B-T13	115	10	175.27	1.05	1.01
B-T14	120	14	179.70	1.07	1.04
B-T15	125	15	183.14	1.09	1.06

Table 5.23: Results for composite beams with openings and with different slab thickness, type C

Beam model	Slab thickness (mm)	$\frac{t}{t_{ref}} x100$ (%)	P_u	$\frac{P_u}{P_o}$	$\frac{P_u}{P_{no}}$
C-T1	105	0	170.59	1.00	0.94
C-T2	110	5	174.40	1.02	0.96
C-T3	115	10	180.17	1.06	0.99
C-T4	120	14	187.77	1.10	1.03
C-T5	125	15	192.64	1.13	1.06
C-T6	105	0	155.92	1.00	0.94
C-T7	110	5	159.99	1.03	0.97
C-T8	115	10	162.80	1.04	0.99
C-T9	120	14	167.64	1.08	1.02
C-T10	125	15	172.11	1.10	1.04
C-T11	105	0	162.67	1.00	0.96
C-T12	110	5	165.72	1.02	0.97
C-T13	115	10	169.33	1.04	1.00
C-T14	120	14	174.60	1.07	1.03
C-T15	125	15	178.93	1.10	1.05

5.5.6 Effect of steel reinforcement (rebar) area

Figures 5.59 to 5.67 show the load-deflection curves, which represent the effect of the steel reinforcing bar area on the composite beams with openings, in a metal-ribbed decking slab.

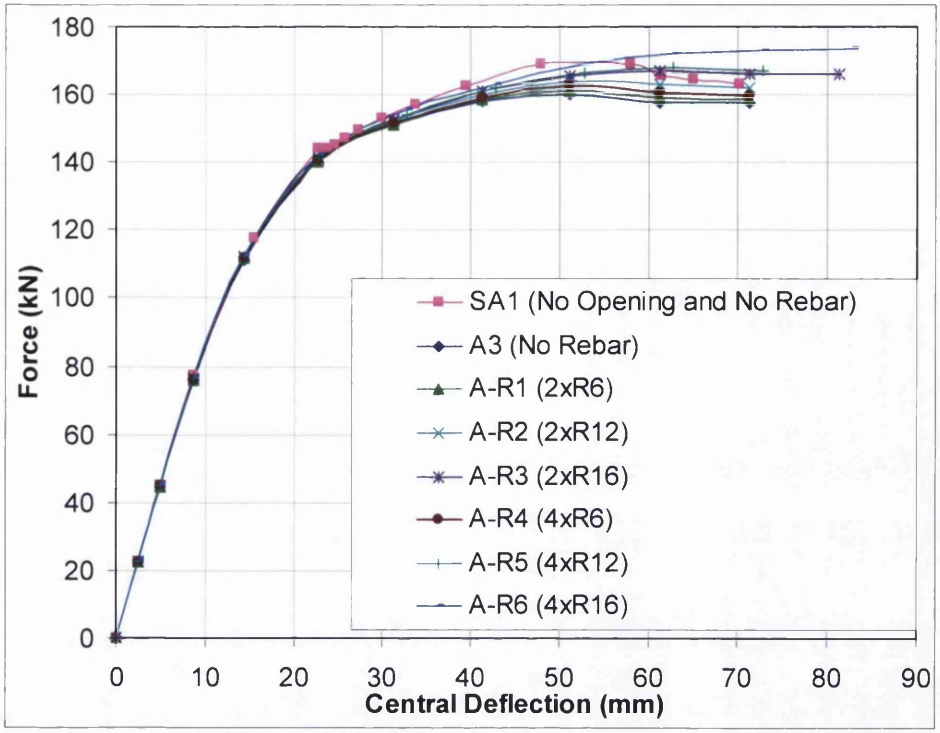

Figure 5.59: Effect of rebar area on ultimate load of composite beam with openings of type A with concrete strength, 43.3 N/mm^2

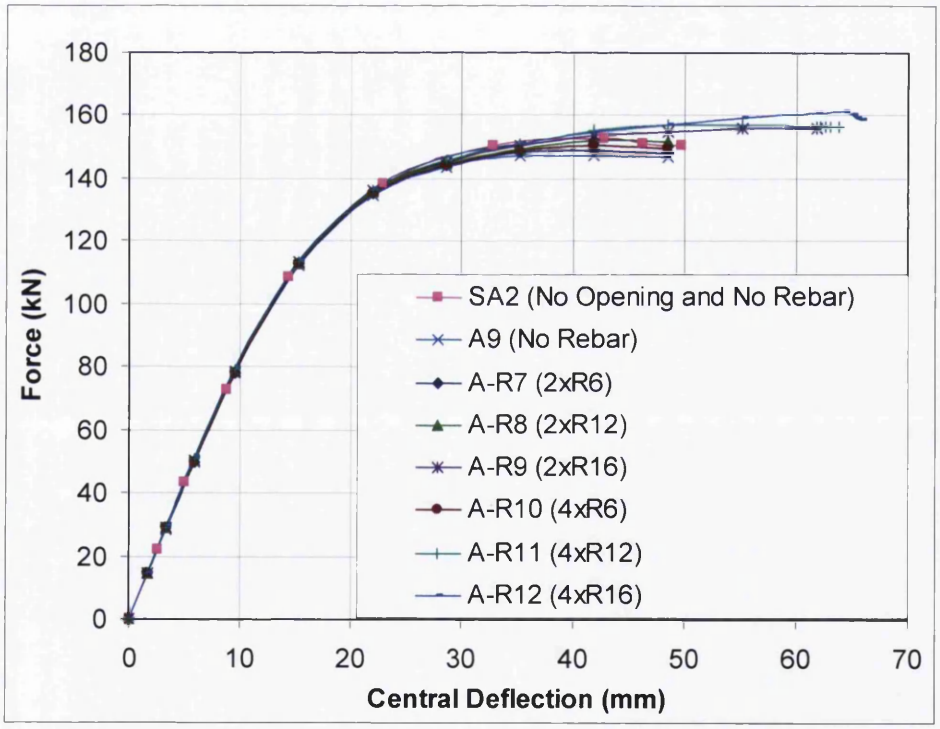

Figure 5.60: Effect of rebar area on ultimate load of composite beam with openings of type A with concrete strength, 26 N/mm^2

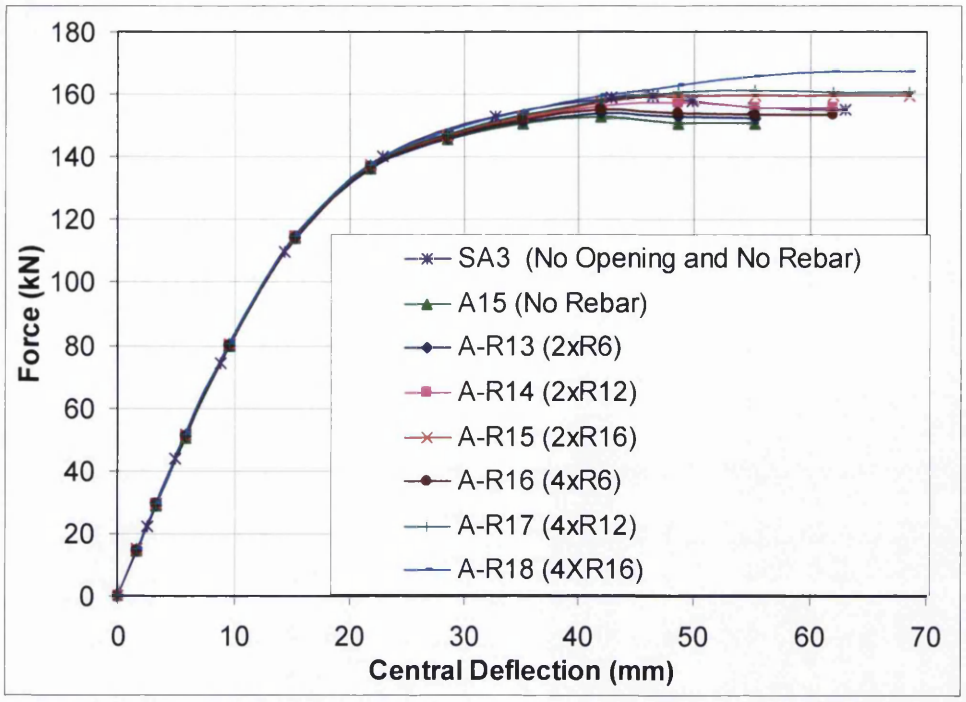

Figure 5.61: Effect of rebar area on ultimate load of composite beam with openings of type A with concrete strength, 35 N/mm^2

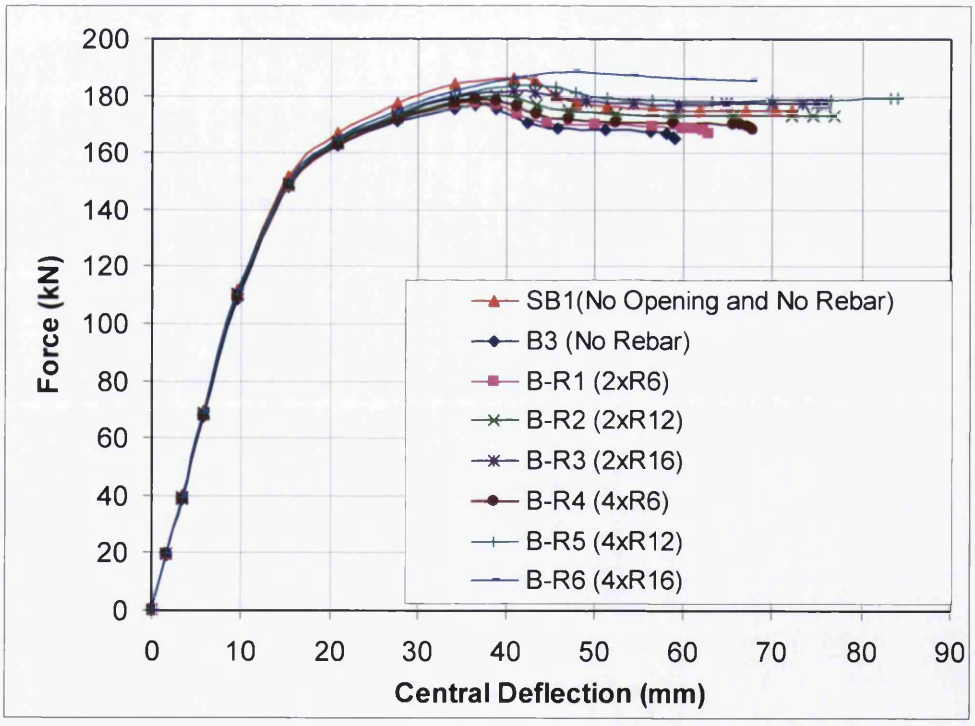

Figure 5.62: Effect of rebar area on ultimate load of composite beam with openings of type B with concrete strength, 43.3 N/mm^2

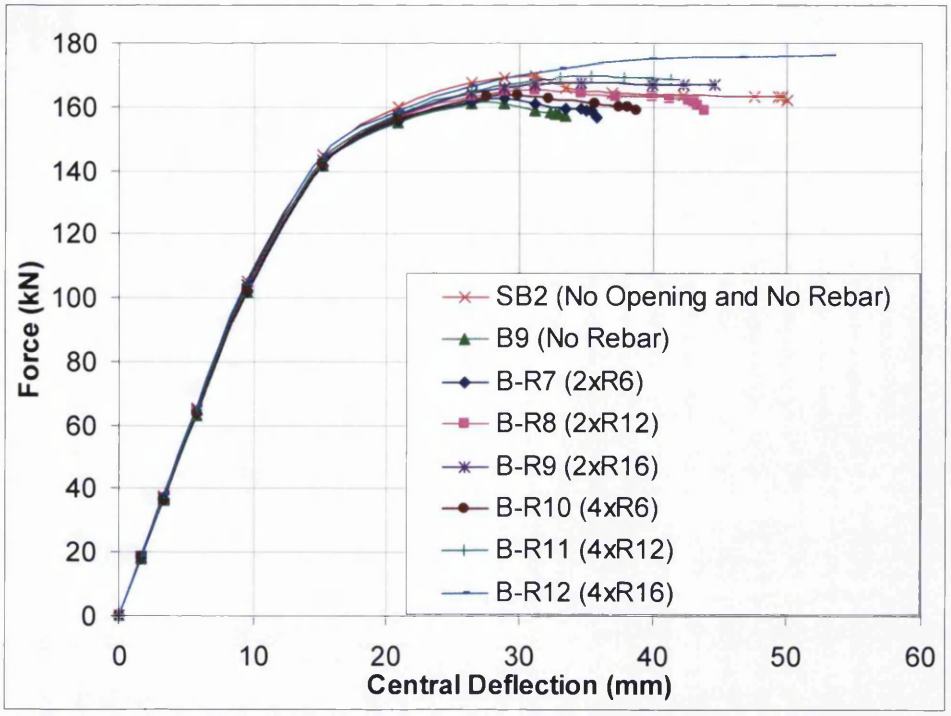

Figure 5.63: Effect of rebar area on ultimate load of composite beam with openings of type B with concrete strength, 26 N/mm^2

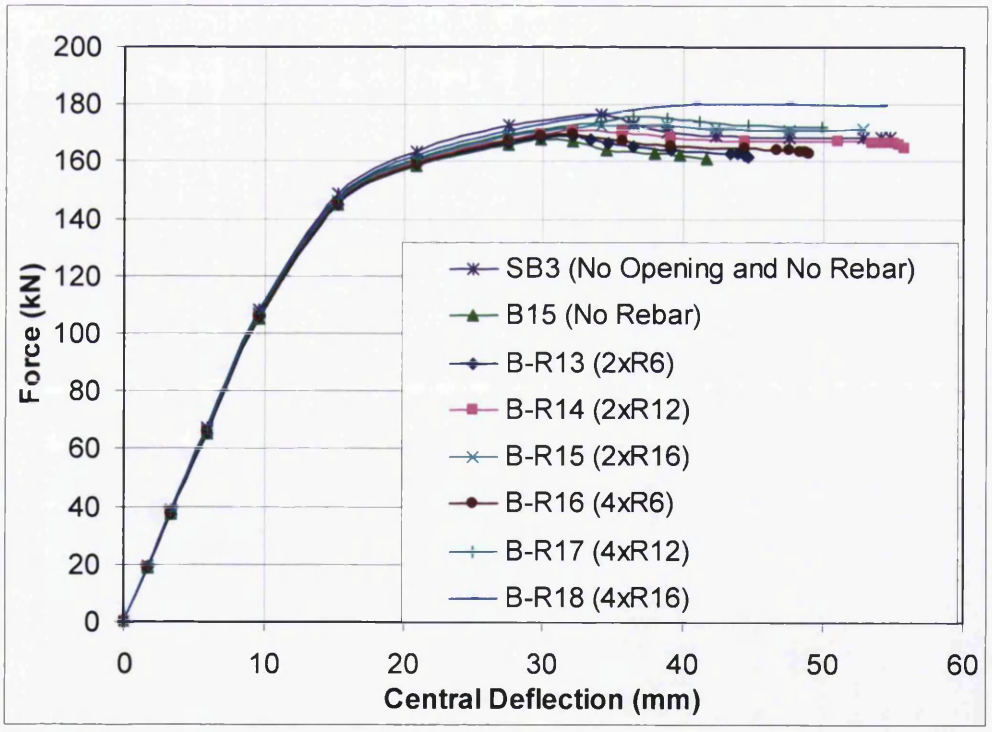

Figure 5.64: Effect of rebar area on ultimate load of composite beam with openings of type B with concrete strength, 35 N/mm^2

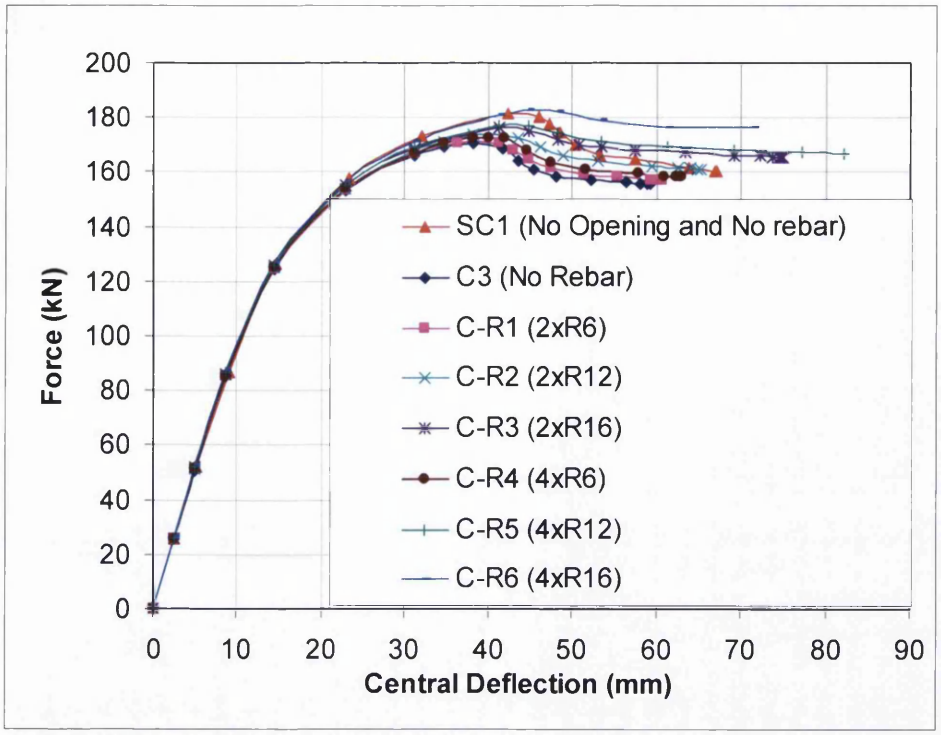

Figure 5.65: Effect of rebar area on ultimate load of composite beam with openings of type C with concrete strength, 43.3 N/mm^2

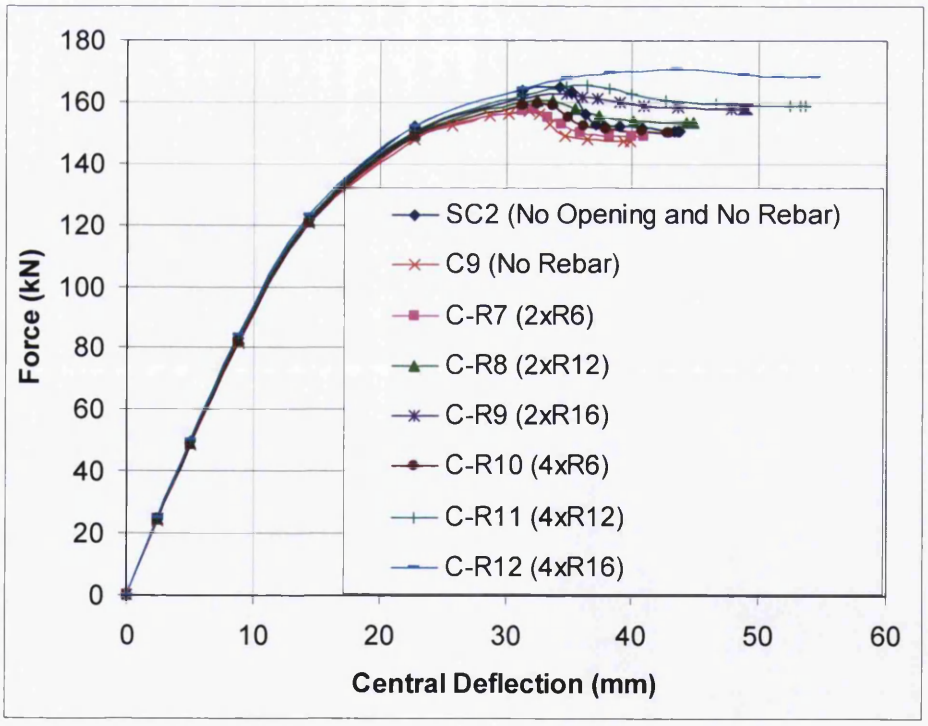

Figure 5.66: Effect of rebar area on ultimate load of composite beam with openings of type C with concrete strength, 26 N/mm^2

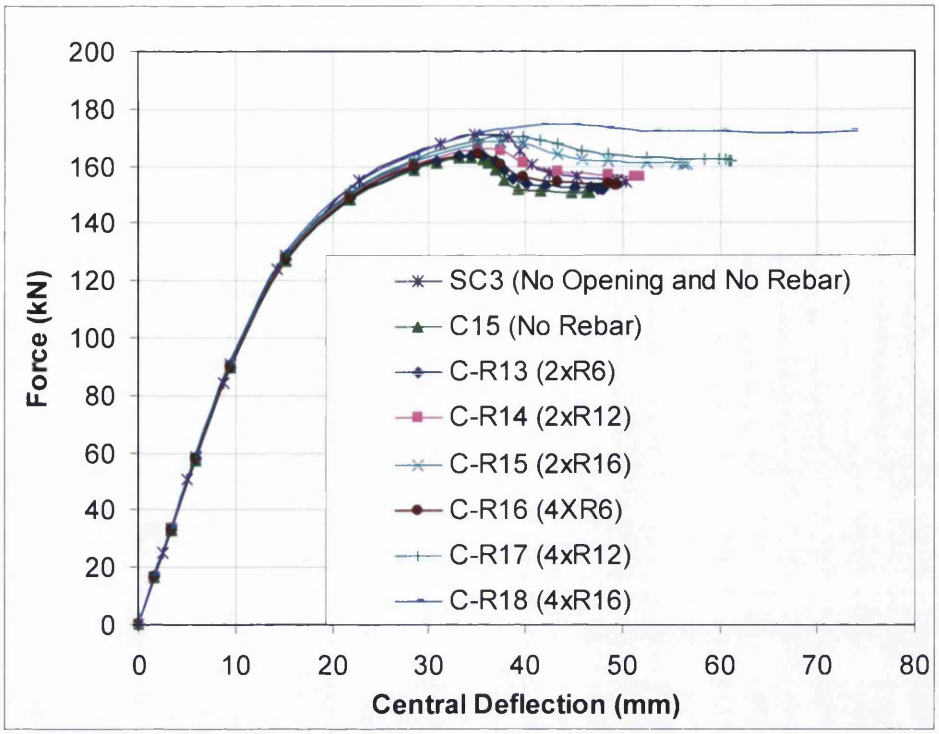

Figure 5.67: Effect of rebar area on ultimate load of composite beam with openings of type C with concrete strength, 35 N/mm^2

It can be observed from load-deflection curves an increase in rebar area results in increase in the ultimate load. There is no effect on beam stiffness in linear range. Most of the load-deflection curve is linear approximately up to 80 kN. Complete results for this study are shown in Table 5.24 to Table 5.26.

In the table P_u is ultimate load for beam with opening reinforced with rebar while P_o is ultimate load for beam with openings and no rebar. It can be observed when two rebar with 6 mm diameter, located outermost side of flange, $\frac{P_u}{P_o}$ ratio up to 1%. When four rebar with 16mm diameter is used, $\frac{P_u}{P_o}$ ratio is increased up to 10%. The maximum $\frac{P_u}{P_o}$ ratio is 1.10, which indicates 10% increment over the openings model without rebar, which is for A-R18 model.

Concrete cross section area in transverse axis was reduced by openings and subsequently reduced the compressive force. Inclusion of rebar has significant effect to enhance the moment resistance of composite beam with openings in metal-ribbed decking. Rebar ratio is the ratio between rebar area and effective concrete area. In all cases, added only 0.2% of rebar will not increase the ultimate load of composite beam with openings compared with a composite beam without openings. However adding more than 2.5% of rebar will increase the ultimate load even over than that of the models without openings which indicate that the beam could be largely over designed. Results have shown that the ideal percentage of rebar to be used is between 0.3% and 1% in order to avoid under or over design the composite beam caused by openings.

This shows that the rebar can be utilized to contribute to composite action. This observation proved that the forced developed by the rebar can be transferred by the shear connector for the cases with opening located at maximum bending moment region of beam span. However, the rebar ratio also is depends on degree of shear interaction. To take into account both factors of openings and rebar in design, a design method has been proposed in Chapter 6 based on numerical result obtained.

It should be mentioned here all models are failed due to bending. It should be borne in mind that in this parametric study, rebars are only to be used to improve the moment capacity of composite beam when the openings are located at the mid-span regions since it is assumes that the yield strength of the reinforcement can be achieved even for the beam designed with partial-interaction and failure occured due to bending. Such suggestion cannot be made for composite beam failed in shear failure.

Nie.et al (2008) and Titoum et. al. (2009) concluded from their observation, for composite beam with degree of shear interaction less than 50%, will fail due to shear failure. Similar conclusion also has been made in Chapter 4, section 4.4.2. Due to this reason, the technique can only be used for composite beam failed in bending with the degree of shear interaction is more than 50%. To develop a practical design method by using this technique, more numerical analyses for different reinforcing bar area has been carried out specifically to study the improvement of moment resistance of composite beam with openings by inclusion of rebar.

Table 5.24: Results for composite beams with openings and with different rebar area, type A

Beam Model	Reinforcing bar area (mm^2)	Rebar Ratio (%)	Opening parameter		P_u	$\frac{P_u}{P_o}$	$\frac{P_u}{P_{no}}$
			a (mm)	f (mm)			
A-R1	(2R6) 56.56	0.2	140	200	161.25	1.01	0.95
A-R2	(2R12) 226.22	0.7	140	200	163.83	1.02	0.97
A-R3	(2R16) 402.18	1.2	140	200	167.02	1.04	0.99
A-R4	(4R6) 113.11	0.3	140	200	162.55	1.02	0.96
A-R5	(4R12) 452.45	1.4	140	200	168.28	1.05	0.99
A-R6	(4R16) 804.35	2.5	140	200	173.51	1.08	1.02
A-R7	(2R6) 56.56	0.2	140	200	148.93	1.01	0.98
A-R8	(2R12) 226.22	0.7	140	200	152.49	1.03	1.00
A-R9	(2R16) 402.18	1.2	140	200	155.97	1.06	1.02
A-R10	(4R6) 113.11	0.3	140	200	150.43	1.02	0.99
A-R11	(4R12) 452.45	1.4	140	200	156.71	1.06	1.03
A-R12	(4R16) 804.35	2.5	140	200	161.51	1.09	1.06
A-R13	(2R6) 56.56	0.2	140	200	153.87	1.01	0.97
A-R14	(2R12) 226.22	0.7	140	200	157.14	1.03	0.99
A-R15	(2R16) 402.18	1.2	140	200	159.65	1.04	1.00
A-R16	(4R6) 113.11	0.3	140	200	155.10	1.02	0.97
A-R17	(4R12) 452.45	1.4	140	200	160.74	1.05	1.01
A-R18	(4R16) 804.35	2.5	140	200	167.41	1.10	1.05

Table 5.25: Results for composite beams with openings and with different rebar area, type B

Beam Model	Reinforcing bar area (mm^2)	Rebar Ratio (%)	Opening parameter		P_u	P_u/P_o	P_u/P_{no}
			a (mm)	f (mm)			
B-R1	(2R6) 56.56	0.2	140	200	177.32	1.01	0.96
B-R2	(2R12) 226.22	0.7	140	200	179.72	1.02	0.98
B-R3	(2R16) 402.18	1.2	140	200	181.50	1.03	0.99
B-R4	(4R6) 113.11	0.3	140	200	178.44	1.01	0.97
B-R5	(4R12) 452.45	1.4	140	200	183.41	1.04	1.00
B-R6	(4R16) 804.35	2.5	140	200	188.06	1.07	1.02
B-R7	(2R6) 56.56	0.2	140	200	162.68	1.01	0.97
B-R8	(2R12) 226.22	0.7	140	200	165.29	1.03	0.99
B-R9	(2R16) 402.18	1.2	140	200	167.35	1.04	1.00
B-R10	(4R6) 113.11	0.3	140	200	163.71	1.02	0.98
B-R11	(4R12) 452.45	1.4	140	200	169.89	1.05	1.01
B-R12	(4R16) 804.35	2.5	140	200	176.00	1.09	1.05
B-R13	(2R6) 56.56	0.2	140	200	168.76	1.01	0.97
B-R14	(2R12) 226.22	0.7	140	200	170.70	1.02	0.98
B-R15	(2R16) 402.18	1.2	140	200	172.57	1.03	0.99
B-R16	(4R6) 113.11	0.3	140	200	169.83	1.01	0.98
B-R17	(4R12) 452.45	1.4	140	200	175.57	1.05	1.01
B-R18	(4R16) 804.35	2.5	140	200	180.05	1.08	1.04

Table 5.26: Results for composite beams with openings and with different rebar area, type C

Beam Model	Reinforcing bar area (mm^2)	Rebar Ratio (%)	Opening parameter		P_u	P_u/P_o	P_u/P_{no}
			a (mm)	f (mm)			
C-R1	(2R6) 56.56	0.2	140	200	170.74	1.00	0.94
C-R2	(2R12) 226.22	0.7	140	200	173.74	1.02	0.96
C-R3	(2R16) 402.18	1.2	140	200	176.09	1.03	0.97
C-R4	(4R6) 113.11	0.3	140	200	172.67	1.01	0.95
C-R5	(4R12) 452.45	1.4	140	200	177.23	1.04	0.98
C-R6	(4R16) 804.35	2.5	140	200	182.71	1.07	1.01
C-R7	(2R6) 56.56	0.2	140	200	157.63	1.01	0.95
C-R8	(2R12) 226.22	0.7	140	200	160.76	1.03	0.97
C-R9	(2R16) 402.18	1.2	140	200	162.49	1.04	0.98
C-R10	(4R6) 113.11	0.3	140	200	159.41	1.02	0.97
C-R11	(4R12) 452.45	1.4	140	200	165.63	1.06	1.00
C-R12	(4R16) 804.35	2.5	140	200	170.38	1.09	1.03
C-R13	(2R6) 56.56	0.2	140	200	163.56	1.01	0.96
C-R14	(2R12) 226.22	0.7	140	200	165.06	1.01	0.97
C-R15	(2R16) 402.18	1.2	140	200	168.30	1.03	0.99
C-R16	(4R6) 113.11	0.3	140	200	164.11	1.01	0.96
C-R17	(4R12) 452.45	1.4	140	200	170.27	1.05	1.00
C-R18	(4R16) 804.35	2.5	140	200	174.39	1.07	1.02

5.6 Conclusion

The effects of openings on composite beams with ribbed-decking slabs were studied. A 3D, non-linear finite element model was developed to investigate these influences. There were three type of decking, A (narrow-ribbed), B (wide-ribbed) and C (wide-ribbed) used in this study base on their dimension. Fifty four composite beam models were used to investigate the effect of this parameter on the ultimate moment capacity. It was found that when openings size in the transverse axis was increase, they had a significant effect on the ultimate load, compared to openings size in longitudinal axis. First part deals with investigation of the opening effect on the ultimate moment capacities of composite beams. Parameters considered include opening sizes in transverse and longitudinal axis, location of the openings and position of load.

When openings size were varied in transverse direction, for type A decking (narrow-ribbed), the results show that by increasing the openings size in transverse direction will decrease the ultimate load of composite beam. The results show that the ultimate load decrease by 2%, 1% and 2% when the opening size is increased by 10% in the direction of transverse axis for model A1, A7 and A8, respectively. The corresponding drop in ultimate load is 9%, 6% and 10%, respectively, when the opening size increased to 50%. For B type model (wide-ribbed), the results show that the ultimate load drops by 2%, 3% and 3%, when the opening size is increased by 10% in the direction of transverse direction for model B1, B7 and B8, respectively. The corresponding drop in ultimate load is 11%, 15% and 12% when the opening size increased to 50%. For C type model, the metal decking used in this group is classified as wide-ribbed. This is similar classification to B groups but different in decking dimension. Similar pattern of load-deflection curve was observed when compared with that of A and C group. The results show that the ultimate load drops by 4%, 3% and 3%, when the opening size is increased by 10% in the transverse direction for model C1, C7 and C8, respectively. The corresponding drop in ultimate load is 12%, 14% and 11% in ultimate load when the opening size increased to 50%. For all cases, with the increase in load, development of high compressive stress is initiated at beam centre and outermost side of opening and then high compressive stress extends to the whole side of opening. For higher openings ratio, development of high compressive

stress is initiated at lower applied load compared to model which has lower opening ratio.

Second parameter considered is openings size in longitudinal direction. Increase the openings size in the longitudinal direction has little effect on the ultimate load. Negligible effect on ultimate load is due to the fact that the width of composite beam flange is not reduced. Reduction in stiffness of the beams is, however, observed in the linear range with increase in the size of openings **(f).** Reduction is attributed due to change of geometry of composite beams in the longitudinal direction. Reduction in stiffness can be associated with opening ratio. Opening ratio is defined by opening size in longitudinal direction divided by beam length. With opening ratio of 10%, the reduction of stiffness is approximately 4% compared with that of a composite beam without opening. For opening ratio 40%, the reduction of stiffness is as high as 22%, as in the case of model B1-f3. From the numerical results, it can be concluded that the effect is significant when opening ratio is more than 20%.

Third parameter considered was openings location with a point load applied at mid-span. Two different locations, 400mm and 800mm were considered in the study. It can be seen that the beam stiffness and ultimate load are least affected when the openings are placed away from the mid-span. Load-deflection curves show that there is reduction on moment capacity of composite beam even when opening is not located at mid-span. However, when applied load location was varied while openings location was constant, the reduction of moment capacity is found to be influenced by applied load location. Load is applied at different locations which are in front of opening (front section), opening centre (central section) and behind opening (end section). Moment is reduced up to 4%, 6% and 7% for load applied at the front section, central section and end section of openings, respectively. It was observed that the moment reduction is more when load is located at opening end section compared to front section. It was also observed that the opening influences more if it is applied within the region of maximum bending moment. For central loading, the maximum bending moment is at the central of the beam while for two point load cases, the maximum bending moment is in between the two loads. Stress contours in composite beam with opening with different load locations shows that for openings located outside maximum bending moment region (load applied at front section), high compressive

stress in slab is formed at mid-span. For load applied at the opening centre and opening end section, high compressive stress in slab is distributed at opening area, along innermost and outermost side of beam flange. The location of high compressive stress is changing from mid-span to opening area due to reduction of slab section.

Fourth parameter considered was two openings with different position .A reduction of ultimate load for two openings located at both side of beam flange is more than that of openings located at one side of beam flange. The difference in ultimate moment between these opening positions is between 3% and 5%. It should be mention, the analyses were carried out using model with openings located away from mid-span. The ultimate moment could be reduced more if openings are located at mid-span of the beam. It can be observed from stress contour, when opening is positioned at both sides of beam flange, high compressive stress developed at corner side of opening. Between these two openings, high compressive stress developed from one opening corner to another opening corner. It shows that the stress distribution is influenced by these two openings. Calculation of effective width should include these two openings even though both opening is located at different cross section. For opening located at one side of flange, high compressive stress is distributed at load location area.

Finally, the parametric study was also conducted to study suitable methods to increase the moment capacity of the composite beams with openings in metal-ribbed decking in order to counter the openings effect in composite beam slab. The aim of this study is to investigate how the beam capacity is increase in order to avoid any too conservative or inadequate in beam design. Three methods were considered, concrete strength, slab thickness and rebar area.

First method was to concrete cube strength increased. The ultimate load is increased by about 10% when the cube strength of composite beam with opening is increased from 26 MPa to 43.3 MPa. It is observed, the beam ultimate load are affected more for lower opening ratio. As in the case of models A1, B1 and C1 which has 10% opening ratio, ultimate load is increased about 7% over the composite beam without openings when the cube strength is increased from 26 MPa to 43.3 MPa. As in the case of model A6, B6 and C6 which has higher opening ratio (50%), the ultimate load is increased about 1% over the composite beam without opening when the cube strength

is increased from 26 MPa to 43.3 MPa. It can be concluded that the ultimate load is increment by increasing cube strength is influence by openings ratio. By increasing the concrete cube strength, for higher openings ratio, the increase in ultimate load is lower compare to smaller openings ratio.

The second method was increasing slab thickness. It is interesting to note that, the ultimate load is increased up to composite beam without openings when the slab thickness is increased by 10% over the thickness of reference model. This result shows that around 10% of slab thickness increment from reference model for composite beam with openings is required to recover lost of composite beam strength caused by openings in slab. In all cases, it is observed that the ultimate load is increased more than composite beam without openings when the slab thickness is increased more than 10% for the thickness of reference model. As in the case of model B-T5, the ultimate load is increased by 7% over the composite beam without openings when the slab thickness is increased by 19% over the thickness of reference model. These results show that the composite beam with openings will be over designed when the slab thickness is increased more than 10% over the thickness of reference model.

The final method was the inclusion of rebar. Concrete area in transverse axis was reduced by openings and subsequently reduced the compressive force. Inclusion of rebar produced significant effect to enhance the moment resistance of a composite beam with openings in metal-ribbed decking. Rebar ratio is the ratio between rebar area and effective concrete area. In all cases, adding 0.2% of rebar will not increase the ultimate load of composite beam with openings up to composite beam without openings. However added 2.5% of rebar will increased the ultimate load over than models without openings. Results show that the ideal percentage of rebar to be used is between 0.3% and 1% in order to avoid under-estimate or over-estimate the composite beam design caused by openings.

Therefore it can be concluded that, to improve the ultimate load of composite beams with openings in metal-ribbed decking slabs, designers should consider the cost implications and they have an option to choose whether to use the cube strength,

overall slab thickness, rebar, or combine technique to counter the effect of the openings.

5.7 References

Nie, J. G., Fan, J., Cai, C.S., (2008). "Experimental study of partially shear-connected composites beams with profiled sheeting" Engineering Structures, 30:1-12.

Titoum, M., Tehami, M., Achour, B., (2009). "Effect of partial shear connection on the behaviour of semi-continuous composite beams" Steel structures, 9(4): 301-313.

Chapter 6

ANALYTICAL METHOD

6.1 Introduction

Parametric studies carried out on composite beams with and without openings in flanges have been described in Chapter 4 and Chapter 5. Although finite element method can be used to determined the ultimate strength of composite beams with openings, it is time consuming and inconvenient to use in design practice. Therefore, it is desirable to obtain practical design equations. In this chapter, the development of a simple design method to predict the ultimate moment capacity of composite beams with openings is presented. The values of ultimate moment capacity thus obtained by the design method are compared with corresponding value from the numerical method.

6.2 Plastic analysis of composite beam with opening in flange

The ultimate strength of composite members depends on the degree of shear connection provided, the compressive resistance of effective concrete slab and tensile

yield resistance of the steel shape. It is determined from its plastic capacity. It is assumed in the design method that strain across the section is sufficiently large that the steel stresses reach at yield throughout the section and that the concrete stresses are at their design strength. The plastic stress blocks are assumed rectangular as opposed to linear in the elastic design. For composite beam with metal-ribbed decking, changing the effective width of the concrete flange could be only modification required to deal with openings in slab design. By neglecting concrete tensile strength, plastic moment capacity of composite beam with opening section, M_c, can be calculated by the following procedure:-

- Find the net effective width of the flange

The net effective width of the flange with opening can be found as,

$$B_{ne} = B_e - 2a \qquad (6\text{-}1)$$

Where,

a= wide of a square openings at the cross-section

B_e=effective width of the beam flange

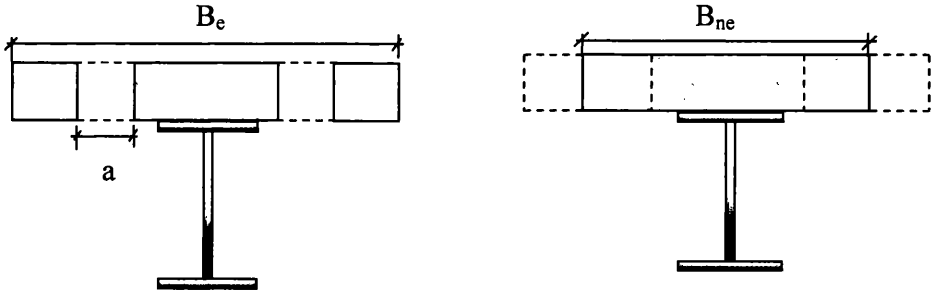

(a) Flange with opening (b) Net effective width

Figure 6.1: Typical composite section composite beams with openings

- Moment capacity

As for the recommendation in design codes such as, EC4 (BSI 1991) and BS5950 (BSI 1990), the plastic neutral axis of the composite section can be located by

comparing the compressive resistance of the effective concrete slab with tensile resistance of steel shape as in Equation (6-1) and equation (6-3), respectively,

$$R_c = 0.45 f_{cu} (D_s - D_p) B_e \tag{6-2}$$

$$R_s = p_y A_s \tag{6-3}$$

To account for openings, modified compressive resistance is given by Equation (6-4)

$$R_c' = \frac{R_c B_{ne}}{B_e} \tag{6-4}$$

There are three possible location of the plastic neutral axis as shown in Figure 6.2.

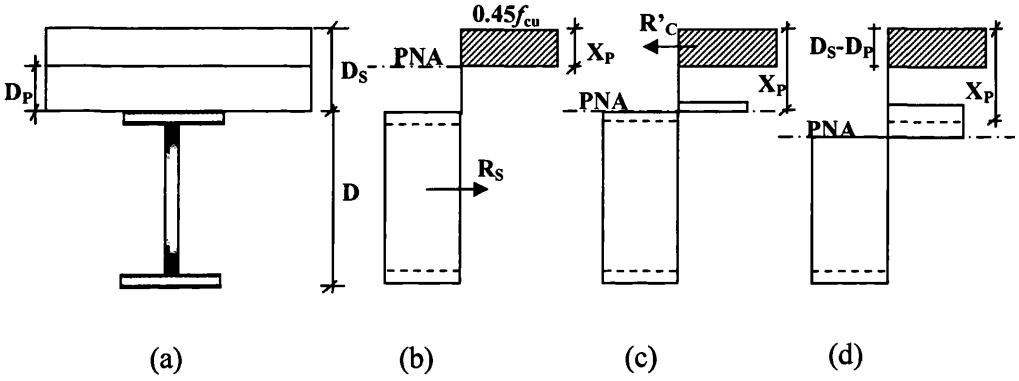

Figure 6.2: Plastic analysis of composite section under positive moment (PNA: plastic neutral axis)

The modified moment capacity, M_c, for full interaction of the composite beam is given by:

- Case 1- Neutral axis in concrete (Figure 6.2 (b))

$$M_c = R_s \left[\frac{D}{2} + D_s - \frac{R_s B_e}{R_c B_{ne}} \left(\frac{D_s - D_p}{2} \right) \right] \tag{6-5}$$

- Case 2- Neutral Axis in steel flange (Figure 6.2 (c))

$$M_c = R_s \frac{D}{2} + \frac{R_c B_{ne}}{B_e}\left(\frac{D_s + D_p}{2}\right) - \frac{\left(R_s - R_c B_{ne}/B_e\right)^2}{R_f}\frac{T}{4} \quad (6\text{-}6)$$

- Case 3- Neutral Axis in steel web (Figure 6.2 (d))

$$M_c = M_s + \frac{R_c B_{ne}}{B_e}\left(\frac{D_s + D_p + D}{2}\right) - \frac{1}{R_w}\left(\frac{R_c B_{ne}}{B_e}\right)^2 \frac{D}{4} \quad (6\text{-}7)$$

However for partial interaction in the composite beam, modified moment capacity M_c is given by:

- Case 4: Plastic neutral axis in the flange

$$M_c = R_s \frac{D}{2} + R_q\left(D_s - \frac{R_q B_e}{R_c B_{ne}}\left(\frac{D_s - D_p}{2}\right)\right) - \frac{\left(R_s - R_q\right)^2}{R_f}\frac{T}{4} \quad (6\text{-}8)$$

- Case 5: Plastic neutral axis in the web

$$M_c = M_s + R_q\left(\frac{D}{2} + D_s - \frac{R_q B_e}{R_c B_{ne}}\left(\frac{D_s - D_p}{2}\right)\right) - \frac{R_q^2}{R_w}\frac{D}{4} \quad (6\text{-}9)$$

6.3 Opening size

A parametric study was conducted using fifty four FE model for various opening sizes across the composite beam flange (100mm, 200mm, 280mm, 340mm, 400mm and 500mm), three different metal-ribbed decking (type A, type B and type C) and various concrete strength (26 N/mm^2, 35 N/mm^2 and 43.3 N/mm^2). Details of the study have been given in Chapter 5. An example of the design calculation to determine moment capacity for model A1 is presented in Appendix H and Appendix I. Modified plastic analysis proposed in section 6.2 was used. Values of moment capacities obtained from the design method are compared with the corresponding value determined by using the finite element method.

Tables 6.1 to 6.3 show the comparison of ultimate moment values. In the table M_{FE} and M_{no} refers to values of composite beam with opening and composite beam without openings, respectively, obtained from numerical model. M_{EC4} and M_{BS5950} refer to the ultimate moment calculated by modified design equation according to EC4 (BSI 1991) and BS5950 (BSI 1990), respectively. A good agreement can be seen between the moments capacities obtained from design equation and the finite element results.

It can be observed that M_{EC4}, the EC4 values are lower than corresponding values predicted by BS 5950, M_{BS5950}. The difference is due to the definition for degree of shear connection between these two codes. The comparison shows most of the predicted value to be on safe side; when the predicted values using modified EC4 and BS5950 equation were lower than finite element values. The mean $\frac{M_{EC4}}{M_{FE}}$ ratio and $\frac{M_{BS5950}}{M_{FE}}$ ratio for 54 numerical models are 0.96 and 0.99, respectively, with standard deviation of 0.02 and 0.01, respectively.

It can be seen from ratio of $\left(\frac{M}{M_{no}}\right)_{FE}$, $\left(\frac{M}{M_{no}}\right)_{EC4}$ and $\left(\frac{M}{M_{no}}\right)_{BS5950}$ that with the presence of openings results are in reduction of the moment capacity of composite beams. Increase in the opening size will decrease a moment capacity of composite beam. For example, as in case of model B12, with the opening ratio of 50%, moment capacity is reduced by 15 % using finite element method. The reduction also confirmed by design method where moment capacity is reduced by 15% and 14% according to EC4 (BSI 1991) and BS5950 (BSI 1990), respectively. By comparing the value from finite element analysis and calculated value from modified equation, the prediction by modification equation can be considered accurate for the design purpose.

Table 6.1: Moment capacity of composite beam between numerical and analytical value (metal decking type A) for opening size parameter

Beam model	Opening Size, a (mm)	f_{cu} (MPa)	k_s (EC4)	k_s (BS5950)	M_{FE} (kN.m)	$\left(\frac{M}{M_{no}}\right)_{FE}$	M_{EC4} (kN.m)	$\frac{M_{EC4}}{M_{FE}}$	$\left(\frac{M}{M_{no}}\right)_{EC4}$	M_{BS5950} (kN.m)	$\frac{M_{BS5950}}{M_{FE}}$	$\left(\frac{M}{M_{no}}\right)_{BS5950}$
A1	50	43.3	0.51	0.60	165.62	0.98	152.31	0.92	1.00	163.33	0.98	1.00
A2	100	43.3	0.51	0.60	162.54	0.96	151.61	0.93	0.99	161.80	1.00	0.99
A3	140	43.3	0.51	0.60	160.06	0.95	150.90	0.94	0.99	160.54	1.00	0.98
A4	170	43.3	0.51	0.60	158.05	0.93	150.27	0.95	0.98	159.38	1.01	0.97
A5	200	43.3	0.51	0.60	155.68	0.92	149.50	0.96	0.98	157.98	1.01	0.97
A6	250	43.3	0.51	0.60	153.88	0.91	147.81	0.96	0.97	154.87	1.01	0.95
A7	50	26	0.68	0.86	151.15	0.99	142.00	0.94	1.00	152.14	1.01	0.99
A8	100	26	0.68	0.86	148.90	0.98	141.24	0.95	0.99	150.55	1.01	0.98
A9	140	26	0.68	0.86	147.66	0.97	140.47	0.95	0.99	148.95	1.01	0.97
A10	170	26	0.68	0.86	146.65	0.96	139.78	0.95	0.98	147.48	1.01	0.97
A11	200	26	0.68	0.86	145.56	0.95	138.95	0.95	0.97	145.71	1.00	0.95
A12	250	26	0.68	0.86	143.49	0.94	137.12	0.96	0.96	141.76	0.99	0.93
A13	50	35	0.61	0.70	156.56	0.98	149.73	0.96	1.00	156.35	1.00	0.99
A14	100	35	0.61	0.70	154.71	0.97	148.92	0.96	0.99	154.91	1.00	0.98
A15	140	35	0.61	0.70	152.80	0.96	148.10	0.97	0.98	153.47	1.00	0.98
A16	170	35	0.61	0.70	151.30	0.95	147.36	0.97	0.98	152.15	1.01	0.97
A17	200	35	0.61	0.70	149.69	0.94	146.47	0.98	0.97	150.55	1.01	0.96
A18	250	35	0.61	0.70	143.49	0.90	144.52	1.01	0.96	147.00	1.02	0.94

Table 6.2: Moment capacity of composite beam between numerical and analytical value (metal decking type B) for opening size parameter

Beam model	Opening Size, a (mm)	f_{cu} (MPa)	k_s (EC4)	k_s (BS5950)	M_{FE} (kN.m)	$\left(\frac{M}{M_{no}}\right)_{FE}$	M_{EC4} (kN.m)	$\frac{M_{EC4}}{M_{FE}}$	$\left(\frac{M}{M_{no}}\right)_{EC4}$	M_{BS5950} (kN.m)	$\frac{M_{BS5950}}{M_{FE}}$	$\left(\frac{M}{M_{no}}\right)_{BS5950}$
B1	50	43.3	0.76	0.89	181.54	0.98	170.19	0.94	0.99	182.60	1.01	0.99
B2	100	43.3	0.76	0.89	178.55	0.96	168.60	0.94	0.98	179.78	1.01	0.97
B3	140	43.3	0.76	0.89	176.42	0.95	167.02	0.95	0.97	176.93	1.00	0.96
B4	170	43.3	0.76	0.89	173.97	0.94	165.58	0.95	0.97	174.33	1.00	0.95
B5	200	43.3	0.76	0.89	172.15	0.93	163.86	0.95	0.96	171.18	0.99	0.93
B6	250	43.3	0.76	0.89	165.53	0.89	160.06	0.97	0.93	164.17	0.99	0.90
B7	50	26	1.00	1.00	165.48	0.97	154.69	0.93	0.99	164.64	0.99	0.98
B8	100	26	1.00	1.00	163.50	0.96	152.97	0.94	0.98	161.07	0.99	0.96
B9	140	26	1.00	1.00	161.07	0.95	151.26	0.94	0.97	157.46	0.98	0.94
B10	170	26	1.00	1.00	157.43	0.93	149.70	0.95	0.96	154.16	0.98	0.93
B11	200	26	1.00	1.00	153.68	0.91	147.83	0.96	0.95	150.17	0.98	0.90
B12	250	26	1.00	1.00	144.61	0.85	143.72	0.99	0.92	141.28	0.98	0.86
B13	50	35	0.91	1.00	171.63	0.97	165.71	0.97	0.99	171.75	1.00	0.99
B14	100	35	0.91	1.00	169.78	0.96	163.88	0.97	0.98	168.52	0.99	0.97
B15	140	35	0.91	1.00	167.46	0.95	162.04	0.97	0.97	165.28	0.99	0.95
B16	170	35	0.91	1.00	165.24	0.94	160.38	0.97	0.96	162.31	0.98	0.94
B17	200	35	0.91	1.00	162.49	0.92	158.38	0.97	0.95	158.72	0.98	0.92
B18	250	35	0.91	1.00	154.53	0.88	153.98	1.00	0.92	150.72	0.98	0.88

Table 6.3: Moment capacity of composite beam between numerical and analytical value (metal decking type C) for opening size parameter

Beam model	Opening Size, a (mm)	f_{cu} (MPa)	k_s (EC4)	k_s (BS5950)	M_{FE} (kN.m)	$\left(\frac{M}{M_{no}}\right)_{FE}$	M_{EC4} (kN.m)	$\frac{M_{EC4}}{M_{FE}}$	$\left(\frac{M}{M_{no}}\right)_{EC4}$	M_{BS5950} (kN.m)	$\frac{M_{BS5950}}{M_{FE}}$	$\left(\frac{M}{M_{no}}\right)_{BS5950}$
C1	50	43.3	0.54	0.63	179.38	0.96	165.57	0.93	0.99	178.27	0.99	0.99
C2	100	43.3	0.54	0.63	175.76	0.94	164.27	0.95	0.99	176.08	1.00	0.98
C3	140	43.3	0.54	0.63	172.73	0.93	162.97	0.96	0.98	173.89	1.01	0.97
C4	170	43.3	0.54	0.63	170.25	0.91	161.78	0.96	0.97	171.90	1.01	0.95
C5	200	43.3	0.54	0.63	167.54	0.90	160.36	0.97	0.96	169.51	1.01	0.94
C6	250	43.3	0.54	0.63	163.32	0.88	157.23	0.97	0.94	164.25	1.01	0.91
C7	50	26	0.71	0.90	163.65	0.97	151.51	0.94	0.99	162.51	0.99	0.99
C8	100	26	0.71	0.90	160.81	0.95	150.10	0.95	0.98	159.73	0.99	0.97
C9	140	26	0.71	0.90	157.86	0.93	148.69	0.95	0.97	156.95	0.99	0.95
C10	170	26	0.71	0.90	156.72	0.93	147.41	0.95	0.97	154.43	0.99	0.94
C11	200	26	0.71	0.90	151.80	0.90	145.87	0.97	0.96	151.40	0.99	0.92
C12	250	26	0.71	0.90	145.98	0.86	142.48	0.99	0.93	144.74	0.98	0.88
C13	50	35	0.63	0.66	169.90	0.97	161.66	0.96	0.99	169.30	1.00	0.99
C14	100	35	0.63	0.66	166.81	0.96	160.15	0.97	0.98	166.87	1.00	0.98
C15	140	35	0.63	0.66	164.71	0.94	158.64	0.98	0.97	164.45	1.00	0.97
C16	170	35	0.63	0.66	162.75	0.93	157.27	0.98	0.97	162.24	1.00	0.95
C17	200	35	0.63	0.66	160.93	0.92	155.63	0.98	0.96	159.60	0.99	0.94
C18	250	35	0.63	0.66	154.48	0.89	152.00	0.98	0.93	153.78	1.00	0.91

6.4 Concrete strength

The values of ratios $\frac{M_{fcu-43.3}}{M_{fcu-26}}$ and $\frac{M_{fcu-43.3}}{M_{no}}$ obtained from the numerical analyses are listed along with the results obtained from design method in Table 6.4. In the table $M_{fcu-43.3}$ represents the values of ultimate moment for model with 43.3 MPa cube strength whereas M_{fcu-26} is for model with 26 MPa cube strength. Design method explained in section 6.2 is used to calculate the analytical results. It is observed from table that maximum variation ratio between analytical and numerical value is 2%. Mean value for $\frac{M_{fcu-43.3}}{M_{fcu-26}}$ ratio of numerical results is 10%. This is confirmed by modified EC4 and BS5950 method, 8% and 11%, respectively. The moment capacity of composite beam with opening also has been compared with composite beam without opening. It can be seen from the table that the most of analytical results obtained from modified EC4 produces conservative prediction of ultimate moment of composite beam with openings in metal-ribbed decking slab.

As in the case of models A1, B1 and C1 which has 10% opening ratio, ultimate load is increased about 6% to 9% over the ultimate load of composite beam without openings when the cube strength is increased from 26 MPa to 43.3 MPa. As in the case of model A6, B6 and C6 which has higher opening ratio (50%), the ultimate load is increased about between -2% and 3% compared to ultimate load of the composite beam without opening when the cube strength is increased from 26 MPa to 43.3 MPa. Similar observation is also obtained from numerical result. It can be observed that the increment of moment capacity is more significant with lower opening ratio. For example, as in the case of model A1, with opening ratio 10% give significant increment in ratio of $\frac{M_{fcu-43.3}}{M_{no}}$ which is 9%. However for model A6, with 50% opening ratio, $\frac{M_{fcu-43.3}}{M_{no}}$ ratio is only 1%. This is also confirmed by analytical value for A1 and A6 which is 7% and 4%, respectively, predicted by modified EC4 and 6% and 1%, respectively, predicted by modified BS5950. It can be concluded that by increasing the concrete cube strength, for higher openings ratio, the increase in ultimate load is lower compare to smaller openings ratio.

Table 6.4: Results for composite beam with openings with different cube strength

Beam Model	f_{cu} (MPa)	M_{FE} (kN)	M_{EC4} (kN)	M_{BS5950} (kN)	Beam Model	f_{cu} (MPa)	Opening Ratio %	M_{FE} (kN)	M_{EC4} (kN)	M_{BS5950} (kN)	FE		EC4		BS 5950	
											$\frac{M_{fcu-43.3}}{M_{fcu-26}}$	$\frac{M_{fcu-43.3}}{M_{no}}$	$\frac{M_{fcu-43.3}}{M_{fcu-26}}$	$\frac{M_{fcu-43.3}}{M_{no}}$	$\frac{M_{fcu-43.3}}{M_{fcu-26}}$	$\frac{M_{fcu-}}{M_{no}}$
A1	43.3	151.15	152.31	163.06	A7	26	10	165.62	142.00	152.14	1.10	1.09	1.07	1.07	1.07	1.06
A2	43.3	148.90	151.61	161.80	A8	26	20	162.54	141.24	150.55	1.09	1.07	1.07	1.06	1.07	1.05
A3	43.3	147.66	150.90	160.54	A9	26	28	160.06	140.47	148.95	1.08	1.05	1.07	1.06	1.08	1.05
A4	43.3	146.65	150.27	159.38	A10	26	34	158.05	139.78	147.48	1.08	1.04	1.08	1.05	1.08	1.04
A5	43.3	145.56	149.5	157.98	A11	26	40	155.68	138.95	145.71	1.07	1.02	1.08	1.05	1.08	1.03
A6	43.3	143.49	147.81	154.87	A12	26	50	153.88	137.12	141.76	1.07	1.01	1.08	1.04	1.09	1.01
B1	43.3	181.54	170.19	182.60	B7	26	10	165.48	154.69	164.64	1.10	1.07	1.10	1.09	1.11	1.09
B2	43.3	178.55	168.60	179.78	B8	26	20	163.50	152.97	161.07	1.09	1.05	1.10	1.08	1.12	1.07
B3	43.3	176.42	167.02	176.93	B9	26	28	161.07	151.26	157.46	1.10	1.04	1.10	1.07	1.12	1.05
B4	43.3	173.97	165.58	174.33	B10	26	34	157.43	149.70	154.16	1.11	1.02	1.11	1.06	1.13	1.04
B5	43.3	172.15	163.86	171.18	B11	26	40	153.68	147.83	150.17	1.12	1.01	1.11	1.05	1.14	1.02
B6	43.3	165.53	160.06	164.17	B12	26	50	144.61	143.72	141.28	1.14	0.98	1.11	1.03	1.16	0.98
C1	43.3	177.17	165.57	178.27	C7	26	10	161.63	151.51	162.51	1.10	1.07	1.09	1.08	1.10	1.08
C2	43.3	173.59	164.27	176.08	C8	26	20	158.82	150.10	159.73	1.09	1.05	1.09	1.08	1.10	1.07
C3	43.3	170.60	162.97	173.89	C9	26	28	155.91	148.69	156.95	1.09	1.03	1.10	1.07	1.11	1.06
C4	43.3	168.15	161.78	171.90	C10	26	34	154.79	147.41	154.43	1.09	1.02	1.10	1.06	1.11	1.04
C5	43.3	165.47	160.36	169.51	C11	26	40	149.93	145.87	151.40	1.10	1.00	1.10	1.05	1.12	1.03
C6	43.3	161.30	157.23	164.25	C12	26	50	144.18	142.48	144.74	1.12	0.98	1.10	1.03	1.13	1.00

6.5 Overall slab thickness

Different values for slab thicknesses were considered to examine the effect of slab thickness on moment capacity of composite beam with opening. Analytical method explained in section 6.2 was used to calculate the prediction results. The comparison of the calculated and numerical results is shown in Tables 6.5 to 6.7. An example of design calculation to determine moment capacity for model A-T2 is presented in Appendix J and Appendix K.

The analytical results of ultimate moment capacity for different overall slab thicknesses are consistent with the sets of numerical results obtained. The mean $\frac{M_{EC4}}{M_{FE}}$ and $\frac{M_{BS5950}}{M_{FE}}$ ratio for 45 numerical models is 0.94 and 0.99, respectively, with standard deviation of 0.02 and 0.01, respectively. Comparison between predicted values and numerical values show that the proposed design equation is sufficiently accurate. The comparison shows also that all predictions of moment capacity from EC4 method (BSI 1991) are on safe side compared to BS5950 method (BSI 1990).

The values at $\frac{M_{FE}}{M_{no}}$, $\frac{M_{EC4}}{M_{no}}$ and $\frac{M_{BS5950}}{M_{no}}$ ratio, show that moment capacity increases with the increase of overall slab thickness. With the increase of composite slab thickness, the lever arm between compression and tension force increases. This consequently increases the moment capacity of composite beam. Interestingly, the increment of moment capacity is as high as 6% over the composite beam without openings as in the case of model B-T5. This is also confirmed by analytical method according to EC4 and BS5950 methods increment being as high as 5% over the composite beam without openings.

Table 6.5: Moment capacity of composite beam between numerical and analytical value (metal decking type A) for overall slab thickness parameter

Beam model	Slab thickness, Ds (mm)	Opening Size, a (mm)	f_{cu} (MPa)	k_s (EC4)	k_s (BS5950)	M_{FE} (kN.m)	$\frac{M_{FE}}{M_{no}}$	M_{EC4} (kN.m)	$\frac{M_{EC4}}{M_{FE}}$	$\frac{M_{EC4}}{M_{no}}$	M_{BS5950} (kN.m)	$\frac{M_{BS5950}}{M_{FE}}$	$\frac{M_{BS5950}}{M_{no}}$
A-T1	105	140	43.3	51%	60%	160.06	0.95	150.90	0.94	0.99	160.54	1.00	0.98
A-T2	110	140	43.3	46%	53%	162.67	0.96	153.13	0.94	1.00	163.84	1.00	1.00
A-T3	115	140	43.3	41%	48%	167.07	0.99	155.35	0.93	1.02	166.30	1.00	1.02
A-T4	120	140	43.3	40%	46%	172.72	1.02	157.57	0.91	1.03	169.18	0.98	1.03
A-T5	125	140	43.3	40%	46%	177.78	1.05	159.80	0.90	1.05	172.07	0.97	1.05
A-T6	105	140	26	68%	86%	147.66	0.97	140.47	0.95	0.99	148.95	1.01	0.97
A-T7	110	140	26	61%	77%	150.57	0.99	142.27	0.94	1.00	151.46	1.01	0.99
A-T8	115	140	26	56%	70%	153.27	1.00	144.06	0.94	1.01	153.97	1.00	1.01
A-T9	120	140	26	51%	64%	156.56	1.03	145.85	0.93	1.02	156.48	1.00	1.02
A-T10	125	140	26	47%	59%	159.61	1.05	147.64	0.93	1.04	159.00	1.00	1.04
A-T11	105	140	35	61%	70%	152.80	0.96	148.10	0.97	0.98	153.47	1.00	0.99
A-T12	110	140	35	55%	63%	155.27	0.97	150.25	0.97	1.00	156.12	1.01	1.01
A-T13	115	140	35	50%	57%	157.52	0.99	152.40	0.97	1.01	158.76	1.01	1.03
A-T14	120	140	35	45%	52%	161.38	1.01	154.55	0.96	1.03	161.40	1.00	1.05
A-T15	125	140	35	42%	48%	165.37	1.04	156.70	0.95	1.04	164.05	0.99	1.06

Table 6.6: Moment capacity of composite beam between numerical and analytical value (metal decking type B) for overall slab thickness parameter

Beam model	Slab thickness, Ds (mm)	Opening Size, a (mm)	f_{cu} (MPa)	k_s (EC4)	k_s (BS5950)	M_{FE} (kN.m)	$\frac{M_{FE}}{M_{no}}$	M_{EC4} (kN.m)	$\frac{M_{EC4}}{M_{FE}}$	$\frac{M_{EC4}}{M_{no}}$	M_{BS5950} (kN.m)	$\frac{M_{BS5950}}{M_{FE}}$	$\frac{M_{BS5950}}{M_{no}}$
B-T1	105	140	43.3	76%	89%	176.42	0.95	167.02	0.95	0.97	176.93	1.00	0.96
B-T2	110	140	43.3	68%	80%	180.31	0.97	170.36	0.94	0.99	181.26	1.00	0.98
B-T3	115	140	43.3	62%	72%	185.61	1.00	173.69	0.94	1.01	185.58	1.00	1.01
B-T4	120	140	43.3	60%	70%	192.20	1.03	177.03	0.92	1.03	189.90	0.98	1.03
B-T5	125	140	43.3	60%	70%	196.19	1.06	180.36	0.92	1.05	194.23	0.97	1.05
B-T6	105	140	26	100%	100%	161.07	0.95	151.26	0.94	0.97	157.46	1.01	0.94
B-T7	110	140	26	92%	116%	164.09	0.97	153.95	0.94	0.99	161.23	1.01	0.97
B-T8	115	140	26	84%	105%	167.50	0.99	156.63	0.94	1.00	165.00	1.00	0.99
B-T9	120	140	26	77%	97%	171.03	1.01	159.32	0.93	1.02	168.76	1.00	1.01
B-T10	125	140	26	71%	89%	174.11	1.03	162.01	0.93	1.04	172.53	1.00	1.03
B-T11	105	140	35	91%	100%	167.46	0.95	162.04	0.97	0.97	165.28	1.00	0.98
B-T12	110	140	35	82%	94%	170.74	0.97	165.27	0.97	0.99	169.25	1.01	1.00
B-T13	115	140	35	74%	86%	175.27	0.99	168.49	0.96	1.01	173.21	1.01	1.02
B-T14	120	140	35	68%	79%	179.70	1.02	171.71	0.96	1.03	177.18	1.00	1.05
B-T15	125	140	35	63%	73%	183.14	1.04	174.94	0.96	1.05	181.15	0.99	1.07

Table 6.7: Moment capacity of composite beam between numerical and analytical value (metal decking type C) for overall slab thickness parameter

Beam model	Slab thickness, Ds (mm)	Opening Size, a (mm)	f_{cu} (MPa)	k_s (EC4)	k_s (BS5950)	M_{FE} (kN.m)	$\frac{M_{FE}}{M_{no}}$	M_{EC4} (kN.m)	$\frac{M_{EC4}}{M_{FE}}$	$\frac{M_{EC4}}{M_{no}}$	M_{BS5950} (kN.m)	$\frac{M_{BS5950}}{M_{FE}}$	$\frac{M_{BS5950}}{M_{no}}$
C-T1	105	140	43.3	54%	63%	170.59	0.93	162.97	0.96	0.98	173.89	1.01	0.97
C-T2	110	140	43.3	53%	62%	174.40	0.95	165.44	0.95	0.99	177.81	1.01	0.98
C-T3	115	140	43.3	53%	62%	180.17	0.98	168.43	0.93	1.01	181.74	1.00	1.01
C-T4	120	140	43.3	53%	62%	187.77	1.02	171.42	0.91	1.03	185.66	0.98	1.03
C-T5	125	140	43.3	53%	62%	192.64	1.05	174.41	0.91	1.05	189.59	0.97	1.05
C-T6	105	140	26	71%	90%	155.92	0.93	148.69	0.95	0.97	156.95	0.99	0.98
C-T7	110	140	26	64%	81%	159.99	0.96	150.76	0.94	0.99	160.37	0.99	0.97
C-T8	115	140	26	60%	75%	162.80	0.97	153.17	0.94	1.00	163.79	0.99	0.99
C-T9	120	140	26	56%	70%	167.64	1.00	155.58	0.93	1.02	167.21	0.99	1.01
C-T10	125	140	26	52%	66%	172.11	1.03	157.99	0.92	1.04	170.63	0.98	1.03
C-T11	105	140	35	63%	66%	162.67	0.94	158.64	0.98	0.97	164.45	1.00	0.99
C-T12	110	140	35	57%	60%	165.72	0.96	161.10	0.97	0.99	167.29	1.00	0.98
C-T13	115	140	35	53%	56%	169.33	0.98	163.99	0.97	1.01	170.89	1.00	1.00
C-T14	120	140	35	52%	54%	174.60	1.01	166.87	0.96	1.02	174.49	0.99	1.02
C-T15	125	140	35	52%	54%	178.93	1.04	169.76	0.95	1.04	178.09	0.98	1.04

6.6 Contribution of steel reinforcement bar (rebar)

When the concrete slab in composite beam is provided with steel reinforcements bar (rebar), the contribution by such reinforcement to compression force of composite beam with openings at mid-span has to be accounted for in predicting the moment capacity. To develop the practical design method, more parametric studies were carried out specifically to study the improvement of moment resistance of composite beam with openings by inclusion of rebar. The plastic moment capacity of composite beam with openings which includes the rebar can be derived from the block-stress. It is assumes that sufficient shear studs are presents where the stress from reinforcing bar, σ_{yr}, is not controlled by shear failure at the steel-concrete interface. The benefit of slip of the shear studs may be helpful as contribution towards ductile behaviour. The ability of metal-ribbed decking to contribute to resistance may be included only when the decking is oriented parallel to the direction of the beam. However the conclusion cannot be made since the contribution not included in this study.

The method to calculate moment capacity has been modified from the method proposed by Loh et. al (2004) and BS5950 (BSI 1991). This can be expressed from the global force equilibrium of the system as

$$\sum F = 0; where \sum F = R_r + R'_c + R_{sc} - R_{ct} - R_{st} \quad (6.10)$$

Figure 6.3 represents the force equilibrium condition of the entire cross-section, which implies that there is zero net axial force acting on the composite steel-concrete section.

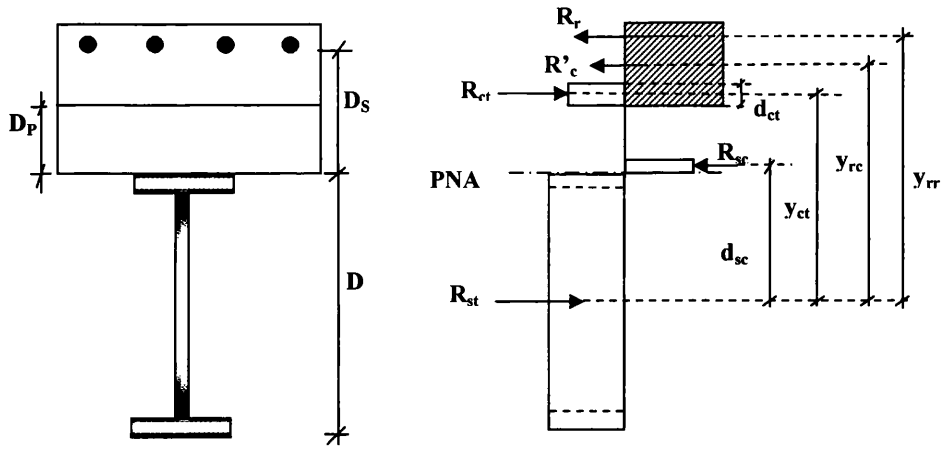

Figure 6.3: Force equilibrium condition of the system

Force contribute by reinforcement is a function of the number of rebar provided over the beam cross-section, area of cross-section of rebar and stress developed in rebar. The value , R_r, may thus be calculated as

$$R_r = NA_r \sigma_{yr} \tag{6.11}$$

In which,

N is the total number of rebar at the cross- section

A_r is the cross-sectional area of rebar

σ_{yr} is the yield stress of rebar

The balance action between shear stud, rebar and concrete can be expressed as

$$R_{ct} = R_r + R'_c - nR_q \tag{6.12}$$

and the depth of concrete in tension d_{ct} may be obtained from

$$d_{ct} = F_{ct} / (0.45 f_{cu} b_{ne}) \tag{6.13}$$

Now the derivation includes the presence of rebar and also the concrete stress block in tension which represent the balance action between shear stud, rebar and concrete.

Knowledge of potential compression and tensile resistance available from the slab and the beam permits the location of neutral axis to proceed. Three cases are possible:

(1) Neutral axis is within the concrete slab
(2) Neutral axis is within the beam's upper flange
(3) Neutral axis is within the beam's web

The composite beam is treated as partial shear connection if

$$R_c+R_r > R_q \tag{6.14}$$

and as full shear connection if

$$R_c+R_r < R_q \tag{6.15}$$

However, for all models in this study, composite beams are fall in partial shear connection. Therefore only case (2) and (3) are possible. Degree of partial shear connection is defined as

$$k_s = \frac{R_c + R_r}{R_q} > 0.7 \tag{6.16}$$

It should be bourn in mind as mention earlier, to make this method valid, ***Rr***, is not controlled by shear failure at the steel-concrete interface. Due to this reason, K is proposed to be more than 0.70 for safety reason. Assumption of K value is based on observation made by Robinson et al. (1973). The ultimate moment of the system can be derived by taking moment about the centre of the beam in tension (Figure 6.3), yield to equation,

$$M_c = \frac{R_c B_{ne}}{B_e} y_c + R_r y_r + R_{sc} y_{sc} + R_{ct} y_{ct} \tag{6.17}$$

where,

y_c = distance from the centre of steel beam in compression to the steel beam in tension.

y_r = distance from the reinforcing bar in compression to the steel beam in tension.

y_{sc} = distance from the centre of concrete in compression to the steel beam in tension.

y_{ct} = distance from the centre of concrete in tension to the steel beam in tension.

Composite beams model were analysed using the present method. Values of moment capacities obtained from the proposed design method are compared with the corresponding values determined by using the finite element method. Tables 6.8 to 6.10 show the comparison of ultimate moment values. An example of design calculation for model A-R1 is presented in Appendix L. In the table M_{FEM} refers to values obtained from numerical model, M_{cpred} refers to the ultimate moment calculated by proposed analytical method and M_{no} corresponds to value of composite beam without openings obtained from numerical method.

In the table, moment capacities obtained from proposed analytical method were compared with corresponding 54 numerical values. Close agreement between the two values is observed. The maximum deviation between numerical and analytical values is ranging from 0.03 to 4. The mean value of the $\frac{M_{c\,pred}}{M_{FE}}$ ratio is 0.99. It is therefore, in all other tables, comparison between predicted values and numerical values show that the proposed design equation is sufficiently accurate.

The ratio of moment capacities obtained from finite element and proposed analytical method to moment capacities of composite beam without opening ($\frac{M_{FE}}{M_{no}}$ *and* $\frac{M_{c\,pred}}{M_{no}}$) shows that moment capacities are increasing with the increase of rebar area. The increase of moment capacity due to increase in rebar area indicates the significant contribution from rebar. Moment capacity obtained from numerical analysis and proposed analytical method show that by providing rebar in slab, moment capacity composite beam with opening is increased up to and can be over the moment capacity of composite beam without opening. As in the case of model B-R12, the moment capacity predicted by proposed analytical method show that the increment is 7% over

the composite beam without openings. This is also confirmed by numerical analysis which the increment is 5 % over the composite beam without openings.

This proved that the force from rebar contributed to compression force. This contribution will consequently increase the total compression force and will increase the lever arm between compression force and tension force subsequently increase the moment capacity of composite beam.

Table 6.8: Moment capacity of composite beam between numerical and analytical value (metal decking type A) for rebar parameter

Beam model	Opening Size, a (mm)	f_{cu} (MPa)	Rebar designation	Number of rebar, N	Rebar area (mm^2)	M_{FE} (kN.m)	$\frac{M_{FE}}{M_{no}}$	$M_{c\,pred}$ (kN.m)	$\frac{M_{c\,pred}}{M_{FE}}$	$\frac{M_{c\,pred}}{M_{no}}$
A-R1	140	43.3	R6	2	56.56	161.25	0.95	161.36	1.00	0.98
A-R2	140	43.3	R12	2	226.22	163.83	0.97	163.52	1.00	1.00
A-R3	140	43.3	R16	2	402.18	167.02	0.99	165.28	0.99	1.01
A-R4	140	43.3	R6	4	113.11	162.55	0.96	162.13	1.00	0.99
A-R5	140	43.3	R12	4	452.45	168.28	0.99	165.70	0.98	1.01
A-R6	140	43.4	R16	4	804.35	173.51	1.02	167.51	0.97	1.02
A-R7	140	26	R6	2	56.56	148.93	0.98	150.25	1.01	0.98
A-R8	140	26	R12	2	226.22	152.49	1.00	153.67	1.01	1.00
A-R9	140	26	R16	2	402.18	155.97	1.02	156.42	1.00	1.02
A-R10	140	26	R6	4	113.11	150.43	0.99	151.48	1.01	0.99
A-R11	140	26	R12	4	452.45	156.71	1.03	157.06	1.00	1.02
A-R12	140	26	R16	4	804.35	161.51	1.06	159.69	0.99	1.04
A-R13	140	35	R6	2	56.56	159.34	1.00	154.55	0.97	0.98
A-R14	140	35	R12	2	226.22	157.14	0.99	157.39	1.00	1.00
A-R15	140	35	R16	2	402.18	159.65	1.00	159.69	1.00	1.01
A-R16	140	35	R6	4	113.11	155.10	0.97	155.56	1.00	0.99
A-R17	140	35	R12	4	452.45	160.74	1.01	160.22	1.00	1.02
A-R18	140	35	R16	4	804.35	167.41	1.05	162.48	0.97	1.03

Table 6.9: Moment capacity of composite beam between numerical and analytical value (metal decking type B) for rebar parameter

Beam model	Opening Size, a (mm)	f_{cu} (MPa)	Rebar designation	Number of rebar, N	Rebar area (mm^2)	M_{FE} (kN.m)	$\frac{M_{FE}}{M_{no}}$	$M_{c\,pred}$ (kN.m)	$\frac{M_{c\,pred}}{M_{FE}}$	$\frac{M_{c\,pred}}{M_{no}}$
B-R1	140	43.3	R6	2	56.56	177.32	0.96	178.30	1.01	0.96
B-R2	140	43.3	R12	2	226.22	179.72	0.98	182.12	1.01	0.99
B-R3	140	43.3	R16	2	402.18	181.50	0.99	185.61	1.02	1.00
B-R4	140	43.3	R6	4	113.11	178.44	0.97	179.63	1.01	0.97
B-R5	140	43.3	R12	4	452.45	183.41	1.00	186.53	1.02	1.01
B-R6	140	43.4	R16	4	804.35	188.06	1.02	191.76	1.02	1.04
B-R7	140	26	R6	2	56.56	162.68	0.97	159.57	0.98	0.95
B-R8	140	26	R12	2	226.22	165.29	0.99	165.40	1.00	0.99
B-R9	140	26	R16	2	402.18	167.35	1.00	170.65	1.02	1.02
B-R10	140	26	R6	4	113.11	163.71	0.98	161.60	0.99	0.96
B-R11	140	26	R12	4	452.45	169.89	1.01	172.01	1.01	1.03
B-R12	140	26	R16	4	804.35	176.00	1.05	179.64	1.02	1.07
B-R13	140	35	R6	2	56.56	168.76	0.97	167.05	0.99	0.96
B-R14	140	35	R12	2	226.22	170.70	0.98	171.95	1.01	0.99
B-R15	140	35	R16	2	402.18	172.57	0.99	176.38	1.02	1.01
B-R16	140	35	R6	4	113.11	169.83	0.98	168.75	0.99	0.97
B-R17	140	35	R12	4	452.45	175.57	1.01	177.53	1.01	1.02
B-R18	140	35	R16	4	804.35	180.05	1.04	184.07	1.02	1.06

Table 6.10: Moment capacity of composite beam between numerical and analytical value (metal decking type C) for rebar parameter

Beam model	Opening Size, a (mm)	f_{cu} (MPa)	Rebar designation	Number of rebar, N	Rebar area (mm^2)	M_{FE} (kN.m)	$\frac{M_{FE}}{M_{no}}$	$M_{c\,pred}$ (kN.m)	$\frac{M_{c\,pred}}{M_{FE}}$	$\frac{M_{c\,pred}}{M_{no}}$
C-R1	140	43.3	R6	2	56.56	170.74	0.94	175.06	1.01	0.97
C-R2	140	43.3	R12	2	226.22	173.74	0.96	178.27	1.01	0.99
C-R3	140	43.3	R16	2	402.18	176.09	0.97	181.15	1.02	1.01
C-R4	140	43.3	R6	4	113.11	172.67	0.95	176.18	1.01	0.98
C-R5	140	43.3	R12	4	452.45	177.23	0.98	181.89	1.01	1.01
C-R6	140	43.4	R16	4	804.35	182.71	1.01	185.97	1.01	1.03
C-R7	140	26	R6	2	56.56	157.63	0.95	158.77	0.99	0.96
C-R8	140	26	R12	2	226.22	160.76	0.97	163.72	1.01	0.99
C-R9	140	26	R16	2	402.18	162.49	0.98	168.09	1.02	1.02
C-R10	140	26	R6	4	113.11	159.41	0.97	160.50	0.99	0.97
C-R11	140	26	R12	4	452.45	165.63	1.00	169.20	1.01	1.03
C-R12	140	26	R16	4	804.35	170.38	1.03	175.17	1.02	1.06
C-R13	140	35	R6	2	56.56	163.56	0.96	165.20	1.00	0.96
C-R14	140	35	R12	2	226.22	165.06	0.97	169.35	1.01	0.99
C-R15	140	35	R16	2	402.18	168.30	0.99	173.04	1.02	1.01
C-R16	140	35	R6	4	113.11	164.11	0.96	166.65	1.00	0.97
C-R17	140	35	R12	4	452.45	170.27	1.00	173.97	1.01	1.02
C-R18	140	35	R16	4	804.35	174.39	1.02	179.08	1.01	1.05

6.7 Calculation of deflection

Deflection of composite beam with opening in metal-ribbed decking slab is calculated as recommended by EC4 (BSI 1991) and Nie. J. (2003). The deflection of beam is considered within serviceability limit state. The effect of slip will be considered in the calculation. From the literature presented in Chapter 2, bending rigidity (EI) of composite beams is calculated using transformed section. When there are openings in composite beam flange, the effect on rigidity is significant as shown in Chapter 5, section 5.8.2. Before calculation of deflection can be carried out, the rigidity of composite beam with openings need to be derived.

To calculate the rigidity of composite beam with opening, conjugate beam method has been used due to its simplicity since this method relies only on the principles of statics (Nie. J. 2006). The conjugate beam method is base on analogy between the relationships among load, shear and bending moment and relationship among M/EI, slope and deflection. Therefore, the slope and deflection can be determined from M/EI by the same operations as those performed to compute shear and bending moment respectively (Kassimali 1999). The method can be applied to different types of loading condition. This method is preferred because of its systematic sign convention and straightforward application. The moment inertia, I, at a cross section where openings are located is less than that other cross-section as shown in Figure 6.4.

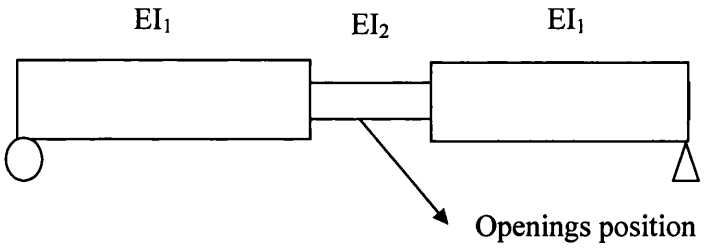

Figure 6.4: Composite beam rigidity

For the case of beam with openings at the mid-span, applied by a point load at the centre, rigidity is derived as follows by referring on diagram shown in Figure 6.5:-

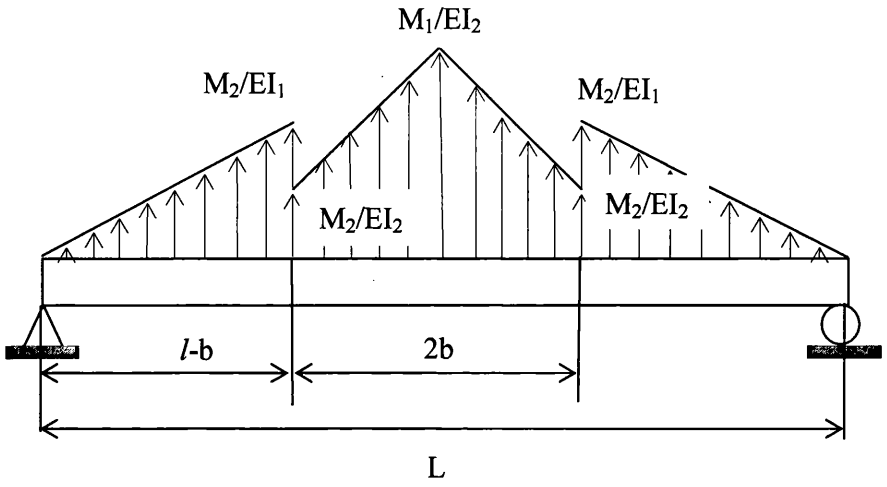

Figure 6.5: Load on the conjugate beam

From the figure, value for M_1, M_2 and l are as follows,

$$M_1 = \frac{PL}{4} \tag{6.18}$$

$$M_2 = \frac{PL}{4l}(l-b) \tag{6.19}$$

$$l = \frac{L}{2} \tag{6.20}$$

Deflection of the composite beam with openings in the flange can, therefore be obtained as,

$$\delta = \frac{P}{6EI_1}(l-b)^3 + \frac{Pb}{12EI_2}\left(6l^2 - 6bl + 3b^2l - b^2\right) \tag{6.21}$$

For beam with no openings in the flange may be obtained from Equation (6.21) by putting b=0 as,

$$\delta = \frac{PL^3}{48EI} \tag{6.22}$$

Equation (6.22) is a typical deflection equation for simply supported beam applied with single point load at mid-span. After Equation (6.21) has been derived for composite beam with openings, prediction of, deflection δ, can be calculated following EC4 standard, as follows (Equation (6.23)),

$$\frac{\delta}{\delta_c} = 1 + 0.3\left[1 - \frac{N}{N_f}\right]\left[\frac{\delta_a}{\delta_c} - 1\right] \tag{6.23}$$

Second method to calculate deflection, Equation (6.21) is combined with the method recommended by Nie. J et. al. (2003) as described in Chapter 2, section 2.8. To consider slip effect, Nie. J et. al (2003) proposed reduced rigidity equation where,

$$B_s = \frac{EI}{(1+\xi)} \tag{6.24}$$

The calculated values of deflection using the proposed method are shown in Table 6.11 and compared with the numerical results. In the table, δ_{FE} is deflection obtained from the numerical method, δ_{EC4} is deflection predicted using EC4 (BSI 1991) and δ_{Nie} is calculated value from Nie. J method (2003). Example of calculation is shown in Appendix M and Appendix N.

Figures 5.20 to 5.25, in Chapter 5, decrease in stiffness in the linear range with the increase of opening size in longitudinal direction has been observed. From this observation, composite beam with different opening size in longitudinal and transverse direction are compared with result obtained from proposed method. Table 6.11 shows the comparison of deflection values.

From the result given in the table, the standard deviation between deflection values obtained from finite element method and EC4 method (δ_{FE} and δ_{EC4}) is found to vary from 0.12 to 1.46, the average ratio, $\frac{\delta_{EC4}}{\delta_{FE}}$ is 0.83. However, the standard deviation between values obtained from finite element method and Nie. J. (2003) method (δ_{FE}

and δ_{Nie}) ranges from 0.02 to 1.07; the average ratio, $\frac{\delta_{Nie}}{\delta_{FE}}$ is 0.92. The calculated deflection is generally in good agreement with finite element results. However calculated result according to Nie. J (2003) method closed to FE values compared to EC4 (BSI 1991) method. Predicted values from EC4 (BSI 1991) method are lower than those by Nie.J (2003) method. For model A1 to C18, where the opening size in transverse direction is investigated, there are no changes in rigidity since the opening size in longitudinal direction is kept constant.

Result from table 6.11 show that the deflection for model A1-f1 to C1-f3 predicted by proposed analytical methods (δ_{EC4} and δ_{Nie}), is found to increase with the increase of opening ratio in longitudinal direction. This is also confirmed by numerical results. Increased in deflection is more significant when the opening ratio is more than 20%. The increased in deflection is due to increased in opening ratio in longitudinal and transverse direction. The increase in opening ratio will reduce the beam section and consequently reduced the rigidity (EI).

Table 6.11: Comparison between numerical and predicted values of deflection for composite beam with openings

Beam model	Opening Size, (mm)		Opening ratio (%)	f_{cu} (MPa)	k_s (EC4)	Load (kN)	δ_{FE} (mm)	*Deflection* δ_{EC4} (mm)	$\delta_{EC4} / \delta_{FE}$	*Deflection* δ_{Nie} (mm)	$\delta_{Nie} / \delta_{FE}$
	a	f									
A4	170	200	10	43.3	0.51	70	8.00	6.24	0.78	6.48	0.81
A10	170	200	10	26	0.68	50	5.80	4.26	0.73	5.00	0.86
A16	170	200	10	35	0.61	65	7.70	5.63	0.73	6.24	0.81
B4	170	200	10	43.3	0.51	90	7.80	6.85	0.88	7.64	0.98
B10	170	200	10	26	0.68	90	8.10	6.24	0.77	8.17	1.01
B16	170	200	10	35	0.61	90	8.35	6.51	0.78	8.49	1.02
C4	170	200	10	43.3	0.51	70	7.00	6.12	0.87	6.04	0.86
C10	170	200	10	26	0.68	65	6.80	5.44	0.80	5.96	0.88
C16	170	200	10	35	0.61	70	7.40	5.99	0.81	6.23	0.84
A1-f1	250	200	10	43.4	0.51	70	8.10	6.36	0.79	6.62	0.82
A1-f2	250	400	20	43.4	0.51	70	8.40	6.62	0.79	6.94	0.83
A1-f3	250	900	45	43.4	0.51	70	9.00	7.30	0.81	7.91	0.88
B1-f1	250	200	10	43.4	0.76	90	7.80	7.02	0.90	7.83	1.00
B1-f2	250	400	20	43.4	0.76	90	8.30	7.38	0.89	8.24	0.99
B1-f3	250	900	45	43.4	0.76	90	9.30	8.33	0.90	9.42	1.01
C1-f1	250	200	10	43.4	0.54	70	7.50	6.27	0.84	6.53	0.87
C1-f2	250	400	20	43.4	0.54	70	7.90	6.57	0.83	6.91	0.87
C1-f3	250	900	45	43.4	0.54	70	8.60	7.43	0.86	7.77	0.90

6.8 Conclusions

Moment capacity equations for composite beam with openings in metal-ribbed decking slab using effective width method were proposed. The proposed equation is based on the ratio between net effective width and gross effective width. Results obtained compared with the value from numerical analysis. The design methods used in EC4 (BSI 1991) and BS 5950 (BSI 1990) were subsequently modified. Agreement is observed between the results for ultimate moment, obtained using the proposed design equations and the corresponding FE analysis. The design method according to EC4 (BSI 1991) is found to be on safe side compared to BS 5950 (BSI 1990). The proposed method was used to calculate the moment capacity of composite beam with openings with different concrete strength and slab thickness.

Secondly, the method to calculate moment capacity of composite beam with openings reinforced with rebar also has been derived. The contribution from the reinforcement to compression force of composite beam with openings at mid-span was accounted in predicting the moment capacity. The plastic moment capacity of composite beam with openings which includes the proposed effective width method and the rebar can be derived from the block-stress. The derivation also is included the degree of shear interaction by taking account the balance action between shear stud, rebar and concrete. The proposed method is sufficiently accurate when compared with results obtained from numerical method.

Finally, formula to determine rigidity of simply supported composite beam with openings loaded under single point load at mid-span has been derived. The proposed equation has been combined with formula proposed by EC4 and Nie. J. (2003) to calculate the deflection of composite beam. The results by the proposed design equation were compared with numerical results and were found reliable to predict the deflection of composite beams with openings.

6.9 References

BSI (1990). BS 5950 Structural use of steel work in building, Part 3, section 3.1: Code of practice for design of composite beams. London, BSI.

BSI (1991). DD ENV 1994-1-1, EC4. Design of composite steel and concrete structures. Part 1.1, General rules and rules for building. London: BSI

Kassamali, A, (1999), Structural Analysis,2nd Ed, PWS Publishing

Loh, H. Y., Uy, B., Bradford, M. A. (2004). "The effect of partial shear connection in the hogging moment regions of composite beam Part II- Analytical study" Journal of Constructional Steel Research, 60(6): 921-962.

Nie, J. G., Cai, C.S., (2003). "Steel-concrete composite beams considering shear slip effects" J Struct Eng, ASCE 129(4): 495-506.

Nie, J. G., Fan, J., Cai, C.S., (2008). "Experimental study of partially shear-connected composites beams with profiled sheeting" Engineering Structures, 30:1-12.

Robinson, H., and, Wallace, I.,W., (1973). "Composite beams with 1-1/2 inch metal deck and partial and full shear connection." The Engineering Journal 16(A-8).

Chapter 7

CONCLUSIONS AND RECOMMENDATIONS

7.1 Introduction

This research has been carried out to study the behaviour of composite beams with openings in metal-ribbed decking slabs. The basic components of the system are metal-ribbed decking, concrete infill and steel beams, connected by a headed shear stud. A numerical model has been developed using the finite element package 'ANSYS'. For composite beams, a full-scale experimental test in a laboratory is very costly. Finite elements method can be used to simulate the experiment to study structural behaviour.

The proposed model has been carefully validated by comparing with experimental data; the model was then used to study the influence of the opening in the composite beam. The FE models have been validated using full-scale experimental test data. It is shown that the finite element and experimental results can be combined efficiently and thus better understanding of the structures could be obtained.

FE model has been used to study the influence of openings in the composite beam. FE is a good alternative method since the variation of parameter can be studied whereas only a limited number of test can be carried out with physical model in view of high cost. Design equations were in accordance with EC4 (BSI 1991) and BS 5950 (BSI 1990). The results obtained from parametric study have resulted in the development of design equations.

7.2 Summaries and conclusions

Based on the findings in this research, following conclusions are made:

(a) Numerical modelling of composite beam with metal-ribbed decking slab.

1) The constitutive model used in modelling the composite beam can be used to represent the nonlinear behaviour of the material used. Very good agreement has been observed by comparing the finite element results with experimental results.

2) Use of solid element to model the shear stud in the finite element idealisation has been shown to predict accurately the ultimate load and load-deflection behaviour of the composite beam. Close agreement was obtained between the experimental and finite element modelling.

3) Deflection values obtained from the finite element analysis ($\delta_{FEM)}$ are found to be close to the corresponding to EC4 method. These values obtained from design method (δ_{EC4}) are higher. This may be because finite element analysis ignores the stiffness of concrete behind the shear stud.

(b) Numerical modelling of composite beams with openings in metal-ribbed decking slabs.

1) For type A decking (narrow-ribbed), all the load-deflection curves are linear up to the first yield load and become non-linear thereafter. Most of the models sustain the linear stage approximately up to 80 kN. The results show that by increasing the openings size in transverse direction will decrease the ultimate load of composite beam. The results show that the ultimate load decrease by 2%, 1% and 2% when the opening size is increased by 10% in the direction of transverse axis for model A1, A7 and A8, respectively. The corresponding drop in ultimate load is 9%, 6% and 10% when the opening size increased to 50%.

2) The load-deflection behaviour for type B decking is linear up to the first yield load averagely equal to 105 kN and it becomes non-linear thereafter. The results show that the ultimate load drops by 2%, 3% and 3%, when the opening size is increased by 10% in the direction of transverse direction for model B1, B7 and B8, respectively. The corresponding drop in ultimate load is 11%, 15% and 12% in ultimate load when the opening size increased to 50%.

3) Load-deflection behaviour of type C decking is almost linear up to 80 to 85 kN and the showed a large deflection with increasing load thereafter. The stiffness of composite section contributed up to 55% of ultimate load. The results show that the ultimate load drops by 4%, 3% and 3%, when the opening size is increased by 10% in the direction of transverse direction for model C1, C7 and C8, respectively. The corresponding drop in ultimate load is 12%, 14% and 11% in ultimate load when the opening size increased to 50%.

4) The initiation and development of stress in ribbed decking slab with openings were obtained from FE stress contour. Generally with the increase in load, development of high compressive stress is initiated at beam centre and outermost side of opening and then high compressive stress extends to the whole sides of opening. For higher openings ratio, development of high compressive stress is initiated at lower applied load compared to model which has lower opening ratio.

5) It was found that increase in the openings size in longitudinal direction does not affect the ultimate load. Reduction in stiffness of the beams is, however, observed in the linear range with increase in the size of openings. Reduction in stiffness can be associated with opening ratio. With opening ratio of 10%, the reduction of stiffness is approximately 4% compared to composite beam without opening. For opening ratio 40%, the reduction of stiffness is as high as 22%, as in the case of model B1-f3. From the numerical results, it can be concluded that the effect is significant when opening ratio is more than 20%.

6) It can be conclude that, for simply supported beam, subjected to central loading, the beam stiffness and ultimate load are least affected when the openings are placed away from the mid-span.

7) The reduction of moment capacity is found to be influenced by load location. Moment is reduced up to 4%, 6% and 7% for load applied at the front section, central section and end section of openings, respectively. It was observed that the moment reduction is more when load is located at opening end section compared to front section. It was also observed that the opening influences more if the load is applied within the region of maximum bending moment.

8) More reduction of ultimate load is observed when two openings are located at both side of flange but at different section compared to the case in which opening is placed at one side of flange at the section. Moment capacity of two openings located at both side of flange is lower than opening located at one side of flange at a section about 3% to 5%. It can be observed that when opening is positioned on both side of beam flange, high compressive stresses are developed at the corner of the openings. It is also observed that the stress distribution is influenced by the presence of two openings.

(c) Parametric study on the method to increased the ultimate moment capacity of the composite beams with openings in metal-ribbed decking composite slabs.

1) It is observed, the beam ultimate load are affected more for lower opening ratio with the increase in concrete cube strength. As in the case of models A1, B1 and C1 which has 10% opening ratio, ultimate load is increased about 7% over the composite beam without openings when the cube strength is increased from 26 MPa to 43.3 MPa. As in the case of model A6, B6 and C6 which has higher opening ratio (50%), the ultimate load is increased about 1% over the composite beam without opening when the cube strength is increased from 26 MPa to 43.3 MPa.

2) It is observed that approximately only 10% slab thickness increment from reference model for composite beam with openings is required to recover the lost of composite beam strength caused by openings in slab. In all cases, it is observed that the ultimate load is increased more than composite beam without openings when the slab thickness is increased more than 10% over the thickness of reference model. As in the case of model B-T5, the ultimate load is increased by 7% over the composite beam without openings when the slab thickness is increased by 19% over the thickness of reference model. These results show that the composite beam with openings will be over design when the slab thickness is increased more than 10% over the thickness of reference model.

3) Inclusion of rebar produced significant effect to enhance the moment resistance of composite beam with openings in metal-ribbed decking. Rebar ratio is the ratio between rebar area and effective concrete area. In all cases, added 0.2% of rebar will not increase the ultimate load of composite beam with openings up to composite beam without openings. However added 2.5% of rebar will increased the ultimate load over than models without openings which indicate that the beam is over design. Results show that the ideal percentage of rebar to be used is between 0.3% and 1% in order to avoid under-estimate or over-estimate the composite beam design caused by openings.

(d) Analytical method.

1) Development of a simple design method to predict the ultimate moment capacity of composite beams with openings is proposed. Changing the effective width of the concrete flange gross to net is the only modification required to deal with openings in slab. Moment capacity calculated by modified design equation according to EC4 and BS5950 show good agreement with the finite element results.

2) It was observed from ratios of $\left(\frac{M}{M_{no}}\right)_{FE}$, $\left(\frac{M}{M_{no}}\right)_{EC4}$ and $\left(\frac{M}{M_{no}}\right)_{BS5950}$ that presence of openings results in reduction of the moment capacity of composite beams. Increase in the opening size will decrease a moment capacity of composite beam. For example, as in case of model B12, with the opening ratio of 50%, moment capacity is reduced by 15 % using finite element method. The reduction also confirmed by design method where moment capacity is reduced by 15% and 14% according to EC4 (BSI 1991) and BS5950 (BSI 1990), respectively. By comparing the value from finite element analysis and calculated value from modified equation, the prediction by modification equation can be considered accurate for the design purpose.

3) Results obtained from FE analysis which shows that the increment of moment capacity is more significant with lower opening ratio. This is also confirmed by analytical value. For example, as in the case of model A1, with opening ratio 10% give significant increment in ratio of $\frac{M_{fcu-43.3}}{M_{no}}$ which is 9%. However for model A6, with 50% opening ratio, $\frac{M_{fcu-43.3}}{M_{no}}$ ratio is only 1%. This is also confirmed by analytical value for A1 and A6 which is 7% and 4%, respectively, predicted by modified EC4 and 6% and 1%, respectively, predicted by modified BS5950. It is observed that $\frac{M_{fcu-43.3}}{M_{no}}$ ratio predicted by modified EC4 method is overestimated compared to numerical method and modified BS5950 method.

4) The method to calculate moment capacity of composite beam with openings reinforced with rebar also has been derived. The contribution from the reinforcement to compression force of composite beam with openings at mid-span was accounted in predicting the moment capacity. The plastic moment capacity of composite beam with openings which includes the proposed effective width method and the rebar can be derived from the block-stress. The derivation also is included the degree of shear interaction by taking account the balance action between shear stud, rebar and concrete. The maximum deviation between numerical and analytical values varies from 0.03 to 4. The mean value of the $\frac{M_{c\,pred}}{M_{FE}}$ ratio is 0.99. It is therefore, concluded that the proposed design equation is sufficiently accurate.

5) Formula to determine rigidity of simply supported composite beam with openings loaded under single point load at mid-span has been derived using conjugate beam method. The rigidity formula then combined with deflection equation proposed by EC4 and Nie.J method. From the results, the standard deviation between deflection values obtained from the finite element method and EC4 method (δ_{FE} and δ_{EC4}), is varieed from 0.12 to 1.46 and that the average ratio, $\frac{\delta_{EC4}}{\delta_{FE}}$ is 0.83. However the standard deviation between deflection values varies from 0.02 to 1.07. The calculated deflection is generally in good agreement with finite element results. However calculated result according to Nie. J (2003) method is more accurate compared to EC4 (BSI 1991) method. Predicted values from EC4 (BSI 1991) method are lower than Nie.J (2003) method. It is also observed from the values obtained from the proposed equation, that there is significant effect on composite beam stiffness when the opening ratio is more than 20%.

7.3 Recommendations for Future Study

The author believes that the work presented in this thesis lays the foundation for better understanding of the nonlinear behaviour of composite beams with openings in metal-ribbed decking slabs under static load. In the author's opinion, further research should be carried out to address the following issues:

1) The present investigation is restricted to the behaviour of composite beam under flexural mode; whereas in practice the composite beam may be subjected to transverse shear; such loading condition should be studied.

2) Investigation is only considered ribbed metal decking having transverse direction to steel beam. Ribbed metal decking having parallel direction to composite beams is not considered. Parallel orientation possibly could contribute to tension/compression force and could help to increase the moment capacity of composite beam with opening in metal-ribbed decking slab.

3) In this study openings are considered only in the flange (slab). However, it is normal to provide openings in the beam also. Study could be carried out to study the combined effect of openings in the flange and the web.

4) It is also important to study the effect of openings which are not within the effective width.

Appendix A: Test arrangement for composite beam and typical results

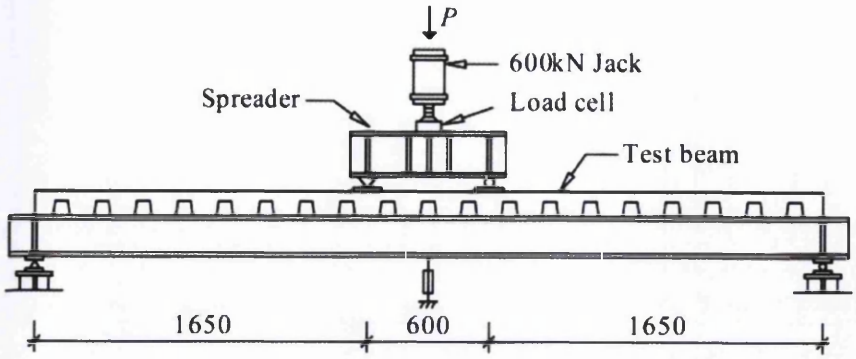

Figure A1: Test arrangement for composite beam

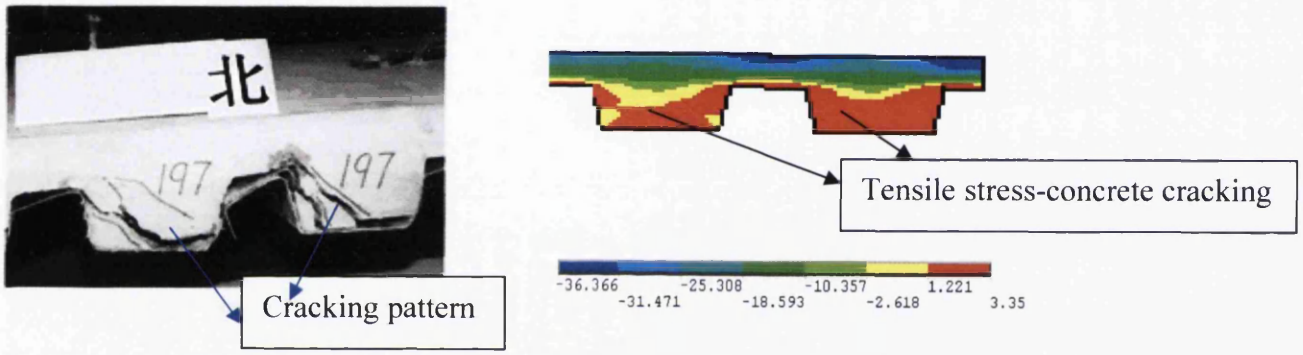

a) Experiment results b) FE results

Figure A2: Typical separation of steel decking and concrete slab

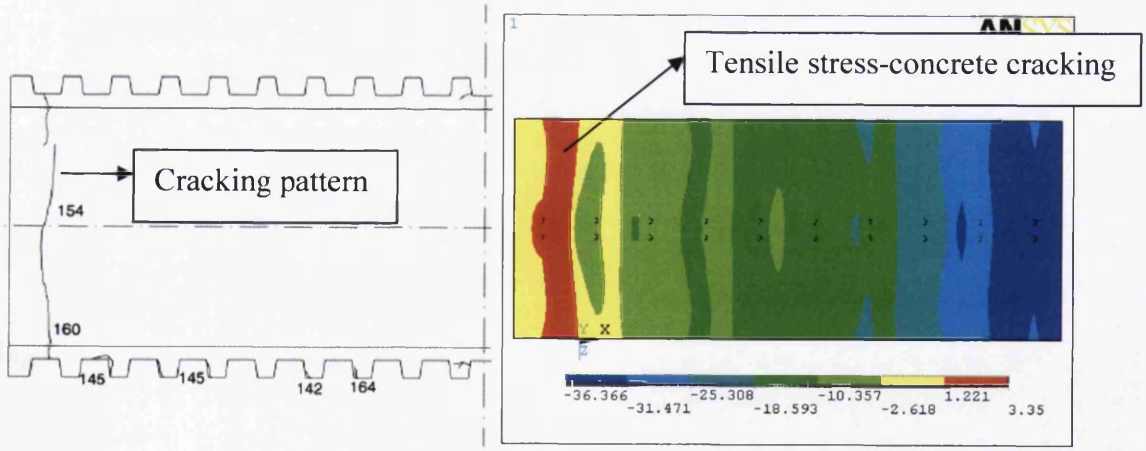

a) Experiment b) FE results

Figure A3: Typical cracking pattern at support area

Appendix B: Yielding sequence of composite beam (SB1)

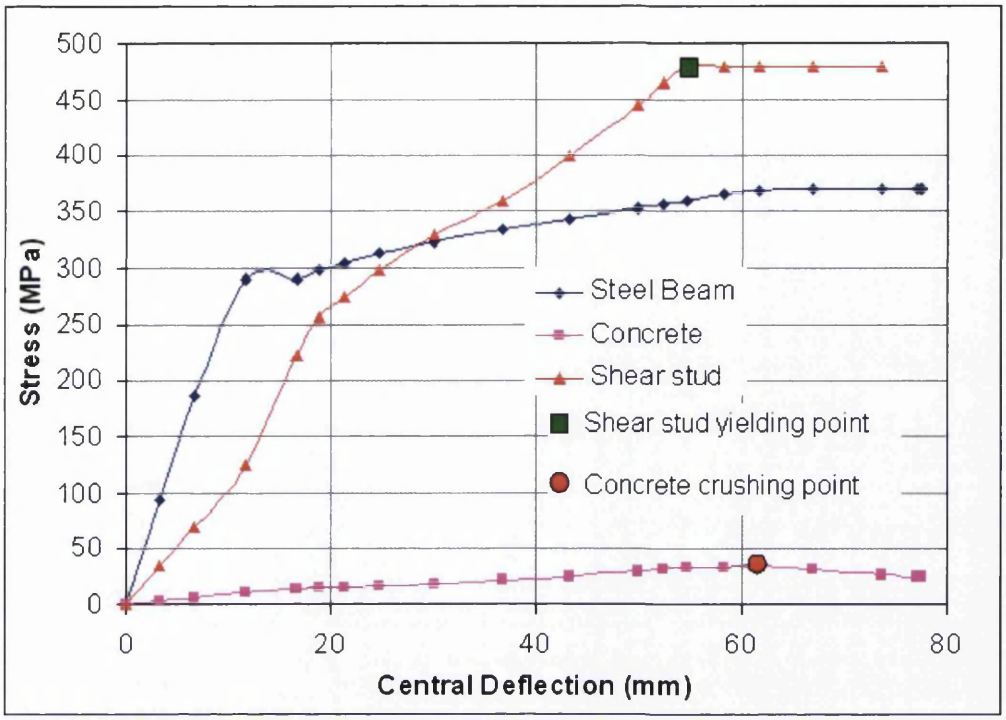

Figure B1: Stress-deflection curve of composite beam component

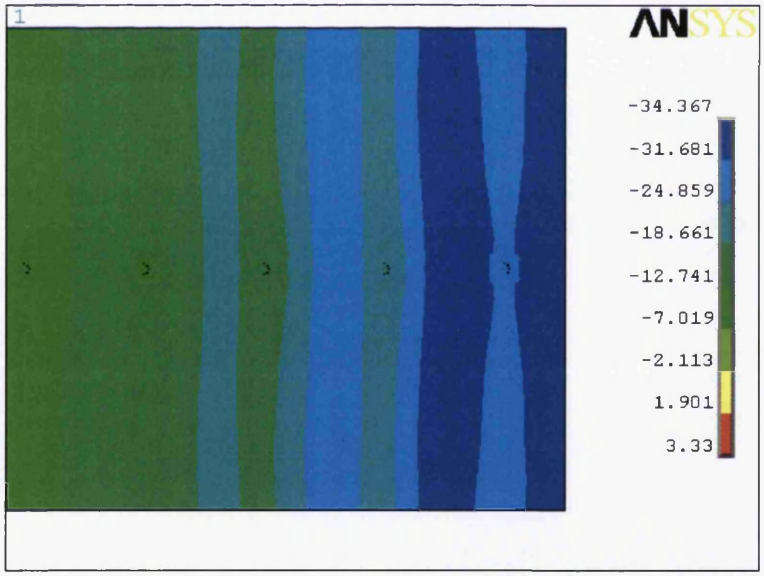

Figure B2: Concrete Stress contours at ultimate stress

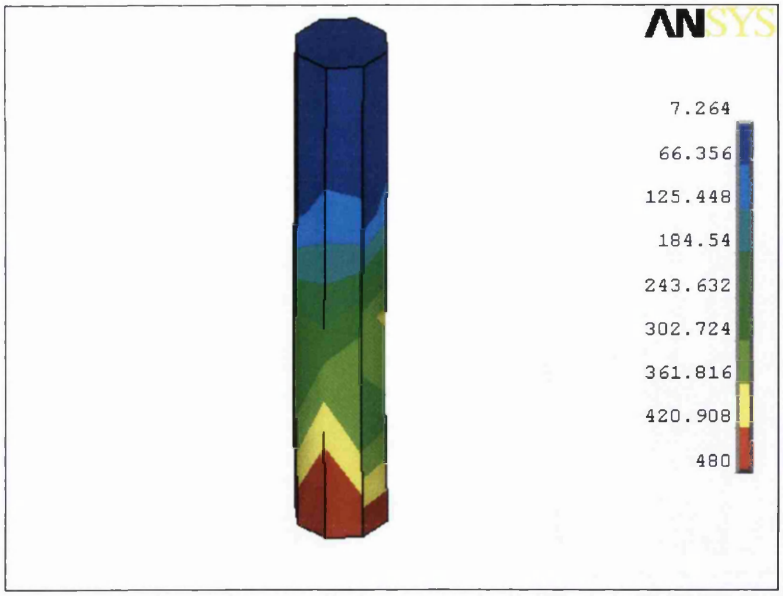

Figure B3: Shear stud connection stress contours at ultimate stress

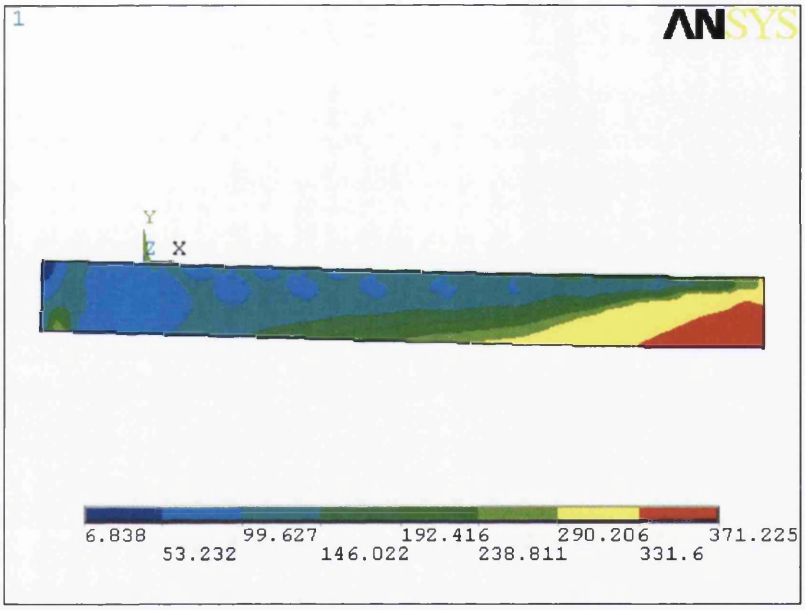

Figure B4: Steel beam stress contours at ultimate stress

Appendix C: Yielding sequence of composite beam (SB2)

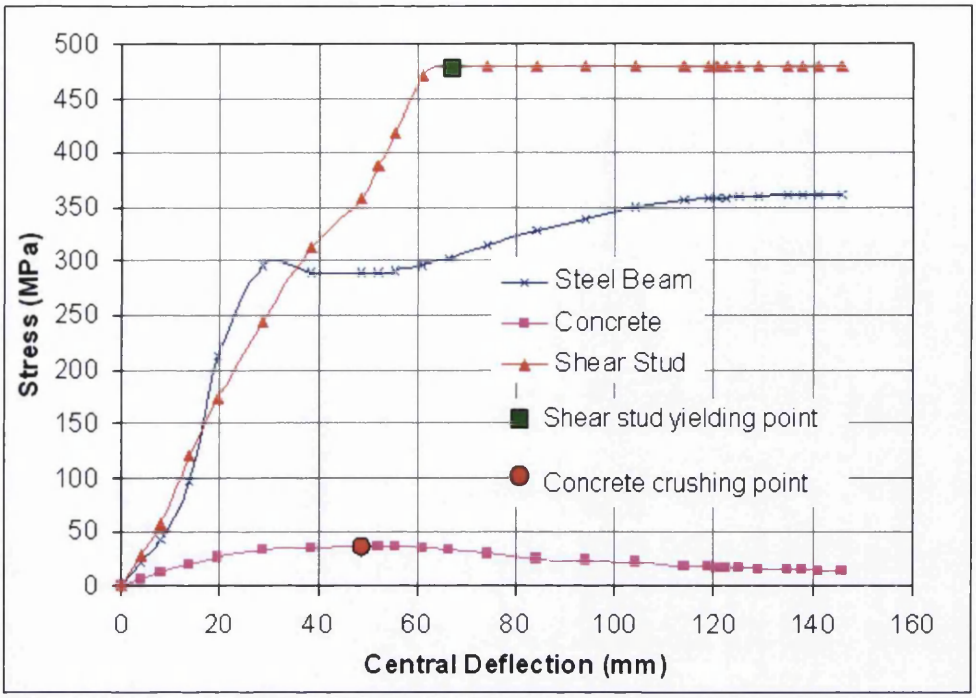

Figure C1: Stress-deflection curve of composite beam component

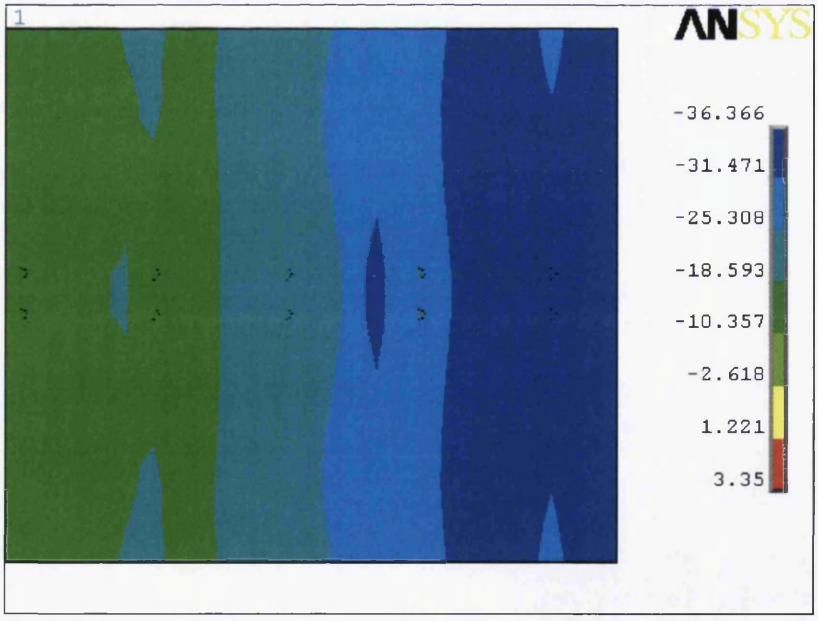

Figure C2: Concrete Stress contours at ultimate stress

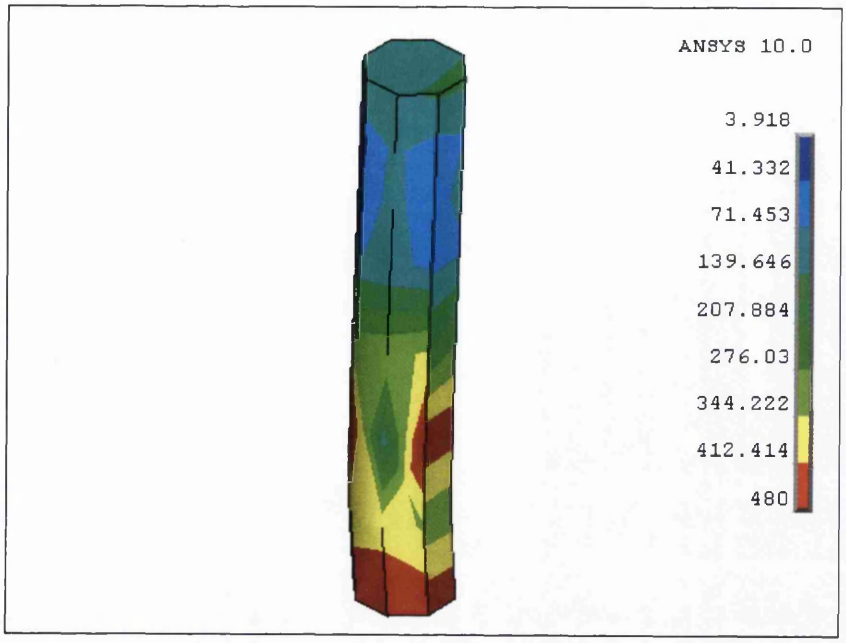

Figure C3: Shear stud connection stress contours at ultimate stress

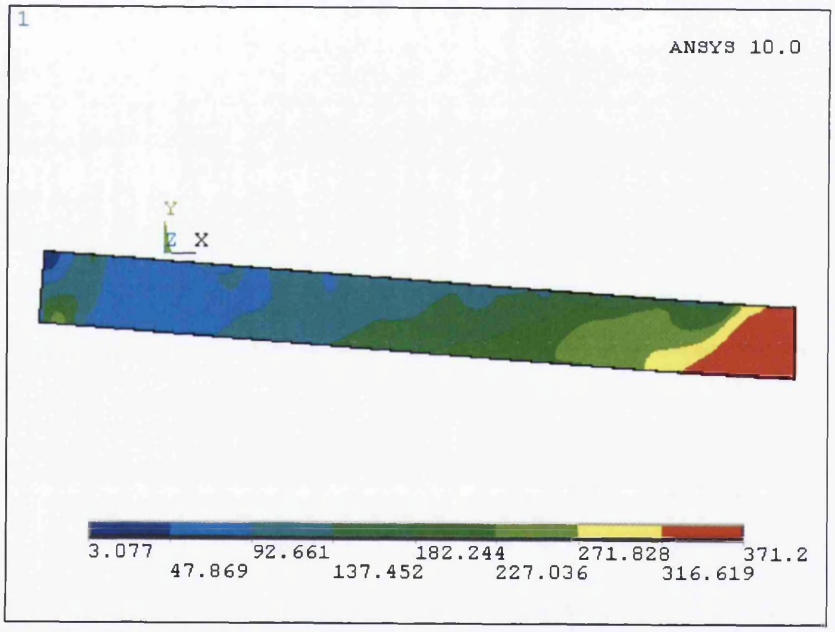

Figure C4: Steel beam stress contours at ultimate stress

Appendix D: Yielding sequence of composite beam (SB3)

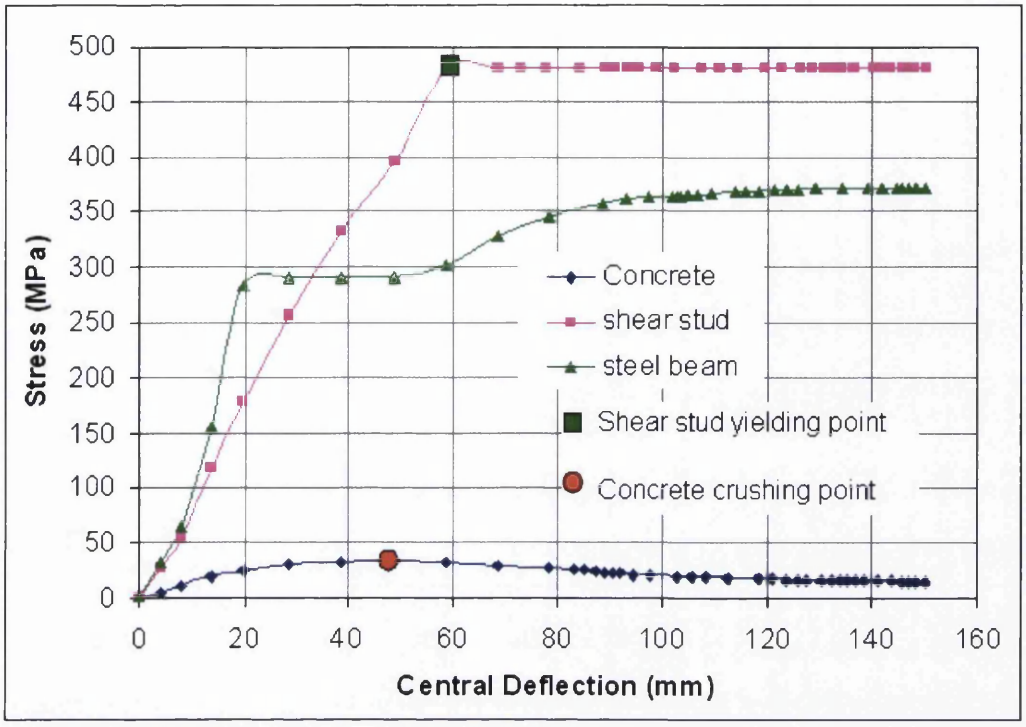

D1: Stress-deflection curve of composite beam component

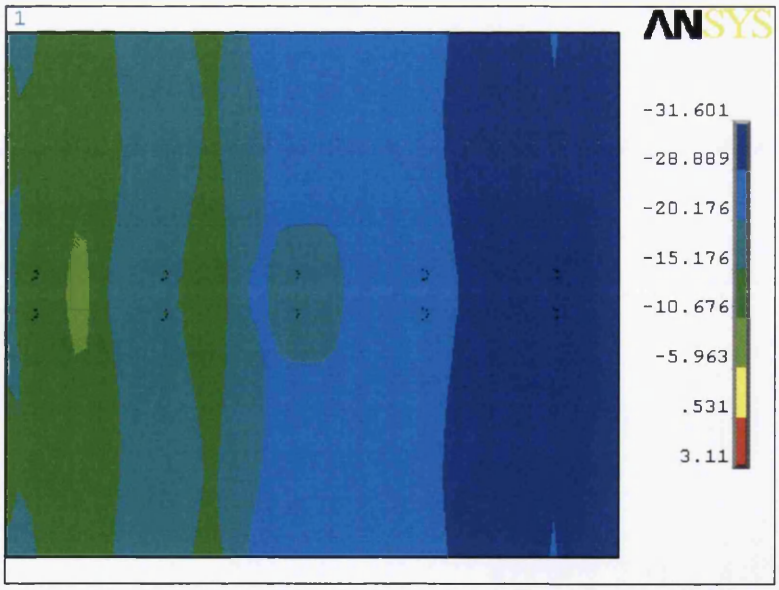

Figure D2: Concrete Stress contours at ultimate stress

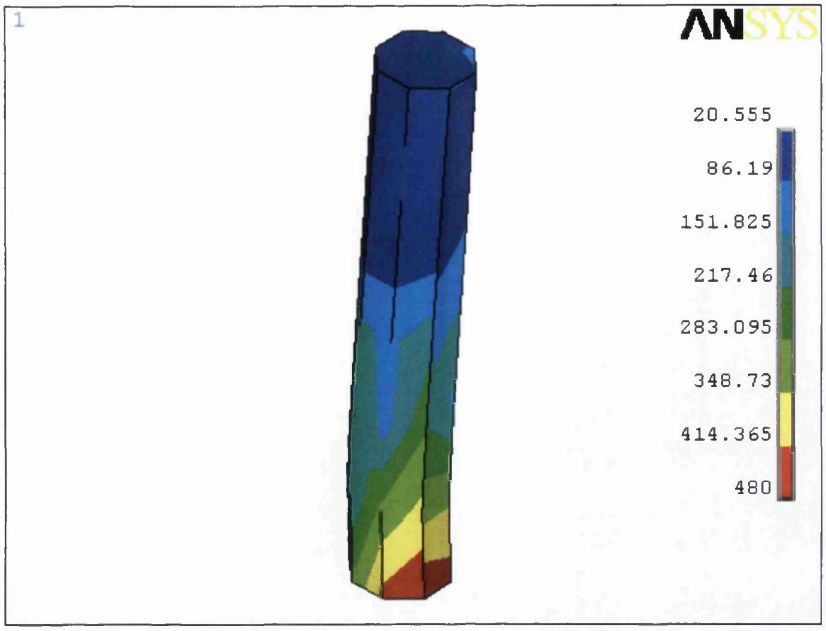

Figure D3: Shear stud connection stress contours at ultimate stress

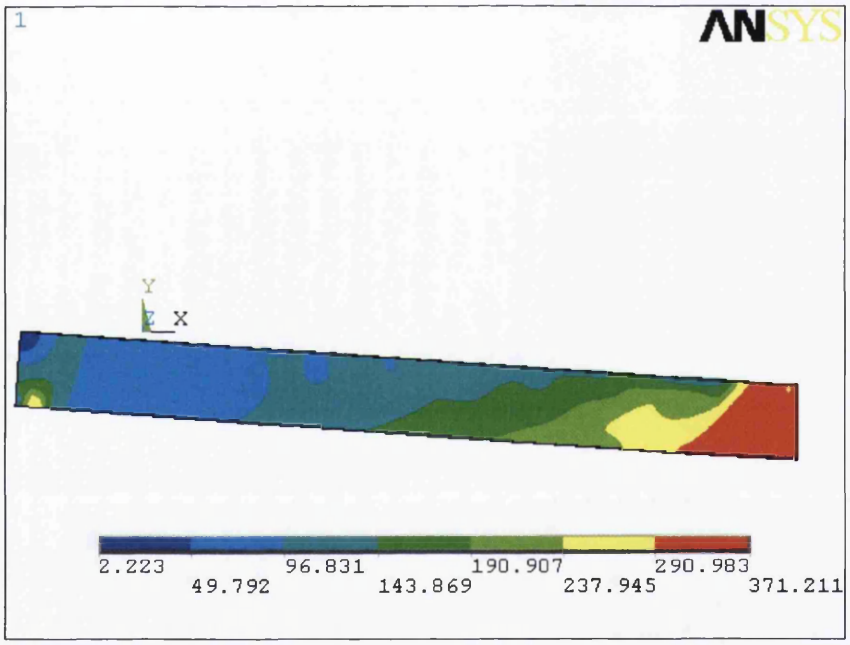

Figure D4: Steel beam stress contours at ultimate stress

Appendix E: Yielding sequence of composite beam (SB4)

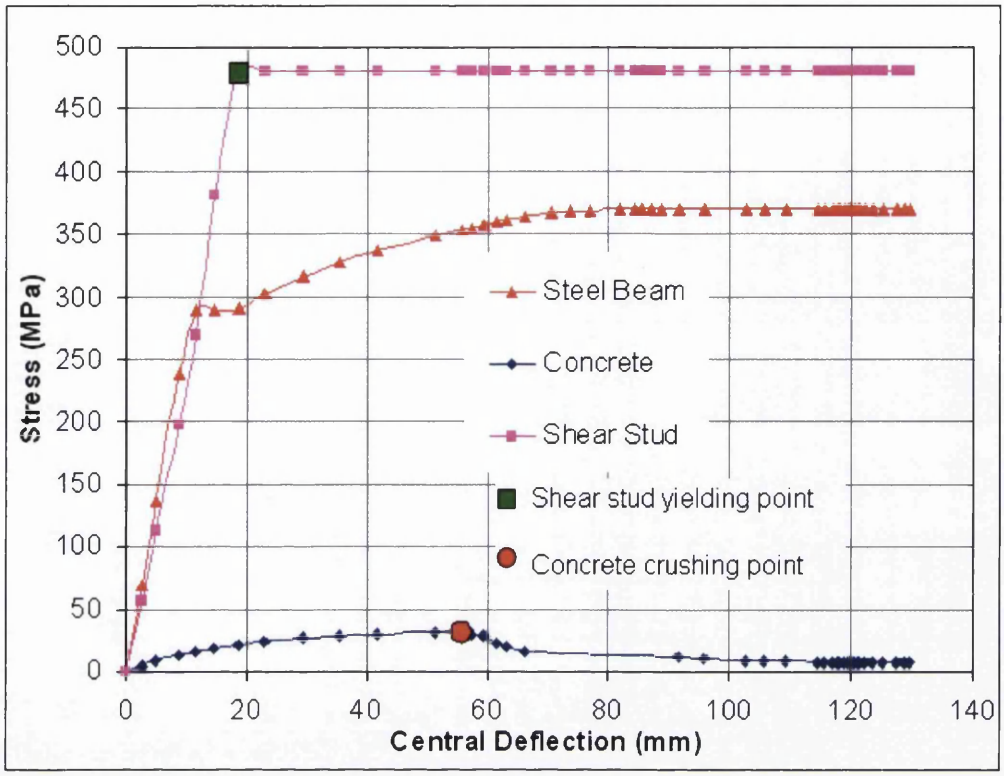

E1: Stress-deflection curve of composite beam component- SB4

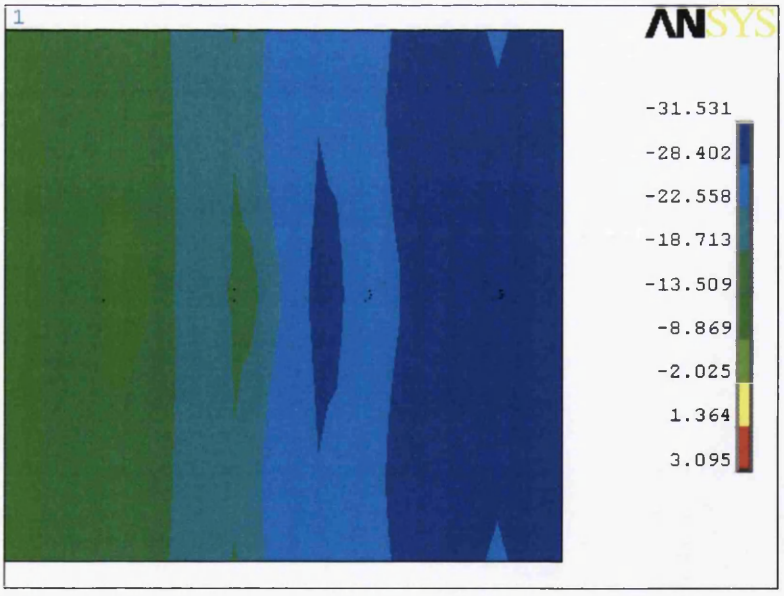

Figure E2: Concrete Stress contours at ultimate stress

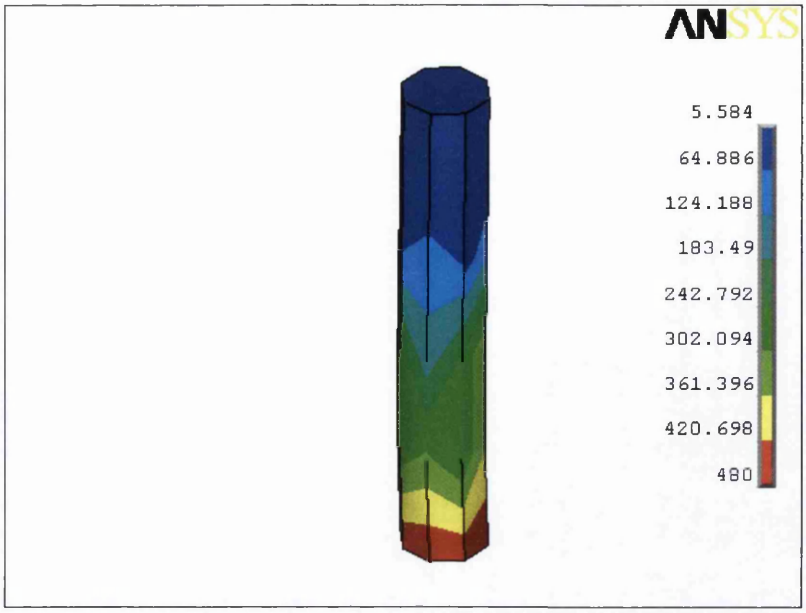

Figure E3: Shear stud connection stress contours at ultimate stress

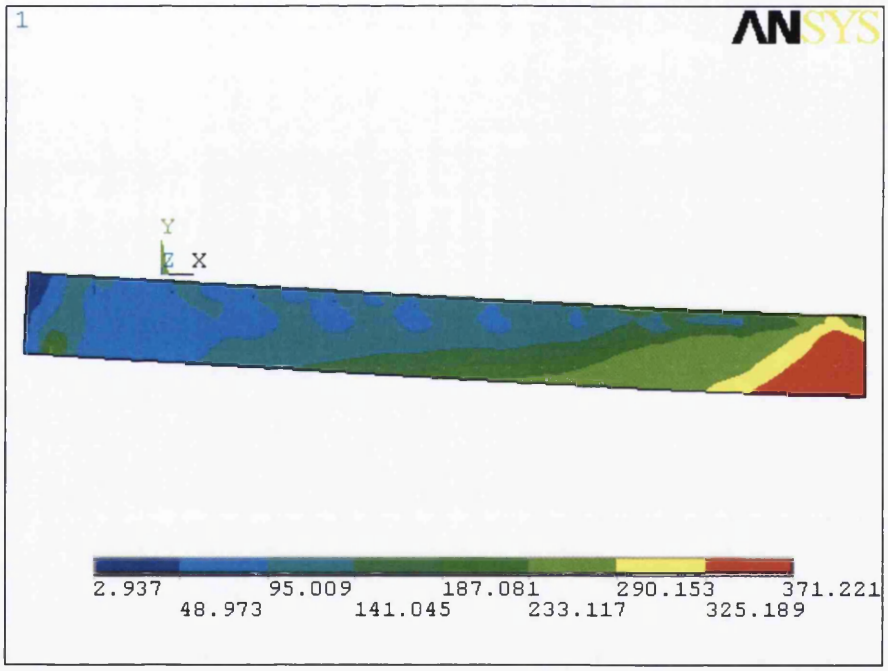

Figure E4: Steel beam stress contours at ultimate stress

Appendix F: Yielding sequence of composite beam (SB5)

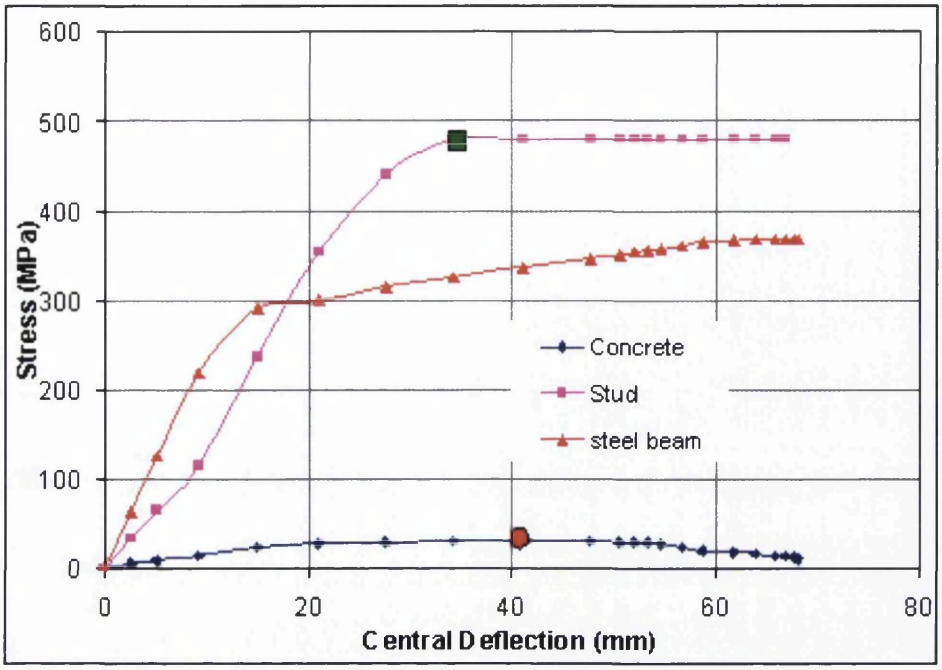

F1: Stress-deflection curve of composite beam component

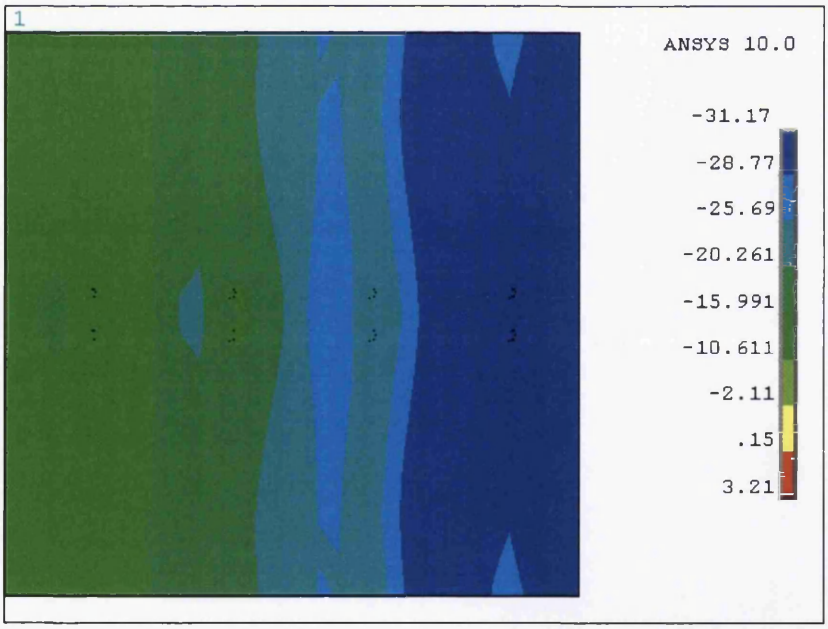

Figure F2: Concrete Stress contours at ultimate stress

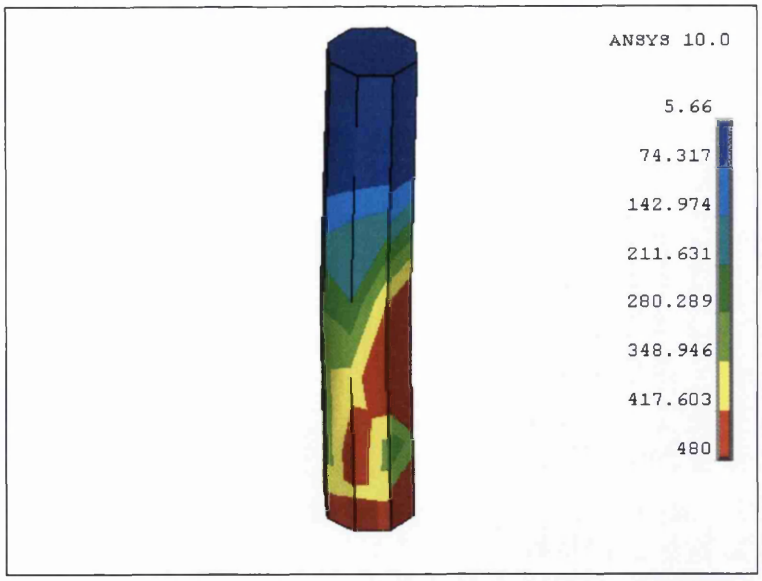

Figure F3: Shear stud connection stress contours at ultimate stress

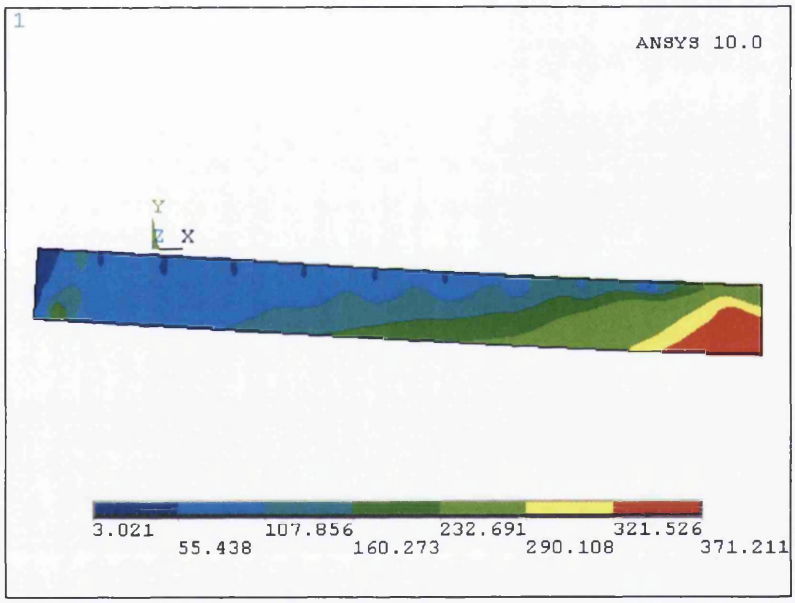

Figure F4: Steel beam stress contours at ultimate stress

Appendix G: Yielding sequence of composite beam (**A1**)

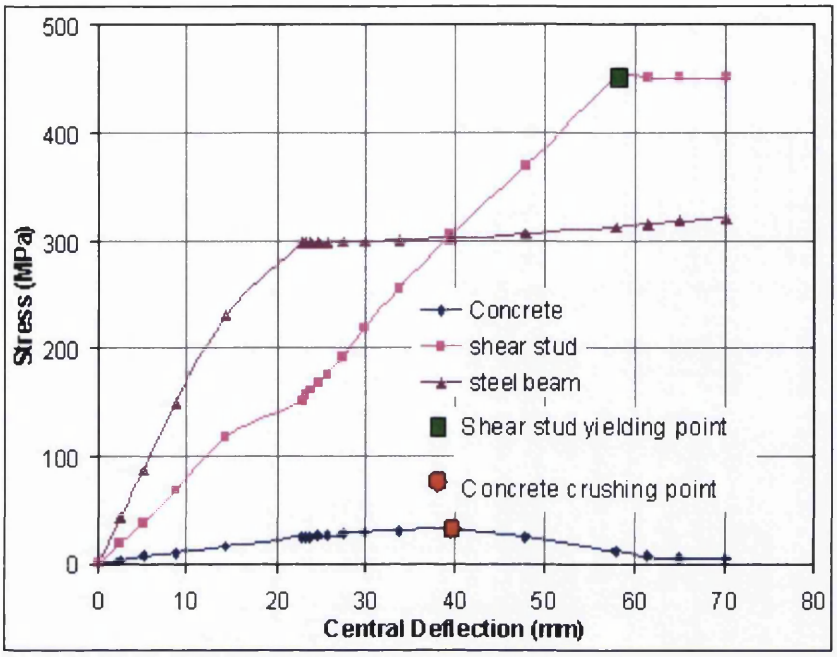

G1: Stress-deflection curve of composite beam component

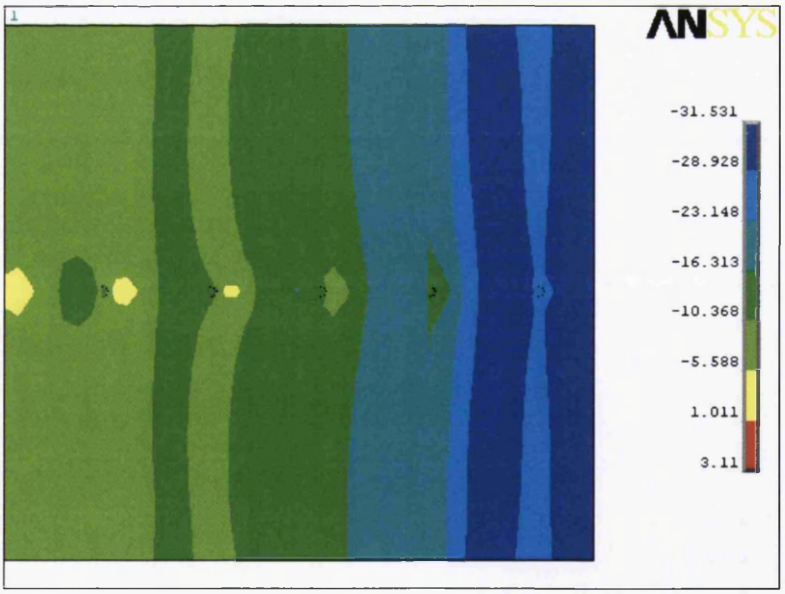

Figure G2: Concrete Stress contours at ultimate stress

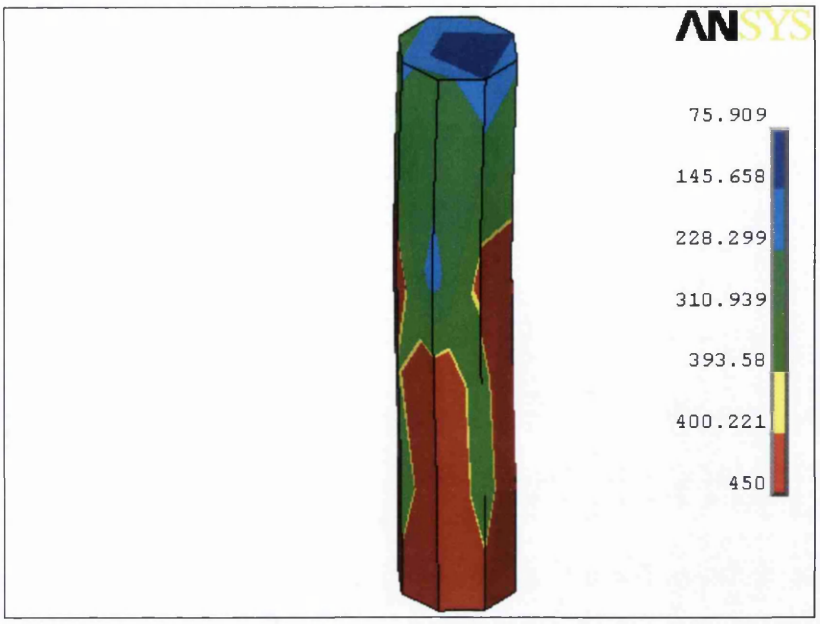

Figure G3: Shear stud connection stress contours at ultimate stress

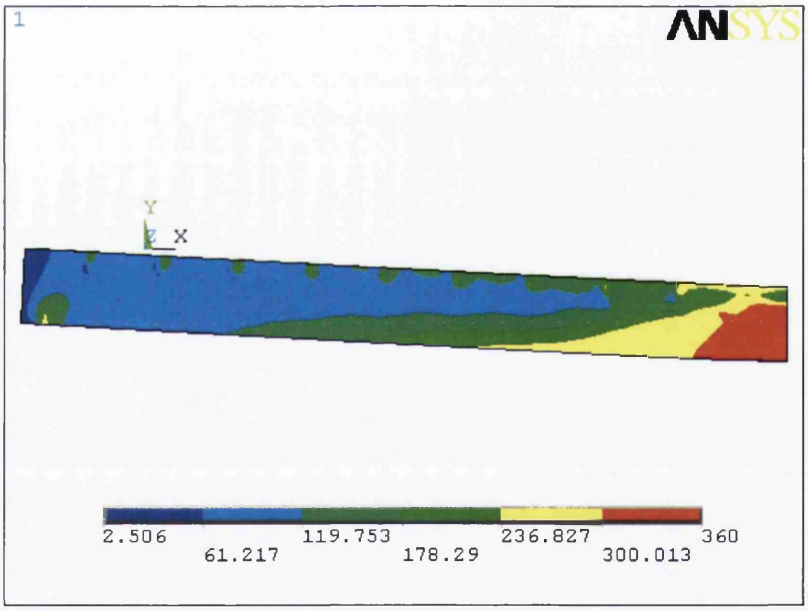

Figure G4: Steel beam stress contours at ultimate stress

Appendix H: Yielding sequence of composite beam (**B1**)

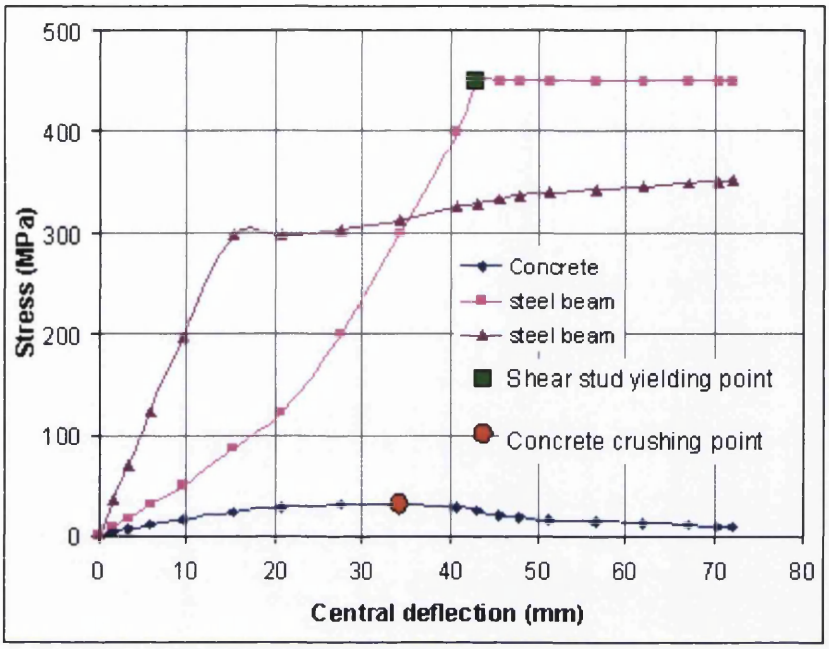

H1: Stress-deflection curve of composite beam component

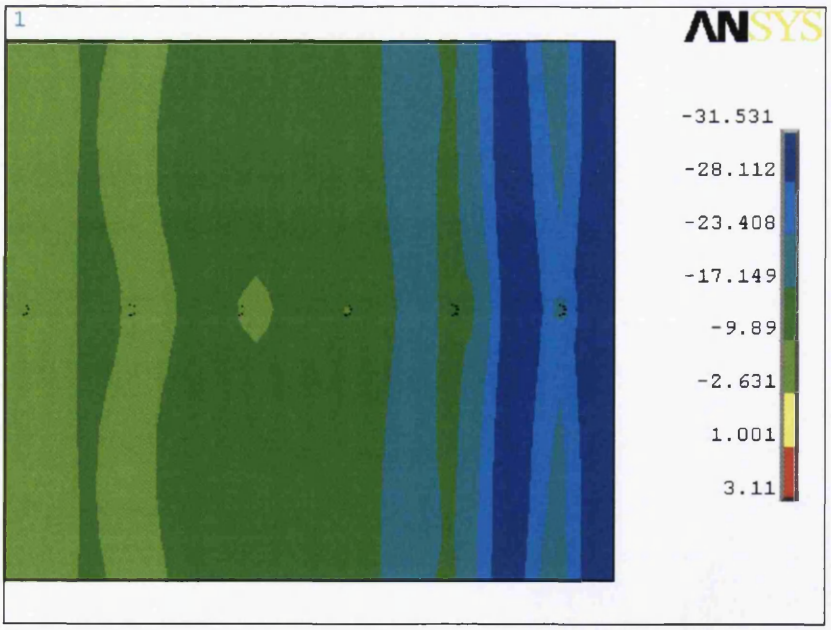

Figure H2: Concrete Stress contours at ultimate stress

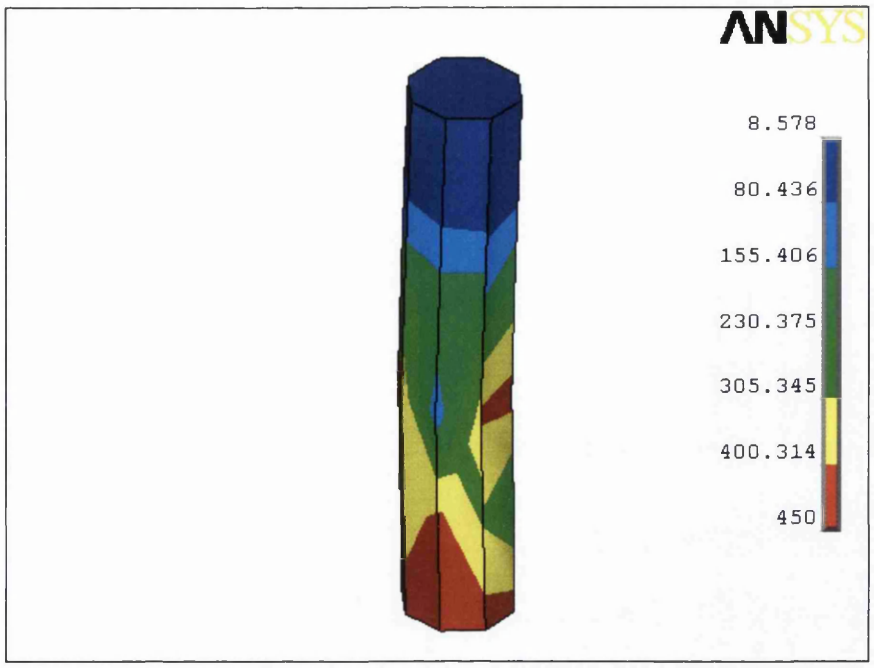

Figure H3: Shear stud connection stress contours at ultimate stress

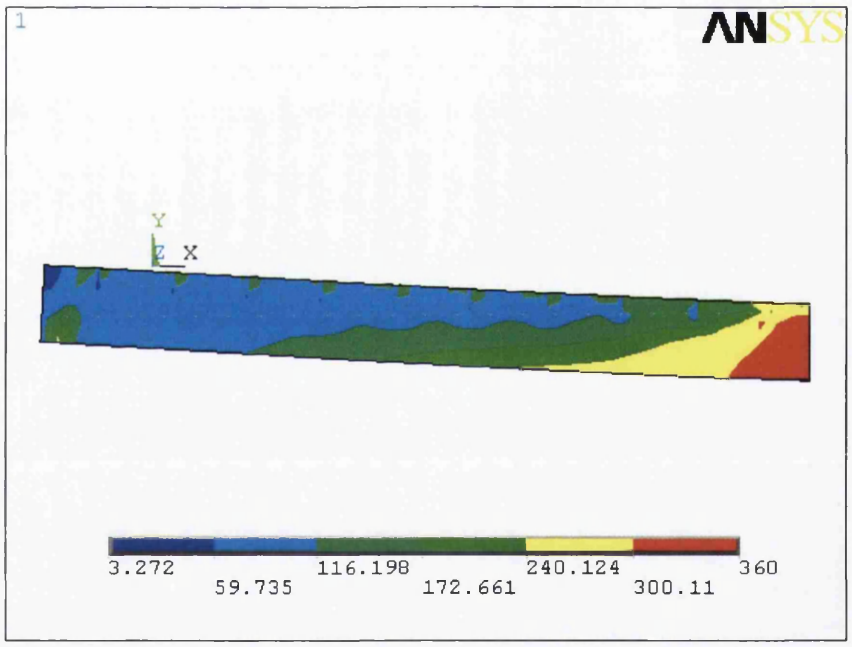

Figure H4: Steel beam stress contours at ultimate stress

Appendix I: Yielding sequence of composite beam (**C1**)

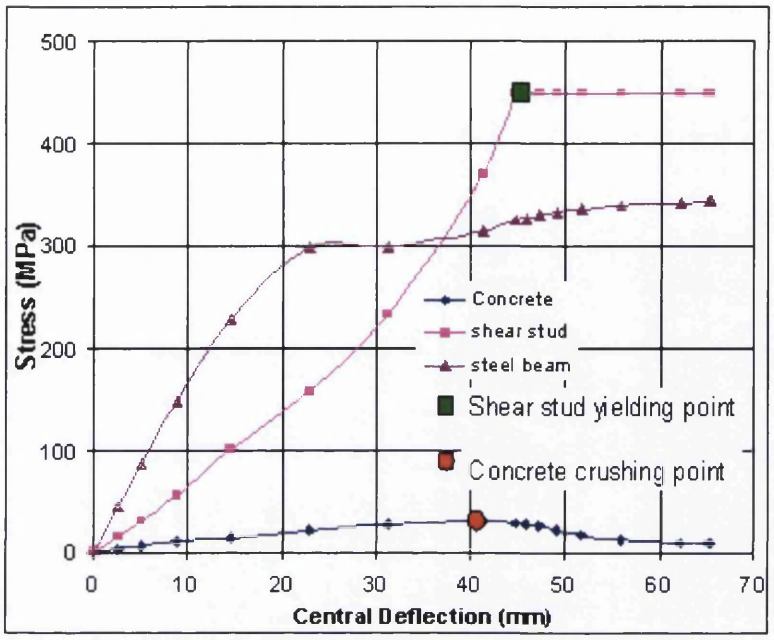

I1: Stress-deflection curve of composite beam component

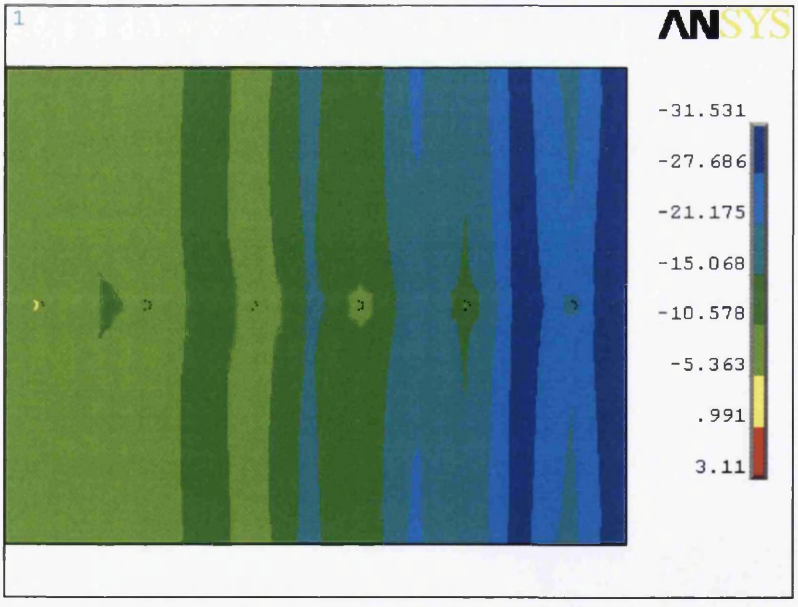

Figure I2: Concrete Stress contours at ultimate stress

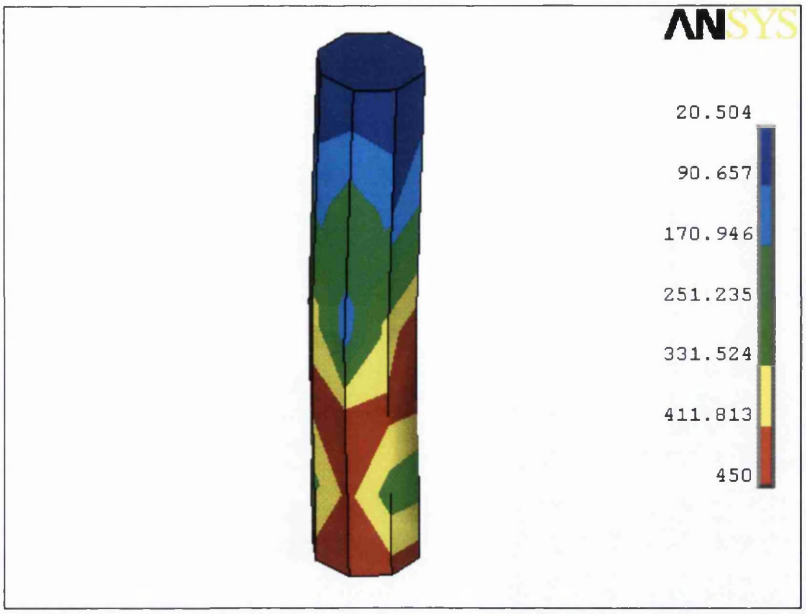

Figure I3: Shear stud connection stress contours at ultimate stress

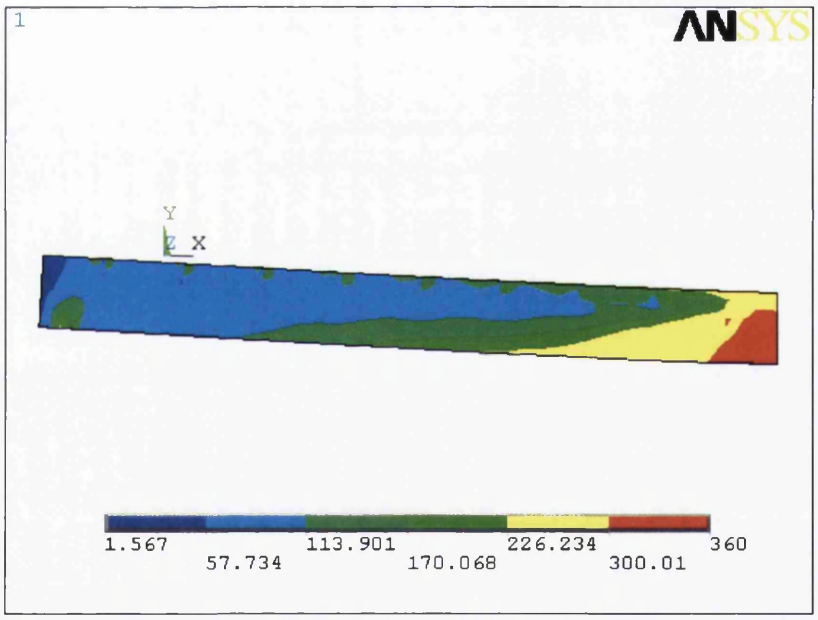

Figure I4: Steel beam stress contours at ultimate stress

Appendix J:

Moment capacity calculation of composite beam with openings in metal-ribbed decking slab using modified plastic analysis according to EC4 for beam A1-T2.

Structural data ***Steel beam section details =>*** **203x133x30**

L =	4000	mm	B =	133.8	mm
D_p =	60	mm	T =	9.6	mm
D_s =	110	mm	t =	6.3	mm
f_{cu} =	43.4	MPa	D =	203.8	mm
f_{sy} =	300	MPa	A =	3732	mm^2
f_u =	450	MPa	Z_p =	3.03E+05	mm^3
Opening, a =	140	mm			

Effective breadth of slab

Be = 720 mm

(Ribs perpendicular to beam)

STRUCTURAL GEOMETRY

Span L = 4000 mm

SLAB DIMENSIONS

B_e =	720	mm
D =	110	mm
f_{cu} =	43.4	N/mm^2
Slab eff. depth D_s =	50	mm

BEAM DIMENSIONS / CLASSIFICATION

B =	133.8	t =	6.3	b/T =	6.96875
T =	9.6	b =	66.9	d/t =	29.3015873
D =	203.8	d =	184.6		

SECTION IS ***PLASTIC***

BEAM PROPERTIES

A =	3731.94	mm^2	S_x =	303117.543	mm^3
I_{xx} =	27543526	mm^4	S_y =	87763.4055	mm^3
I_{yy} =	3836401	mm^4	u =	0.9	
r_x =	85.90975	mm	x =	21.22916667	
r_y =	32.0623	mm	f_{sy} =	300	N/mm^2
Z_x =	2702996	mm^3			
Z_y =	573453.1	mm^3			

Resistance of slab in compression

R_c = 0.45 fcu Be (Ds-Dp)

$$R'_c = \frac{R_c B_{ne}}{B_e}$$

R'_c = 703.08 kN

Resistance of steel section in tension

R_s = A f_{ys}
= 1119.582 kN

Resistance of steel flange section

R_f = 385.344 kN

Resistance of steel web section

R_w = 348.894 kN

Case2 R_s>R_c>R_w
Plastic Neutral axis lies in steel flange

$$M_c = R_s \frac{D}{2} + \frac{R_c B_{ne}}{B_e}\left(\frac{D_s + D_p}{2}\right) - \frac{\left(R_s - R_c B_{ne} / B_e\right)^2}{R_f}\frac{T}{4}$$

M_c = 172.7668 kNm

Degree of shear connection

Number of shear connector per trough	=	1		
Spacing	=	200	mm	
Diameter	=	19	mm	
Normal Height , H	=	95	mm	
Height as welded, h	=	95	mm	
Rib width , ba	=	80	mm	ba = average width of rib

Number of shear connector in half span, N = 10

P_{rd} = $0.8f_u(\pi d^2/4)$ = 102.08358 KN 81.666864 (Factored)
or
P_{rd} = $0.29\alpha d^2(f_{ck}E_{cm})^{1/2}$ = 112.71994 KN 90.17594982 (Factored)

Strength	C20/25	C25/30	C30/37	C35/45	C40/50	C45/55	C50/60
E_{cm}	29	30.5	32	33.5	35	36	37

$f_{cm}= f_{ck}+8$
$f_{cm}=$ 42.20941
$E_{cm}=22[(f_{cm})/10]^{0.3}$
$E_{cm}=$ 33.88796
c = 0.2 [(h/d)+1] for 3 <= h/d <= 4 = 1.2
c = 1 for h/d> 4 1

h/d = 5 (if greater than 4, stud considered as ductiled)

α = 1

E_{cm} = 33887.96 (Check with table provided)

Reduction factor for profile shape

$$r_p = \frac{0.70}{\sqrt{n}}\frac{b_a}{D_p}\left(\frac{h-D_p}{D_p}\right) \le 1.0(n=1), 0.8(n=2)$$

r_p= 0.5444 =< 1
r_p= 0.5444

Lowest P_{rd} Final P_{rd}

81.666864 44.46307 kN

For full shear connection:-

15.81267316

Total shear resistance, R_q

R_q = 444.6307 kN

RE-EVALUATING THE NUETRAL AXIS POSITION FOR PARTIAL INTERACTION

Case4 $R_q > R_w$
Plastic Neutral axis lies in flange

$$M_c = R_s \frac{D}{2} + R_q \left(D_s - \frac{R_q B_e}{R_c B_{ne}} \left(\frac{D_s - D_p}{2} \right) \right) - \frac{(R_s - R_q)^2}{R_f} \frac{T}{4}$$

M_c = 153.1278 kNm

Shear interaction = Provided/partial

0.63

Minimum degree of shear connection (At=Ab), N/Nf >= 0.25+0.03L

0.37

Appendix K:

Moment capacity calculation of composite beam with openings in metal-ribbed decking slab using modified plastic analysis according to BS 5950 for beam A1-T2.

Structural data ***Steel beam section details =>*** **203x133x30**

L =	4000	mm	B =	133.8	mm
D_p =	60	mm	T =	9.6	mm
D_s =	110	mm	t =	6.3	mm
f_{cu} =	43.4	MPa	D =	203.8	mm
f_{sy} =	300	MPa	A =	3732	mm^2
f_u =	450	MPa	Z_p =	3.03E+05	mm^3
Opening, a =	140	mm			

Effective breadth of slab

B_e = 720

(Ribs perpendicular to beam)

STRUCTURAL GEOMETRY

Span L = 4000 mm

SLAB DIMENSIONS

B_e =	720	mm
D =	110	mm
f_{cu} =	43.4	N/mm^2
Slab eff. depth D_s =	50	mm

BEAM DIMENSIONS / CLASSIFICATION

B =	133.8	t =	6.3	b/T =	6.96875
T =	9.6	b =	66.9	d/t =	29.3015873
D =	203.8	d =	184.6		

SECTION IS PLASTIC

BEAM PROPERTIES

A =	3731.94	mm^2	S_x =	303117.543	mm^3
I_{xx} =	27543526	mm^4	S_y =	87763.4055	mm^3
I_{yy} =	3836401	mm^4	u =	0.9	
r_x =	85.90975	mm	x =	21.22916667	
r_y =	32.0623	mm	f_{sy} =	300	N/mm^2
Z_x =	2702996	mm^3			
Z_y =	573453.1	mm^3			

Resistance of slab in compression

R_c = $0.45 f_{cu} B_e (D_s - D_p)$

$$R'_c = \frac{R_c B_{ne}}{B_e}$$

R'_c = 703.08 kN

Resistance of steel section in tension

R_s = $A f_{ys}$
= 1119.582 kN

Resistance of steel flange section

R_f = 385.344 kN

Resistance of steel web section

R_w = 348.894 kN

Case2 $R_s > R_c > R_w$
Plastic Neutral axis lies in steel flange

$$M_c = R_s \frac{D}{2} + \frac{R_c B_{ne}}{B_e}\left(\frac{D_s + D_p}{2}\right) - \frac{\left(R_s - R_c B_{ne} / B_e\right)^2}{R_f}\frac{T}{4}$$

M_c = 172.7668 kNm

Degree of shear connection

Number of shear connector per trough	=	1		
Spacing	=	200	mm	
Diameter	=	19	mm	
Normal Height , H	=	95	mm	
Height as welded, h	=	95	mm	
Rib width , ba	=	80	mm	ba = average width of rib

Number of shear connector in half span, N = 10

Table 21.4 , Steel Designers' Manual, SCI

Dimension odf stud Shear connector			Characteristic strength of concrete (N/mm2)			
Diameter	**Nominal Height**	**As-welded Height**	**25**	**30**	**35**	**40**
25	100	95	146	154	161	168
22	100	95	119	126	132	139
19	100	95	95	100	104	109
19	75	70	82	87	91	96
16	75	70	70	74	78	82
13	65	60	44	47	49	52

For concrete of characteristic strength greater than 40 N/mm^2 use the value for 40 N/mm^2

Resistance of shear connector:

From table 21.4 , Steel Designers' Manual, SCI

Characteristic strength = 109 kN

Design strength,q (Normal concrete) = 87.2 kN

Design strength,q (Lightweight concrete) = 78.48 kN

Check Rib = ba/Dp = 0.11663 < 2 narrow-rib

Reduction factor for profile shape

$$r_p = \frac{0.85}{\sqrt{n}} \frac{b_a}{D_p} \left(\frac{h - D_p}{D_p} \right) \leq 1.0(n=1), 0.8(n=2)$$

r_p= 0.661111 =< 1

r_p= 0.661111 *BS 5950: Part 3 Clause 5.4.7.2*

Total resistance of shear connectors

R_q = r_p x q x N

= 576.4889 kN

RE-EVALUATING THE NUETRAL AXIS POSITION FOR PARTIAL INTERACTION

Case4 $R_q > R_w$
Plastic Neutral axis lies in flange

$$M_c = R_s \frac{D}{2} + R_q \left(D_s - \frac{R_q B_e}{R_c B_{ne}} \left(\frac{D_s - D_p}{2} \right) \right) - \frac{(R_s - R_q)^2}{R_f} \frac{T}{4}$$

M_c = 163.8449 kNm

Actual no. of connector hlf span = 10
No. of Full shear connector = 13.551

Degree of shear connector = Actual/Full = 0.74

$$\boxed{K \geq \frac{L-6}{10}; \geq 0.4}$$

K = 0.74 > 0.4 O.K

Appendix L:

Moment capacity calculation of composite beam with openings in metal-ribbed decking slab reinforced with rebar for beam A-R1.

Structural data

L =	4000	mm
D_p =	60	mm
D_s =	105	mm
f_{cu} =	43.4	MPa
f_{sy} =	300	MPa
f_u, shear stud =	450	MPa
f_r, rebar =	460	MPa
Diameter rebar =	6	mm
Number of rebar =	2	
distance of rebar, d_r= from top of slab	10	mm

Steel beam section details => 203x133x30

B =	133.8	mm	Opening, a =	140	mm
T =	9.6	mm	Number , =	2	
t =	6.3	mm			
D =	203.8	mm			
A =	3731.94	mm^2			
Z_p =	303117.543	mm^3			

(Ribs perpendicular to beam)
STRUCTURAL GEOMETRY

Span L = 4000 mm

SLAB DIMENSIONS

Be =	1000	mm
D =	105	mm
f_{cu} =	43.4	N/mm^2

Slab effective. depth D_s = 45mm

BEAM DIMENSIONS / CLASSIFICATION

B =	133.8	t =	6.3	b/T =	6.96875
T =	9.6	b =	66.9	d/t =	29.3015873
D =	203.8	d =	184.6		

SECTION IS PLASTIC

BEAM PROPERTIES

A =	3731.94	mm^2	S_x =	303117.543	mm^3
I_{xx} =	27543526	mm^4	S_y =	87763.4055	mm^3
I_{yy} =	3836401	mm^4	u =	0.9	
r_x =	85.90975	mm	x =	21.22916667	
r_y =	32.0623	mm	f_{sy} =	300	N/mm^2
Z_x =	2702996	mm^3			
Z_y =	573453.1	mm^3			

Effective breadth of slab

B_e = 1000

B_{ne} = 720

R_r = 26.01576 kN

$$R_c' = \frac{R_c B_{ne}}{B_e} = 610.80075 \text{ kN}$$

R_s = A f_{ys}

= 1119.582 kN

R_f = 385.344 kN

R_w = 348.894 kN

Partial Interaction infromation:-

Degree of shear connection

Number of shear connector per trough	=	1		
Spacing	=	200	mm	
Diameter	=	19	mm	
Normal Height , H	=	95	mm	
Height as welded, h	=	95	mm	
Rib width , ba	=	80	mm	ba = average width of rib
Number of shear connector in half span, N	=	10		

Check Rib = ba/Dp = 1.333333 < 2 narrow-rib

Resistance of shear connector:

Characteristic strength = 109 kN
(From table 21.4 , Steel Designers' Manual, SCI)

Design strength,q = 87.2 kN

$$r_p = \frac{0.85}{\sqrt{n}} \frac{b_a}{D_p} \left(\frac{h - D_p}{D_p} \right) \leq 1.0(n=1), 0.8(n=2)$$

r_p= 0.661111111 =< 1 (Take the limit value if it over)

r_p= 0.661111111 BS 5950: Part 3 Clause 5.4.7.2

Total resistance of shear connectors

R_q = r_p x q x N

= 576.4888889 kN (For normal weight concrete)

Check the design condition,

$R_c+R_r > R_q$

Partial interaction design

R_{ct} = $R'_c+R_r - R_q$
= 60.32762111 kN

t_{ct} = $R_{ct}/ (0.45f_{cu}b_{ne})$
= 4.444563878 mm

$R_r+R_c+R_{sc}$ = $R_{ct} + R_{ss}$
R_{sc} = $R_{ct} + Rss - Rc - Rr$ and R_{ss} = R_s-R_{sc}
R_{sc} = $(R_{ct} + R_s - R_c - R_r)/2$
= 271.5465556 kN 848.0354 =R_{ss}

A_{sc} = 905.1551852 mm2

Locate neutral axis, Flange area, BT = 1284.48 mm

Neutral axis in flange

Calculation for neutral axis in flange:-

R_{sc} = $t_1 \times b \times f_{ys}$

t_1 = 6.764986436 mm

y_{sc} = $= (A_s D - bt_1^2)/ 2(A_s - bt_1) - t_1/2$

= 130.0634637 mm

y_c = $y_{sc} + t_1/2 + Ds - (D_s - D_p)$

y_c = 215.945957 mm

y_r = $y_{sc} + t_1/2 + D_s - D_r$

= 228.445957 mm

y_{ct} = $y_{sc} + t_1/2 + t_{ct}/2 + D_p$

= 195.6682389 mm

M_c = $R'_c y_c + R_r y_r + R_{sc} y_{sc} - R_{ct} y_{ct}$

= 161.3572339 kNm

Appendix M:

Example of deflection calculation for beam A1-f1 using EC4 method.

Structural data			**Steel beam section details =>**		**203x133x30**
L =	4000	mm	B =	133.8	mm
D_p =	60	mm	T =	9.6	mm
D_s =	105	mm	t =	6.3	mm
f_{cu} =	43	MPa	D =	203.8	mm
f_{ys} =	300	MPa	A =	3731.94	mm^2
			Z_p =	303117.5	mm^3

Opening Parameter

a =	250	mm
f =	200	mm

$E_{concrete}$ =	26499.00788	
E_{steel} =	206000	
n =	7.773875948	
b_e=	1000	mm
t_c =	45	mm

(Ribs perpendicular to beam)
STRUCTURAL GEOMETRY

Span	L =	4000	mm	

SLAB DIMENSIONS

B_e =	1000	mm
D =	105	mm
f_{cu} =	43	N/mm^2
Slab eff. depth D_s =	45mm	

BEAM DIMENSIONS / CLASSIFICATION

B =	133.8	t =	6.3	b/T =	6.96875
T =	9.6	b =	66.9	d/t =	29.3015873
D =	203.8	d =	184.6		
		SECTION IS		PLASTIC	

BEAM PROPERTIES

A =	3731.94	mm^2	Sx =	303117.5	mm^3
I_{xx} =	27543525.73	mm^4	Sy =	87763.41	mm^3
I_{yy} =	3836400.912	mm^4	u =	0.9	
r_x =	85.90974687	mm	x =	21.22917	
r_y =	32.06229948	mm	py =	300	N/mm^2
Z_x =	2702995.655	mm^3			
Z_y =	573453.0511	mm^3			

Rigidity of section without openings-B1

Moment inertia of composite section

Section	Transform section	Distance from top of slab to centroid (y)mm	Ay	Ay^2	Ilocal in steel unit
Concrete	5788.618226	22.5	130243.9	2930488	976829.3257
Steel	3731.94	206.9	772138.4	1.6E+08	27543525.73
Total	9520.558226		902382.3	1.63E+08	28520355.05

$y_{centroid}$ = 902382.2961 / 9520.558226 = 94.78249853 mm

$I_{composite}$ = 105676226.4 mm^4 83117754

EI = 21769302647

Rigidity of section with openings-B2

Moment inertia of composite section

Section	Transform section	Distance from top of slab to centroid (y)mm	Ay	Ay^2	Ilocal in steel unit
Concrete	2894.309113	22.5	65121.96	1465244	488414.6629
Steel	3731.94	206.9	772138.4	1.6E+08	27543525.73
Total	6626.249113		837260.3	1.61E+08	28031940.39

$y_{centroid}$ = 837260.341 / 6626.249113 = 126.3550957 mm

$I_{composite}$ = 83460505.9 mm^4 67316156

EI = 17192864215

$$\frac{\delta}{\delta_c} = 1 + 0.3\left[1 - \frac{N}{N_f}\right]\left[\frac{\delta_a}{\delta_c} - 1\right]$$

Deflection of steel acting alone

$$\delta_a = \frac{Pl^3}{48\,EI}$$

I_s = 27543525.73
δ_a = 16.4493986 mm

Using conjugate beam method (Point load at central)

$$\delta_c = \frac{P}{6B_1}(l-b)^3 + \frac{Pb}{12B_2}\left(6l^2 - 6bl + 3b^2l - b^2\right)$$

1-s = 0.494080745
(δ_a/δ_c)-1 = 2.572230277
δ = 6.360454671 mm

Appendix N:

Example of deflection calculation for beam A1-f1 using Nie. J. method.

Structural data			**Steel beam section details =>**		**203x133x30**
L =	4000	mm	B =	133.8	mm
D_p =	60	mm	T =	9.6	mm
D_s =	105	mm	t =	6.3	mm
f_{cu} =	43	MPa	D =	203.8	mm
f_{ys} =	300	MPa	A =	3731.94	mm^2
			Zp =	303117.5	mm^3

Opening Parameter

a =	250	mm
f =	200	mm
$E_{concrete}$ =	26499.00788	
E_{steel} =	206000	
n =	7.773875948	
b_e=	1000	mm
t_c =	45	mm

(Ribs perpendicular to beam)
STRUCTURAL GEOMETRY

SLAB DIMENSIONS

				Be =	1000	mm
Span	L =	4000	mm	D =	105	mm
				fcu =	43	N/mm^2
				Slab eff. depth Ds =		45mm

BEAM DIMENSIONS / CLASSIFICATION

B =	133.8	t =	6.3	b/T =	6.96875
T =	9.6	b =	66.9	d/t =	29.3015873
D =	203.8	d =	184.6		

SECTION IS PLASTIC

BEAM PROPERTIES

A =	3731.94	mm^2	S_x =	303117.5	mm^3
I_{xx} =	27543525.73	mm^4	S_y =	87763.41	mm^3
I_{yy} =	3836400.912	mm^4	u =	0.9	
r_x =	85.90974687	mm	x =	21.22917	
r_y =	32.06229948	mm	f_{ys} =	300	N/mm^2
Z_x =	2702995.655	mm^3			
Z_y =	573453.0511	mm^3			

Rigidity of section without openings-B1

Moment inertia of composite section

Section	Transform section	Distance from top of slab to centroid (y)mm	Ay	Ay^2	I local in steel unit
Concrete	5788.618226	22.5	130243.9	2930488	976829.3257
Steel	3731.94	206.9	772138.4	1.6E+08	27543525.73
Total	9520.558226		902382.3	1.63E+08	28520355.05

$y_{centroid}$ = 902382.2961 / 9520.558226 = 94.78249853 mm

$I_{composite}$= 105676226.4 mm^4 83117754

EI = 21769302647

$$\frac{1}{A_o} = \frac{n}{k_c A_c} + \frac{1}{A_a} \qquad \begin{aligned} A_c &= nA_a \\ I_c &= nI_a \end{aligned}$$

A_c = 29011.6386

$1/A_o$ = 0.000535914

A_o = 1865.97 mm^2

$$\frac{1}{A'} = d_c^{\,2} + \frac{I_o}{A_o} \qquad I_o = \frac{k_c I_c}{n} + I_a$$

I_c =	214119952.2	mm^4	0.000214	m^4
I_o =	55087051.46	mm^4	5.51E-05	m^4
d_c =	184.4	mm	0.1844	m
1/A' =	63525.29843	mm^2	0.063525	m^2
A' =	1.57418E-05	mm^2	15.74176	m^2

k_s = 0.505919255

Nfull 19.766

Nprov = 10

p_f= 101.1838511 mm

Pitch, p = 200 mm

$$V_u = k_t P_{rd} \qquad K = 0.66 V_u$$

P_{rd}	=	81.666864	
k_t	=	0.544444444	
pitch,p	=	200	mm
V_u	=	44.4630704	
K	=	29.34562646	

$$\alpha^2 = \frac{k}{pE_a I_o A'}$$

α^2 = 0.821378547 m^{-2}

$$\beta = \frac{A' p d_c}{k}$$

β = 1.97834E-05 m/kN

$$\eta = \frac{24(EI)_c \beta}{L^2 h}$$

η = 2.091988524

$$\varepsilon_s = \eta \left[0.5 - \frac{1}{(\alpha L)} \right]$$

ε_s = 0.468925416

1+ ε_s = 1.468925416

B/ (1+ ε_s) = 14819.88289

B_1 = 14819.88289

Rigidity of section with openings-B2

Moment inertia of composite section

Section	Transform section	Distance from top of slab to centroid (y)mm	Ay	Ay^2	I local in steel unit
Concrete	2894.309113	22.5	65121.96	1465244	488414.6629
Steel	3731.94	206.9	772138.4	1.6E+08	27543525.73
Total	6626.249113		837260.3	1.61E+08	28031940.39

$y_{centroid}$ = 837260.341 / 6626.249113 = 126.3550957 mm

$I_{composite}$ = 83460505.9 mm^4 67316156

EI = 17192864215

$$\frac{1}{A_o} = \frac{n}{k_c A_c} + \frac{1}{A_a} \qquad \begin{aligned} A_c &= nA_a \\ I_c &= nI_a \end{aligned}$$

A_c = 29011.6386

$1/A_o$ = 0.000535914

A_o = 1865.97 mm^2

$$\frac{1}{A'} = d_c^{\,2} + \frac{I_o}{A_o} \qquad I_o = \frac{k_c I_c}{n} + I_a$$

I_c =	214119952.2	mm^4	0.000214	m^4
I_o =	55087051.46	mm^4	5.51E-05	m^4
d_c =	184.4	mm	0.1844	m
1/A' =	63525.29843	mm^2	0.063525	m^2
A' =	1.57418E-05	mm^2	15.74176	m^2

k_s = 0.505919255

Nfull 19.766

Nprov = 10

p_r = 101.1838511 mm

Pitch, p = 200 mm

$$V_u = k_t P_{rd} \qquad K = 0.66 V_u$$

P_{rd}	=	81.666864	
k_t	=	0.544444444	
pitch,p	=	200	mm
V_u	=	44.4630704	
K	=	29.34562646	

$$\alpha^2 = \frac{k}{pE_a I_o A'}$$

α^2 = 0.821378547 m^{-2}

$$\beta = \frac{A' p d_c}{k}$$

β = 1.97834E-05 m/kN

$$\eta = \frac{24(EI)_c \beta}{L^2 h}$$

η = 1.652201507

$$\varepsilon_s = \eta\left[0.5 - \frac{1}{(\alpha L)}\right]$$

ε_s = 0.370345855

1+ ε_s = 1.370345855

B/ (1+ ε_s) = 12546.3686

B_2 = 12546.3686

Using conjugate beam method - Point load at central

$$\Delta = \frac{P}{6B_1}(l-b)^3 + \frac{Pb}{12B_2}\left(6l^2 - 6bl + 3b^2 l - b^2\right)$$

Δ = 6.618276386 mm

Publications

The author has four jointed international publications.

The publications are:

- Bahrom S and Xiao R.Y "Numerical modelling of composite beam with openings in metal-ribbed decking slab'', Proceeding in 15th International Conference on Composite Structures, Porto, June 2009, Paper No. 113.

- Xiao R.Y and Baharom S., "Numerical Modelling of the Effect of Opening Location in Composite Beam Flanges with Deformed Decking Floors'', 11th International Conference on Civil, Structural and Environmental Engineering Computing, (CC2007 and AICC2007), St. Julians, Malta,18-21 September 2007.

- Baharom S. and Xiao R.Y., "Finite element modelling of composite beam with opening in ribbed decking slab'', 6th International Conference on Steel and Structural Engineering (ICSAS'07), St Catherine's College, Oxford, July 24th- 27th 2007.

- Baharom. S. and Xiao R.Y., "Comparison between Modelling of Ribbed Decking Composite Slabs With and Without Slip in Finite Element Analysis''. CST 2006: The Eighth International Conference on Computational Structures Technology, Las Palmas de Gran Canaria, Spain, 12-15 September 2006.